Engineering approach to highly-glycolytic cancer models and systems exploration of COVID-19 vascular complications

AA Meyer

orcid.org/0000-0003-0429-3878

Thesis accepted in fulfilment of the requirements for the degree Doctor of Philosophy in Engineering with Mechanical Engineering at the North-West University

Promoter: Prof EH Mathews

Graduation: May 2022

Student number: 31554857

ABSTRACT

Title: Engineering approach to highly-glycolytic cancer models and systems exploration of COVID-19 vascular complications

Student: Albertus Abram Meyer

Promoter: Prof Edward Henry Mathews

Keywords: Cancer, glucose deprivation, coronavirus disease of 2019, coronary heart disease, engineering approach

In this thesis, engineering approaches are applied to two major medical research diseases, namely cancer and coronavirus disease of 2019 (COVID-19).

The first approach (Part A) provides new preclinical cell culture *(in vitro)* cancer models for metabolic treatments. In engineering experimental modelling, models are intended to investigate, improve and/or simulate a practical problem. For this process to be accurate, the small-scale model should be designed within the bounds of scaling validity. This ensures that the small-scale model accurately represents the full-scale model.

This engineering experimental modelling principle was applied to *in vitro* (cell cultures) cancer models to develop alternative methods for metabolic cancer treatments, i.e., glucose deprivation (GD). *In vitro* cancer models do not necessarily focus on aspects that are important for quantification in a realistic environment. Current microenvironments of *in vitro* cancer models are optimised for cell growth and do not mimic physiological conditions.

This results in glucose and glutamine concentrations (the main energy sources for cell growth) being much higher in cell cultures than in typical cancer patients' concentrations. In addition, *in vitro* glucose concentrations of metabolic treatments are tested at much lower levels than what is achievable in humans. Furthermore, cancer cells are exposed to GD at much shorter durations than typical clinical metabolic treatments in humans.

These discrepancies could partly result in untranslatable results and misrepresenting data used to develop *in vivo* (human) metabolic cancer treatments. Therefore, novel replicable metabolic *in vitro* methods were developed within the bounds of scaling validity, i.e., at achievable glucose and glutamine concentrations. The results obtained from these new methods are the following:

- Cancer and non-cancer cells stabilise after 20 days when exposed to physiological glucose and glutamine concentrations. Therefore, moderate long-term GD should only be implemented at least 20 days after cells were exposed to physiological conditions.

- Cancer cells were affected more than non-cancer cells after exposure to long-term moderate GD, with respective minimum cell growth after treatment of 62% and 84%.
- Long-term moderate GD is not sufficiently effective to achieve remission. Therefore, additional therapies are needed.
- Cancer cells are most vulnerable approximately 26 days after moderate GD. Additional therapies were implemented at this point.

Cells were exposed to the following extra therapies during metabolic treatments: (i) very low short-term GD, (ii) very low short-term glucose and glutamine deprivation, and (iii) different doses of two different chemotherapies. Results of these extra therapies were the following:

(i) Short-term GD decreased cancer cell growth further than long-term moderate GD; the minimum cancer cell growth after treatment was 15%.

(ii) The addition of short-term glutamine deprivation did not decrease cell growth any further; the minimum cancer cell growth after treatment was 16%.

(iii) Long-term moderate GD increased the efficacy of chemotherapy on some of the cancer cell lines.

The insights gained from these tests were further used to develop a hypothetical non-toxic long-and short-term metabolic treatment for future clinical trials. This hypothetical method provides an alternative, non-toxic way to decrease circulating blood glucose levels. Most aspects of this proposed method have been shown to be safe in non-cancer patients. Therefore, future work should aim to implement such therapies on cancer patients in clinical trials.

The second approach (Part B) provides a systems engineering approach to medical research, which provides a holistic view of factors that influence disease severity and therapeutic insights on COVID-19. Traditionally, medical research employs a reductionist approach, which entails dividing complex systems into smaller parts and focusing on these smaller parts to solve the problem. This leads to an in-depth understanding of only the smaller aspects and not the larger overall problem.

Furthermore, the whole-system interaction and cause-and-effect are not adequately considered. This reductionistic approach is seen in numerous medical studies of severe COVID-19 cases and deaths due to COVID-19 in patients with chronic cardiovascular comorbidities.

Part B of this study aimed to apply a systems-based engineering approach to integrate an existing systems-based coronary heart disease (CHD) model with the activated pathogenetic pathways seen in severe COVID-19 complications. This new integraded model was developed to help explain the mechanisms of interaction of severe COVID-19 on the vascular system. The new *integrated CHD/COVID-19 model* provides the following insight:

- This fully integrated model presents a visual explanation of the pathogenetic mechanisms of interaction between CHD and COVID-19 complications.
- A detailed integrated explanation of a death spiral as a result of interactions between *Inflammation*, endothelial cell injury, *Hypercoagulability* and hypoxia.
- The model also presents how this *death spiral* is aggravated through the following CHD hallmarks: *Hyperglycaemia/Hyperinsulinaemia, Hypercholesterolaemia*, and/or *Hypertension*.
- A strong association between CHD and COVID-19 for all the investigated *health factors* and *pharmaceutical interventions*, except for β-blockers, was found.
- The new model shows how different *health factors* (stress, exercise, smoking, etc.) and *pharmaceutical interventions* (statins, salicylates, thrombin inhibitors, etc.) may either aggravate or suppress COVID-19 severity.

With the insight gained from this new model, recommendations are made for future research in potential new pharmacotherapeutics and personalised computational analysis to help assess the risk of a patient with severe COVID-19 vascular complications.

DEDICATION

I dedicate this study to the following people:

My grandmother, Joey Geldenhuis, whose love and passion for people inspired me to always ensure that my work helps others.

A friend, Elinza Mostert, may your soul rest in peace and may the battle you faced inspire novel cancer treatments.

All those who lost their loved ones due to cancer and COVID-19, may your hearts be healed again.

ACKNOWLEDGEMENTS

First and foremost, I would like to thank my heavenly father, Jesus Christ, for blessing me with the ability to pursue my PhD. All the glory and honour goes to Him alone. Furthermore, several people have guided me throughout this study, and I want to thank each of them individually:

- My supervisor, Prof Edward Mathews, thank you for the guidance, advice and creative ideas that inspired this research. When faced with complex problems, I will always remember to*: "Gather all the information until you understand all the detail and then develop a simplified solution."*
- To the *Centre for Research and Continued Engineering Development, Human Sim International (Pty) Ltd* and its sister companies for the bursary to pursue my PhD.
- A grateful thank you to Prof Annie Joubert and Dr. Michelle Visagie from the *University of Pretoria* for their financial contributions from the following grants: *National Research Foundation, Cancer Association of South Africa, South Africa Medical Research Council, Struwig-Germeshuysen Kankernavorsingstrust* and *The School of Medicine Research Committee of the University of Pretoria.* More specifically, thank you to Dr. Michelle Visagie for her exemptional experimental work done at the *University of Pretoria Physiology Department* cell culture laboratories.
- Thank you to the mentors I had throughout my study, Mr. George Mathews, for the initial support at the start of the research. Dr. Jean van Laar for your "open door policy" and willingness to help where needed. Dr. Andries Gous, for your assistance with the COVID-19 research. Dr. Marc Mathews for the initial development of the CHD model.
- Great appreciation to Dr. Nelis Willers and Mrs. Riana Willers for the time they took to review my thesis and their impeccable insight. I will always remember the following advice: *"You do not write for yourself, but you write for the reader, through their perspective*."
- To my friends and colleagues who always believed in me. Thank you for encouraging me and keeping me sane. I will make up for the lost social time in the near future.
- To my family. Thank you to my dad, Hennie, for all your prayers and support. To my brother, Niél, a big thank you for your motivation and abundant love. Mostly thank you to my mother, Hannelie, for her valuable assistance in structuring my document and for the endless motivation to never give up. I treasure you all.

Lastly, but most importantly, a special thank you to my wife, Marné. I will always cherish the love and support you have provided me during this study. Thank you for always listening and knowing what to say when I need it most. You are truly a blessing from God.

PREFACE

Novelty of research outputs is an important aspect of a PhD. In this thesis, three chapters have already been published/accepted in accredited scientific journals and results of one chapter has been presented at an international conference. Subsequently, Chapter 3 has been submitted for publication. The co-author declarations are provided in Appendix A.

The article and conference proceeding citations, corresponding chapters, appendices and contributions made by Albertus Abram Meyer towards these research outputs are described here.

Published/accepted articles

1. **Chapter 2** has already been successfully published in the medical scientific journal, *Nutrition* (impact factor 3.6 at the time of writing) with the following title: *In vitro quantification: long-term effect of glucose deprivation on various cancer cell lines.* DOI number: 10.1016/j.nut.2020.110748 (see Appendix B for the published manuscript).

The following contributions were made by Albertus Abram Meyer:

- Formal analysis: Application of statistical and formal techniques to analyse the study data.
- Visualisation: Preparation, creation of graphical presentation and visualisation of the study data.
- Writing, reviewing and editing: Preparation, critical review, write-up revisions of the manuscript and final approval of the version to be published.

2. **Chapter 5** has already been successfully published in the medical scientific journal, *Medical Hypotheses* (impact factor 1.3 at the time of writing) with the following title: *A hypothetical method for controlling highly glycolytic cancers and metastases.* DOI number: 10.1016/j.mehy.2018.06.014 (see Appendix C for the published manuscript).

The following contributions were made by Albertus Abram Meyer:

- Methodology: Integration of detailed methodology of the proposed long-term glucose deprivation *Press* treatment.
- Investigation: Research concerning correct medical equipment, medication dosages and durations as well as correspondence and verification with experts in the respective fields.
- Writing, review and editing: Preparation, critical review and write-up revisions of the manuscript and final approval of the version to be published.

3. **Chapter 6** has already been successfully published in a special edition research topic of Frontiers in Cardiovascular Medicine (impact factor 6.0 at the time of writing), namely “What do we know about COVID-19 implications for cardiovascular disease?”. The manuscript title: *Using a systems approach to explore the mechanisms of interaction between severe COVID-19 and its coronary heart disease complications.* DOI number: 10.3389/fcvm.2022.737592 (see Appendix D for the published manuscript).

The following contributions were made by Albertus Abram Meyer:

- Formal analysis: Substantial contributions to the conception and design of the work. Development of the methodology used to integrate current literature with the model.
- Methodology: Design and integration of detailed methodology used to integrate current COVID-19 literature into the CHD model.
- Investigation: Research concerning literature of activated biomarkers, traits and hallmarks reported in patients, as well as correspondence and verification of this with experts in these fields.
- Visualisation: Preparation, creation of graphical presentation and visualisation of the study data.
- Writing, review and editing: Preparation, critical review, revising it critically for important intellectual content, write-up revisions of the manuscript and final approval of the version to be published.

4. **Chapter 3** has been submitted for publication and has been preliminarily accepted with revisions in the scientific medical journal *Cancer Cell International* (impact factor 5.7 at the time of writing) with the following title: *In vitro quantification: combined long and short-term metabolic effects on different cancer cell lines.* The manuscript is currently under review.

The following contributions were made by Albertus Abram Meyer:

- Formal analysis: Application of statistical and formal techniques to analyse the study data.
- Visualisation: Preparation, creation of graphical presentation and visualisation of the study data.
- Writing, review and editing: Preparation, critical review, write-up revisions of the manuscript and final approval of the version to be published.

Conference proceeding

The results of **Chapter 2** were also presented as an oral presentation at the 3rd World Congress on Cancer: New strategies to prevent, diagnose and treat Cancer based on Precision Medicine, Top Hotel Praha & Congress Centre, Prague, Czech Republic from 23-25 September 2019. Title of the conference proceeding: *"Ketogenic diet as a cancer treatment: In vitro Quantification."*

The following contributions were made by Albertus Abram Meyer:

- Formal analysis: Application of statistical and formal techniques to analyse the study data.
- Visualisation: Preparation, visualisation of the study data and creation of the graphical presentation.

TABLE OF CONTENTS

LIST OF TABLES

LIST OF FIGURES

LIST OF APPENDICES

ABBREVIATIONS AND ACRONYMS

ACE	Angiotensin-converting-enzyme
ATP	Adenosine Triphosphate
BDNF	Brain-derived neurotrophic factor
BG	Blood Glucose
BNP	B-type natriuretic peptide
CHD	Coronary Heart Disease
COVID-19	Coronavirus disease of 2019
COX	Cyclooxygenase
CRP	C-reactive protein
DCA	Dichloroacetate
DMEM	Dulbecco’s Modified Eagle’s Medium
DSR	Differential Stress Resistance
DSS	Differential Stress Sensitisation
D-dimer	Fibrin degradation product D
EC	Endothelial cell
ECG	Electrocardiography
EGF	Epidermal Growth Factor
EGFR	Estimated Glomerular Filtration Rate
FCS	Foetal Calf Serum
FDG	Fluorodeoxyglucose
FFA	Free fatty acids
GCF	Gingival crevicular fluid

GD	Glucose Deprivation
GKI	Glucose-Ketone Index
GKIC	Glucose-Ketone Index Calculator
HbA1c	Glycated haemoglobin A1c
HDL	High-density lipoprotein
HeLa	Henrietta Lacks
HF12M	Ham’s F-12 Medium
Hs	Homocysteine
ICAM	Intracellular adhesion molecule
IGF-1	Insulin-like growth factor-1
IL	Interleukin
KD-R	Restricted Ketogenic Diet
LDL	Low-density lipoprotein
MAPK	Mitogen-activated protein kinase
MCF-7	Michigan Cancer Foundation (metastatic breast cancer cell)
MCF-10A	Michigan Cancer Foundation (non-cancer immortalised cell)
MCP	Monocyte chemoattractant protein
MDA-MB-231	M.D. Anderson Metastasis Breast cancer cell line
MIF	Macrophage migration inhibitory factor
MMP	Matrix metalloproteinase
MPO	Myeloperoxidase
mSLP	Mitochondrial Substrate Level Phosphorylation
MTE	Metabolic Treatment Efficacy

NFκβ	Nuclear factor-kappa-beta
NLRP3	Nod-like receptor family pyrin domain containing 3
NO	Nitric oxide
NO-NSAID	Nitric oxide-non-steroidal anti-inflammatory drug
OPG	Osteoprotegerin
oxLDL	Oxidised LDL
PAI	Plasminogen activator inhibitor
PDGF	Platelet-derived growth factor
PET	Positron Emission Tomography
PERCIST	PET Response Criteria In Solid Tumours
P. gingivalis	Porphyromonas gingivalis
PI3K	Phosphatidylinositol 3-kinase
PKM2	Pyruvate Kinase M2
RANKL	Receptor activator of nuclear factor kappa-beta ligand
ROS	Reactive oxygen species
SARS-CoV-2	Severe acute respiratory syndrome coronavirus 2
SCD-40	Recombinant human sCD40 ligand
SMC	Smooth muscle cell
SSRI	Serotonin reuptake inhibitors
SUV	Standardized Uptake Value
TF	Tissue factor
TMAO	Oxidation product of trimethylamine
TNF-α	Tumour necrosis factor-alpha

VCAM	Vascular cell adhesion molecule
vWF	von Willebrand factor
β-blocker	Beta-adrenergic antagonists

CHAPTER 1
INTRODUCTION

"We cannot solve our problems with the same thinking we used when we created them."

Albert Einstein[1]

[1]AZ Quotes, "Albert Einstein Quotes About Problem Solving." [Online]. Available: https://www.azquotes.com/author/4399-Albert_Einstein/tag/problem-solving. [Accessed: 21-Nov-2021].

1.1 PREAMBLE

This thesis makes several novel contributions to the medical field by applying engineering principles to medical research. These contributions are made in cancer and coronavirus disease of 2019 (COVID-19) research fields.

Since two different engineering approaches were applied to two disease areas separately, hence the main body of the thesis is divided into two Parts (A and B). Part A consists of an engineering experimental modelling approach to develop more physiologically correct metabolic preclinical cancer cell culture models. Part B provides an engineering systems approach that fully explains the pathogenic pathways and vascular complications seen in most critically ill COVID-19 patients.

As a result of the two approaches, the layout of this thesis is slightly different compared to a typical PhD thesis, in that the two Parts (A and B) each consists of separate chapters, with the sections of each chapter including the typical PhD thesis chapters, i.e., (i) Background (containing the literature review providing the rationale and need for the study, the problem statement and objectives); (ii) Methodology; (iii) Results; (iv) Discussion; (v) Conclusions; (vi) Novel contributions; and (vii) Dissemination of results. Part A and B's overall limitations, recommendations for future work and conclusions are detailed in the final chapter (Chapter 7).

In this introductory chapter, the general background is given to provide an overview of the two main problems addressed in this thesis and presented as Part A and Part B. For each of the main study problems, the corresponding overall aims and specific objectives to address these aims are provided. The chapter is concluded with the layout of the thesis, including a brief outline of each chapter.

1.2 BACKGROUND TO THE THESIS

Engineering has played a pivotal role in medical discoveries and clinical translation over the last century [1]. Since the invention of the X-ray in 1895, several Nobel Prizes have been awarded for novel health technology development [1]. These ground-breaking inventions have ideally positioned the integration of engineering and medical sciences to address significant challenges in medicine and health care [1].

In this thesis, two engineering approaches are applied to different challenges in two major disease areas in medical research. Engineering experimental modelling is applied to the field of cancer, while engineering systems-integration is applied to COVID-19 disease.

1.2.1 Engineering experimental modelling

The first approach, engineering experimental modelling, involves using the principle of similarity to develop small-scale *in vitro* cancer models that mimic metabolic cancer treatments. The overarching concept and abstract reasoning of similarity are applicable in this study. Therefore, only an overview of model similarity laws is discussed.

The principle of similarity originated from dimensional analysis and is historically rooted in aerodynamics [2]. In engineering, it is used to simplify complex problems by developing tractably solvable models. Two models are considered completely similar if all relevant dimensionless parameters have the same corresponding values for the small- and large-scale models [2]. The rewards of creating similarity models can be spectacular: It allows a model as small as a children's toy to provide insight into the dynamics of an aeroplane [3], thus producing incalculable savings in time and money in the design process [4].

Consider the simple example in Figure 1.1 of the airflow around a full-scaled aircraft wing prototype (left) and small-scaled aerofoil model (right). The small-scaled model is considered to be dynamically similar if the flow around them (denoted by U_p and U_m) is such that the homogenous points' forces are proportionate in magnitude [2]. To achieve such similarity, the model's dimensions must be within the bounds of scaling validity (i.e., all three dimensions between the models were scaled proportionately, by a factor of 10 [2]).

Dynamic similarity thus ensures that the simplified small-scaled aerofoil model accurately simulates the full-scaled aircraft wing prototype (within the bounds of scaling validity) [5]. If the small-scale model is designed outside the validity bounds, it will generate incomparable results [2]. The consequences of designing outside of these validity bounds may be catastrophic. In this case, the full-scaled aeroplane wing would not be designed correctly and could fail during flight.

Unfortunately, complete similarity is impossible in practice, and the small-scale and real-world models are rarely ever close to perfect [3]. Nevertheless, similarity ultimately helps the experimenter to identify which parameters are essential to control, within specific boundary conditions, during experimental tests [4]. Most importantly, not all parameters are equally important; their relative importance depends on the situation [4]. Therefore, the experimenter should always ask how this mismatch will affect the results obtained from the experiments [4].

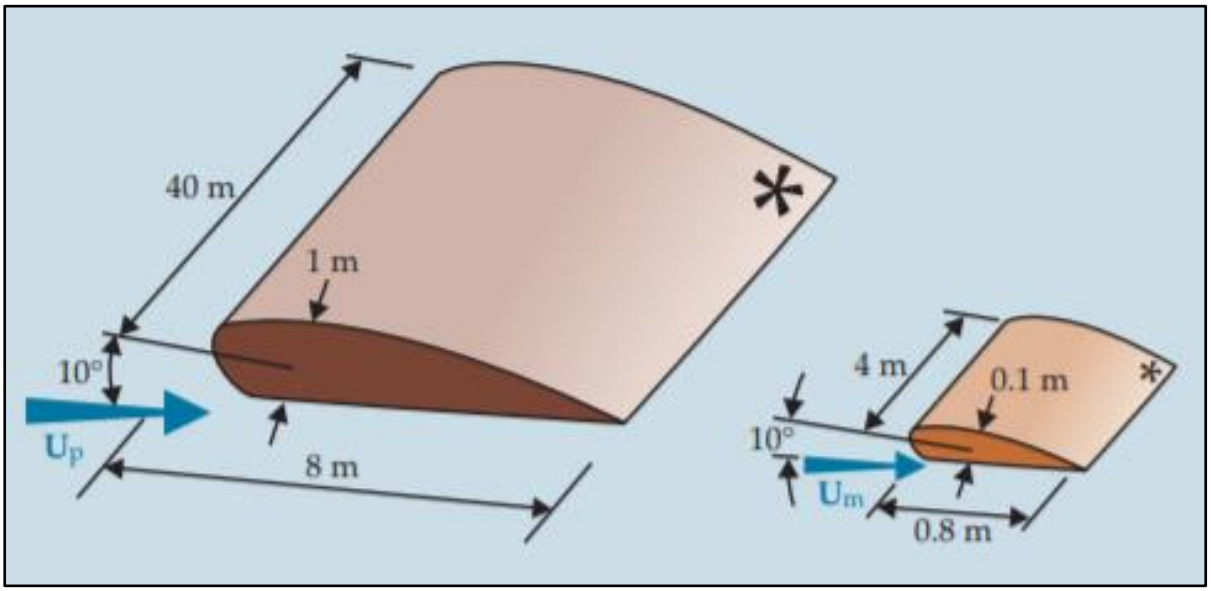

Figure 1.1. Dynamically similar full (left) and small (right) scale aerofoil models [2].

Consider preclinical cancer cell culture *(in vitro)* models, which is the initial step in cancer treatment's novel drug development process. All cancer treatments start in the laboratory, where the treatment's efficacy is initially tested on cancer cells[2-4]. If the relevant efficacy is achieved, then the drug moves on to be tested in animals *(in vivo)* [2-4]. If successful, the drug moves to clinical trials where it is tested in humans and, if found to be safe and effective, eventually approved for commercial use[2-4].

This novel drug development process is a time-consuming and costly process. For example, a new oncology drug may take ten years to be developed and approved, with the entire process amounting to approximately R17 billion [6].

Despite extensive research conducted in the past decade, the success rate for developing a new drug for cancer treatment is still the lowest of all major diseases [7]. The overall probability of success rate is as low as 3.4% [7]. This highlights the susceptibility of preclinical cancer models to poorly predicting outcomes in human clinical trials [8]–[12].

In view of the fact that data generated from these preclinical studies should support the advancement of novel drug development in human clinical trials, preclinical models should be as translatable to human clinical trials as possible.

[2]National Cancer Institute, “Phases of clinical trials,” 2020. [Online]. Available: https://www.cancer.gov/about-cancer/treatment/clinical-trials/what-are-trials/phases. [Accessed: 20-Mar-2020].
[3]U.S. Food & Drug Administration, “The drug development process - Step 3: Clinical Research,” 2018. [Online]. Available: https://www.fda.gov/patients/drug-development-process/step-3-clinical-research. [Accessed: 20-Mar-2020].
[4]U.S. Department of Health & Human Services, “Examination of clinical trial costs and barriers for drug development,” 2014. [Online]. Available: https://aspe.hhs.gov/report/examination-clinical-trial-costs-and-barriers-drug-development. [Accessed: 20-Mar-2020].

Various studies have investigated the translatability of preclinical models to clinical practice and all conclude that preclinical *in vitro* cancer models are not translatable and should be redesigned [12]–[14].

In the previous airfoil example, dynamic similarity was met on certain boundary conditions. In the same way, the metabolic similarity between *in vitro* cancer models and humans can, and should, be met if the metabolic nutrients are modelled within certain validity bounds. Cancer cells' primary metabolites provided in *in vitro* cancer models to sustain cell growth are glucose and glutamine [15] – making these two metabolites the important variables to isolate for similarity between *in vitro* cancer models and human cancer cell conditions.

By applying the principle of similarity, one would expect that the glucose and glutamine concentrations in *in vitro* cancer models would be aligned to typical concentrations seen in humans. More importantly, that these concentrations do not exceed the upper and lower boundary limits, i.e., maximum and minimum concentrations of glucose and glutamine before a severe event would occur (death).

Unfortunately, this is not the case since the initial glucose and glutamine concentrations are much higher (above the upper limit) than typical cancer patients' levels during metabolic treatments [16]–[33]. Likewise, the concentrations also drop to concentrations far below the lower limits [16]–[33]. Furthermore, the treatment exposure time of *in vitro* cancer models does not mimic treatment durations in human clinical trials (hours vs. months) [16]–[33]. These studies are individually analysed in detail in Chapter 2.

What is important to note about these discrepancies is that they are outside the bounds of validity. This concept is illustrated in Figure 1.2, with typical concentrations of glucose (top graphs) and glutamine (bottom graphs) in metabolic treatments investigated in current *in vitro* cancer models (left) and humans (right). The upper and lower bounds of glucose and glutamine concentrations achievable in humans are indicated with dashed red lines.

The values of glucose and glutamine are later discussed in detail in Chapters 2 to 5. What is important to denote from Figure 1.2 is the red shaded boxes highlighting that *in vitro* cancer models are applied outside the validity bounds. Therefore, there is a need to develop new *in vitro* cancer models within these bounds, including similar treatment durations.

These aspects of *in vitro* cancer models have not yet been thoroughly investigated from an engineering point of view. They are fully addressed in **Part A** of this thesis, entitled **Engineering experimental modelling for *in vitro* cancer glucose models.**

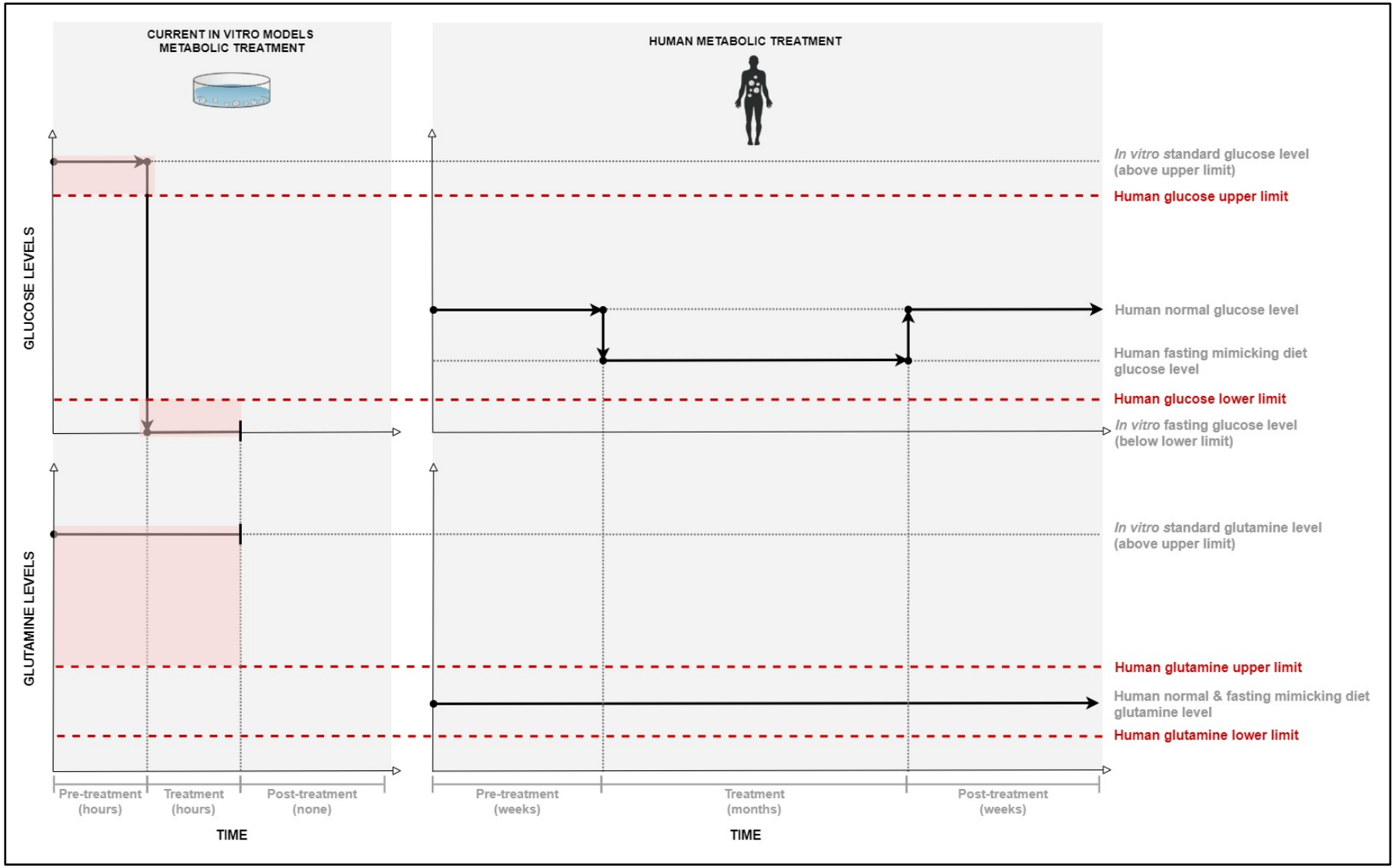

Figure 1.2. Glucose and glutamine levels in cancer models (left) and humans (right).

1.2.2 Engineering systems-integration

Medical research methods primarily follow a reductionistic approach [34], [35]. A reductionistic approach entails breaking down a disease into its smallest biological elements (cellular interactions) and investigating each element in detail [34], [35]. Subsequently, such an approach helps gain a detailed understanding of the mechanisms of interaction of each biological element [35], [36].

Figure 1.3 illustrates this reductionistic approach, where the “Black-Box” represents the disease and the internal connections inside the “Black-Box” represent the biological elements. The inputs and outputs of the “Black-Box” are not important but rather the detailed interactions between each element. Although this is necessary for advanced knowledge of diseases, only the smaller parts of the disease are understood, increasing complexity and delaying the development of treatments.

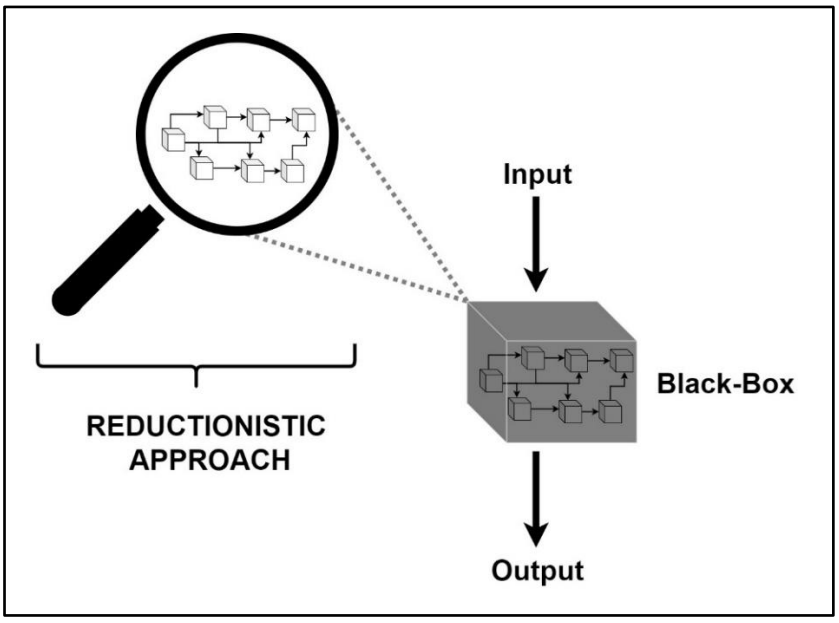

Figure 1.3. Visual representation of the Black-Box method.

In contrast, complex problems in engineering are primarily solved using a different approach, namely a systems approach [37]. Instead of focusing on the detailed interactions between each element, a systems approach rather focuses on the inputs and outputs of each element within the system and their effect on the entire system. Such a systems approach provides a more holistic and integrated understanding of each element's role within the system.

Consider Figure 1.4, which shows the difference between these two approaches. As discussed, the reductionistic approach (left) focuses on the detailed elements inside the

"Black-Boxes". On the other hand, the systems approach (right) focuses on the inputs and outputs of each "Black-Box" and ultimately the resulting input and output of the entire system.

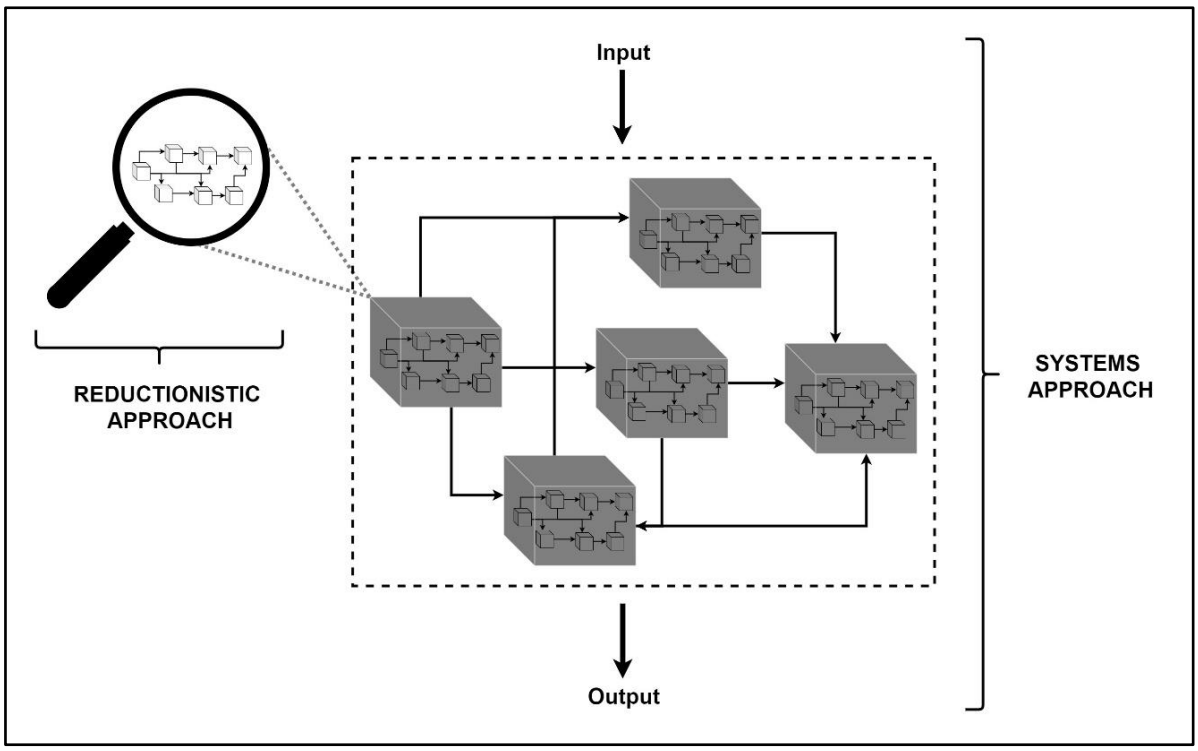

Figure 1.4. Reductionistic vs systems approach.

Since the declaration of COVID-19 as a pandemic in March 2020 [38], a reductionistic approach was followed to help gain a better understanding of the disease [39]. The prevailing viewpoints in literature were that most severe cases of COVID-19 either (i) result in cardiovascular complications [40]–[44] and/or (ii) cardiovascular complications are seen in patients with pre-existing cardiovascular comorbidities [45]–[49].

Although this is valuable insight, these studies followed a reductionistic approach by solely investigating each vascular-related complication at a detailed cellular level. With a holistic systems approach, the focus is instead on how these vascular complications influence each other.

In this thesis, a systems approach was followed to investigate the mechanisms of interaction COVID-19 has on these vascular complications, which are observed in most patients with severe COVID-19 [38]–[42]. The insight gained from this systems approach should assist in a better understanding and explanation of why most deaths occur in these individuals.

The pathogenesis of cardiovascular disease and COVID-19 were integrated to thoroughly investigate these vascular complications. Most of the vascular complications seen in severe

COVID-19 patients have been included in a previous risk-based integrated model of coronary heart disease (CHD) [8], [9]. This CHD model was integrated with severe COVID-19 complications, thereby developing a new *integrated CHD/COVID-19 model*.

The systems approach and model outcomes are detailed in **Part B** of this thesis**,** entitled **A systems engineering approach to explore the mechanisms of interaction between severe COVID-19 and its CHD complications.**

1.3 PROBLEM STATEMENTS, AIMS AND OBJECTIVES

This section provides the main problem statements, overall aims and specific objectives for each of the two approaches presented in Parts A and B of the thesis. These main problems were investigated in several sub-studies, each with its own research objectives detailed in Chapters 2 to 5 (Part A) and Chapter 6 (Part B).

1.3.1 Part A: Engineering experimental modelling for *in vitro* cancer glucose models

Problem statement: Current microenvironments of *in vitro* cancer cells are optimised for cell growth and not to mimic physiological conditions. This results in glucose and glutamine concentrations being much higher than typical cancer patients' concentrations. In addition, *in vitro* glucose concentrations of metabolic treatments are tested at much lower levels than what is achievable in humans. These discrepancies could partly result in untranslatable results and misrepresenting data used to develop *in vivo* metabolic cancer treatments.

Aim: The aim of Part A of this study was to develop new long-term metabolic *in vitro* methods by applying an engineering experimental modelling approach, which addresses the glucose and glutamine discrepancies between *in vitro* cancer models and clinical metabolic cancer treatments.

Research objectives: The research objectives with reference to the respective chapters in which they are addressed are the following:

1. Develop new *in vitro* cancer models that mimic typical cancer patients' glucose and glutamine levels (Chapter 2).
2. Develop long-term glucose deprivation tests that model glucose deprivation concentrations of humans during metabolic treatments for investigating the effect on cancer and non-cancer cell growth (Chapter 2).
3. Investigate the effect of additional very low, yet achievable, short-term glucose only and combined glucose and glutamine deprivation on cancer and non-cancer cell growth combined with long-term glucose deprivation (Chapter 3).
4. Investigate the effect of chemotherapy on cancer and non-cancer cell growth when administered at typical cancer patients' glucose and glutamine concentrations (Chapter 4).

5. Investigate the effect that additional non-metabolic chemotherapy treatment has on cancer and non-cancer cell growth when combined with long term glucose deprivation (Chapter 4).
6. Determine if a lower chemotherapy dosage combined with glucose deprivation will have a similar therapeutic effect compared to a higher chemotherapy dosage administered without glucose deprivation (Chapter 4).
7. Develop a non-toxic glucose deprivation method to investigate the effect of combined short- and long-term metabolic treatments (Chapter 5).

1.3.2 Part B: A systems engineering approach to severe COVID-19 and its vascular complications

Problem statement: Most severe COVID-19 cases either result in cardiovascular complications and/or cardiovascular complications are seen in patients with pre-existing cardiovascular comorbidities. However, the mechanisms of interaction of COVID-19 on the vascular system are not yet fully understood.

Aim: The aim of Part B of this study was to help explain the mechanisms of interaction of severe COVID-19 on the vascular system, by using a systems engineering approach to integrate an existing CHD model with the activated pathogenetic pathways seen in patients with severe COVID-19.

Research objectives: The research objectives, which are all addressed in Chapter 6, are the following:

1. To develop an *integrated CHD/COVID-19 model*, which explains the mechanisms of interaction of severe COVID-19 on the vascular system.
2. To use the *integrated CHD/COVID-19 model* to
   (a) investigate why some patients with severe COVID-19 experience sudden death,
   (b) examine the effect of CHD comorbidities on COVID-19 severity,
   (c) examine how different *health factors* influence COVID-19 severity, and
   (d) explore how various CHD *pharmaceutical interventions* could help reduce an individual's risk of developing severe COVID-19.

1.4 OUTLINE OF THE THESIS

The thesis is presented as seven chapters, each relating to the overall theme of the thesis, namely applying engineering approaches to medical research. An outline of the chapters in this thesis is provided in Table 1.1.

Table 1.1. Chapters of the thesis and respective outline of each chapter.

CHAPTER	CONTENTS OF THE CHAPTER
Chapter 1: Introduction	General background to provide an overview of the two main problems addressed in this thesis. The problem statements, aims and objectives for each part are provided.
PART A: ENGINEERING EXPERIMENTAL MODELLING FOR IN VITRO CANCER MODELS	
Chapter 2: Long-term energy restriction for cancer treatment	A novel method to conduct long-term *in vitro* glucose deprivation tests on cancer cells, referred to as the *Press* treatment, is provided in this chapter.
Chapter 3: Combined long- and short-term energy restriction for cancer treatment	This chapter explores the addition of two different metabolic short-term treatments in combination with the *Press* treatment. These short-term treatments are referred to as *Pulse* treatments. Therefore, this chapter explores a combined metabolic *Press-Pulse* treatment.
Chapter 4: Long-term energy restriction in combination with short-term chemotherapy for cancer treatment	The addition of two different *Pulse* treatments, in combination with the *Press* treatment, are investigated. These *Pulse* treatments are non-metabolic (chemotherapy); hence this chapter explores a combined non-metabolic *Press-Pulse* treatment.
Chapter 5: An energy restriction method for highly-glycolytic cancers	In this chapter, the insights gained from the preceding chapters are used to develop a hypothetical non-toxic *Press-Pulse* therapy. After additional future work and ethical clearance, this therapy may hopefully be implemented in human clinical trials.
PART B: A SYSTEMS ENGINEERING APPROACH TO EXPLORE THE MECHANISMS OF INTERACTION BETWEEN SEVERE COVID-19 AND ITS CHD COMPLICATIONS	
Chapter 6: Integrated CHD/COVID-19 model	This chapter details how a systems approach can explore the mechanisms of cardiovascular complications in COVID-19. For this purpose, a new *integrated CHD/COVID-19 model* was developed by integrating the activated pathogenetic pathways of severe COVID-19 into an existing CHD model.
Chapter 7: Limitations, recommendations and conclusions	The concluding chapter provides the study's limitations, recommendations for future work and overall conclusions for Parts A and B.

Chapter 7 is followed by a **Glossary** of frequently used words and a list of all the **References** used in this thesis. Finally, the **Appendices** are provided in sequential order in which they are referred to in the thesis.

PART A

ENGINEERING EXPERIMENTAL MODELLING FOR *IN VITRO* CANCER MODELS

CHAPTER 2
LONG-TERM ENERGY RESTRICTION FOR CANCER TREATMENT

"Criticism may not be agreeable, but it is necessary. It fulfils the same function as pain in the human body. It calls attention to an unhealthy state of things."

Winston Churchill[5]

[5]AZ Quotes, "Winston Churchill Quotes About Criticism." [Online]. Available: https://www.azquotes.com/author/2886-Winston_Churchill/tag/criticism. [Accessed: 21-Nov-2021].

2.1 PREAMBLE

This chapter presents the main problem with the current *in vitro* cancer glucose models that investigate metabolic cancer treatment, i.e., glucose deprivation (GD). The chapter starts with a literature review, introducing the problems with current GD *in vitro* cancer methods and explains how this may have major effects on validity, reproducibility and physiological relevance. The objectives addressed in this chapter are provided.

Then follows the methods and materials used to develop these new long-term GD *in vitro* cancer models. The results are presented, and the significance to literature is discussed. The chapter concludes with the main findings and additions to these new methods, addressed in the next chapter (Chapter 3).

2.2 LITERATURE REVIEW

There has been an increase in the understanding of the benefits of strict glucose control during the treatment of highly-glycolytic cancers [15], [50].

Various nutritional strategies are used to decrease circulating blood glucose (BG) levels and elevate ketone bodies for therapeutic purposes [51]. These nutritional strategies include various fasting regimes [52], [53], restricted ketogenic diet (KD-R) [54], calorie restriction [54] and ketone supplementation [55] in combination with the use of diabetic medication (e.g. metformin). The most established of these nutritional strategies, the KD-R, has shown therapeutic effects on various types of cancer when used in combination with adjuvant therapies [51], [56]–[61].

These studies point to a therapeutic window created by the high glucose uptake of certain cancer cell types (highly-glycolytic cancers) compared to that of non-cancer cells. Despite the large therapeutic evidence of the benefits of nutritional strategies, the trials up to now show inconsistent variability in therapeutic responses [51], [62]. Furthermore, a review by Winter *et al.* stated that: *"…nutritional strategies targeting glycaemic modulation to exploit the observed tumour glucose-dependency have not yet been thoroughly investigated in clinical trials and existing clinical data is limited."* [51] Similarly, a more recent review on the subject emphasised the need for further investigation of glucose-lowering nutritional strategies on different cancer cells, both in molecular studies and clinical practice [62].

By applying the engineering experimental modelling approach, as discussed in Chapter 1, Section 1.2.1, several problems with the current *in vitro* cancer models were found. These problems are summarised in Table 2.1 in the following three categories:

(i) The initial glucose concentration of the growth medium does not mimic concentrations in cancer patients.

(ii) The glucose concentration used for metabolic treatments are is not achievable in humans.

(iii) The time periods that the cells are exposed to the experimental conditions do not simulate the time frames of real-world metabolic therapies [63].

Problem number (i) originates from the fact that the average human physiological BG concentration is approximately 6 mmol/L [64] and that of cancer patients approximately 6.5 mmol/L [64], [65]. However, most glucose concentrations of *in vitro* cell cultures microenvironments are either 11.1 or 25.52 mmol/L [66]. The cell lines must therefore be stabilised at 6.5 mmol/L before the different treatments can be investigated in order to correctly simulate cancer patients' glucose conditions [63].

Most experiments/treatments are conducted at glucose concentrations close to 0 mmol/L [17]–[19], [26]–[33], [67]. Achieving a 0 mmol/L glucose level is not possible in patients and leads to problem number (ii).

Lastly, the cancer cells are often not exposed to experimental conditions over a long enough period to simulate real-world metabolic therapies. As the effect of a KD-R is over months [56], [61], [68], data for at least 90 days is needed to see initial and longer-term effects. This is contrary to most *in vitro* tests, which are conducted over periods measured in days or even hours, leading to problem number (iii). It is clear that not one experiment correctly addressed all three problems.

Table 2.1. Comparison of in vitro testing methods and resulting metabolic problems

Problem (i): Initial conditions	**Problem (ii): Treatment conditions**	**Problem (iii): Treatment period**	**Ref**
Initial glucose concentrations do not represent cancer patients' concentrations of 6.5 (mmol/L)	Treatment glucose concentration (mmol/L)	Duration of treatment	
11.1	0 – 2.78	2 days	[20]
25.52	0 – 2.5	2 days	[21]
25.52	0	6 hours	[22]
25.52	0 – 5	1 day	[16]
25.52	0 - 5.6	5 days	[23]
11.1	0	18 hours	[17]
25.52	0.5	5 days	[26]
25.52	5.5	2 days	[24]
11.1	0	14 days	[27]
25.52 & 11.1	4.17	1 day	[25]
25.52	0	1 day	[28]
25.52	0	1 day	[29]
25.52	0	2 days	[30]
25.52	0	4 days	[31]
15	0	2 days	[32]
25.52	0	3 days	[33]
11.1	0	3 days	[18]
25.52	0	3 days	[19]

This chapter will endeavour to add to the existing pool of knowledge in preclinical data for long-term GD strategies. Some of the research questions that will be investigated are the following:

1. Can *in vitro* tests be conducted on cancer cells at typical *in vivo* physiological BG concentrations of typical cancer patients (6.5 mmol/L)? *In vitro* tests are usually done at four times higher BG levels [69]. As the aim of the investigation is BG control, the BG baseline should be correct to have confidence in the results.
2. The ketogenic diet does not work for all cancer patients [58]. Therefore, what is the effect of long-term GD on different cancer cell lines?
3. At what cell growth rate (for metabolic treatments) will cancer cell lines recover and after what treatment period?
4. When will the *in vitro* cancer line be at its most vulnerable, assuming that they recover? Therefore, when does a potential therapeutic window for short-term adjuvant therapies open? This *in vitro* data could direct future human *in vivo* tests as to when cancer growths are at their most vulnerable.

The question may be asked why mouse models are not used for the present glycolytic study [70]. One important reason is the difference between the BG microenvironments between mice and humans [69]–[71].

Studies with cancer-bearing mice and humans show that in humans, the BG environment increases by 1.15-fold [65], while in mice, it decreases by 2.1-fold very shortly after invasion by highly-glycolytic cancers [72]. This can *inter alia* be attributed to the large difference in metabolic parameters between humans and mice [71].

For instance, mice have a 7.5-fold greater basal metabolic rate than humans [71], with a 10-15 fold higher relative basal glucose turnover rate [71]. This means that rodents are under much greater metabolic constraints than humans.

With such a high basal glucose demand in mice, together with the added high glucose demand of highly-gycolytic cancers, it is important to either sustain adequate glycogen storages or to use very high levels of energy-expensive gluconeogenesis in order to provide for the upregulated glucose demand.

However, mice have two-fold less liver and 4.5-fold fewer muscle glycogen stores than humans [71]. Furthermore, the mouse will have to overeat in order to supply the added BG demand of highly glycolytic cancers *via* gluconeogenesis [71].

Glucose availability to cancer cells (which is the effect to study) is thus much lower in mice compared to humans. Metabolic (glycolytic) effects on highly glycolytic cancers can therefore not always be accurately extrapolated to human responses from mice studies.

Furthermore, one would not have full control over BG levels in mice. On the other hand, one will have full control over the *in vitro* microenvironment. BG control in a cancer model is important as human BG control is much tighter than that of mice [69], [70]. Therefore, in this study, it is proposed that properly developed *in vitro* cancer models could potentially be more relevant for obtaining long-term metabolic data for humans than using *in vivo* mice models.

2.3 OBJECTIVES

Research objectives for this chapter:

1. Develop new *in vitro* cancer models that mimic typical cancer patients' glucose and glutamine levels.
2. Develop long-term glucose deprivation tests that model glucose deprivation concentrations of humans during metabolic treatments for investigating the effect on cancer and non-cancer cell growth.

2.4 METHODS AND MATERIALS

2.4.1 Cell lines

Since this study focuses on GD and all cells use glucose for cell growth [15], the type of cell line was not important. It was only necessary to conduct these tests on more than one cancer cell line and at least one non-cancer cell line. This should help one gain insight into the effect of long-term GD on the different cell lines.

Therefore, tests were conducted on four cell lines i.e. three cancer and one non-cancer cell line. Of the cancer cell lines, two were metastatic breast cancer cell lines, namely the highly glycolytic M.D. Anderson metastasis breast cancer (MDA-MB)-231 and the less glycolytic Michigan Cancer Foundation (MCF-7) cells. The third cancer cell line was the Henrietta Lacks (HeLa) cervical cancer cell line. The non-cancer cell line used was a spontaneously immortalised non-cancer breast cell line (MCF-10A).

These cell lines are commercially available from the American Tissue Culture Collection (ATCC), Maryland, United States of America. All reagents were obtained from (Sigma Chemical Co) (St. Louis, Missouri, United States of America).

2.4.2 Concentration levels of glucose and glutamine

Glucose

In order to stay within the bounds of validity for glucose concentrations, a value of 6.5 mmol/L was used as the initial condition to mimic glucose levels of typical cancer patients [65].

An average BG level as low as 1 mmol/L has been reported during fasting [73]. BG levels as low as 4 mmol/L were reported for cancer patients on a ketogenic diet [51]. Values for a combination of fasting, KD-R and metformin use could not be found. It is assumed that 3.5 mmol/L could be achieved in patients during a KD-R with the addition of fasting and metformin.

A value of 3.5 mmol/L was chosen as the glucose concentration during long-term GD, which replicates glucose-lowering nutritional strategies in combination with pharmaceutical agents such as metformin.

Glutamine

Glutamine levels in standard cultivation of cancer cells is 4 mmol/L and 2 mmol/L for non-cancer cells, which are also more than four times higher than human physiological plasma

glutamine levels of 0.6-0.9 mmol/L [74]–[76]. A constant physiological glutamine concentration of 0.6 mmol/L was chosen during the long-term GD, i.e., cells were not exposed to glutamine deprivation.

2.4.3 Initial cell growth conditions of negative controls

Cells were initially grown and maintained in 25 cm^2 tissue culture flasks in a humidified atmosphere at 37 °C, 5% CO_2 in a Forma Scientific water-jacketed incubator (Ohio, United States of America). All reagents were obtained from (Sigma Chemical Co) (St. Louis, Missouri, United States of America) unless specified otherwise.

Negative control for cancer cell lines

Experimental Condition 0 for the negative control cancer cell lines was cultured in DMEM with 25.52 mmol/L glucose and 4 mmol/L L-glutamine supplemented with 10% dialysed heat-inactivated FCS (56 °C, 30 min), 100 units/mL penicillin G, 100 µg/mL streptomycin and amphotericin B (0.25 µg/L).

Negative control for non-cancer cell line

Experimental Condition 0 for the non-cancer breast cancer cell line was cultured in a ratio of 50% DMEM to 50% Ham's F-12 medium (HF12M) containing 17.56 mmol/L glucose and 2 mmol/L L-glutamine, with the addition of 10% dialysed FCS (56 °C, 30 min), 500 ng/mL hydrocortisone, 20 ng/mL epidermal growth factor (EGF), 100 ng/ml cholera toxin, 10 µg/mL insulin, 100 units/mL penicillin G, 100 µg/mL streptomycin and 0.25 µg/L amphotericin B.

Cell lines exposed to treatment

All of the treated cancer and non-cancer cell lines were cultured using the same conditions as described for the negative controls. The only difference between the treated cell lines and negative controls was the concentrations of glucose and glutamine. The respective changes in concentrations of glucose and glutamine for the treated cell lines will now be discussed.

2.4.4 Experimental procedure conditions

The different conditions of glucose and glutamine, as well as the exposure durations, are summarised in Table 2.2. Cancer and non-cancer cell lines were initially grown in their standard cell culture conditions, namely DMEM (Condition 0).

After enough cells were cultivated, all cell lines were exposed to typical physiological glucose (6.5 mmol/L) and glutamine (0.6 mmol/L) levels of cancer patients, namely condition 1. Cells

were exposed to this condition on day 0 until cell growth stability was reached on day 30. Growth stability was regarded as a period of very little variation in cell growth.

Thereafter, cells were exposed to long-term GD (Condition 2) to 3.5 mmol/L glucose. Cells were maintained at this condition from day 0 (Day 30 after Condition 1) until day 82. This condition replicated long-term glucose-lowering nutritional strategies in combination with pharmaceutical agents such as metformin.

Table 2.2. Cell culture glucose and glutamine conditions as well as exposure days.

Metabolic condition number	Glucose (mmol/L)	Glutamine (mmol/L)	Days
Initial cell culture growth			
0	25.52 (cancer cells) & 17.56 (non-cancer cells)	4 (cancer cells) & 2 (non-cancer cells)	0
Stabilisation in physiological conditions			
1	6.5 (all cells)	0.6 (all cells)	0-30
Long-term glucose deprivation			
2	3.5 (all cells)	0.6 (all cells)	0*-82

Note: *Day 0 in Condition 2 is actually day 31, the day after cells stabilised in physiological conditions.

2.4.5 Measuring relative cell growth

Crystal violet staining and spectrophotometry [77], [78] were used here to interpret cell density, proliferation and cell viability.

Upon termination of the experiment, cells were fixed with 1% gluteraldehyde (100 µL) at room temperature for 45 min. Gluteraldehyde was replaced with 0.1% crystal violet (100 µL) at room temperature for 90 min. Plates were thereafter left to dry, 0.2% triton X-100 (200 µL) was added to the flasks and incubated overnight to solubilise the crystal violet.

The solubilised dye was transferred to a new 96-well plate where the absorbance was determined using an EPOCH Microplate Reader (Biotek Instruments, Inc. (Winooski, Vermont, United States of America)) at a wavelength of 570 nm.

Quantitative data were collected via spectrophotometry from three independent repeats for all experiments in the long-term GD study. Each data set in Figure 2.1 and Figure 2.2 represents the average Relative Cell Growth (RCG).

This RCG was calculated as a change in percentage of cell growth between the treated cells and their respective negative controls, denoted by Equation 2.1:

$$Relative\ Cell\ Growth = \frac{Instantaneous\ cell\ growth\ of\ treated\ cells}{Instantaneous\ cell\ growth\ of\ respective\ negative\ controls} \times 100 \qquad (2.1)$$

Three independent repeats were produced for each data set. The error bars illustrated on each data point in Figure 2.1 and Figure 2.2 represent the standard deviations of three independent tests.

2.5 RESULTS AND DISCUSSION

Figure 2.1 presents the results of cells exposed to typical human glucose and glutamine concentrations of 6.5 mmol/L and 0.6 mmol/L, respectively (Condition 1). The non-cancer cell line (MCF-10A) showed little change in RCG, remaining at approximately 100% during the entire exposure time.

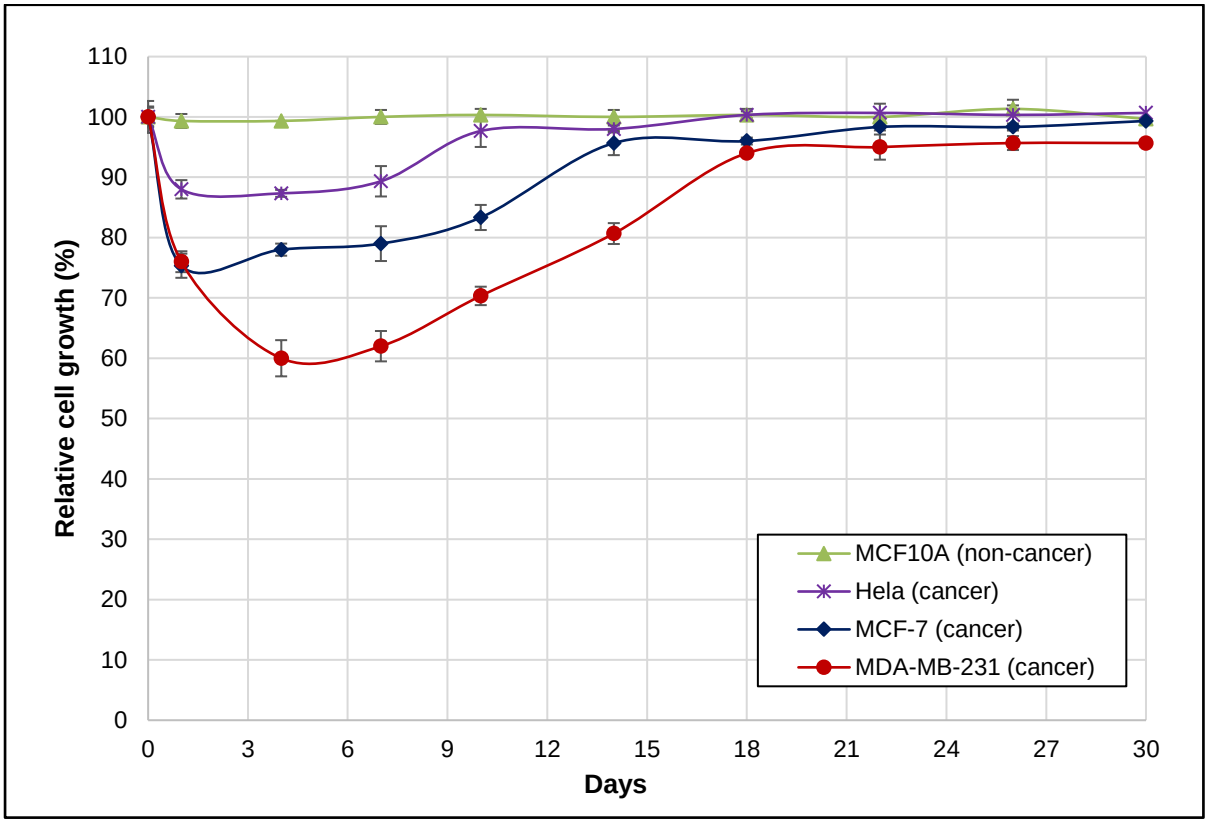

Note: After stabilisation was reached on day 30 the cells were cultivated in long-term GD concentrations (Condition 2). The glucose and glutamine concentrations were 3.5 mmol/L and 0.6 mmol/L, respectively. The glucose concentration was chosen to mimic a combination of KD-R and glucose-lowering medication such as metformin. Glucose concentration was 25.52 mmol/L and glutamine 4 mmol/L before time zero. From day zero, glucose and glutamine concentrations were 6.5 mmol/L and 0.6 mmol/L, respectively.

Figure 2.1. RCG of cells exposed to typical human glucose concentrations.

On the other hand, the three cancer cell lines present, at first, a decrease in RCG but later recover and stabilise within 30 days. The cancer cell lines all recover at different rates, which could be due to differences in metabolic dependence. Since the cancer cell line that took the longest to recover and achieved the lowest RCG, is more glucose avid than the other cancer cell lines [79], [80].

An important observation this data provides is that the cell lines are able to proliferate in such 'low' glucose cell culture media without adverse effects on cell viability. This human glucose and glutamine concentration *in vitro* media condition offers a more appropriate model for human *in vivo* conditions. Tests conducted in these new conditions should yield a more realistic baseline for further GD studies.

The cell lines' responses to this long-term GD, Condition 2, is shown in Figure 2.2. All cell lines present a decrease in RCG from day zero until day 30. Thereafter the cells recovered, yet not fully, and stabilised after approximately 65 days of exposure.

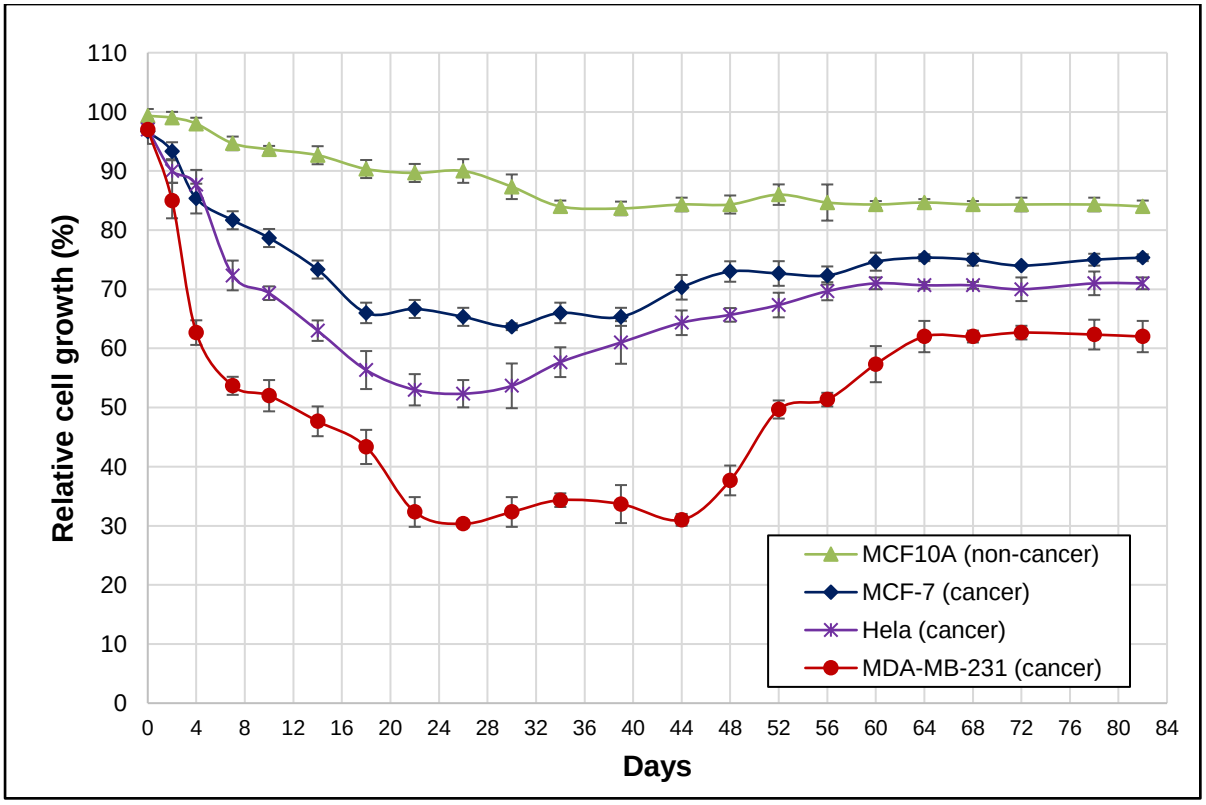

Note: Day zero is after initial exposure to medium containing 6.5 mmol/L glucose, glucose and glutamine concentrations from day zero were 3.5 mmol/l and 0.6 mmol/L respectively.

Figure 2.2. RCG of cell lines during long-term glucose deprivation conditions.

From the results illustrated in Figure 2.2, the following four important observations are made:

1. The cell lines reacted differently to long-term glucose deprivation.
2. All cancer cell lines were affected more severely than the non-cancer cell line.
3. Long-term GD did not reduce RCG enough to achieve full remission. Additional therapies are needed to achieve full remission.
4. Minimum RCG for all cell lines was achieved at approximately 26 days after GD was started.

Further insights were gained by evaluating the data of each cell line in more detail. Table 2.3 gives a summary of the RCG recovery point, days until RCG recovery point, minimum RCG and days until the minimum RCG rate was achieved. As expected, the cancer cell line that was affected the most was the highly glycolytic metastatic breast cancer cell line (MDA-MB-231). This cell line's minimum RCG decreased to 30% (±0.58%) on day 26 and stabilised at 62% (±2.65%).

Table 2.3. Comparison of RCG after cells were exposed to long-term GD.

Cell lines	RCG recovery point (mean ± SD)	Days until RCG recovery point	Minimum RCG (mean ± SD)	Days until minimum RCG
MCF-10A (non-cancer)	84 ± 1.00%	34	84 ± 1.00%	34
MCF-7 (breast cancer)	75 ± 2.00%	60	65 ± 2.00%	26
HeLa (cervical cancer)	71 ± 1.00%	60	52.33 ± 2.31%	26
MDA-MB-231 (breast cancer)	62 ± 2.65%	64	30 ± 0.58%	26
Average days until minimum cell growth (excluding non-cancer cell line)				26

Note: RCG, relative cell growth, GD, glucose deprivation, SD, standard deviation, MCF-10A, non-cancer, breast cell line, MCF-7, metastatic luminal breast cell line, HeLa, glycolytic cervical cancer cell line, MDA-MB-231, highly glycolytic metastatic breast cell line.

Furthermore, the least affected cell line was the non-cancer MCF-10A cell line, with its RCG decreasing only to 84% (±1.00%) after 34 days and stabilising at this level for the duration of the experiment. This reduction in RCG rate could be assumed to be similar to the regular "weight loss" experienced during strict dietary restriction.

Figure 2.2 and Table 2.3 both show that the cancer cell lines' RCG rate increases again after the minimum levels were reached. This emphasises the need for adjuvant therapies to be implemented in combination with long-term glucose deprivation. Examples of extra therapies are chemotherapy, radiation, hyperbaric or other extra metabolic treatments [81].

These extra therapies should be implemented at the most vulnerable point (minimum RCG), thus achieving the maximum effect. The most therapeutic time would be the point where the least cancer cells survive. From the data provided in Figure 2.2 and Table 2.3**,** this most therapeutic point would be on the day the minimum RCG rate was reached. All three cancer cell lines reached this point on day 26.

The MDA-MB-231 cancer cell line remained at this vulnerable point for 22 days (day 22-44), which provides a wide therapeutic window to implement adjuvant therapies. Although this insight adds value to such therapies, future human clinical trials would need to be done to validate this therapeutic window.

Another valuable insight is shown in Figure 2.2, which may prove valuable for personalised treatment regimens, is that the therapeutic effect is higher in the highly glycolytic cell line than for the less glycolytic ones.

Future decisions on metabolic treatment should thus be made based on the metabolic activity of cancer (Standard Uptake Value (SUV)) rather than on the type of cancer. Glucose metabolic activity can be measured by [18F]-fluorodeoxyglucose based Positron Emission Tomography (PET) scans and the cancer cells' respective SUVs [82]–[85].

2.6 CONCLUSIONS

The need for more clinical data on long-term GD treatments for cancers (e.g. fasting, KD-R etc.) is well described in literature. The results of this study contributed to the available pool of knowledge in a number of ways.

Firstly, it illustrated that *in vitro* cancer tests can successfully be done at a human *in vivo* BG microenvironment of 6.5 mmol/L. This provides more confidence in results than the typically used *in vitro* BG microenvironment of 25.5 mmol/L. This method is repeatable, and future long-term GD tests should be stabilised in human glucose conditions before GD starts. Therefore, the first objective detailed in Section 2.3 was achieved.

Secondly, the next objective (detailed in Section 2.3) was also achieved by developing successful repeatable long-term metabolic *in vitro* cancer tests, which mimic human GD concentrations. The results showed that long-term GD affects different cancer cell lines differently. It is suspected that the SUVs of cancers will be used in the future as standard practice to establish the usefulness of GD treatment (e.g. nutritional etc.). Future research should establish these SUVs.

Thirdly, as full cancer extinction is not possible with long-term GD deprivation alone, adjuvant therapies are needed. This was a first *in vitro* attempt to establish the potentially best therapeutic time for adjuvant therapy implementation. For the cancer cell lines investigated, the 26 day period after a BG level of 3.5 mmol/L is reached seems to be a sensible adjuvant time target. Future tests should explore the effect of adding metabolic and non-metabolic short-term adjuvant therapies at these instances.

2.7 NOVEL CONTRIBUTIONS

2.7.1 Novel contributions from new repeatable methods

Standard cancer cell cultivation is done in high glucose Dulbecco's Modified Eagle's Medium (DMEM) at a glucose level of 25.52 mmol/L. This represents a four-fold higher concentration above physiological conditions of 6.5 mmol/L, which could cast doubt over the validity of GD treatments. Subsequently, glutamine levels in standard cultivation of cancer cells are 4 mmol/L, 4-8 times higher than human physiological plasma glutamine levels of 0.5-0.9 mmol/L.

This chapter presents a novel, repeatable method for long-term tests on cells cultivated in typical human physiological glucose (6.5 mmol/L) and glutamine (0.6 mmol/L) concentrations. This allows cells to stabilise in human physiological glucose and glutamine concentrations before long-term GD tests are conducted.

Moreover, GD tests are typically conducted at very low glucose concentrations which are unachievable in humans. Therefore, this new method provides long-term GD tests conducted at achievable low glucose concentrations of 3 mmol/L.

In addition to achievable glucose concentrations, current preclinical *in vitro* GD tests are short-term based (24 hours to 7 days), whereas glucose-lowering diets are implemented over months in practice. Therefore, this chapter also presented a repeatable long-term (90 days) *in vitro* GD method that mimics practical glucose-lowering diet durations.

2.7.2 Novel contributions from results

These new results provide the following holistic insights into future GD's long-term *in vitro* tests:

- All of the cancer cells presented a lower RCG rate than the non-cancer cell line after long-term GD treatment.
- Long-term GD is cell line dependent, i.e. it had a different effect on all cancer cell lines.

- All of the cancer cell lines' RCG started to increase after approximately 26 days. Therefore, future tests should combine adjuvant therapies with long-term GD treatment.
- The investigated cancer cells are most vulnerable (lowest RCG) after being exposed to GD for 26 days. Future tests could implement adjuvant therapies at approximately 26 day intervals during long-term GD.

2.8 DISSEMINATION OF RESULTS

This chapter has already been successfully published in the medical scientific journal, *Nutrition* with the following title: *In vitro quantification: long-term effect of glucose deprivation on various cancer cell lines.* DOI number: 10.1016/j.nut.2020.110748 (see Appendix B for the published manuscript).

The results were also presented as an oral presentation at the 3rd World Congress on Cancer: New strategies to prevent, diagnose and treat Cancer based on Precision Medicine, Top Hotel Praha & Congress Centre, Prague, Czech Republic from 23-25 September 2019. Title of the conference proceeding: *"Ketogenic diet as a cancer treatment: In vitro quantification."*

Furthermore, the published manuscript developed from this chapter has already been recognised within the cancer research scientific community, evident from the following citations:

1. R. J. Klement, C. E. Champ, U. Kämmerer, P.S. Koebrunner, K. Krage, G. Schäfer, et al. "Impact of a ketogenic diet intervention during radiotherapy on body composition: III-final results of the KETOCOMP study for breast cancer patients," Breast Cancer Res., vol. 22, no. 94, pp. 1–14, 2020. doi:10.1186/s13058-020-01331-5.
2. I. Kareva and J. S. Brown, "Estrogen as an Essential Resource and the Coexistence of ER+ and ER– Cancer Cells," Front. Ecol. Evol., vol. 9, no. August, pp. 1–15, 2021. doi:10.3389/fevo.2021.673082.
3. R. Maldonado, C. A. Talana, C. Song, A. Dixon, K. Uehara, and M. Weichhaus, "β-hydroxybutyrate does not alter the effects of glucose deprivation on breast cancer cells," Oncol. Lett., vol. 65, no. 21, pp. 1–13, 2020. doi:10.3892/ol.2020.12326.

CHAPTER 3
COMBINED LONG-AND SHORT-TERM ENERGY RESTRICTION FOR CANCER TREATMENT

"Everything is energy and that's all there is to it."

Albert Einstein[6]

[6]AZ Quotes, "Albert Einstein Quotes About Energy." [Online]. Available: https://www.azquotes.com/author/4399-Albert_Einstein/tag/energy. [Accessed: 21-Nov-2021].

3.1 PREAMBLE

This chapter explores the addition of two different metabolic short-term treatments (referred to as *Pulse* treatments) to the long-term GD treatment (referred to as *Press* treatment). The two *Pulse* treatments are (i) short-term very low glucose-only deprivation and (ii) combined short-term very low glucose and glutamine deprivation. This combined method is referred to as the *Press-Pulse* treatment.

The chapter starts with a detailed literature review, which provides insight into the need to investigate these treatments. This leads to this chapter's objective, which is followed by the methods and subsequent results. A summary of the main findings follows.

Thereafter, the outcomes of the two different *Press-Pulse* treatments are discussed. Furthermore, a comparison between *Press* only and metabolic *Press-Pulse* treatments is also drawn. A proposal is given that combines non-metabolic short-term *Pulse* therapies, namely chemotherapy. The chapter concludes with the main differences of each treatment and novel contributions.

3.2 LITERATURE REVIEW

More than 40% of cancers metastasise to the brain [69], [86]–[89]. The brain is protected by the blood-brain barrier, which restricts most substances [90]. This, in return, complicates most chemotherapy regimens. Metabolic treatments do not experience similar severe barriers.

The benefits of metabolic control in the treatment of highly-glycolytic cancers have therefore received more interest lately [15], [50], [91], [92]. Glucose and glutamine are, amongst others, vital metabolites for both healthy and cancer cells [76], [78], [93]–[96]. These metabolites are a common topic in current cancer metabolism research [15], [94], [97]. Their uptake is upregulated in most solid cancers in relation to healthy cells. A therapeutic window may be created when certain cancer cells are deprived of these metabolites [76], [78], [93]–[96].

The therapeutic window of depriving cancer cells of glucose is currently exploited in ongoing clinical trials *via* glucose-lowering nutritional strategies and/or glutamine inhibitors [51], [62], [95]. However, as discussed in Chapter 2, Section 2.2, the trials show inconsistent variability in therapeutic responses [51], [62].

As investigated in Chapter 2, long-term GD was undertaken in an attempt to simulate how a long-term glucose reduction (BG: 3.5 mmol/L for 90 days) would affect different cancer cell lines. The results showed the following [63]:

- The cell lines reacted differently to long-term glucose deprivation.
- All cancer cell lines were affected more severely than the non-cancer cell line.
- Long-term GD did not reduce RCG enough to achieve full remission.

The question may be asked whether full remission could be achieved if both short-and long-term GD are implemented simultaneously. This idea of combining both short- and long-term therapies is based on an evolutionary concept of mass extinction known as the *Press-Pulse* theory [98], [99]. The theory is that mass extinction only occurs when both gradual environmental changes (referred to as *Press*) and acute disruptive events (referred to as *Pulses*) happen simultaneously [98], [99].

Although the theory originated from ecology [98], [100] and paleobiology [101], the *Press-Pulse* concept has been applied to other fields successfully [102]. Therefore, the effect of *Press* and *Pulse* changes are not restricted to a specific element in nature.

This concept of *Press-Pulse* is illustrated in Figure 3.1, where the change of a given variable of interest is seen over time. Firstly, the *Press* remedy decreases the variable to a new equilibrium (no mass extinction). Thereafter, the *Pulse* remedy further decreases the variable to a new equilibrium (still no mass extinction). Finally, the combination of *Press-Pulse* remedies decreases the variable of interest to mass extinction.

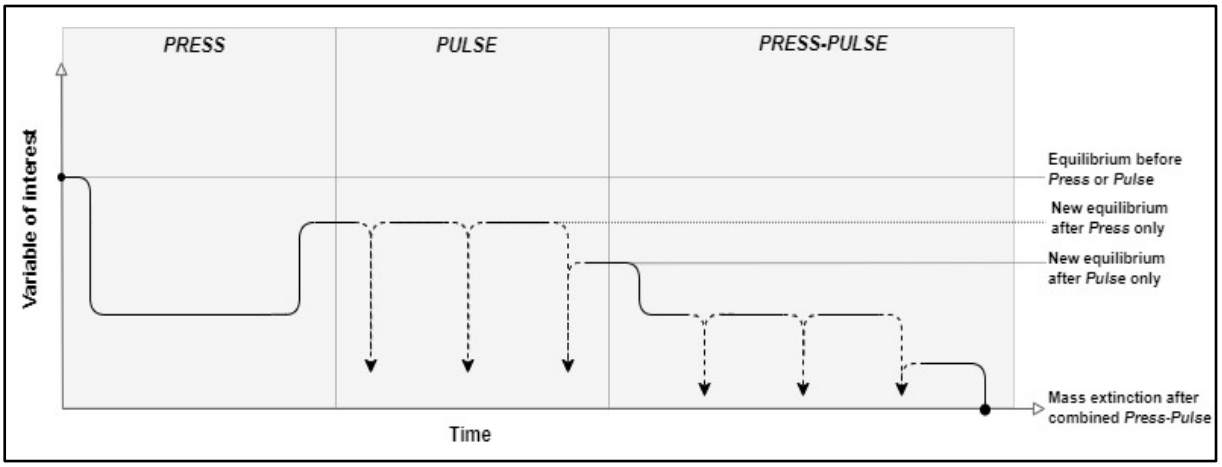

Figure 3.1. *Press-Pulse* theory of mass extinction.

Both short *(Pulse)* and long-term *(Press)* metabolic treatments have been implemented separately [63], [77], [78]. However, full remission of cancer cells was not achieved. Therefore, the combination of *Press-Pulse* should be investigated. The combination of *Press-Pulse* for cancer treatment has recently been proposed by Seyfried *et al.* [103]. However, such a treatment has not yet been investigated in *in vitro* cancer models. Therefore, the tests

conducted in this chapter are the first attempt at conducting metabolic *Press-Pulse* treatments on cancer cells.

Since glucose is usually the main fuel for most highly-glycolytic cancers [15], [50], [93], [94], [104], [105], this study investigates the combined effect of both short-term *(Pulse)* and long-term *(Press)* glucose deprivation.

Glutamine, the most abundant amino acid, is also an important energy source for some cancers [106]–[108]. As discussed in Chapter 2, Section 2.4.2, glutamine levels in standard cell culture are usually 4 mmol/L [16], [21]–[23]. This is much higher than a normal healthy human's plasma glutamine levels of 0.6-0.9 mmol/L [74]–[76]. For a further accurate representation of the microenvironment, a concentration of 0.6 mmol/L glutamine was used in this study.

At present, it is difficult to achieve long-term *(Press)* glutamine deprivation in humans. However, short term *(Pulse)* treatment is possible and could be beneficial [109]. Therefore, in addition to short-term glucose deprivation, glutamine was also implemented as a short-term *(Pulse)* deprivation treatment, together with a glucose *Pulse*.

The *(Pulse)* metabolic treatments will therefore serve as adjuvant therapies during the long-term *(Press)* glucose deprivation. Since engineering experimental modelling principles are applied in this study, both the *Press* and *Pulse* treatment concentrations for glucose and glutamine should stay within the bounds of validity.

Fortunately, the long-term GD *(Press)* concentration for glucose has already been defined within the bounds of validity in Chapter 2, Section 2.4.2. These same long-term GD concentrations of 3.5 mmol/L will thus be used as the glucose *Press* condition for the tests conducted in this chapter. The appropriate glucose and glutamine concentrations for the *Pulse* conditions are discussed in the sections that follow.

3.2.1 Minimum safe human levels of blood glucose and glutamine *Pulse* conditions

Since the very low short-term GD of 1 mmol/L is very low, the question may be asked whether this could be safely achieved in humans for short periods. Scientific evidence on the safety of very low BG levels is limited [110]. Nevertheless, data from some clinical studies and case reports of 117 individuals were found. These studies provide the mean and minimum BG levels of patients and are provided in Table 3.1 [73], [111]–[116]. The average of these values was 2.7 mmol/L for the mean BG values and 1.6 mmol/L for the minimum BG values. The lowest BG level was 0.5 mmol/L.

Clinical practice has strict criteria that act as a limitation to studies on real-life hypoglycaemic events e.g., individuals with Type 1 diabetes. With lack of scientific data, it might be beneficial to also investigate other sources for data on severe hypoglycaemia.

Asymptomatic hypoglycaemia is one of the most common symptoms of diabetes, especially for Type 1 insulin-dependent diabetics (T1D) [117]. A possible source of large-scale data of T1D patient's BG levels is online diabetes forums and vlogs.

Table 3.1. Scientific evidence of low BG levels in humans [73], [111]–[116]**.**

Clinical studies	Number of patients	Mean BG (mmol/L)	Minimum BG (mmol/L)	Ref
Non-diabetic patients with chronic renal failure on maintenance haemodialysis.	21	-	2.1	[111]
Diabetic patients on maintenance haemodialysis.	21	2.7	1.2	[112]
Leucine-induced hypoglycaemia in healthy during administration of chlorpropamide.	25	2.4	1.3	[113]
Leucine-induced hypoglycaemia in healthy during administration of ultralente insulin.	22	3.5	1.8	[113]
Role of Glucagon, Catecholamines, and Growth Hormone in Human Glucose Counter regulation.	13	2.9	2.0	[114]
Resistance to Symptomatic Insulin Reactions after Fasting.	9	2.1	0.5	[115]
Effect of acute hypoglycaemia on brain function and activation.	6	2.5	2.4	[116]
Averages	-	**2.7**	**1.6**	-

Diabetes Daily forums and *YouTube* video logs (vlogs) were used to gather relevant information. *"Diabetes Daily*[7]*"* was created in 2005 as an online platform to support diabetes forums, newsletters and blogs, which help people gain the support and inspiration needed for a diabetic lifestyle with over 10 million yearly site visits[7].

In total, 1 040 diabetics' lowest recorded BG levels were recorded from online forums on *Diabetics Daily*[7-11] and from the comments of four different vlogs on *YouTube*[12-15]. All participants used personal glucose monitors to measure their BG levels. These lowest recorded BG levels are illustrated in Figure 3.2.

[7]Diabetes Daily, "Diabetes Daily forum 1," 2005. [Online]. Available: https://www.diabetesdaily.com/forum/testing-blood-sugar/16155-whats-lowest-blood-sugar-level-youve-had-10. [Accessed: 19-Feb-2018].
[8]Diabetes Daily, "Diabetes Daily forum 2," 2005. [Online]. Available: https://www.diabetesdaily.com/forum/testing-blood-sugar/16155-whats-lowest-blood-sugar-level-youve-had/. [Accessed: 12-Apr-2018].
[9]Diabetes Daily, "Diabetes Daily forum 3," 2005. [Online]. Available: https://www.diabetesdaily.com/forum/type-1-diabetes/8597-lowest-you-ever-came/. [Accessed: 12-Apr-2018].
[10]Diabetes Daily, "Diabetes Daily forum 4," 2005. [Online]. Available: https://www.diabetesdaily.com/forum/type-1-diabetes/2635-whats-lowest-what-reaction/. [Accessed: 12-Apr-2018].
[11]Diabetes Daily, "Diabetes Daily forum 5," 2005. [Online]. Available: https://www.diabetesdaily.com/forum/promotions-surveys-and-trial-recruitment/114563-how-low-bg-have-you-measured/. [Accessed: 28-Mar-2018].
[12]YouTube, "YouTube vlog 1," 2005. [Online]. Available: https://www.youtube.com/watch?v=h3M1rWWk9IQ. [Accessed: 10-Apr-2018].
[13]YouTube, "YouTube vlog 2," 2005. [Online]. Available: https://www.youtube.com/watch?v=CuYdDpB1tDI. [Accessed: 28-Mar-2018].
[14]YouTube, "YouTube vlog 3," 2005. [Online]. Available: https://www.youtube.com/watch?v=UpSc1WS7dPA. [Accessed: 03-Apr-2018].
[15]YouTube, "YouTube vlog 4," 2005. [Online]. Available: https://www.youtube.com/watch?v=aGW88bp8jRw. [Accessed: 10-Apr-2018].

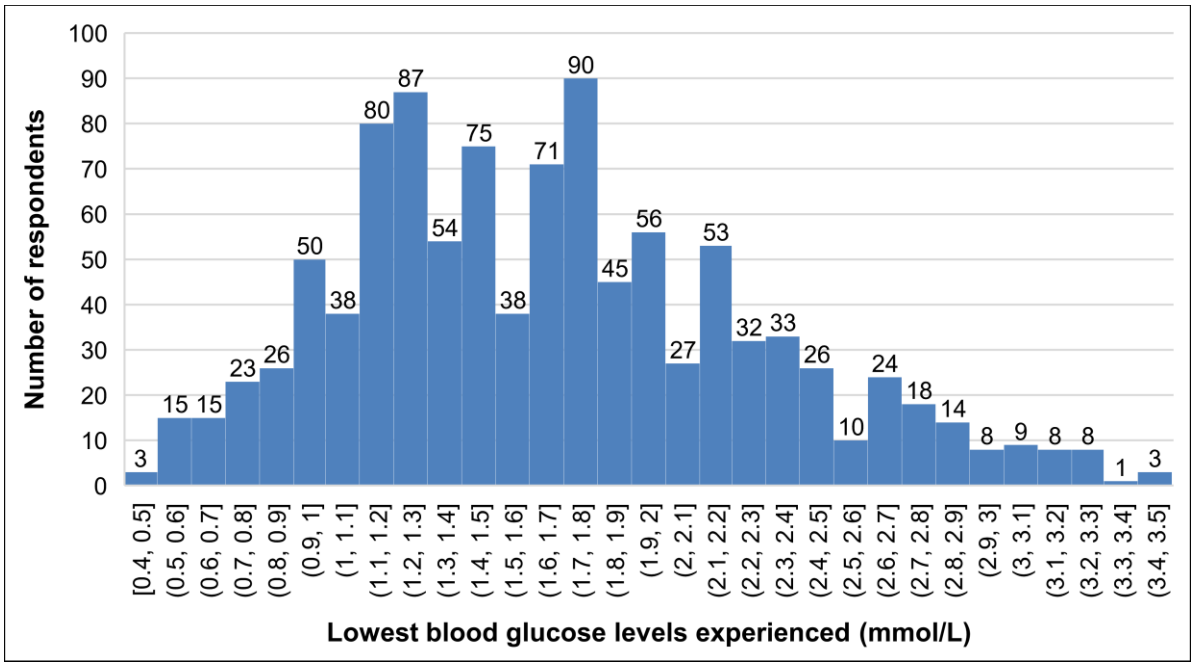

Note: The values in the different ranges are included when square brackets "[]" are used and excluded when round brackets "()" are used.

Figure 3.2. Lowest BG levels of respondents.

A summary of the statistical analyses is represented in Table 3.2. A total of 95% of the respondents have experienced a BG level below 2.8 mmol/L. The mean of these lowest recorded BG levels was 1.67 mmol/L. The lowest BG reading was 0.4 mmol/L. All the respondents reported no long-term ill effects.

These records are obviously anecdotal. However, the sheer amount of data helps to offset the potentially unreliable nature of the self-reported measurements. The anecdotal data's similarity to that of the data from the clinical studies described earlier also provides some encouraging pointers. There is thus a possibility that humans may survive severe hypoglycaemia for short periods with few adverse effects. More research is, however, needed.

Table 3.2. Summary of data after statistical analyses.

Description	Value
Number of respondents.	1 040
Mean BG (mmol/L).	1.67
Standard deviation (σ).	0.6
95% confidence interval: upper limit.	1.70
95% confidence interval: lower limit.	1.64
Minimum BG (mmol/L).	0.4

3.3 OBJECTIVES

Research objective for this chapter:

1. To investigate the effect of additional very low, yet achievable, short-term glucose only and combined glucose and glutamine deprivation on cancer and non-cancer cell growth combined with long term glucose deprivation.

3.4 METHODS AND MATERIALS

3.4.1 Cell lines

As described in Chapter 2, Section 2.4.1, the same cell lines were used in this chapter, namely two breast cancer cell lines (MDA-MB-231 and MCF-7), one cervical cancer cell line (HeLa) and the non-cancer breast cell line (MCF-10A).

3.4.2 Concentration levels of glucose and glutamine

All tests conducted in this chapter was done on cells after they were stabilised in typical cancer patients' glucose (6.5 mmol/L) and glutamine (0.6 mmol/L) concentrations. The results of this stabilisation were previously presented in Figure 2.1 (Chapter 2). The *Press-Pulse* treatment was thus tested after this stable and physiologically correct *in vitro* cancer model was developed.

The values of the *Pulse* conditions were based on previous research on short-term very low glucose and glutamine *Pulse* deprivation [77], [78]. These studies resulted in decreased cell density, rounded cells and apoptosis induction when exposed to very low glucose (<3 mmol/L) and glutamine (<0.5 mmol/L) concentrations for 2-6 hours [77], [78].

Glucose

As discussed, the same *Press* glucose conceration of 3.5 mmol/L that was used in Chapter 2 will be used here. This concentration was derived from the following: typical cancer patients on a KD-R have presented BG levels as low as 4 mmol/L [51]. A further lowering of circulating BG levels to 3.5 mmol/L could potentially be achieved with fasting and/or metformin.

Based on the extensive review of the literature and the fact that glucose *Pulses* will only be implemented over a period of 3 hours. A concentration of 1 mmol/L was chosen for the *Pulse* glucose condition.

Glutamine

Similar to Chapter 2, Section 2.4.2, no long-term glutamine *Press* was conducted. Therefore, glutamine was kept constant at a physiological glutamine concentration of 0.6 mmol/L [80]–[82].

Although glutamine was not reduced for the *Press* conditions, glutamine was decreased during the *Pulse* conditions. A minimum short-term concentration of 0.25 mmol/L (for 3 hours) was used as the glutamine *Pulse* concentration. This value of 0.25 mmol/L for glutamine is also very low, but these levels have been achieved in patients before [118]. Although future work is needed, it is assumed that these levels could be achieved in humans for the 3-hour duration.

The very low glucose and glutamine conditions could possibly be recreated in patients using either a pharmacological procedure for glucose *Pulses* [81] or a mechanical procedure such as hemodiafiltration for combined glucose and glutamine *Pulses* [119]. These procedures are further discussed in Chapter 5.

3.4.3 Initial cell growth conditions of negative controls

The same procedure for initial cell growth and conditions for the negative controls were used for these tests. Refer to Chapter 2, Section 2.4.3 for a detailed description. Also, all of the treated cell lines were cultured using the same conditions as described for the negative controls, with the only difference being the concentrations of glucose and glutamine. The respective changes in concentrations of glucose and glutamine for the treated cell lines will now be discussed.

3.4.4 Experimental procedure conditions

Before the metabolic *Press-Pulse* treatment started (before day 0), cells were cultured in standard cell culture media (Condition 0). Thereafter, the cell lines were stabilised in typical cancer patients' glucose (6.5 mmol/L) and glutamine (0.6 mmol/L), namely Condition 1. Therefore, the results are not detailed in this chapter; refer back to Figure 2.1, Chapter 2.

The experimental procedure is divided into two parallel tests of metabolic *Press-Pulse* treatments (Treatment 1 and 2). The respective glucose and glutamine conditions for the two *Press-Pulse* treatments are summarised in Table 3.3.

Both Treatment 1 and 2 started with a glucose *Press* of 3.5 mmol/L and maintaining glutamine at 0.6 mmol/L on day 0 for 118 days, namely Condition 2. On days 50, 71 and 92, two different *Pulses* were given. For the cell lines in Treatment 1 glucose was reduced to 1 mmol/L for three

hours (glutamine kept at 0.6 mmol/L), namely Condition 3a. For Treatment 2 a combined glucose *Pulse* 1 mmol/L and glutamine *Pulse* to 0.25 mmol/L was done for three hours), namely Condition 3b. These short-term exposure durations are three hours since previous *in vitro* tests of three-hour glucose and glutamine deprivation has previously been successfully conducted [77], [78].

After the *Press-Pulse* treatment (days 118-160), cells were cultuivated back into typical cancer patients' glucose (6.5 mmol/L) and glutamine (0.6 mmol/L) concentrations), namely Condition 1. This was done to investigate whether cells 'recover' after such treatment.

Table 3.3. Cell culture glucose and glutamine conditions as well as exposure days.

Metabolic condition number	Glucose (mmol/L)	Glutamine (mmol/L)	Days
Negative controls in standard cell culture conditions			
0	25.52 (cancer cells) 17.56 (non-cancer cells)	4.0 (cancer cells) 2.0 (non-cancer cells)	0-160
Typical cancer patients physiological conditions			
1	6.5	0.6	118-160
Glucose Press for all cell lines			
2	3.5	0.6	0-118
Treatment 1: Glucose-only Pulse			
3a	1.0	0.6	50, 71, 92
Treatment 2: Combined glucose and glutamine Pulse			
3b	1.0	0.25	50, 71, 92

3.4.5 Measuring relative cell growth

The same procedure used to calculate RCG as detailed in Chapter 2, Section 2.4.5, was used in this chapter.

3.5 RESULTS

Quantitative data were collected *via* spectrophotometry from three independent repeats for all experiments. Same as in Chapter 2, each data point in Figure 3.3 to Figure 3.6 represent the average relative cell growth. This was calculated as a change in percentage between the treated cells and their respective negative controls, namely cells maintained in optimal growth conditions DMEM (error bars illustrate the standard deviations).

Several drug response metrics exist to test the efficacy of preclinical *in vitro* cancer treatments [120]. The most relevant is the GR_{50}, the drug concentration that reduces the RCG rate by 50% [121]. Therefore, from the results, the metabolic *Press-Pulse* therapy is effective if the RCG rate decreased by more than 50% after treatment.

3.5.1 Glucose-only *Pulses*

Figure 3.3 shows the response to long-term *(Press)* GD (Condition 2) for 118 days with glucose-only *metabolic Pulses* (Condition 3a) on days 50, 71 and 92. The cell lines' glucose and glutamine concentrations were then taken back (in the after-treatment recovery period) to typical cancer patients' values of 6.5 mmol/L and 0.6 mmol/L, respectively, for the period 118 to 160 days.

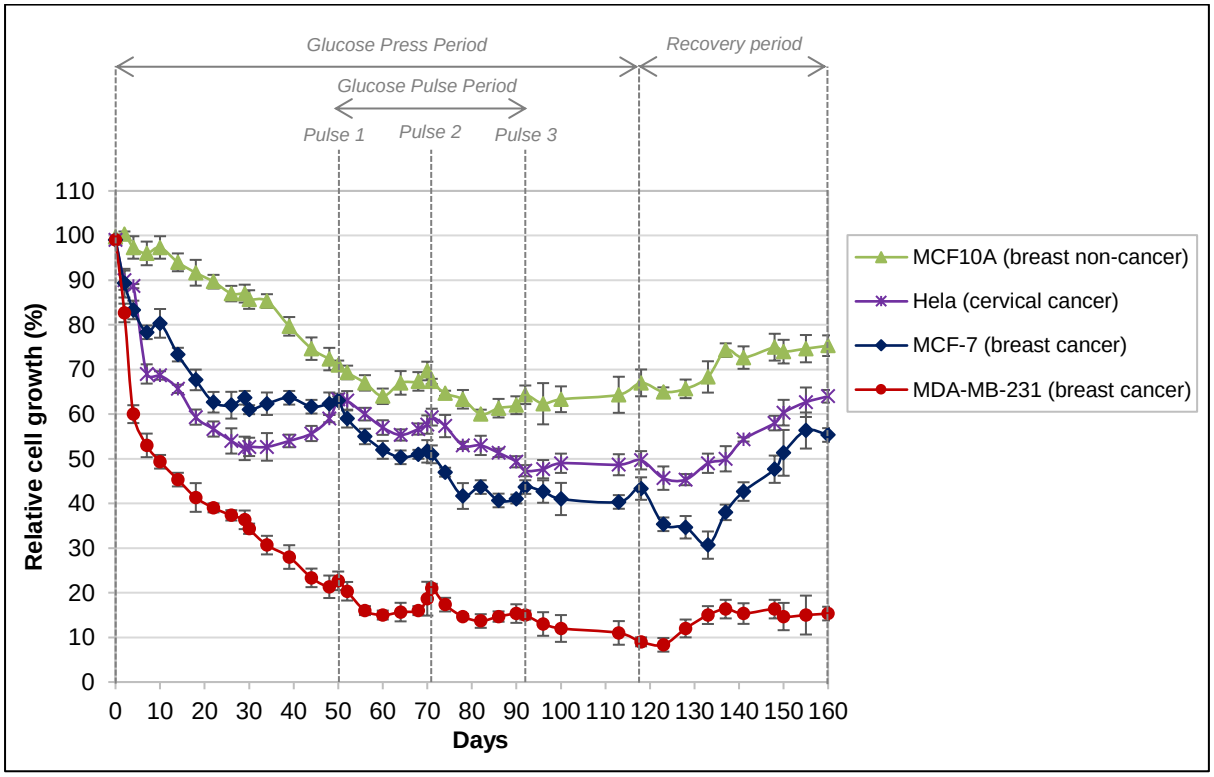

Note: Long-term *Press* glucose deprivation was done at 3.5 mmol/L and metabolic *Pulses* at 1 mmol/L glucose on days 50, 71 and 92 while maintaining glutamine at 0.6 mmol/L.

Figure 3.3. Long-term *Press* glucose deprivation metabolic glucose-only *Pulses*.

All cell lines reacted differently to the treatment. After 160 days the RCG rates were the following: the non-cancer cell line (MCF10A) was affected the least, stabilising at 75.33±2.31%, the cancer cell lines Hela, MCF-7 and MDA-MB-231 stabilised at 64.00±1.41%, 55.33±1.53% and 15.33±1.53% respectively. All cell lines were affected after each *metabolic Pulse.* RCG increased again, when taken back to typical cancer patients' physiological concentrations after the *Press* therapy was stopped on day 118.

MDA-MB-231 was affected the most by the treatment, with a minimum RCG of 8.33±1.53% on day 123, 5 days after the *Press* therapy was stopped. This cell line has shown to have high proliferation rates and intrinsic resistance to cell death, when allowed to grow in nutrient and space-limiting conditions and is termed an aggressive cancer cell line [122]. It is interesting that this aggressive cancer cell line should be the most susceptible to the *Press-Pulse* metabolic treatment. It has previously been hypothesised that highly glycolytic cancers and metastases will be the most severely impacted by metabolic treatment [63], [81], [119].

3.5.2 Glucose and glutamine *Pulses*

Figure 3.4 shows the response to long-term *Press* GD (Condition 2 in Table 3.3) for days 0-118, with both glucose and glutamine *metabolic Pulses* (Condition 3b in Table 3.3) on days 50, 71 & 92. The recovery period (days 118-160) was at typical cancer patients' glucose and glutamine concentrations.

There was very little difference between the results of glucose-only *Pulses* (Figure 3.3) and the combined glucose and glutamine *Pulses* (Figure 3.4).

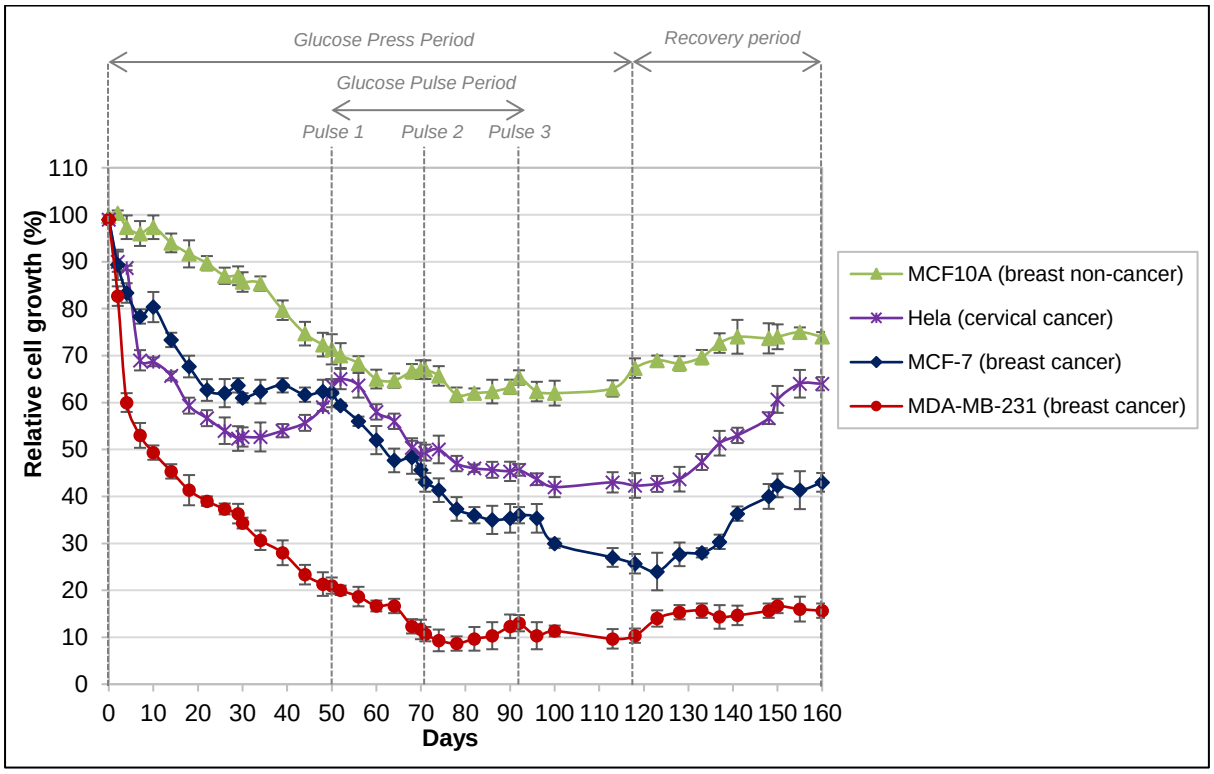

Note: Long-term *Press* glucose deprivation done at 3.5 mmol/L with metabolic *Pulse* of 1 mmol/L glucose and 0.25 mmol/L glutamine on days 50, 71 and 92.

Figure 3.4. Long-term GD *Press* with combined glucose and glutamine *Pulses*.

Figure 3.5 A to D present overlays of Figure 3.3 and Figure 3.4 comparing how the different cell lines responded to the different *metabolic Pulse* treatments. Figure 3.5A shows that only the MCF-7 cancer cell line had a small positive therapeutic response to the combined glutamine and glucose *metabolic Pulse* in relation to the glucose-only *Pulse*. Figure 3.5 B, C and D give the other three cell lines responses. The results for glucose-only and combined glucose and glutamine *metabolic Pulses* showed little difference.

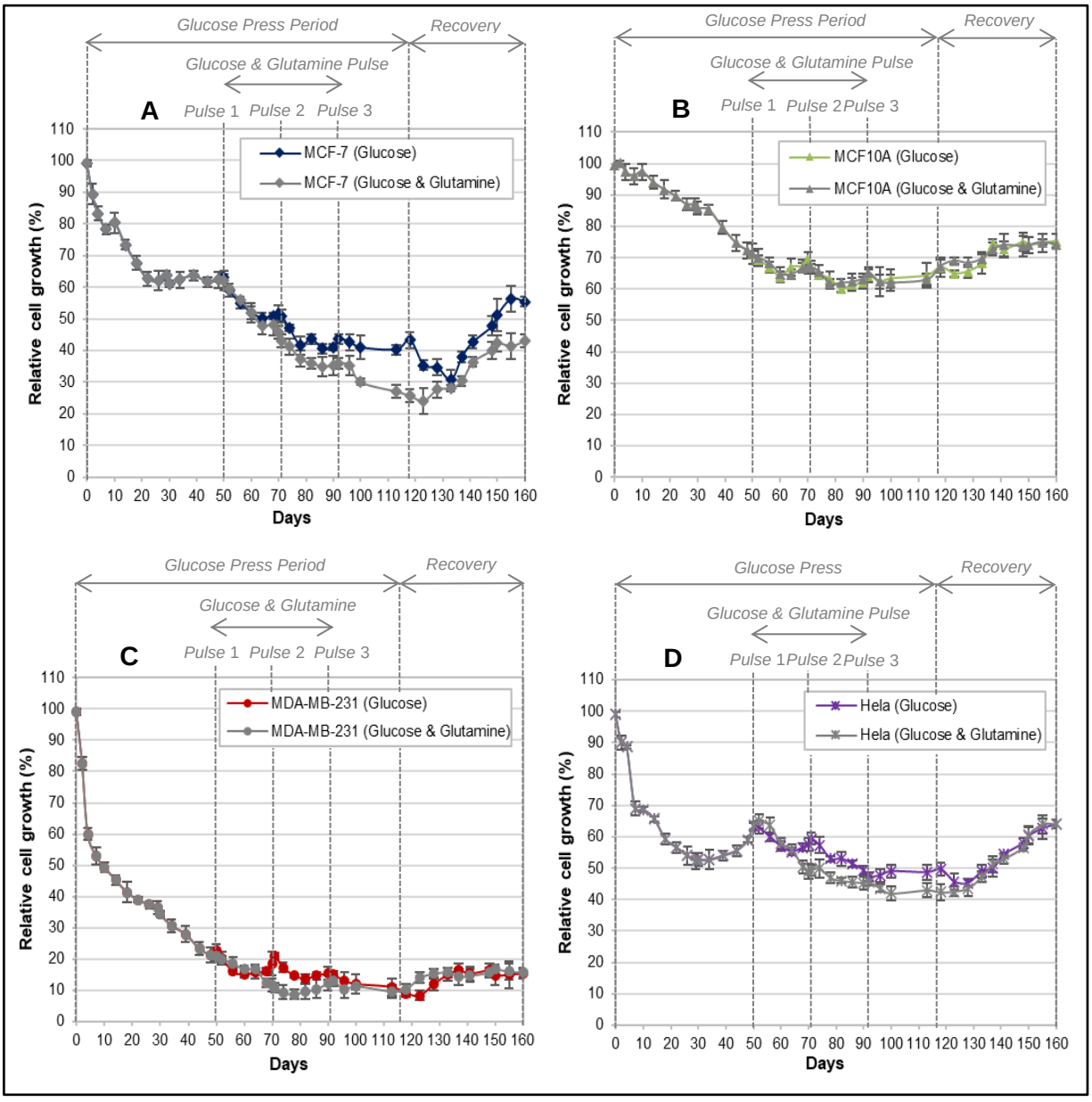

Note: Long-term *Press* glucose deprivation done at 3.5 mmol/L with metabolic *Pulses* on days 50, 71 and 92: (i) glucose-only Pulse (1 mmol/L) and (ii) combined glucose (1 mmol/L) and glutamine (0.25 mmol/L) *Pulses*.

Figure 3.5. Comparison of different cell lines' RCG after *Press-Pulse* treatments.

3.5.3 Recovery period

During the recovery period of days 118-160, all treatments were stopped. All cells were thus taken back to typical cancer patients' glucose and glutamine levels. Figure 3.3 and Figure 3.4 show that all of the cell lines' RCG rates increased and later stabilised. This indicates some form of 'recovery'.

More specifically, from day 130 onwards the MCF-7 and HeLa cell lines demonstrate a similar recovery rate which is much faster than the other two cell lines. These cell lines may have changed their energy sources used for cell growth, from glucose & glutamine to lactate. Lactate is a by-product of glucose metabolism. Evidence in literature shows that MCF-7 and HeLa cell lines have the ability to switch from glucose to lactate as an additional energy source [123].

Furthermore, new information shows that cancer cells obtain their energy from mitochondrial substrate level phosphorylation (mSLP) in the glutaminolysis pathway [124]–[126]. As with lactate (the by-product of glucose metabolism) the end-products of mSLP could also be used by these cells as an alternative energy source [125]. It is known that succinate, rather than lactate, is the end-product of the glutaminolysis pathway.

Therefore, the cell lines that recovered, namely MCF-7 and Hela, may alternatively obtain energy for ATP synthesis from the newly discovered glutaminolysis pathway. This is further discussed in Chapter 7, Section 7.2.2.

As for the most affected cell line, namely MDA-MB-231, did not 'recover' as well as the other cell lines with only 15% RCG on day 160. This could suggest a potential benefit of metabolic *Press-Pulse* treatment for breast cancer patients having tumours with similar characteristics to the MDA-MB-231 cell line. Future clinical trials are needed to confirm this.

3.6 DISCUSSION

In this study short-term metabolic *Pulses* were added to the metabolic long-term *Press* treatment that was investigated in Chapter 2 [63]. The RCG rates at the end of the *Press* only (black bars) [63] and the *Press/Pulse* (grey bars) treatments are summarised in Figure 3.6.

Comparing the results in Figure 3.6 for the *Press* only method (Chapter 2) [63] with the combined *Press-Pulse* method, the following can be seen:

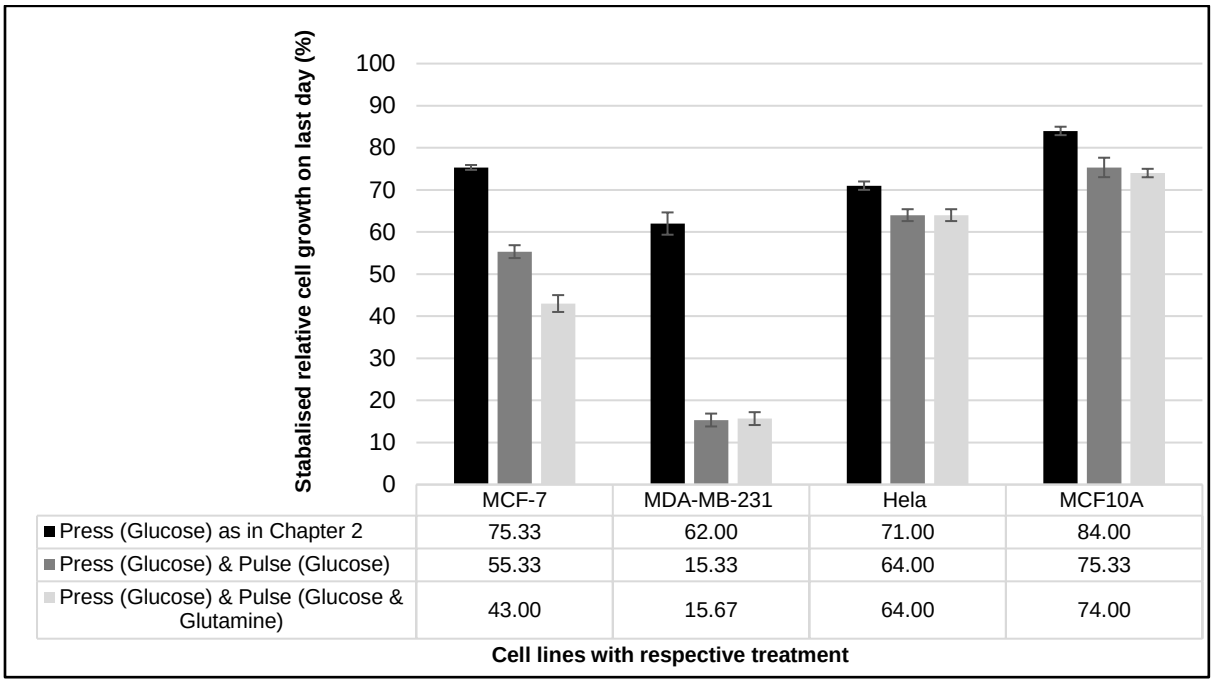

	MCF-7	MDA-MB-231	Hela	MCF10A
Press (Glucose) as in Chapter 2	75.33	62.00	71.00	84.00
Press (Glucose) & Pulse (Glucose)	55.33	15.33	64.00	75.33
Press (Glucose) & Pulse (Glucose & Glutamine)	43.00	15.67	64.00	74.00

Figure 3.6. RCG comparison between glucose *Press* and *Press-Pulse* treatments.

1. The non-cancer cell line (MCF10A) stabilised at 84% and at approximately 75% (Figure 3.6) for the glucose-only *Press* (Chapter 2) [63] and the combined *Press-Pulse* metabolic therapy respectively.

2. The most aggressive cancer cell line, namely MDA-MB-231 was the most affected by the *Press-Pulse* therapy. For the *Press* only therapies, RCG stabilised at 62% after *Press* treatment (Chapter 2). The RCG for the two *Press-Pulse* therapies (tests (a) and (b)) stabilised at a very low value of approximately 15%, 42 days after the *Press* therapy was stopped and 68 days after the last *Pulse.*

   If the most aggressive tumorigenic cell line is close to full remission with *Press-Pulse* therapy, one wonders if this effect could be replicated in some cancer patients with aggressive highly glycolytic tumours and metastases. The problem is to find out who these patients could be.

   A pilot study is currently under way to measure fluorodeoxyglucose (FDG) uptake (measure of glucose metabolism) of these *in vitro* cell lines. This could potentially provide a test to link high glucose metabolism with effectiveness of glucose deprivation studies in the tested cell lines. The FDG uptake from these tests could then potentially be linked to the FDG uptake values of patients' tumours. This is further discussed in the future research Section 7.2.2 (Chapter 7).

3. Only the MCF-7 cell lines showed some sensitivity to the additional glutamine *Pulses.* RCG decreased from 75% for the glucose-only *Press* therapy (Chapter 2) [63], while it

decreased to 55% for the glucose *Press* combined with the glucose *Pulses.* RCG decreased further to 43% when a glutamine *Pulse* was added. This suggests that the MCF-7 cell line subsists, at least partially, on glutamine in addition to glucose.

4. The Hela cell line was the least affected by the metabolic therapies, with 71% RCG for the *Press* only (Chapter 2) [63] and 64% for the two *Press-Pulse* therapies. This will also be explored in the future pilot study, investigating the FDG uptake of cell lines, see Chapter 7, Section 7.2.2.
5. It is clear that the *Press-Pulse* treatment benefits cell lines MCF-7 and MDA-MB-231 more than a *Press* only treatment, but less so for the Hela cell line. However, a downward growth trend was still observed for all the cancer cell lines after the last (third) *Pulse*. It is suggested that future tests be extended to at least five *Pulses*.
6. The increase in RCG of MCF-7 and HeLa from day 130 onwards, after the *Press-Pulse* treatment, hint at these cell lines' ability to change their energy sources from glucose and glutamine to other energy sources. There is evidence that these cells switch from glucose to lactate for cell growth [123]. Future research is needed to confirm this.
7. There is evidence that the estimated adenosine triphosphate (ATP) production of MCF-7 is less dependent on glycolytic than oxidative metabolic pathways compared to the MDA-MB-231 cell line [127]. This could partially explain the resistance the MCF-7 cell line has to *Press-Pulse* glucose deprivation conditions.

3.7 CONCLUSIONS

The potential benefits of metabolic control in the treatment of highly-glycolytic cancers have become more evident. Past studies have researched, separately, the effects of both long-term and short-term GD on cancer cell lines.

However, there is a lack of studies combining the two in a *Press-Pulse* methodology. This methodology is based on the evolutionary concept of mass extinction which shows that full extinction only occurs when gradual long-term *(Press)* and acute short-term *(Pulses)* occur simultaneously.

The objective of this chapter, as detailed in Section 3.3, was achieved by testing both short-and long-term GD effects on different cancer and non-cancer cell lines. The method was based on the previously developed experimental procedure detailed in Chapter 2.

Although all the cell lines showed reduced RCG rates, only the aggressive MDA-MB-231 cancer cell line showed sufficient response for a potential glucose-only *Press-Pulse* treatment.

Whereas, both MDA-MB-231 and MCF-7 RCG rates were below 50% after the combined glucose and glutamine *Press-Pulse* therapy.

Future work was also proposed to investigate which cancer patients could be candidates for such metabolic treatments. The data also suggested that non-metabolic *Pulses*, beyond the current metabolic *Pulses* used in this chapter, could yield better results.

3.8 NOVEL CONTRIBUTIONS

3.8.1 Novel contributions from new repeatable methods

This chapter presented the addition of short-term metabolic *(Pulse)* treatments combined with long-term GD *(Press)* treatment, i.e. a long-term metabolic *Press-Pulse* treatment tested on different cancer and non-cancer cell lines. Very low short-term glucose-only and glucose and glutamine deprivation have not been investigated in combination with long-term GD *Press* treatment. This chapter thus provides a novel repeatable metabolic *Press-Pulse* method conducted on different cancer and non-cancer cells.

3.8.2 Novel contributions from results

The results of these novel methods provide the following novel insights into future long-term metabolic *Press-Pulse in vitro* tests:

- Similar to the long-term GD *Press* treatment in Chapter 2, all cell lines reacted differently to the *Press-Pulse* treatment.
- After the *Press-Pulse* therapy was stopped, the cancer cell lines stabilised at lower values than the previous long-term GD *Press* treatment.
- One of the breast cancer cell lines, namely MDA-MB-231, was nearly eradicated with the *Press-Pulse* treatment.
- Only one cancer cell line, namely MCF-7, displayed a slightly lower RCG for the combined glutamine and glucose *Pulse* than the glucose-only *Pulse.* The other cell lines showed similar RCG rates when comparing the two different *Pulse* treatments.

3.8.3 Dissemination of results

This chapter has been submitted for publication and has been preliminarily accepted with revisions to the scientific medical journal *Cancer Cell International* with the following title: *In vitro quantification: combined long and short-term metabolic effects on different cancer cell lines.*

CHAPTER 4
LONG-TERM ENERGY RESTRICTION IN COMBINATION WITH SHORT-TERM CHEMOTHERAPY FOR CANCER TREATMENT

"It is not the strongest of the species that survive, nor the most intelligent, but the one most responsive to change."

Charles Darwin[16]

[16]Your Fates, "Survival Quotes." [Online]. Available: https://www.yourfates.com/survival-quotes/. [Accessed: 21-Nov-2021].

4.1 PREAMBLE

The following chapter investigates a non-metabolic *Pulse* treatment that is combined with long-term GD *Press* treatment. Two different chemotherapies, namely paclitaxel and carmustine, are administered separately as the *Pulse* treatments.

The chapter provides a literature review of the need to investigate chemotherapy in combination with GD, which leads to the objectives of this chapter. The same methods were used for both chemotherapies, namely, chemotherapy administered at three different dosages while being exposed to one of the following treatments: (1) typical cancer patients' glucose and glutamine concentrations or (2) long-term GD.

The results and discussions are combined and divided into two sections: paclitaxel (Section 4.5.1) and carmustine (Section 4.5.2). Each section contains the results of Treatment 1 and 2. The chapter concludes with a conclusion of the main findings and implications to literature and this chapter's novel contributions.

4.2 LITERATURE REVIEW

Since the inception of chemotherapy in the 1940s, it is still one of the principal modes of treatment for many cancer patients [128]. However, the main drawback of this type of therapy is that non-cancer cells are often severely affected, resulting in various toxic side effects in cancer patients [129]. These cytotoxic effects are especially evident in carmustine treatment, which is an alkylating agent capable of crossing the blood-brain barrier[17].

Fortunately, several studies have shown that short-term starvation/fasting could reduce these toxic side effects [25], [53], [130]–[134]. However, one of the challenges of fasting is that it increases the risk of cachexia in cancer patients [54], [135]. To lower the risk of cachexia from fasting and fasting-mimicking diets such as a KD-R have been used in its place [54], [91], [131].

The prevailing point of view in the field is thus that fasting-mimicking diets should allow an increase in chemotherapy dosage administration while maintaining quality of life [136]. However, few have investigated the long-term therapeutic effects of chemotherapy when combined with fasting-mimicking diets. Could the same therapeutic effect be achieved at a lower dose when combined with fasting-mimicking diets instead of increasing chemotherapy? This study will investigate these effects in new preclinical models.

[17]National Institute of Health, "National Center for Biotechnology Information, PubChemo database, Carmustine." [Online]. Available: https://pubchem.ncbi.nlm.nih.gov/compound/Carmustine. [Accessed: 12-Apr-2020].

Current preclinical studies have evaluated the effect of fasting on chemotherapy toxicty [25], [53], [130]–[134]. However, similar to Chapters 2 and 3, these studies are not conducted at clinically relevant metabolic concentrations. Therefore, in this chapter the *in vitro* tests will be designed to mimic long-term clinical treatments of chemotherapy administered in combination with fasting-mimicking diets.

The two chemotherapies used are the following:

(i) Carmustine (bis-chloroethylnitrosourea), which is most frequently used as an antineoplastic agent in the treatment of brain tumours [137]. Here the possibility of its use is explored on breast (MDA-MB-231, MCF-7) and cervical (HeLa) cancer cell lines.

(ii) Paclitaxel, which is one of the most commonly used chemotherapies due to its effective treatment on various cancers, especially breast cancer [138].

4.3 OBJECTIVES

Research objectives for this chapter:

1. To investigate the effect of chemotherapy on cancer and non-cancer cell growth when administered at typical cancer patients' glucose and glutamine concentrations.
2. To investigate the effect that additional non-metabolic chemotherapy treatment has on cancer and non-cancer cell growth when combined with long-term glucose deprivation.
3. To determine if a lower chemotherapy dosage combined with glucose deprivation will have a similar therapeutic effect compared to a higher chemotherapy dosage administered without glucose deprivation.

4.4 METHODS AND MATERIALS

4.4.1 Cell lines

As described in Chapter 2, Section 2.4.1, the same cell lines were used in this chapter, namely two breast cancer cell lines (MDA-MB-231 and MCF-7), one cervical cancer cell line (HeLa) and the non-cancer breast cell line (MCF-10A).

4.4.2 Concentration levels of glucose and glutamine

The same glucose and glutamine concentrations of typical cancer patients and long-term GD *(Press)* that were used in Chapter 2 and 3 were used here. These conditions are summarised in Table 4.1. Condition 1 provides the physiological glucose and glutamine concentrations of typical cancer patients. Condition 2 gives the long-term GD concentrations.

Table 4.1. Cell culture microenvironment conditions for the experimental procedure.

Metabolic condition number	Conditions	Glucose (mmol/L)	Glutamine (mmol/L)
1	Typical cancer patients' concentrations	6.5	0.6
2	Long-term glucose deprivation concentrations	3.5	0.6

4.4.3 Chemotherapy conditions: paclitaxel and carmustine

The efficacy of paclitaxel used as a monotherapy has been studied at different dosages, infusion times and administration cycles [139]. The most widely used dose in humans, infusion time and administration cycle is 175 mg/m^2 at a 3-hour intravenous infusion rate, which is administered every 3 weeks [139].

Therefore, to replicate the most widely used paclitaxel therapy, the *in vitro* experiments were set up accordingly. Cells were exposed to an infusion time of 3-hours and exposed at 21-day intervals. The administration cycle of 21 days is also in close proximity to the most vulnerable point when cells are exposed to long-term GD (minimum RCG on day 26). See Table 2.3 in Section 2.5 of Chapter 2.

Since paclitaxel is well established in clinical practice, the pharmacokinetics of paclitaxel used as a monotherapy was considered to determine the different dosages [139]. Further, it is important to consider clinically relevant dosages of approved cancer drugs when re-evaluating them in preclinical studies [9]. However, determining the most clinically relevant dose in cell culture is still a controversial topic [140], [141].

Therefore, for this study the concentration of paclitaxel that presents optimal antiproliferative activity for these cancer cell lines was used, namely 1 μM [142]. In addition to this, lower (half) and higher (double) concentrations of 0.5 μM and 2 μM were used respectively, see Table 4.2. These concentrations are still well below the maximum plasma concentration of 5.1 μM, which is achieved in cancer patients at the most widely used dose of 175 mg/m^2, 3-hour intravenous infusion, every 21 days [139].

Table 4.2. Different chemotherapy dosages for paclitaxel and carmustine.

Dosage	Paclitaxel concentration (μM)	Carmustine concentration (μM)	Exposure day(s)
Minimum	0.5	10	29,50,71 & 50,71,92
Standard	1	50	29,50,71 & 50,71,92
Maximum	2	100	29,50,71 & 50,71,92

Determining the most clinically relevant dose in cell culture is still a controversial topic [140], [141] and beyond the scope of this study. Here we are only concerned about the relevant glucose and glutamine concentrations. The carmustine dosages were also based on previous preclinical tests, which present optimal antiproliferative activity at dosages of 50 μM to 100 μM [143]. Therefore, for this study, the optimal dosages 50 μM and 100 μM were used, as well as a much lower concentration of 10 μM (see Table 4.2). The same exposure times and chemotherapy cycles of paclitaxel were used for carmustine, namely 3 hours every 21 days.

After chemotherapy administration, cells were washed three times with 3 ml of the respective cell culture medium the cells were exposed to. Thereafter, new medium was added to the cells with the respective glucose and glutamine concentrations.

4.4.4 Initial cell growth conditions of negative controls

The same procedure for initial cell growth and conditions for the negative controls were used for these tests. Refer to Chapter 2, Section 2.4.3 for a detailed description. Also, all of the treated cell lines were cultured using the same conditions as described for the negative controls, with the only difference being glucose and glutamine concentrations and chemotherapy exposures.

4.4.5 Experimental procedure conditions

Before the non-metabolic *Press-Pulse* treatment started (before day 0), cells were cultured in standard cell culture media (Condition 0). Thereafter, the cell lines were stabilised in typical cancer patients' glucose (6.5 mmol/L) and glutamine (0.6 mmol/L), namely Condition 1. Therefore, the results are not detailed in this chapter; refer back to Figure 2.1, Chapter 2.

A thorough methodology was developed to reduce unfavourable factors such as overpopulation of controls, incubation space and contamination. Two non-metabolic Press-Pulse tests were conducted in parallel for each chemotherapy, namely Treatment 1: Chemotherapy *Pulse* at physiological glucose levels, and Treatment 2: Glucose *Press* with chemotherapy *Pulses*. The methodology is described here.

Treatment 1: Chemotherapy *Pulse* at physiological glucose levels (Chemo without GD)

Treatment 1 consists of long-term GD before chemotherapy, days 0-29. These tests were conducted to model current clinical practice of chemotherapy administered to cancer patients that followed long-term KD-R prior to chemotherapy. The same long-term GD *Press* treatment glucose and glutamine concentrations as in Chapters 2 and 3 were used here, namely 3.5 mmol/L glucose and 0.6 mmol/L glutamine (see Condition 2, Table 4.1).

After the long-term GD, cells were exposed to each of the three different chemotherapy dosages separately. These dosages were administered every 21 days, namely days 29, 50 and 71. Between each cycle of chemotherapy (days 29 to 71), cells were exposed to typical cancer patients' glucose and glutamine concentrations as described by Condition 1 in Table 4.1.

After the three cycles of chemotherapy, cells were maintained in Condition 1 until day 100. This was implemented to investigate the cell lines' response after Treatment 1, i.e., to examine whether RCG will increase, decrease or remain the same.

Treatment 2: Glucose *Press* with chemotherapy *Pulses* (Chemo with GD)

Treatment 2 also entailed the same long-term GD *Press* treatment as in Chapters 2 and 3, namely 3.5 mmol/L glucose and 0.6 mmol/L glutamine (see Condition 2, Table 4.1). Cells were exposed to this condition for four months, days 0 to 118. This duration of GD replicates typical long-term KD-R [144].

During the long-term GD, cells were exposed to each of the three different chemotherapy dosages. These dosages were administered every 21 days, namely days 50, 71 and 92. Between each cycle of chemotherapy (days 50 to 92), cells were maintained in the long-term GD condition.

Thereafter, on day 118, cells were exposed to typical cancer patients' glucose and glutamine concentrations (Condition 1). Cells were maintained at these concentrations until day 160. This was implemented to examine the cell lines' response after the Treatment 2, i.e., whether RCG will increase, decrease, or remain the same.

4.4.6 Measuring relative cell growth

The same procedure used to calculate RCG as detailed in Chapter 2, Section 2.4.5, was used in this chapter.

4.5 RESULTS AND DISCUSSION

Each data point denoted in Figure 4.1 to Figure 4.10 represent the average RCG rates, with the error bars illustrating the standard deviations of the three independent repeats per data point.

Similar to Chapter 3, the non-metabolic *Press-Pulse* therapy is considered to be effective if the RCG rate decreases by more than 50% after treatment. The following sections will discuss the results obtained for both paclitaxel and carmustine separately.

4.5.1 Paclitaxel treatments

4.5.1.1. Treatment 1 results: Paclitaxel Pulse without glucose deprivation

Figure 4.1 (A-C) illustrates the different cell lines' RCG rates during Treatment 1 with paclitaxel. Before comparing the paclitaxel treatment efficacy. The effect of GD before paclitaxel administration is assessed.

GD before paclitaxel treatment affected all cell lines and mostly affected the MDA-MB-231 cancer cell line. The non-cancer cell line MCF-10A also presented a decrease in RCG. This is in agreement with the previous long-term GD tests done in Chapters 2 and 3.

After this initial GD of days 0 to 30, the cells were exposed to typical cancer patients' glucose and glutamine concentrations. All cells were then administered with three cycles of paclitaxel.

Firstly, the results of the lowest paclitaxel dose (0.5 μM) are presented in Figure 4.1A. A therapeutic effect was not evident at this dosage in any of the cell lines, since RCG rates remained fairly stable throughout the treatment, see days 30 to 100.

Secondly, a higher dose of 1 μM (Figure 4.1B), a therapeutic response can be seen in the MCF-7 and MDA-MB-231 cancer cell lines. These cancer cell lines presented a continuous decrease in RCG after each administration of paclitaxel. On the other hand, the Hela cancer cell line's RCG remained stable after each paclitaxel administration. Fortunately, the non-cancer cell line's RCG remained considerably stable and at similar RCG rates as the lower 0.5 μM dose. This could hint at similar low toxicity levels at a paclitaxel concentration of 0.5 μM and 1 μM.

Lastly, the highest dose of 2 μM (Figure 4.1C) represented the most therapeutic response in all cancer cell lines. RCG decreased dramatically in all three cancer cell lines after each administration of paclitaxel. This is regrettably also true for the non-cancer cell line MCF-10A, which also presented a rapid decrease in RCG. Fortunately, the non-cancer cell line's RCG rate resulted in a much higher RCG than the cancer cell lines.

Paclitaxel is one of the most commonly used chemotherapies due to its effective treatment on various cancers [138]. These results are thus in line with clinical practice, given that all cancer cell lines' RCG rates decreased at similar rates. However, paclitaxel used in cancer patients has toxicity issues [145]–[148]. This is also represented by the decrease in the non-cancer cell line MCF-10A.

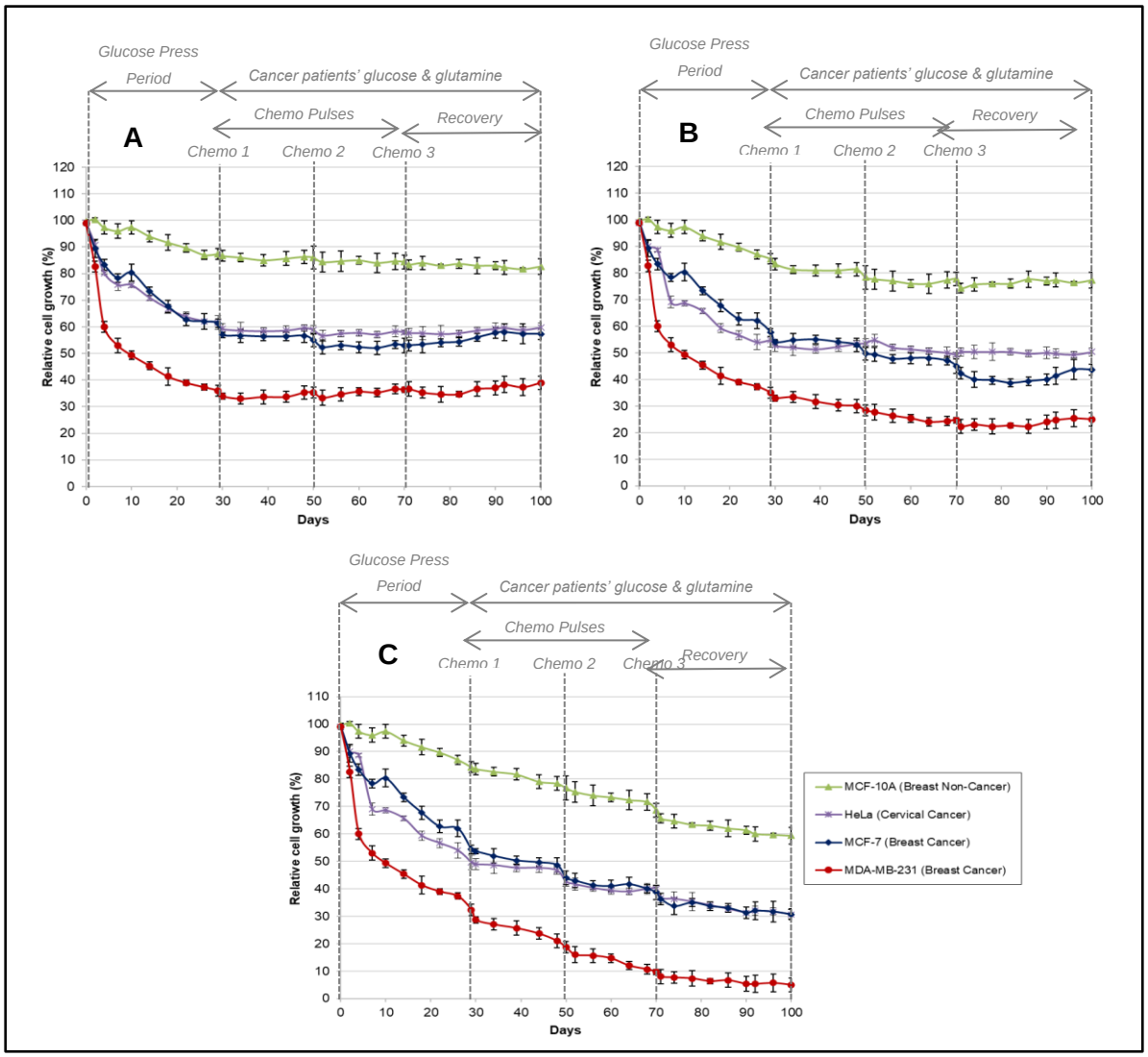

Note: Glucose 6.5 mmol/L and glutamine 0.6 mmol/L with paclitaxel dosages of (A) 0.5 μM, (B) 1 μM and (C) 2 μM.

Figure 4.1. Paclitaxel administered without GD at different dosages.

4.5.1.2. Treatment 2 results: Paclitaxel Pulse with glucose deprivation Press

All cells were exposed to a glucose concentration of 3.5 mmol/L and administered with the same paclitaxel procedure as described earlier. The effects of this treatment on the different cell lines are illustrated in Figure 4.2 (A-C).

GD before paclitaxel treatment (days 0 to 30) affected all cell lines and mostly affected the MDA-MB-231 cancer cell line. The non-cancer cell line MCF-10A also presented a decrease in RCG. This is in agreement with the previous long-term GD tests done in Chapters 2 and 3.

The additional GD after paclitaxel treatment (days 70 to 100) appeared to stabilise the RCG of all cells at the respective levels. This is evident since RCG increased slightly once cells were reverted back to typical cancer patients' glucose concentrations after treatment.

Firstly, considering the lowest dosage of 0.5 μM (Figure 4.2A), the MCF-7 cancer and MCF-10 non-cancer cell lines were mostly affected. Unfortunately, at this dosage the non-cancer cell line's RCG is lower than two of the three cancer cell lines. This hints at the fact that the risk of toxicity might outweigh the therapeutic efficacy.

Secondly, at the slightly higher dose of 1 μM (Figure 4.2B), all cell lines showed aggressive decreases in RCG after each cycle of paclitaxel. This is especially true for the MDA-MB-231 cancer cell line. The non-cancer cell line resulted in a similar RCG rate as the previous dose of 0.5 μM. Fortunately, in this case all cancer cell lines resulted in a lower RCG than the non-cancer cell line. Therefore, at a higher dose of 1 μM paclitaxel combined with GD; the therapeutic efficacy might outweigh the risk of toxicity.

Lastly, the cells' response to the highest dose of 2 μM (Figure 4.2C) shows similar detrimental effects on all cell lines. A very aggressive decrease in RCG for the cancer cell lines presents a high therapeutic potential for these cancer cells. However, the non-cancer cell line is significantly affected and could therefore result in much higher toxicity levels. Although these results are limited to a single non-cancer cell line, caution should be taken when cancer patients are administered high dosages of paclitaxel in combination with GD.

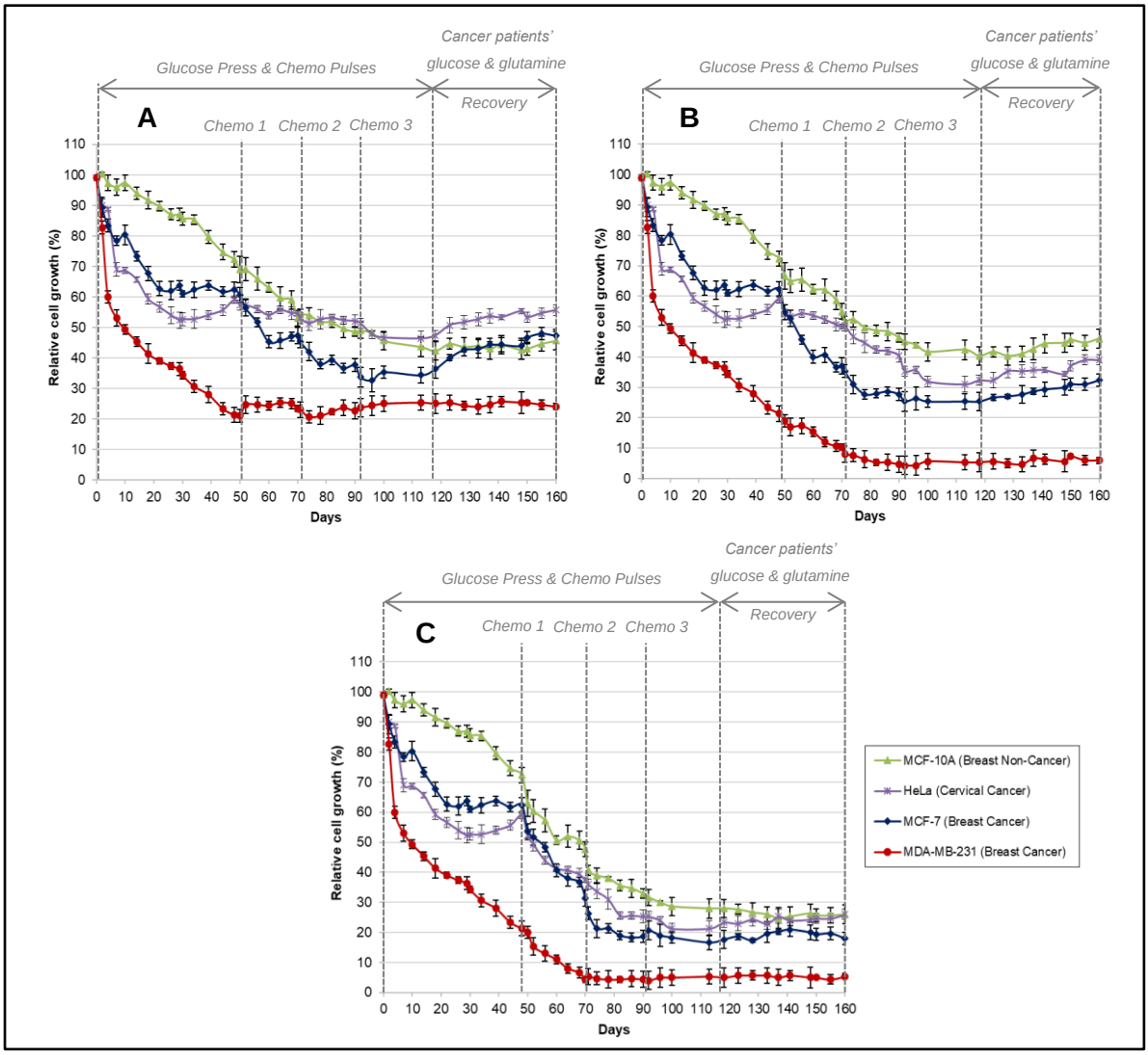

Note: Glucose 6.5 mmol/L and glutamine 0.6 mmol/L, paclitaxel dosages of (A) 0.5 μM, (B) 1 μM and (C) 2 μM.

Figure 4.2. Paclitaxel administered with GD at different dosages.

Now that both results were given, these results can be compared to investigate the benefits and possible disadvantages of paclitaxel combined with long-term GD.

4.5.1.3. Comparison between paclitaxel administered with and without GD

To illustrate the effect of paclitaxel treatment with and without GD, the overall decrease in RCG was calculated. This was done by subtracting the RCG after Treatment 1 (day 100) with the final RCG after Treatment 2 (day 160). These results are presented in Figure 4.3.

At first glance this graph illustrates the increased therapeutic efficacy of paclitaxel when GD is added as a combination treatment. However, as previously highlighted, lower toxicity is evident in treatment without GD than with GD. This is made clear by evaluating the RCG of the non-cancer cell line (MCF-10A), which shows a decrease in RCG of more than 30% with GD than without GD for all dosages of paclitaxel.

In contrast to this, treatment with GD resulted in an additional decrease in RCG of more than 10% in all three cancer cell lines for at least one of the different paclitaxel dosages. It follows then that treatment with GD acquires a higher positive therapeutic response at the tested dosages. However, toxicity might become a problem for dosages above 1 μM in combination with GD.

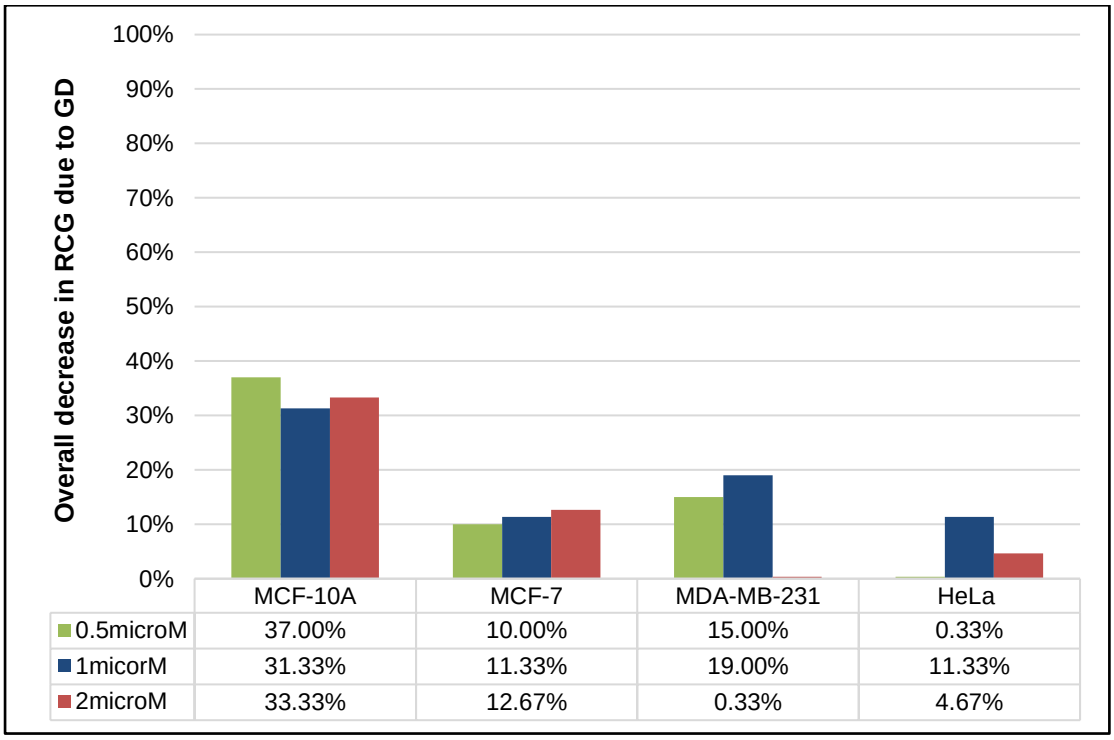

	MCF-10A	MCF-7	MDA-MB-231	HeLa
0.5microM	37.00%	10.00%	15.00%	0.33%
1micorM	31.33%	11.33%	19.00%	11.33%
2microM	33.33%	12.67%	0.33%	4.67%

Figure 4.3. Overall decrease in RCG due to GD at different paclitaxel dosages.

With a closer inspection of each cancer cell line's response, more insight is gained. The breast cancer cell line MCF-7 is a mitochondrial oxidative phosphorylation phenotype cell line and is thus less dependent on glycolysis [149]. Furthermore, it has a lower metastatic potential and is less aggressive [150]. These attributes contribute to the expectation that MCF-7 would show increased resistance to additional GD treatment than the other breast cancer cell line, namely MDA-MB-231.

This was indeed the case since Figure 4.3 illustrates that the RCG of MCF-7 was higher than MDA-MB-231 after both treatments and for all dosages of paclitaxel. Despite this, RCG decreased by an additional 10 to 12% for the respective paclitaxel dosages combined with GD.

The other breast cancer cell line, MDA-MB-231, mainly uses glycolysis rather than mitochondrial respiration to produce energy [80]. This presents elevated glycolytic activity under normoxic conditions [79]. This may partially explain the high therapeutic response of MDA-MB-231 to paclitaxel treatment combined with GD.

On the other hand, MDA-MB-231 also has higher proliferation rates and intrinsic resistance to cell death when grown in nutrient and space limiting conditions [122]. Nonetheless, this cell line still experienced the most therapeutic effect after both treatments, especially when paclitaxel was combined with GD.

Lastly, the HeLa cervical cancer cell line is the oldest and most distributed immortalised cell line and is known for its aggressive cell growth rates [151]. Like the MCF-7 cancer cell line, the HeLa cells also present less glycolysis dependency and are more dependent on glutamine for energy production [152]. As a result, the HeLa cell lines were not expected to present significant differences between paclitaxel treatment with or without GD.

This was indeed the case, especially at the lowest dose of paclitaxel (0.5 μM) where the HeLa cell lines only displayed a 0.33% difference in RCG between treatment with and without GD, see Figure 4.3.

Previous studies of preclinical models provide possible explanations for the increased therapeutic efficacy of chemotherapy when GD is added. These are differential cellular responses between cancer and non-cancer cells, namely Differential Stress Resistance (DSR) and Differential Stress Sensitisation (DSS) [131], [136]. To further elaborate:

- DSR decreases the toxicity of chemotherapy on non-cancer cells and thus causes a protective effect for these cells [136]. During DR, non-cancer cells re-invest energy in maintenance and repair that contribute to resistance to chemotherapy, while tumour cells are unable to slow down growth due to mutations in tumour suppressor genes and mitogenic pathways [136].
- DSS, on the other hand, increases the efficacy of chemotherapy on cancer cells [131], [136]. Moreover, the low serum levels of glucose achieved under KD-R impose extra stress on some types of cancer cells; since their energy needs under these circumstances are primarily met by means of glycolysis, which is inhibited under conditions of low glucose [131], [136]. Meanwhile, under GD conditions, regular cells tend to switch over to alternative energy sources [131], [136].

The DSS effect is clearly illustrated in Figure 4.3 for the MDA-MB-231 and MCF-7 cancer cell lines, less likely so for the HeLa cell line. This was, however, expected due to the HeLa cell line's lower dependency on glucose for energy.

On the other hand, in Figure 4.3, the DSR protective effect on the non-cancer cell line (MCF-10A) is not noticeable since RCG decreases with the addition of GD. This could be due to, amongst others, the following:

- Non-cancer cell lines can switch their main energy sources to ketones under GD conditions [15], [153]. However, the cell culture media did not contain ketones or other main energy sources for the cells to use other than glucose and glutamine.
- Paclitaxel is known to be more toxic to *in vitro* non-cancer cells more than to *in vivo* mouse models.

Therefore, the question remains whether a lower dosage of paclitaxel can be used to achieve a similar efficacy than a higher dosage (without the added toxicity of higher dosages), by adding an adjacent therapy such as GD. This is explored in the next section.

4.5.1.4. Dosage comparison of paclitaxel administration with and without GD

If cell lines are similarly affected by lower chemotherapy dosages when combined with GD than at higher dosages without GD. This would substantially impact chemotherapy dosages administered in practice and future designs of clinical trials evaluating long-term KD-R.

Figure 4.4 (A-C) compares the RCG rates between paclitaxel administered at 0.5 μM with GD and a higher dose of 1 μM without GD. All cancer cell lines show a similar therapeutic response, even though only half of the paclitaxel concentration was administered to the cells combined with GD.

Conversely, the non-cancer cell line (MCF-10A) presents a much lower RCG when the lower 0.5 μM dose is combined with GD. This may give rise to additional toxicity when paclitaxel treatment is combined with GD.

Figure 4.5 (A-C) presents a comparison between the higher paclitaxel dosages of 1 μM with GD and a dosage of 2 μM without GD. These results present similar decreases in the two breast cancer cell lines at a lower paclitaxel dosage combined with GD than at a higher paclitaxel dose without GD.

However, the HeLa cancer cell line seems to end at the same RCG rate. This is achieved at a much slower rate when combined with GD. Furthermore, the non-cancer cell line (MCF-10A) once again shows a much higher toxicity problem since RCG is lower when GD is combined with paclitaxel.

In summary, all of the cell lines present similar therapeutic efficacy at lower dosages of paclitaxel when combined with GD than higher dosages without GD. However, toxicity remains an issue since the non-cancer cell line presents much lower RCG rates when paclitaxel is administered during long-term GD.

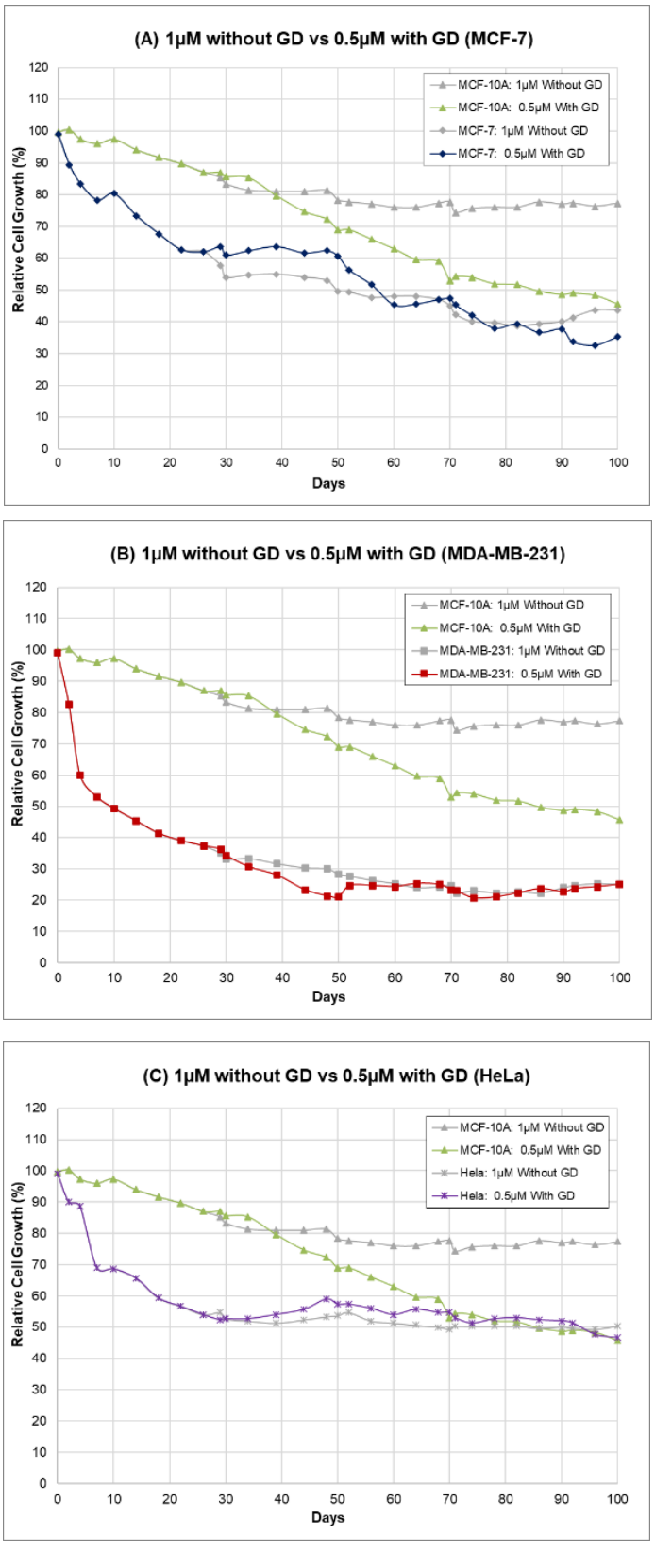

Note: Paclitaxel administered at a high dosage (1 μM) at typical cancer patients' glucose concentration on 6.5 mmol/L vs a fifth of the dosage (0.5 μM) at a glucose deprivation concentration of 3.5 mmol/L. The figure is separated by the different cancer cell lines (A) MCF-7, (B) MDA-MB-231, (C) HeLa with the non-cancer cell line MCF-10A also shown in (A-C).

Figure 4.4. Lower paclitaxel dosages: 0.5 μM with GD vs 1 μM without GD.

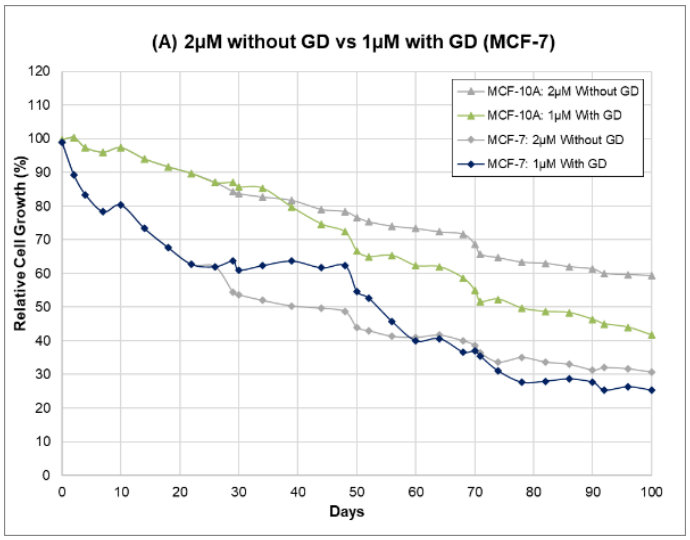

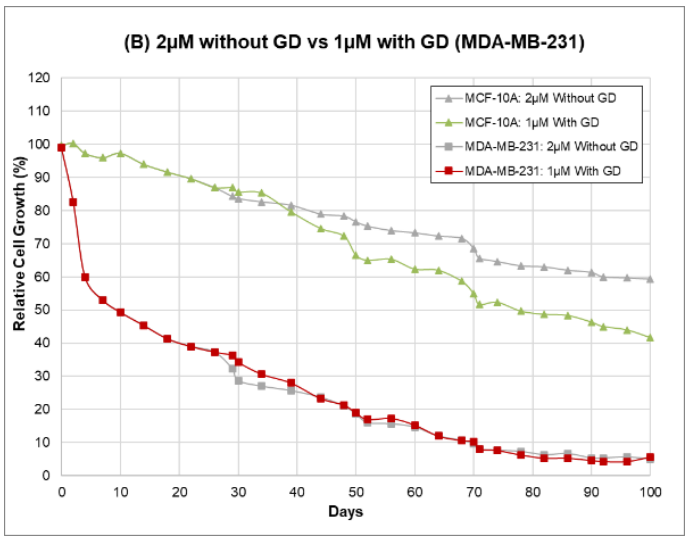

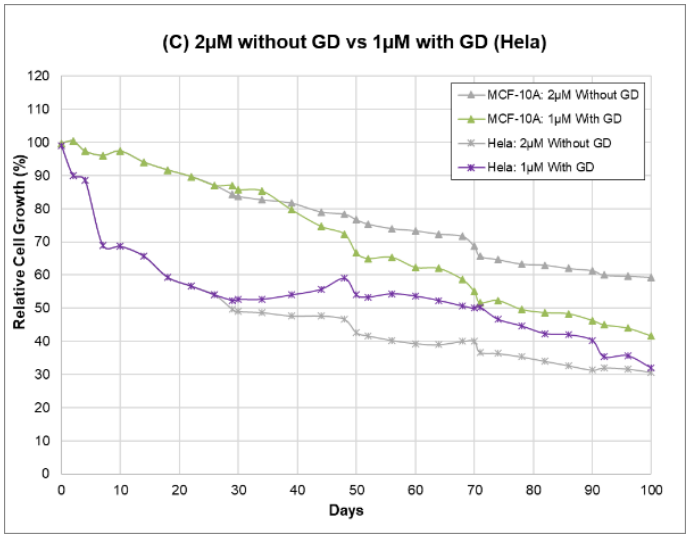

Note: Paclitaxel administered at a high dosage (2 μM) at typical cancer patients' glucose concentration on 6.5 mmol/L vs half the dosage (1 μM) at a glucose deprivation concentration of 3.5 mmol/L. Figure 4.5 is separated by the different cancer cell lines (A) MCF-7, (B) MDA-MB-231, (C) HeLa with the non-cancer cell line MCF-10A also shown in (A-C).

Figure 4.5. Higher paclitaxel dosages: 1 μM with GD vs 2 μM without GD.

4.5.2 Carmustine treatments

4.5.2.1. Treatment 1 results: Carmustine Pulse without glucose deprivation

Figure 4.6 (A-C) illustrates the different cell lines' RCG rates during Treatment 1 with carmustine. Before comparing the carmustine treatment efficacy, the effect of GD before carmustine administration is assessed.

The RCG rates of all cell lines decreased, with the MDA-MB-231 cancer cell line affected the most. The non-cancer cell line, MCF-10A, also presented a decrease in RCG. These results are in agreement with the previous long-term GD tests done in Chapters 2 and 3.

After this initial GD of days 0 to 30, the cells were exposed to typical cancer patients' glucose and glutamine concentrations. All cells were then administered with three cycles of carmustine.

Firstly, at the lowest dosage of 10 μM (Figure 4.6A), all cancer cell lines presented a slight increase in RCG after each administration. Whereas, the non-cancer cell line was negatively affected, constituting to a continuous decrease in RCG. Fortunately, the non-cancer cell line's RCG rate is still slightly higher than the cancer cell lines. This indicates that therapeutic efficacy outweighs the risk of toxicity at this concentration.

Secondly, for a dose of 50 μM (Figure 4.6B), a similar response to the previous 10 μM is seen in the non-cancer cell line and for the two cancer cell lines, namely MCF-7 and HeLa. However, RCG in these three cell lines are slightly lower. Nevertheless, the MDA-MB-231 cancer cells now shows a slight decrease in RCG rather than a slight increase after each cycle of carmustine. Fortunately, the non-cancer cell line's RCG rate is still slightly higher than the cancer cell lines. This indicates that therapeutic efficacy outweighs the risk of toxicity at this concentration.

Lastly, the highest dose of 100 μM (Figure 4.6C) represents a very different response to the other dosages. The MDA-MB-231 cancer cell line shows, once again, a decrease in RCG after each administration of carmustine.

The non-cancer cell line is highly affected, decreasing to a RCG rate below the two cancer cell lines MCF-7 and HeLa. Therefore, at this high dosage, the risk of toxicity could outweigh the therapeutic benefit. Subsequently, these cancer cell lines both illustrate an aggressive increase in RCG after each carmustine cycle. This confirms the idea that carmustine does not present any therapeutic potential for these cancer cell lines.

This slight increase in RCG rates of MCF-7 and HeLa cancer cell lines could be due to a higher glucose concentration. The next set of results will explore whether adding GD will reverse this increased RCG.

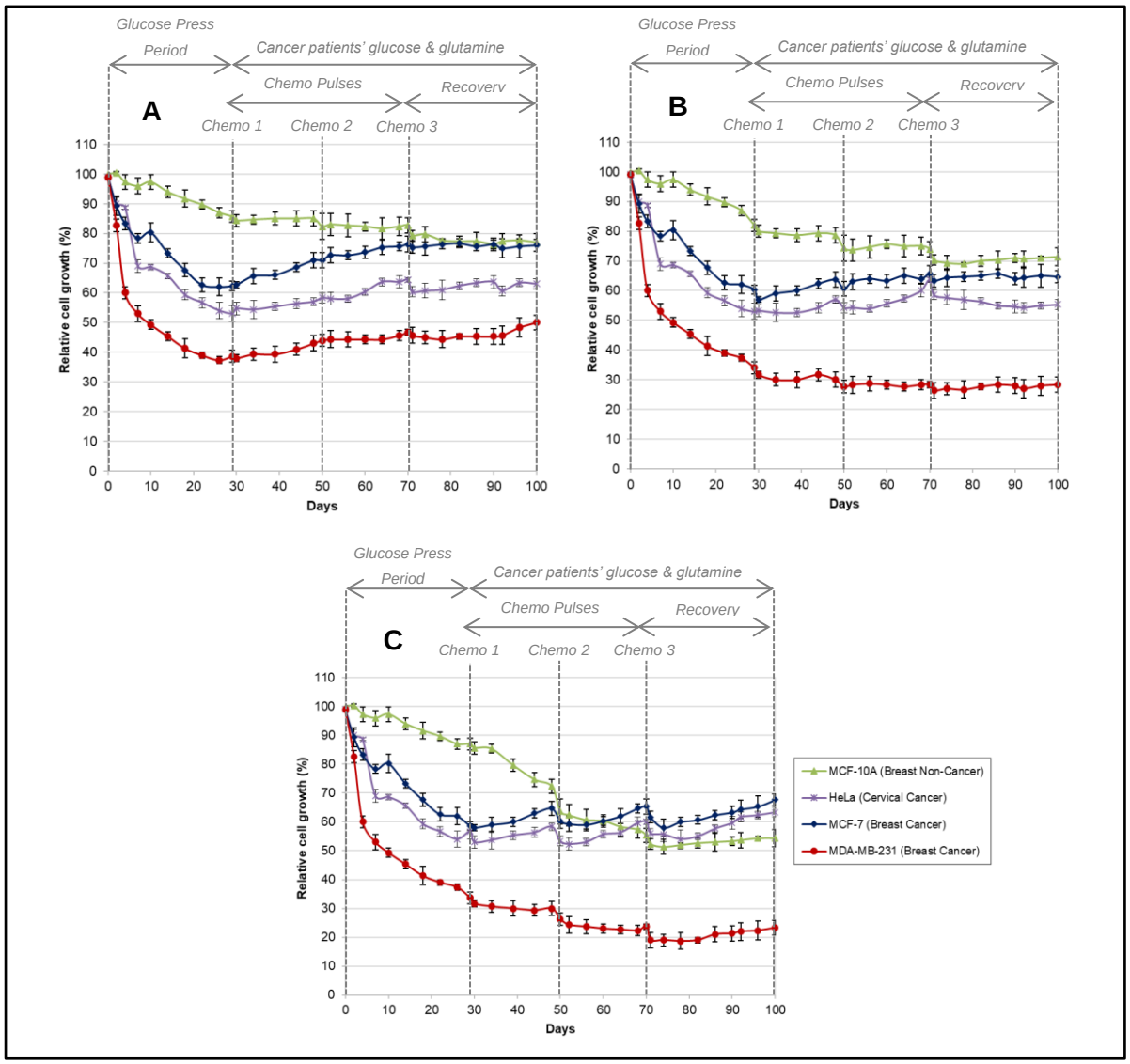

Note: glucose 6.5 mmol/L and glutamine 0.6 mmol/L, carmustine dosages of (A) 10 μM, (B) 50 μM and (C) 100 μM.

Figure 4.6. Carmustine administered without GD at different dosages.

4.5.2.2. Treatment 2 results: Carmustine Pulse with glucose deprivation Press

For the combination of chemotherapy and GD, three cycles of carmustine were administered to the different cancer cells while being exposed to a similar KD-R and fasting glucose concentration of 3.5 mmol/L. These results are illustrated in Figure 4.7 (A-C). The same dosages of carmustine, as previously described, were used, namely 10 μM, 50 μM and 100 μM.

In terms of the results from the therapy, most cell lines show a decrease in RCG during the GD before chemotherapy started, especially the cancer cell line MDA-MB-231. This result is similar to the previous GD done in Chapters 2 and 3. Likewise, the additional 30 days of GD after three cycles of chemotherapy resulted in further suppression of RCG recovery.

When considering the lowest dose of 10 μM (Figure 4.7A), all cell lines maintained their RCG rates from day 50 to 160, they did not show any further decrease after each cycle of carmustine. These reults indicate that carmustine does not affect the RCG rates of these cancer cell lines at such a low dosage.

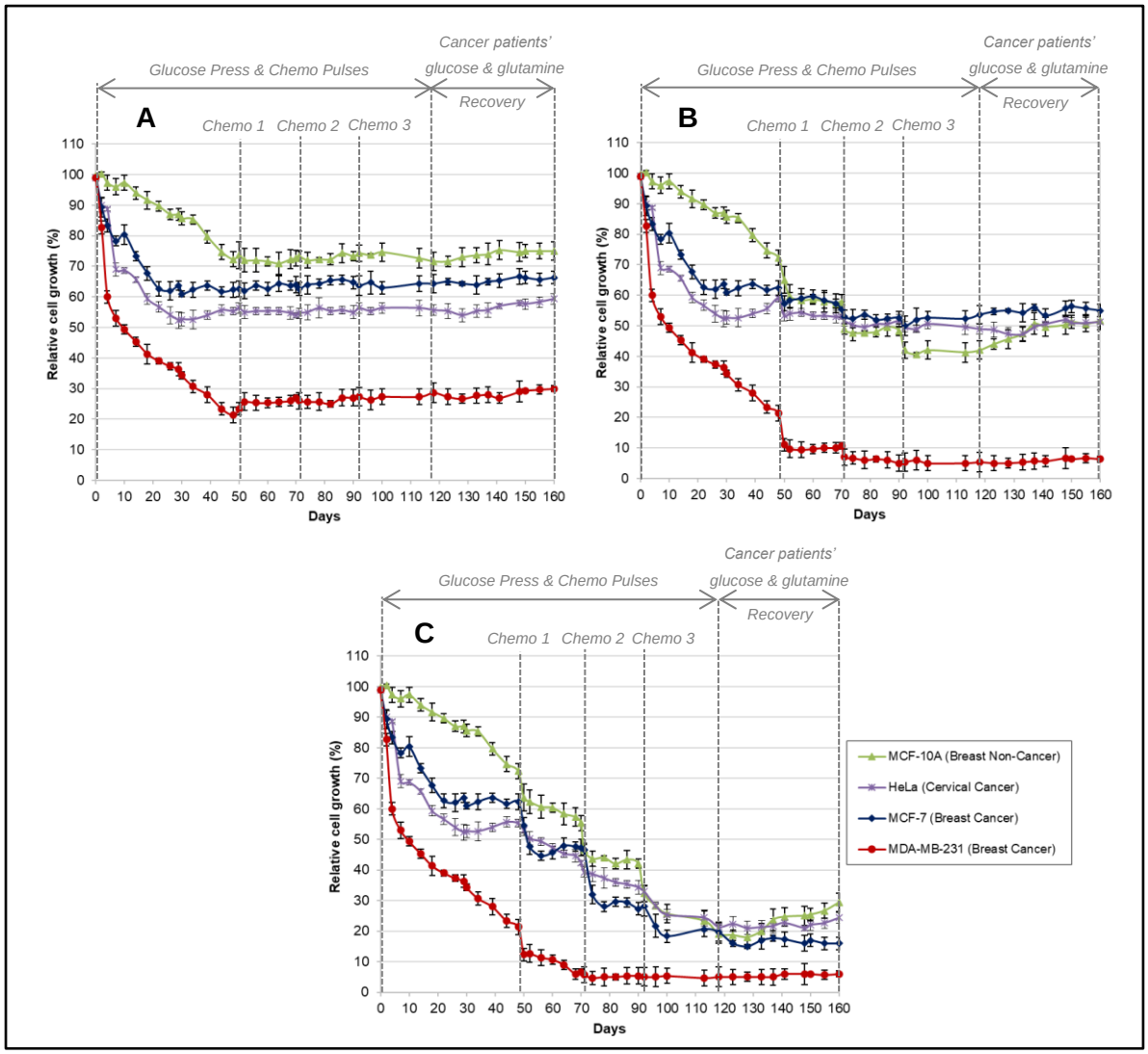

Note: Glucose 6.5 mmol/L and glutamine 0.6 mmol/L, carmustine dosages of (A) 10 μM, (B) 50 μM and (C) 100 μM.

Figure 4.7. Carmustine administered with GD at different dosages.

At the slightly higher dose of 50 μM (Figure 4.7B), all cell lines showed aggressive decreases in RCG rates, decreasing after each cycle of carmustine. The two cell lines that were most affected were the non-cancer cell line MCF-10A and the cancer cell line MDA-MB-231. The response of MDA-MB-231 shows a high therapeutic efficacy potential. However, this is

suppressed by the higher toxic potential shown by MCF-10A. Similar to Treatment 1, the MC-7 and HeLa cancer cell lines showed resistance to this treatment and resulted in higher RCG rates than the non-cancer cell line.

Lastly, the response to the highest dose of 100 μM (Figure 4.7C) presents a detrimental effect to all cell lines. A very aggressive decrease in RCG rates are seen in all cell lines. On the one hand this presents a high therapeutic potential for the cancer cells, on the other hand, this could lead to much higher toxicity.

Now that both results were given, these results can be compared to investigate the benefits and possible disadvantages of carmustine combined with long-term GD.

4.5.2.3. Comparison between carmustine administered with and without GD

The respective RCG rates of each cell line at the end of the two different treatments were compared. These results are illustrated in Figure 4.8 and discussed here.

Firstly, as previously highlighted, slightly lower toxicity is evident in cells after treatment without GD than with GD. This is made clear in Figure 4.8 by the higher decrease in RCG rate of the non-cancer cell line (MCF-10A) with GD than without GD, especially at higher dosages of carmustine.

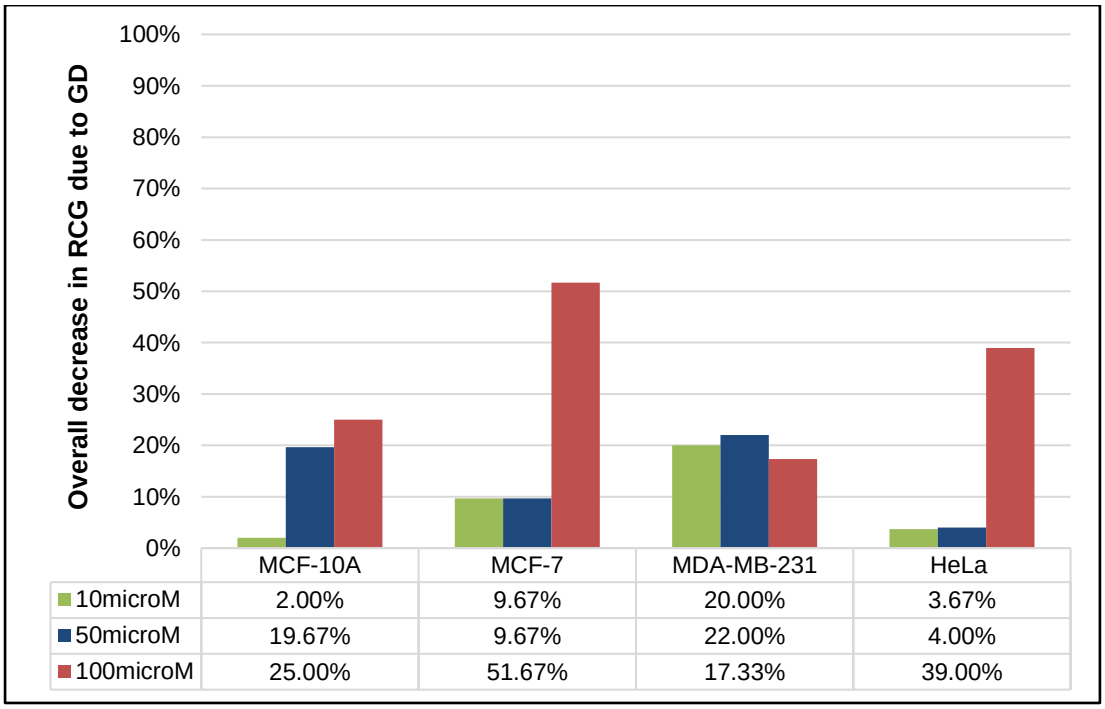

	MCF-10A	MCF-7	MDA-MB-231	HeLa
10microM	2.00%	9.67%	20.00%	3.67%
50microM	19.67%	9.67%	22.00%	4.00%
100microM	25.00%	51.67%	17.33%	39.00%

Figure 4.8. Overall decrease in RCG due to GD at different carmustine dosages.

In contrast to this, treatment with GD resulted in an additional decrease in RCG of more than 20% in all three cancer cell lines for at least one of the different carmustine dosages. It follows then that treatment with GD acquires a higher positive therapeutic response at the tested carmustine dosages. However, toxicity might become a problem for dosages above 50 μM in combination with GD.

On closer inspection of each cancer cell line, more insight is gained. Firstly, the MCF-7 breast cancer cell line is a mitochondrial oxidative phosphorylation phenotype cell line which is less dependent on glycolysis [149]. This cell line is also defined as poorly aggressive with a low metastatic potential [150]. Therefore, it was expected that this cell line would show more resistance to GD treatment than the other breast cancer cell line MDA-MB-231.

This was indeed the case. Figure 4.8 illustrated that at lower dosages of carmustine (10 μM and 50 μM), where the addition of GD decreased RCG rate by approximately 10%. However, at a much higher dose of 100 μM, treatment with GD decreased RCG by a further 51.67%.

In contrast, the other breast cancer cell line (MDA-MB-231) presents elevated glycolytic activity under normoxic conditions [79]. These cells mainly use glycolysis rather than mitochondrial respiration to produce the energy required for cell functioning and proliferation [80]. Therefore, it was expected that MDA-MB-231 would show a higher therapeutic response to the added GD treatment. This was indeed the case, with the addition of GD resulting in an additional decrease in RCG of approximately 20% for all dosages of carmustine.

Lastly, the cervical cancer cell line (HeLa), also presents aggressive growth and doubles on average every 24 hours [151]. Its primary source of energy is mostly glutamine rather than glucose, thus demonstrating dependence on oxidative phosphorylation for growth [152]. Therefore, resistance to GD was expected for this cell line since its dependency on glucose for proliferation is lower.

This resistance to GD treatment is especially evident at the lower dosages of carmustine (10 μM and 50 μM). This is illustrated in Figure 4.8 by the slight additional decrease in RCG of only 3.67% and 4.00%, respectively when GD was added. However, at the highest dose of carmustine (100 μM), the HeLa cancer cell line presented a much different response. Treatment with GD resulted in an additional decrease in RCG of 39%.

Another significant observation illustrated in Figure 4.8 is that the therapeutic efficacy of GD is greater at higher dosages of carmustine. At first glance, this may appear opportunistic; however, on closer inspection of the non-cancer cell line, toxicity becomes a problem at higher carmustine dosages.

Therefore, the question remains whether a lower dosage of carmustine can be used to achieve a similar efficacy than a higher dosage (without the added toxicity of higher dosages), by adding an adjacent therapy such as GD. This is explored in the next section.

4.5.2.4. Dosage comparison of carmustine administered with and without GD

If cell lines are similarly affected by lower chemotherapy dosages when combined with GD than at higher dosages without GD. This would substantially impact chemotherapy dosages administered in practice and future designs of clinical trials evaluating long-term KD-R.

Figure 4.9 (A-C) present the different cell lines RCG after being exposed to a lower dose of 10 μM carmustine with GD and a higher dose of 50 μM carmustine without GD. All four cell lines show similar RCG rates throughout the respective treatment durations. These results show that when combining GD with lower dosages of carmustine, the potential therapeutic efficacy outweighs the potential toxicity in these cancer cell lines.

Furthermore, Figure 4.10 (A-C) presents the different cell lines response of RCG after exposure to carmustine dosages of 50 μM with GD and a higher dosage of 100 μM without GD. Once again, these results show that the potential toxicity might outweigh the therapeutic efficacy for MCF-7 and HeLa cancer cell lines but not for the MDA-MB-231 cancer cell line.

In summary, all of the cell lines present similar therapeutic efficacy at lower dosages of carmustine when combined with GD than higher dosages without GD.

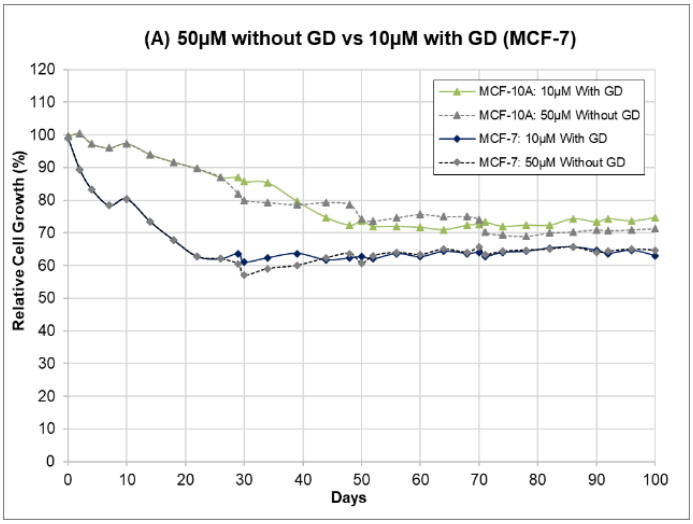

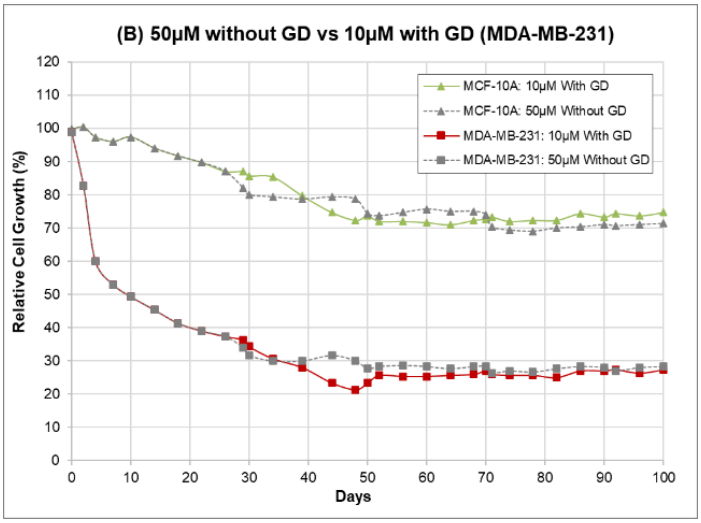

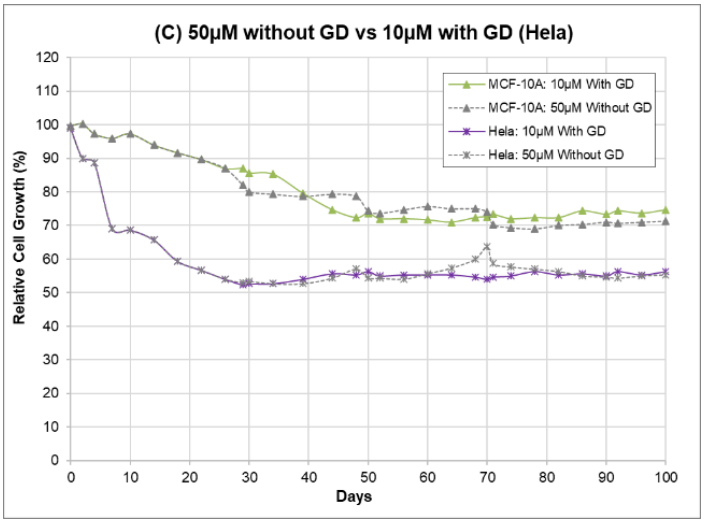

Note: Carmustine administered at a high dosage (50 μM) at typical cancer patients' glucose concentration on 6.5 mmol/L vs a fifth of the dosage (10 μM) at a glucose deprivation concentration of 3.5 mmol/L. Figure 20 is separated by the different cancer cell lines (A) MCF-7, (B) MDA-MB-231, (C) HeLa with the non-cancer cell line MCF-10A also shown in (A-C).

Figure 4.9. Lower carmustine dosages: 10 μM with GD vs 50 μM without GD.

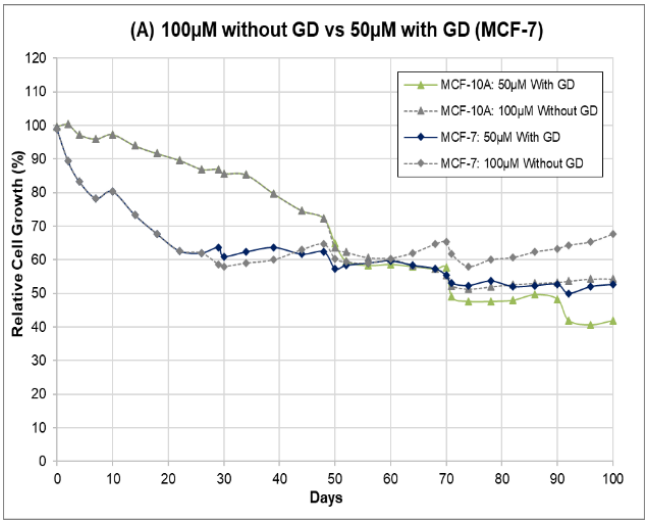

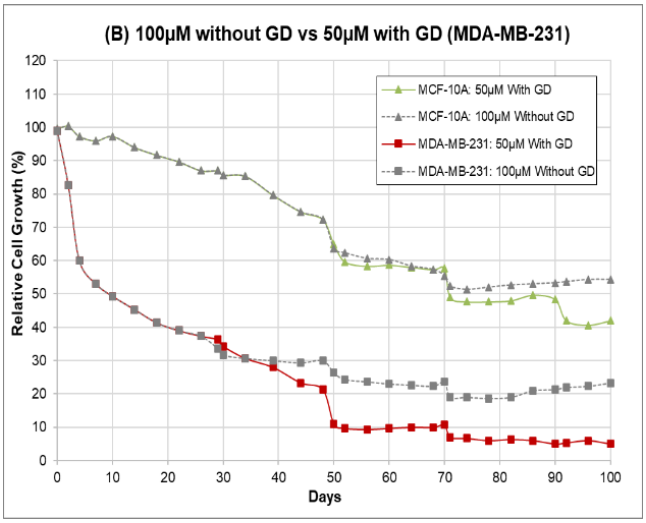

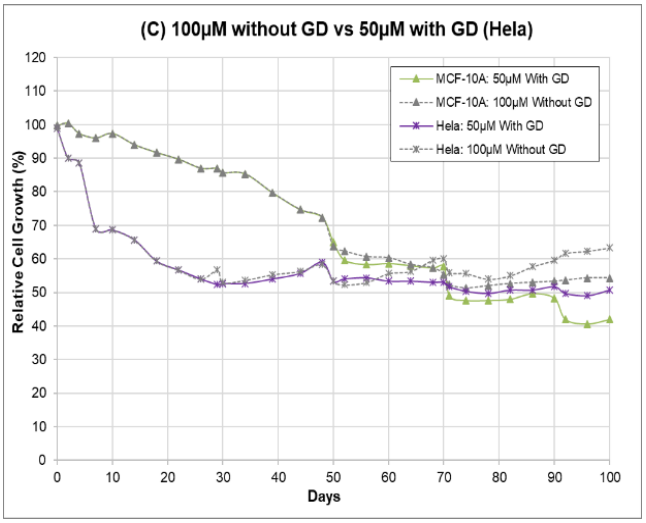

Note: Carmustine administered at a high dosage (100 μM) at typical cancer patients' glucose concentration on 6.5 mmol/L vs half the dosage (50 μM) at a glucose deprivation concentration of 3.5 mmol/L. Figure 21 is separated by the different cancer cell lines (A) MCF-7, (B) MDA-MB-231, (C) HeLa with the non-cancer cell line MCF-10A also shown in (A-C).

Figure 4.10. Higher carmustine dosages: 50 μM with GD vs 100 μM without GD.

4.6 CONCLUSIONS

This chapter explored the addition of a non-metabolic *Pulse* treatment, namely chemotherapy (paclitaxel and carmustine), to the long-term GD *Press* treatment. Furthermore, current *in vitro* tests of chemotherapy administered during metabolic treatments, KD-R, do not accurately model clinical studies.

Therefore, this study acts as a starting point to accurately model such therapies *in vitro*. This was successfully done by exposing cells to chemotherapy at typical cancer patients' glucose and glutamine concentrations, similar to Chapter 2. Thereby achieving the first objective, as outlined in Section 4.3.

The results of the combined *Press-Pulse* treatment (chemotherapy with GD) presented an increase in the efficacy of chemotherapy. The scope of the increase in efficacy was potentially linked to the cell lines need for glycolysis. However, further tests are needed to prove this statement. Therefore, the second objective, as outlined in Section 4.3, was achieved.

Furthermore, the results showed that exposure to lower dosages of chemotherapy combined with GD achieves similar RCG rates in cells as at higher dosages without GD. However, some of the cancer cell lines presented more resistance increased toxicity when combined with GD. Therefore, the last objective, as outlined in Section 4.3, was achieved.

Future work of similar tests conducted on more cancer and non-cancer cell lines should provide better insight into whether toxicity outweighs therapeutic efficacy or *visa-versa*.

4.7 NOVEL CONTRIBUTIONS

4.7.1 Novel contributions from new repeatable methods

This chapter presented the following novel preclinical chemotherapy methods:

- Cancer cells were exposed to long-term paclitaxel chemotherapy, administered at glucose and glutamine levels of typical cancer patients.
- A non-metabolic short-term *(Pulse)* adjuvant therapy, namely paclitaxel, was administered to cells in combination with long-term GD *(Press)* treatment.
- The effect of GD was tested by exposing cells to different dosages of paclitaxel during long-term GD *(Press)* treatment.

4.7.2 Novel contributions from results: Paclitaxel

The results of these novel methods provide the following novel insights into future *in vitro* tests:

- A similar reduction in RCG of cancer cells was reached when a lower dose of paclitaxel was administered in combination with GD than when a higher dose was administered without GD.
- Paclitaxel demonstrates a higher toxic effect on non-cancer cells when administered in combination with long-term GD than without GD.
- Non-cancer cell RCG rates were at times lower than some cancer cell lines' RCG rates when paclitaxel was administered with GD.
- Similar to Chapter 3, all cell lines reacted differently to the non-metabolic *Press-Pulse* treatment. Therefore, the therapeutic effect of paclitaxel combined with GD is cell line dependent.

4.7.3 Novel contributions from results: Carmustine

The results of these novel methods provide the following novel insights into future *in vitro* tests:

- A similar reduction in RCG of cancer cells was reached when a lower dose of carmustine was administered in combination with GD than when a higher dose was administered without GD.
- Carmustine demonstrates a higher toxic effect on non-cancer cells when administered in combination with long-term GD than without GD. Non-cancer cell RCG rates were similar to some cancer cell lines RCG rates when carmustine was administered with GD.
- Similar to Chapter 3, all cell lines reacted differently to the non-metabolic *Press-Pulse* treatment. Therefore, the therapeutic effect of carmustine combined with GD is cell line dependent.

CHAPTER 5
AN ENERGY RESTRICTION METHOD FOR HIGHLY-GLYCOLYTIC CANCERS

"Truth in science can be defined as the working hypothesis best suited to open the way to the next better one."

Konrad Lorenz[18]

[18]Quote Master, "Quotes About Hypothesis." [Online]. Available: https://www.quotemaster.org/Hypothesis. [Accessed: 21-Nov-2021].

5.1 PREAMBLE

Chapters 2-4 explored long-term GD *Press* treatments alone and combined with metabolic (short-term very low GD) and non-metabolic (chemotherapy) *Pulse* treatments on *in vitro* cancer cells. This chapter combines the outcomes of chapters 2-4 to develop a non-toxic short-and long-term metabolic method for cancer patients i.e. the objective of this chapter.

The chapter starts with a literature review of current short-and long-term metabolic control strategies used on cancer patients in clinical practice. The detailed methodology envisaged from insights gained in chapters 2-4 follows this. The chapter concludes with a discussion of the method's implication to clinical practice, a conclusion, and this chapter's novel contributions.

5.2 LITERATURE REVIEW

5.2.1 Current metabolic control strategies

5.2.1.1. Short-term (Pulse) pharmacological glucose and glutamine deprivation strategies

Antiglycolytic therapies such as the glycolysis inhibitor 2-deoxyglucose (2-DG), show dose limitations due to toxicity. Fortunately, a KD-R has helped to reduce this toxicity. However, this still doesn't fully exploit the potential of antiglycolytic approaches. [154]

The same toxicity problems are found in compounds that inhibit the various glutamine metabolism cycles in cancer cells [155]. These toxicities mostly include gastrointestinal and neurotoxicity when one of the following inhibitors were administered: acivicin, 6-diazo-5-oxo-L-norleucine (DON), and azaserine [76].

Therefore, it is deemed necessary to propose non-toxic, short-term methods to reduce both glucose and glutamine without inducing undesirable toxicity. However, the addition of glutamine deprivation (as discussed in Chapter 3) does not prove to add a large enough therapeutic benefit. It was decided not to focus on glutamine deprivation in this method.

5.2.1.2. Long-term (Press) glucose deprivation strategies

The most common glucose lowering diet was developed to treat epilepsy, namely KD-R [156]. The KD-R has recently been shown to increase the therapeutic efficacy of different standard of care cancer treatments such as chemotherapy and radiotherapy [56], [58]–[61], [144], [157]–[159].

Moreover, numerous preclinical studies provide evidence of a potential therapeutic effect for different cancers including; breast and ovarian [16], [160], colon [161], gastric [162], lung [59], [157], neuroblastoma [163], [164], pancreatic [59], [165] and prostate [166]–[168] cancers.

The KD-R consists of high fat and low carbohydrates and proteins, with the ratio of fats to carbohydrates usually 3:1 [169]. Long-term intake of this high fat and low carbohydrate ratio forces the body's metabolism into a state of nutritional ketosis [54], [169]

Ketosis occurs when circulating glucose levels are reduced, resulting in a decrease in glycolytic and pentose phosphate pathways used for cellular energy [170], [171]. The energy required for cellular metabolism is then supplied by water-soluble ketone bodies (D-β-hydroxybutyrate and acetoacetate) produced from the adipocyte-derived fatty acids and ketogenic dietary fat [54].

In other words, the body burns fat instead of glucose to provide energy to cells. Additional supplementation of exogenous ketones such as medium-chain triglycerides, ketone salts and/or esters can be added to a KD-R; to help maintain this state of nutritional ketosis [55]. Restricted calorie intake and/or including short-term fasting further reduce or maintain circulating BG levels without the addition of pharmaceuticals [134], [135], [172].

On the other hand, different pharmaceuticals could be used as a long-term BG deprivation strategy [93], [103]. One of the most common BG lowering medicines is metformin, which is used as an antidiabetic (BG reducing) medication [173]. Fortunately, metformin has been shown to reduce the incidence and mortality of different cancers by mimicking nutritional deprivation [80], [174]–[178].

Another factor that could influence long-term BG levels is stress [93], [179]. More specifically, stress stimulates the physiological hypothalamic-pituitary-adrenocortical response that increases BG via the secretion of glucocorticoids, endogenous opioids, and catecholamines [180]. These responses can further lead to immunosuppression, which could promote post-treatment metastasis [180].

Furthermore, stress can also increase factors that may promote tumorigenesis, namely insulin-like growth factor (IGF-10), catecholamines and/or glucocorticoids [103]. Therefore, it is important to ensure that multiple stress management strategies are included, such as exercise [93], yoga, music, meditation etc., in addition to pharmacological methods [103].

5.3 OBJECTIVES

Research objective for this chapter:

1. To develop a non-toxic glucose deprivation method to investigate the effect of combined short-and long-term metabolic treatments.

5.4 METHODS AND MATERIALS

5.4.1 Preamble

The methodology proposed in this section is illustrated in Figure 5.1 [81]**.** The full method consists of the following various steps:

1. Cancer identification
2. Proposed long-term (Press) glucose deprivation
3. Hypothesised short-term (Pulse) glucose deprivation
4. Suppression of glucose counter-regulation
5. Cerebral glucose demand control
6. Effects and safety of pharmacological agents
7. Extra patient safety measures

The two main procedures are the long-term (*Press* [103]) and short-term (*Pulse* [103]) GD strategies.

The proposed methodology only consists of standard medical procedures that have been tested on non-cancer patients. However, some of the procedures are yet to be tested on cancer patients. These differences are indicated in Figure 5.1 as “green tick marks” for standard procedures in cancer patients and “orange tick marks” if the procedure has not been tested on cancer patients.

5.4.2 Cancer identification

As novel drugs are tested on human subjects, ethical considerations are of utmost importance. Therefore, adherence to the principles of Good Clinical Practice (GCP), including Human Subject Protection (HSP), is universally recognised as a critical requirement to the ethical conduct of research involving human subjects [181].

Therefore, *Visit 1,* as shown in Figure 5.1, is the first step to identify whether the cancer patients meet all of the necessary inclusion criteria to take part in this novel treatment. The inclusion criteria will be in line with the necessary requirements to ensure that the patient's treatment risks are thoroughly explained. Also, to determine whether the treatment will have a therapeutic effect on the patient's tumour.

This leads to the second step *(Visit* 2*),* where the patient's tumour is examined to determine if it is sufficiently glucose avid. This should safeguard the possibility of the treatment having an antitumor effect. A well-established imaging technique, namely PET with the glucose radiotracer, FDG, will be used [182].

The patient's tumour metabolises FDG the same way it would metabolise glucose. The quantity of metabolised FDG relative to non-tumour tissue is produced as an image on the PET scanner. A semi-quantitative method is then used to calculate the SUV from this image [183]. Research shows that untreated glucose avid solid tumours typically have an SUV higher than 5.0 [93]. Therefore, only patients with an SUV of 5.0 or higher should be included in this treatment.

This first scan will also act as the initial scan to establish the metabolic and physical characteristics of the patient's tumour before and after the glucose-deprivation therapy (Visits 2 and 4 in Figure 5.1). These scans should be evaluated using the PET response criteria in solid tumours (PERCIST) [184].

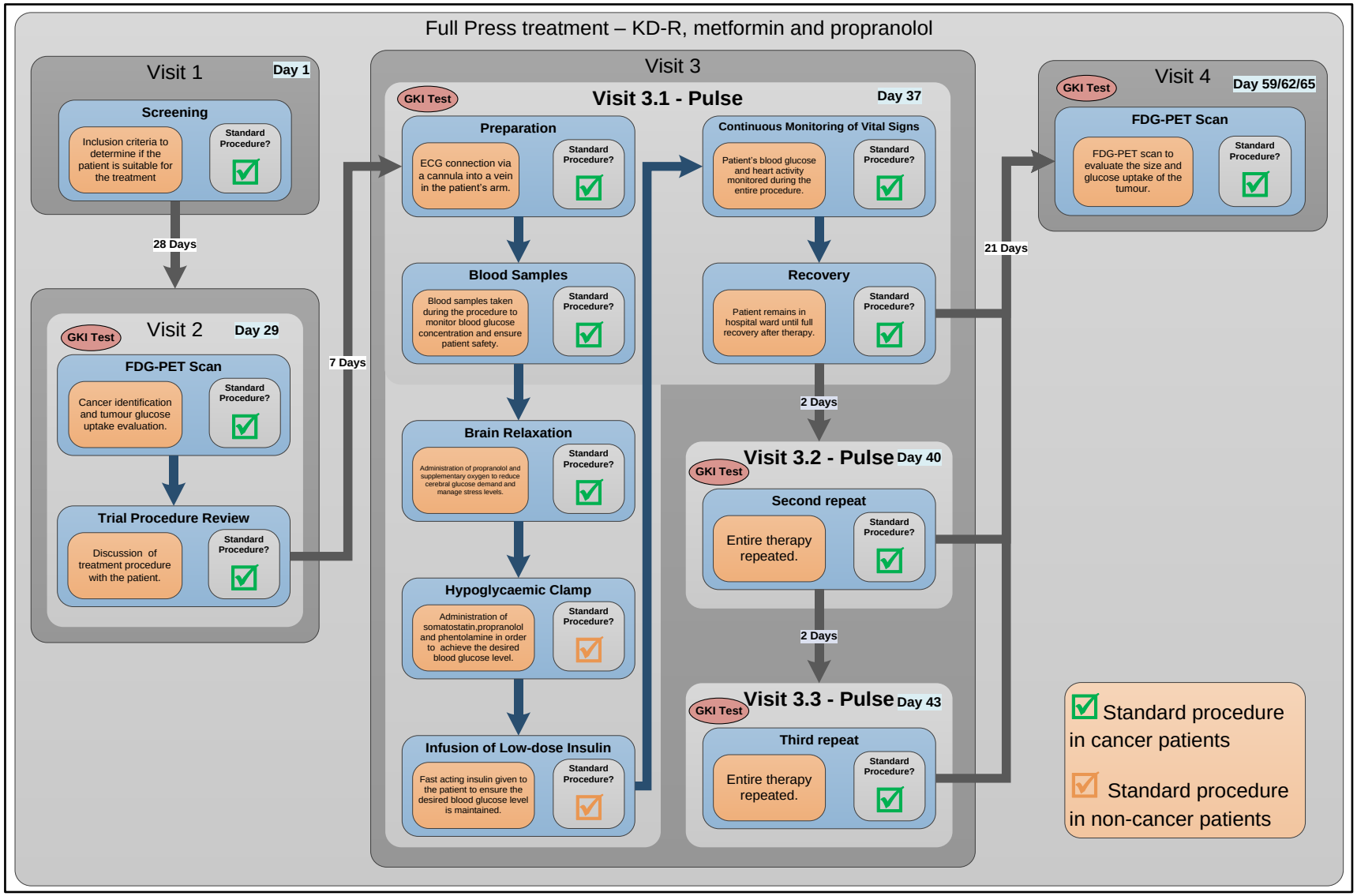

Note: Fluorodeoxyglucose based Positron Emission Tomography (FDG-PET), Electrocardiography (ECG), Glucose Ketone Index (GKI), Restricted Ketogenic Diet (KD-R).

Figure 5.1. Proposed *Press-Pulse* cancer treatment.

5.4.3 Proposed long-term glucose deprivation (*Press*)

The long-term GD should start directly after patients have passed the initial screening procedure in *Visit 1* and continue until *Visit 4*. As described in Section 5.2.1.2, similar long-term GD strategies are suggested for this treatment. This includes dietary control *via* a KD-R in combination with metformin and stress lowering agents (β-blockers).

A strict personalised KD-R will be developed for each patient by a nutritionist that will ensure BG and ketone levels are reduced to therapeutic levels [165], [171], [185]. These therapeutic levels will be monitored via a glucose-ketone index calculator (GKIC) [186]. Research shows that a manageable nutritional ketosis state is at a GKI value of less than 2.0 (preferably 1.0) [186]. Patients will undergo GKI tests before each visit during the entire treatment to ensure these GKI levels are maintained.

Certain long-term use of β-blockers such as propranolol, to reduce cancer patients' stress levels, have shown to slightly increase non-diabetic patients' BG levels [187]. Fortunately, there is a selective β_1-blocker (atenolol) that does not significantly affect glucose metabolism [188].

Therefore, atenolol should be administered to patients on a patient-specific dosage regime starting with 50 mg per day [189]. A dosage of 500 mg per day of metformin is proposed for nondiabetic patients, which will be adjusted as per BG levels of each patient[19]. These dosages will continually be adjusted during the weeks leading up to *Visits 3.1-3.3*.

5.4.4 Hypothesised short-term glucose deprivation (*Pulse*)

The short-term *in vitro* results of Chapters 2-4 [63]**,** along with previous studies [77], [78] were used to develop the therapeutic periods and BG levels for the *Pulse* treatment. The target for the very low short-term BG level (*Pulse* treatment) is between 1 and 2 mmol/L. The use of low-dose insulin in combination with glucose counter-regulation suppression should be sufficient to achieve such low levels [114].

Glucose counter-regulation has safely been achieved by suppressing glucagon secretion *via* administration of somatostatin; and by blocking epinephrine and norepinephrine actions *via* α and β-blockers (specifically the adrenergic antagonists, phentolamine and propranolol) [114], [190]. Moreover, the short-term use of propranolol impairs glucose recovery in patients after insulin-induced hypoglycaemia [191]. This will help achieve such low levels of circulating BG during the short-term *(Pulse)* treatment.

[19]Drugs.com, "Metformin - FDA Professional Drug Information," 2018. [Online]. Available: https://www.drugs.com/pro/metformin.html#Table1. [Accessed: 20-Mar-2018].

Fortunately, this is not the first time such a procedure is proposed. Rizza, Cryer and Gerich successfully carried out this method on non-cancer patients in 1979 [114]. The patients' BG levels decreased to 2 mmol/L for an *inter alia* 90 minutes. The proposed *Pulse* treatment will therefore be a replication of their method, since the procedure has been ethically approved for non-cancer patients.

There are, however, a few differences between their method and the proposed *Pulse* treatment. The first difference is that the duration at which BG levels were maintained at 2 mmol/L (90 minutes) will be doubled to 180 minutes. This coincides with the *in vitro* tests done in Chapters 2-4 [63].

Secondly, the treatment will be repeated two or three times, as shown in *Visits 3.2* and *3.3* in Figure 5.1**)**. These repeating *Pulses* are similar to the three *Pulses* done in the *in vitro* tests. However, instead of separating the *Pulses* with 21 days, the *Pulses* should only be two days apart. The shorter time between *Pulses* was chosen since a shorter treatment would be easier for cancer patients to maintain a strict KD-R. Furthermore, results of RCG in Chapters 2-4 showed no significant changes between each *Pulse* treatment.

5.4.5 Suppression of glucose counter-regulation

An initial dose of 0.04 IU/kg rapid-acting insulin will be administered to patients at *Visit 3* to achieve the desired 2 mmol/L BG level [114]. This dosage typically achieves such low BG levels within 15 minutes [114], [192]. The patient's BG counter-regulation should further be suppressed during the 180 minutes by administering the combination of somatostatin, phentolamine and propranolol. This step is referred to as the "Hypoglycaemic Clamp" step of *Visit 3* in Figure 5.1.

The respective dosages that have been used to maintain this hypoglycaemic clamp are somatostatin at 250 µg/h, phentolamine at 500 µg/min and propranolol at 80 µg/min [114]. As an inherent safety feature, glucose is expected to slowly appear in the blood. Therefore, additional low-dose insulin should be administered at 0.014 IU/kg (if necessary) to maintain BG levels at 2 mmol/L.

5.4.6 Controlling of cerebral glucose demand

The brain forms a large part of the bodies glucose utilisation, consuming at least 25% of all circulating glucose supply while only receiving 15% of total blood flow [193]. The human brain only accounts for approximately 2% of total body weight while demanding approximately 20% of the total body energy consumption [194].

This amounts to a 10-times higher cerebral energy requirement per gram of tissue than the whole-body average. Moreover, in a fasted state, the brain consumes approximately 60% of circulating glucose [195], [196].

It is, therefore, crucial to address the brain's energy and metabolic needs, especially when considering potential short-term glucose-lowering therapies [81], [86], [93]. Very low BG levels generally contribute to neurogenic and/or neuroglycopenic symptoms [197]–[199]. Neurogenic (adrenergic) symptoms include palpitations, tremors, hunger, or sweating, whereas neuroglycopenic symptoms (shortage of glucose in the brain) often include behavioural changes, difficulty thinking, and/or frank confusion [197]–[199].

In severe cases, it can lead to short-term cognitive impairment requiring external assistance for recovery [200], seizure, coma, and even death [197]–[199]. If BG levels fall below 1 mmol/L for an extended period of time, neuronal death could occur [201]. These complex responses to low BG levels and associated neurological risks further illustrate the importance of controlling the brain's energy and metabolic needs.

The energy produced by the mitochondria in the brain is almost entirely derived from the oxygen-dependent metabolism of glucose [202]. Consequently, a decrease in oxygen supply to the brain *via* cerebral blood flow could result in severe ischemic brain damage [202]. Therefore, the appropriate oxygen delivery to the brain is an important aspect of patient care [203]. Supplemental oxygen could be administered *via* low-flow nasal cannula, simple face masks, non-rebreather masks, or Venturi masks [203].

In addition to the supplemental oxygen, the aforementioned β-blocker (propranolol) also acts as a relaxant to decrease metabolic stimuli in the brain [194], [204]. This step is illustrated in Figure 5.1 by the "Brain Relaxation" step of *Visit 3*.

It is important to note that the proposed GD procedure was done on non-cancer patients without permanent adverse neurological effects [114]. However, this treatment is proposed for cancer patients and therefore, extra safety precautions are discussed in the next sections.

5.4.7 Pharmacological agents' previous use in cancer patients

Safety is the most important aspect to consider when hypothesising a new treatment. The pharmacological agents proposed in this treatment have all safely been administered to cancer patients. Some have even been shown to have a positive effect on cancer control.

Several *in vitro* and *in vivo* studies provide evidence of the β-adrenergic inhibitor, propranolol, to inhibit the development of metastases [205]–[207]. For example, propranolol has been

administered to breast cancer patients in phase two clinical trial [205]. The outcomes of this trial show how propranolol can safely inhibit several pathways related to metastasis [205].

Furthermore, the long-term use of propranolol has been shown to reduce breast cancer-specific mortality [208], [209], enhance the survival rate of prostate cancer and reduce metastases [210]. The use of atenolol and propranolol should also inhibit the tumour promoting effects of stress hormones (epinephrine and/or norepinephrine) [211], [212].

The other two pharmaceutical agents used at *Visit 3.1* for the hypoglycaemic clamp (somatostatin and phentolamine) have also been used in cancer treatments. Somatostatin has been shown to inhibit the growth of pancreatic and breast cancer cells *in vitro* and has also been used to treat pituitary, insulinomas and carcinoid tumours [213]–[215]. Phentolamine, on the other hand, has been used in cancer patients to alleviate pain [216].

Metformin has been used to treat type 2 diabetes mellitus patients since its discovery in 1950 [173]. Recent studies present several epidemiologic, clinical and preclinical evidence pertaining to its therapeutic effect on different cancers [16], [174], [177], [217]. Therefore, its use in diabetic cancer patients is common but less common in non-diabetic cancer patients. Therefore, dosages and BG levels of each patient should continuously be monitored to ensure that nothing more than what is needed is administered.

It should be noted that insulin has been found to stimulate glycolysis and are overexpressed in cancer cells, driving growth and proliferation [93], [218]. Therefore, the use of insulin to decrease BG levels is not ideal. However, the proposed dosage is low (similar to basal rates), and the procedure has previously been ethically approved on non-cancer patients [114]. For these reasons, the use of insulin should be sufficient. Future research should focus on rapidly reducing BG levels without the use of insulin.

5.4.8 Initial extra patient safety precautions

Patient safety is the most important factor of any novel medical treatment. To ensure patient safety, the possible safety risks and measures are discussed here.

Extra safety precautions: Short-term *(Pulse)* BG deprivation

The main risk factor in the proposed method is the short-term *(Pulse)* BG deprivation treatment. Therefore, it is important that this step is piloted in a hospital.

The patients will therefore be in a controlled environment where specialists such as an oncologist and endocrinologist can continuously monitor their vital statistics. Continuous

monitoring of vitals should include, but not be limited to, the following: BG, electrocardiography (ECG), blood pressure, heart rate, oxygen saturation, carbon dioxide saturation arterial pH, Na^+, K^+, Ca^{2+} and Cl^-, as illustrated in Figure 5.1 by the “Continuous Monitoring of Vital Signs” step of *Visit 3*.

Since insulin is produced naturally by the pancreas to regulate BG levels, the administration of additional insulin to decrease BG could lead to the aforementioned hypoglycaemic problems. The dosages of each patient should continuously be monitored to ensure patient safety [219].

The patients are expected to develop various hypoglycaemic symptoms during the short-term severe GD and less so during the long-term glucose deprivation. These symptoms are expected to mainly be neurogenic such as sweating, hunger, and paraesthesia, palpitations, tremor, and anxiety [190]. Nevertheless, uncontrollable excessive hypoglycaemia is always a risk and therefore, emergency glucose infusion should be on hand.

The previously described reduction in cerebral glucose demand should minimise these neurogenic symptoms during hypoglycaemic BG levels. Fortunately, if any cognitive impairment resides, full cognitive recovery is expected after one and a half days of severe hypoglycaemia [220].

The proposed supplemental oxygen for cerebral glucose demand is an extra safety precaution. Since previous short-term very low BG levels (as low as 0.5 mmol/L) has been achieved without any adverse events, see Table 3.1 in Chapter 3. Moreover, the study done by Rizza, Cryer, and Gerich [114] (on which the short-term *(Pulse)* treatment was developed) safely achieved a BG value of 2 mmol/L without supplemental oxygen.

Another extra safety precaution is the administration of exogenous ketone supplements, which is an important energy source for the brain during the hypoglycaemic clamp and nutritional ketosis [171]. Examples of exogenous ketones are medium-chain triglycerides l, ketone salts and/or esters.

If the cancer treatment is successful, rapid cell death of cancer cells could lead to acute tumour lysis syndrome such as hyperkalaemia, hyperphosphataemia, hypercalcaemia, or hyperuricaemia [221], [222]. For this reason, blood gas analysis of potassium (> 6 mmol/L or 25% increase from baseline), phosphate (> 2 mmol/L or 25% increase from baseline), calcium (> 1.75 mmol/L or 25% change from baseline), and uric acid (> 476µmol/L or 25% increase from baseline) should continuously be monitored [221], [223], [224].

If the patient experiences any of these symptoms, the doctor must take the necessary precaution measures to ensure that the symptoms are resolved. It is advised that the following intravenous fluid is on hand, namely isotonic sodium bicarbonate [224], [225] and rasburicase (or allopurinol) [221], [224], [225].

Extra safety precautions: Long-term *(Pulse)* BG deprivation

Regarding safety of the less strenuous long-term *(Press)* GD therapy, the KD-R is a well-established safe diet [59]. Further, for more than 30 years, atenolol has been used safely as a stress suppression treatment[20]. On the other hand, the administration of metformin could result in metformin-associated lactic acidosis.

This is only a potential risk, since metformin-associated lactic acidosis rare [226]. However, it is important to ensure that metformin dosage is either reduced or discontinues when a patient's estimated glomerular filtration rate is <30 mL/min/1.73 m^2 [226]. Lactic acidosis can also be treated by administering dichloroacetate[21]. Dichloroacetate could potentially also enhance cancer cell death since DCA has shown to have an anti-cancer effect in both *in vitro* and *in vivo* models [227].

Lastly, if any patient experiences severe symptoms, GD treatment must be stopped immediately, and the necessary precaution measures should be followed to ensure patients safety.

5.5 CONCLUSIONS

Most cancer cells have a higher energy demand for glucose compared to non-cancer cells. They are also less flexible to metabolic changes and struggle to metabolise nutrients other than glucose and glutamine as efficiently. In this chapter, a hypothetical method was proposed that capitalises on this therapeutic window *via* BG deprivation.

The method consists of moderate long-term *(Press)* GD and more intense (very low) short-term *(Pulse)* GD. The moderate long-term *(Press)* GD has previously been shown to be effective and safe in cancer patients [17, 34]. Whereas the short-term *(Pulse)* GD treatment has been shown to be effective in *in vitro* cancer cell models [78], [228] (also see Chapter 2) and proven to be safe in non-cancer patients [114].

Previous studies of very low GD treatments used glucose inhibitors, which led to problems with toxicity [103]. The newly proposed very low GD *Pulse* treatment should not have such problems.

[20]FDA, "U.S. Food & Drug Administration," 2018. [Online]. Available: https://www.accessdata.fda.gov/scripts/cder/ob/results_product.cfm?Appl_Type=A&Appl_No=072303. [Accessed: 04-Jun-2018].
[21]National Institutes of Health, "PubChem - Dichloroacetic Acid," 2018. [Online]. Available: https://pubchem.ncbi.nlm.nih.gov/compound/6597#section=Information-Sources. [Accessed: 31-May-2018].

Therefore, this chapter's research objective, as detailed in Section 5.3, was achieved. Furthermore, this treatment method could further be refined by adding other non-metabolic treatments such as chemotherapy.

As shown in Chapter 4, cancer cells are more vulnerable to chemotherapy during long-term GD. This has also been confirmed in other studies [25], [53], [130]–[134]. However, as shown in the results, toxicity might become an issue when GD is combined with higher dosages of chemotherapy. It is therefore prudent to ensure that the efficacy always outweighs toxicity.

5.6 NOVEL CONTRIBUTIONS

5.6.1 Novel contributions from the new non-toxic method

Current glucose inhibitors, which are used to achieve very low glucose levels in patients, have problems with toxicity. In this chapter, a non-toxic *Press-Pulse* method was developed to reduce a cancer patient's blood glucose to very low levels (without the concomitant toxicity) for a short-term period. Such a detailed method does not exist in literature. This method forms the basis of a comprehensive protocol that may be used, after approval, for future metabolic clinical trials.

5.6.2 Dissemination of results

This chapter has already been successfully published in the medical scientific journal, *Medical Hypotheses* (impact factor 1.3 at the time of writing) with the following title: *A hypothetical method for controlling highly glycolytic cancers and metastases.* DOI number: 10.1016/j.mehy.2018.06.014 (see Appendix C for the published manuscript).

The manuscript has also been recognised within the cancer research scientific community, evident from the following citations:

1. R. J. Klement. "The emerging role of ketogenic diets in cancer treatment." Curr Opin Clin Nutr Metab Care, vol. 22, pp. 129-34, 2019. doi:10.1097/MCO.0000000000000540.
2. R. M. Baiardo, A. Zangrillo, V. Gregorc, F. Ciceri, L. Dagna, Y. Tshomba, *et al.* "How to obtain severe hypoglycemia without causing brain or cardiac damage." Medical Hypotheses, vol. 130, 2019. doi:10.1016/j.mehy.2019.109276.
3. E. H. Mathews, M. H. Visagie, A. A. Meyer, A. M. Joubert, G. E. Mathews. "In vitro quantification: Long-term effect of glucose deprivation on various cancer cell lines." Nutrition, vol. 74, 2020. doi:10.1016/j.nut.2020.110748

PART B:

A SYSTEMS ENGINEERING APPROACH TO EXPLORE THE MECHANISMS OF INTERACTION BETWEEN SEVERE COVID-19 AND ITS CHD COMPLICATIONS

CHAPTER 6
INTEGRATED CHD/COVID-19 MODEL

"Learn to see. Everything connects to everything else."

Leonardo da Vinci[22]

[22]Goodreads, "Leonardo da Vinci Quotes." [Online]. Available: https://www.goodreads.com/quotes/679908-learn-how-to-see-realize-that-everything-connects-to-everything . [Accessed: 21-Nov-2021].

6.1 PREAMBLE

This chapter focuses on a systems engineering approach to explore the mechanisms of cardiovascular complications in coronavirus disease of 2019 (COVID-19). The chapter starts with an extensive review of current literature on COVID-19 and its cardiovascular complications. This includes the description of an existing CHD model and the need to integrate this model with the phenomenology of COVID-19. The objectives and respective sections in which they are addressed follow. The methods used to integrate the existing CHD model with the pathogenic pathways of COVID-19 activated CHD biomarkers and traits are presented.

A discussion of the resulting model suggests systematically how the pathogenesis of nine *health factors* (e.g., stress, exercise, smoking) and seven *pharmaceutical interventions* (e.g., statins, salicylates, thrombin inhibitors) may either aggravate or suppress COVID-19 severity. These insights are valuable in identifying new *pharmaceutical interventions*, help understand how *health factors* influence COVID-19 severity and give a fully integrated explanation for the COVID-19 *death spiral* phenomenon seen in some patients.

With insight gained from this chapter, recommendations are made for future research questions. The chapter concludes with the novel contributions of this chapter.

6.2 LITERATURE REVIEW

The coronavirus disease of 2019 (COVID-19) is caused by the infection of severe acute respiratory syndrome coronavirus 2 (SARS-CoV-2), which first emerged in December 2019 in Wuhan, China [229]. In March 2020, the World Health Organisation declared this disease a pandemic [38]. As of 8 August 2021, the total number of confirmed global deaths were 4 285 421 [230].

It is widely accepted that COVID-19 severity is increased by respiratory complications such as hypoxia. Critically ill patients developing hypoxemia require supplemental oxygen and/or mechanical ventilation [42], [231]. Although this condition is respiratory-related, this hypoxia is fuelled by vascular complications, documented in numerous autopsies [40]–[44]. Moreover, pre-existing cardiovascular-related comorbidities are known risk factors that increase COVID-19 severity. These comorbidities include, amongst others, *Hypertension*, *Hyperglycaemia/Hyperinsulinaemia*, obesity and/or chronic cardiac disease [45]–[49].

Furthermore, hospitalised critically ill (severe) COVID-19 patients experience cardiovascular complications such as cardiac injury, thrombosis, arrhythmia, heart failure and myocardial

infarction [232]–[236]. This is again substantiated by autopsies that present various findings of vasculature damage that leads to a state of *Hypercoagulability* in deceased COVID-19 patients [40]–[44].

Most severe COVID-19 patients also experience a chronic heightened *Inflammatory state*, especially within the alveoli and pulmonary capillaries [237]–[239]. This may be as a result of the dysregulated hyperimmune response [237] and/or direct viral infection mediating inflammatory cell infiltration [46], [239].

Therefore, the prevailing viewpoints in literature are that most severe cases of COVID-19 (i) result in cardiovascular complications [40]–[44] and/or (ii) are seen in patients with pre-existing cardiovascular comorbidities [45]–[49]. A need therefore exists to further investigate the underlying mechanisms/pathogenesis between cardiovascular disease and Covid-19.

To fully investigate this, the pathogenesis of cardiovascular disease and COVID-19 needs to be integrated. Fortunately, most of the above mentioned vascular COVID-19 effects are also seen in an existing model of coronary heart disease (CHD) shown in Figure 6.1 [240], [241]. These effects are depicted in Figure 6.1 as the following CHD hallmarks (yellow boxes): *(A) Hypercoagulability, (B) Hypercholesterolaemia, (C) Hyperglycaemia/Hyperinsulinaemia, (D) Inflammatory state,* and *(E) Hypertension.*

Hypercholesterolaemia is a common CHD risk factor, known to aggravate vascular cell dysfunction, aggravate coagulation and upregulate inflammation [242]–[244]. The *Hypercholesterolaemia* CHD hallmark, *(B)* in Figure 6.1, has only been partially linked to COVID-19 through high circulating cholesterol levels that may make a person more susceptible to infection [245].

Although this might still be controversial, a recent molecular study showed that SARS-CoV-2 requires cholesterol for viral entry [246]. Subsequently, another molecular study (yet unpublished) showed how cholesterol optimally positions furin for priming SARS-CoV-2[23]. In other words, cholesterol improves binding to ACE2 receptors while producing a more infectious virion[23].

Another association is envisaged between increased COVID-19 severity and *Hypercholesterolaemia,* through vascular complications that arise from high cholesterol levels. Since both *Hypercoagulability* and *Inflammation* are known risk factors for COVID-19 and *Hypercholesterolaemia* influences both these hallmarks [240], *Hypercholesterolaemia* was also included in the *integrated CHD*/COVID-19 *model* (more detailed discussions are given in Section 6.5.2.1 and Section 6.5.4).

[23]H. Wang, Z. Yuan, M. A. Pavel, and S. B. Hansen, “The role of high cholesterol in age-related COVID19 lethality.,” bioRxiv (Preprint), pp. 1–17, 2020.

All of the CHD Hallmarks identified in the CHD model (Figure 6.1) play a significant role in COVID-19 severity. In this chapter the CHD pathogenic pathways are integrated with those of severe COVID-19 complications, using a systems-based approach.

6.3 OBJECTIVES

The research objectives for this chapter are the following:

1. To develop an *integrated CHD/COVID-19 model*, which explains the mechanisms of interaction of severe COVID-19 on the vascular system.
2. To use the *integrated CHD/COVID-19 model* to
   (a) investigate why some patients with severe COVID-19 experience sudden death,
   (b) examine the effect of CHD comorbidities on COVID-19 severity,
   (c) examine how different *health factors* influence COVID-19 severity, and
   (d) explore how various CHD *pharmaceutical interventions* could help reduce an individual's risk of developing severe COVID-19.

6.4 METHODS

The methodology to develop the pathogenic pathways for the *integrated CHD/*COVID-19 *model* is divided into three parts, namely:

- Section 6.4.1 describes the existing CHD model [240].
- Section 6.4.2 discusses the systems-based method for integration (Figure 2) of COVID-19 factors into the CHD model (Figure 6.1). The outcome of this method is depicted in Figure 6.3 to Figure 6.6 and Figure 6.8 to Figure 6.10. Its implications are discussed in the results Sections 6.5.1 and 6.5.2.
- Section 6.4.3 describes the method to evaluate the effects on COVID-19 severity of *health factors* (blue ovals) and *pharmaceutical interventions* (blue boxes) as depicted in Figure 6.1. The relevant pathogenic pathways that are activated are discussed in more detail in the results Sections 6.5.3 and 6.5.4.

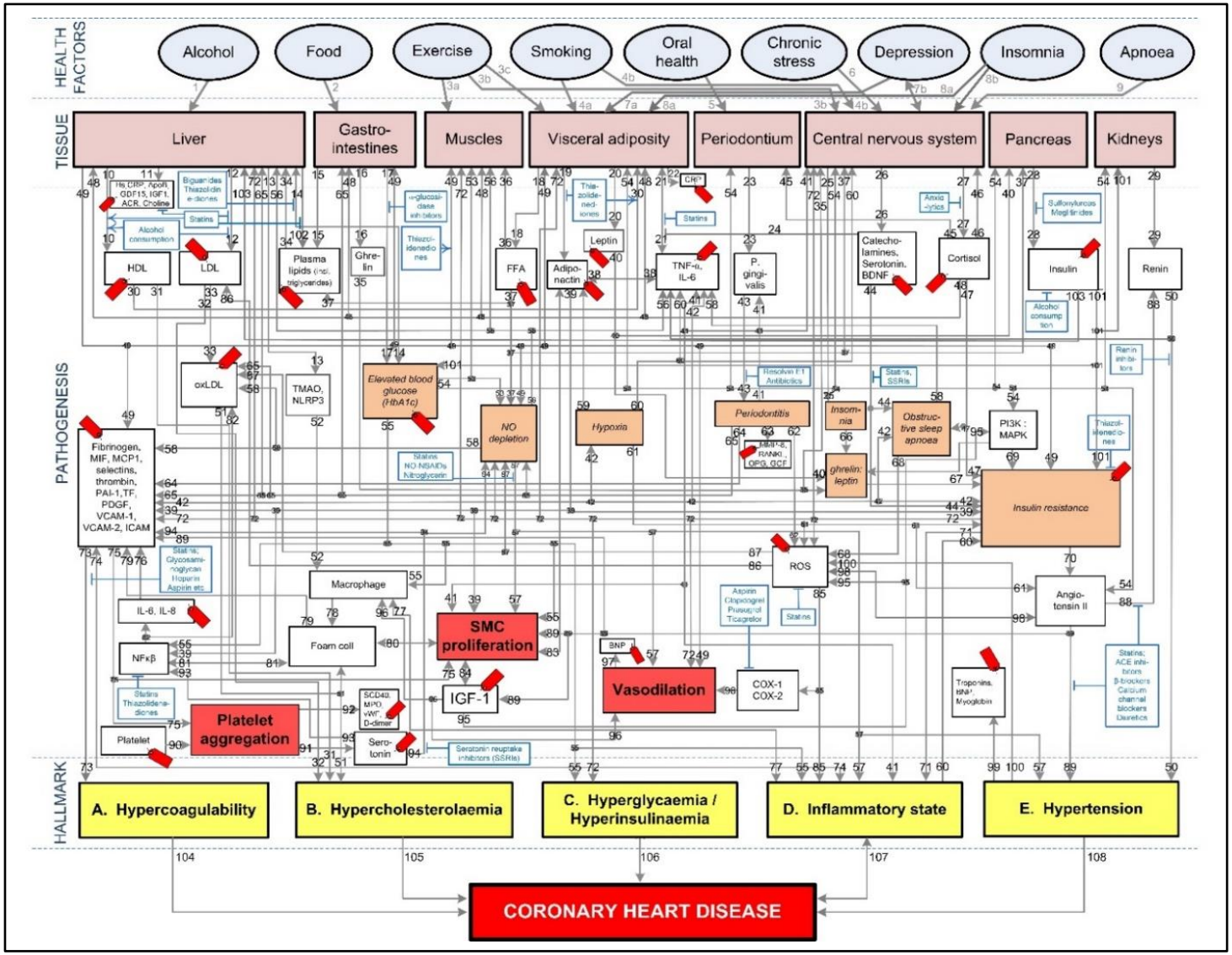

Note: The affective pathway of pharmaceuticals, blue boxes, is shown in Figure 6.1 and salient serological biomarkers are indicated by the red tags (🏷). The blunted blue arrows denote antagonise or inhibit and pointed blue arrows denote up-regulate or facilitate. Refer to the Abbreviations section at the beginning of the thesis and the Glossary section at the end of the thesis for the abbreviations and definitions.

Figure 6.1. CHD model before integration with COVID-19 [240], [241], [247]–[250].

6.4.1 Description of existing CHD model

The existing CHD model (Figure 6.1) was developed as a PhD study, extensively described in [240]. The mode is available online from the university [240]. Some results and implications of the model were published [241], [247]–[250]. Hence, only the relevant salient elements are discussed here. The model defined CHD as the incidence of atherosclerosis, coronary artery disease, or myocardial infarction [240]. Subsequently, results for cardiovascular disease were interpreted as CHD only in scenarios where the effect of a stroke could be accounted for [240].

Although cerebrovascular disease is also a component of cardiovascular disease it was thus not addressed here. This proposed *integrated CHD/*COVID-19 *model* is therefore based primarily on CHD attributes, with focus on vascular complications induced by the SARS-CoV-2 virus. It is acknowledged that other pathogenic pathways may exist, such as the cerebrovascular ones [251], which should warrant further research in an extended model.

The CHD model, presented in Figure 6.1, was developed by analysing the effect of different *health factors* (blue ovals) on *body tissues* (pink boxes) and investigating the respective *pathogenesis* (grey lines with numbers), *traits* (orange boxes) and activated *biomarkers* (white boxes) related to an increased risk of CHD [240], [241], [247]–[250].

Each grey line and respective number in the CHD model correspond to a certain pathogenesis pathway that could typically be present in a CHD patient. These pathways are visual representations of previously published literature, which link the effects of *health factors* (blue ovals) to the relevant *tissues* (pink boxes) and subsequently to the hallmarks of CHD (yellow boxes) [240], [241], [247]–[250].

The traits are represented in the lightly shaded orange boxes. Biomarkers are indicated as white boxes, with those that are typically measured, denoted with red tags *(✎)*. The *pharmaceutical interventions*, acting on the respective pathways are indicated as blue boxes, where blunted blue arrows *(⊣)* denote antagonise or inhibit and pointed blue arrows *(→)* denote up-regulate or facilitate [240], [241], [247]–[250].

6.4.2 Systems-based integration of COVID-19 factors into the CHD model

The systems-based integration methodology discussed here is depicted as three phases in a flow chart in Figure 6.2. The iterative approach followed here is to ensure that only pathways discussed in literature, with substantial evidence, are included. Figure 6.3 shows the COVID-19 pathways in green, with all other pathways of the original model in Figure 6.1 transparent.

Phase 1: SARS-CoV-2 and CHD

SARS-CoV-2, which causes Covid-19, was incorporated into the existing CHD model by investigating pathogenic pathways and biomarkers reported in literature. These biomarkers and pathways were either included or excluded based on the following five steps, presented in Figure 6.2 (Phase 1).

Step (1): Firstly, the relevant tissue (denoted as pink boxes in the right-hand corner of Figure 6.3) through which the SARS-CoV-2 virus (green oval in Figure 6.3) enters the body is evaluated. Although Endothelial Cell (EC) injury was discussed as the critical element in CHD in [240], it is not shown in Figure 6.1. EC injury is added as a green box between pathways 110, 111, 112, and 116 at the bottom of Figure 6.3.

Step (2): The activated CHD related biomarkers, traits or hallmarks, reported in severe COVID-19 patients are then identified from literature. These are respectively denoted in Figure 6.3 as white, orange and yellow boxes.

Step (3): In this step the identified CHD biomarkers, traits or hallmarks found in literature are evaluated, in order to determine whether the activation of these occurs directly or indirectly as a result of the SARS-CoV-2 virus. Steps (4) and (5) describe the two possible outcomes of the identification process.

Step (4): If the activation occurs directly, as determined in Step (3), then a new (green) pathway leading from the virus to the respective CHD biomarker, trait or hallmark is added to the integrated model in Figure 6.3.

Step (5): If the activation occurs indirectly, as determined in Step (3), then a new biomarker or trait is added to the model, e.g., the inflammatory cytokines in the top, right-hand white box between pathways 107, 108 and 115 in Figure 6.3. A biomarker or trait is only added if its respective pathway eventually leads to the activation of a CHD hallmark.

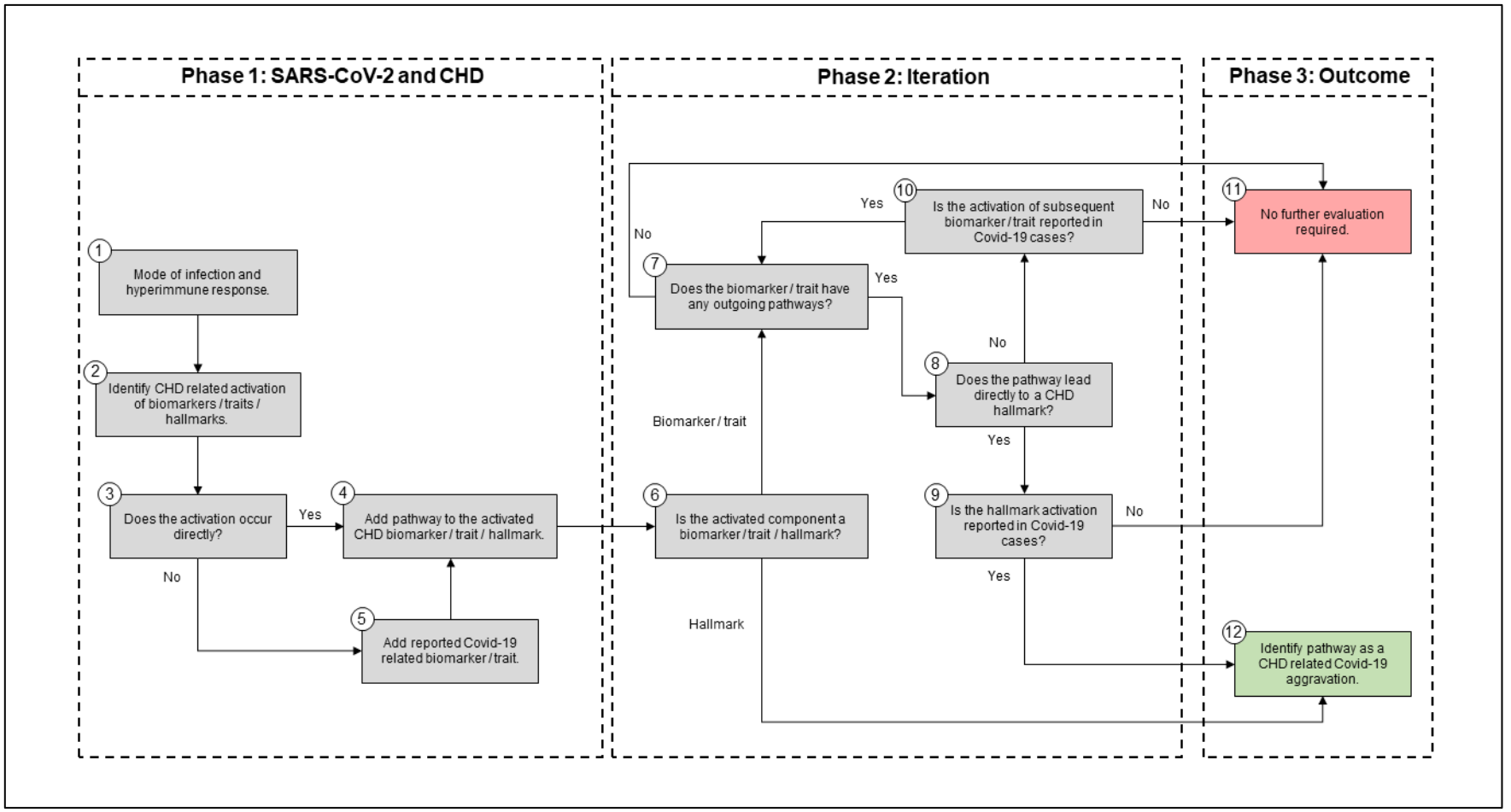

Figure 6.2. Methodology used to develop an Integrated CHD/COVID-19 model.

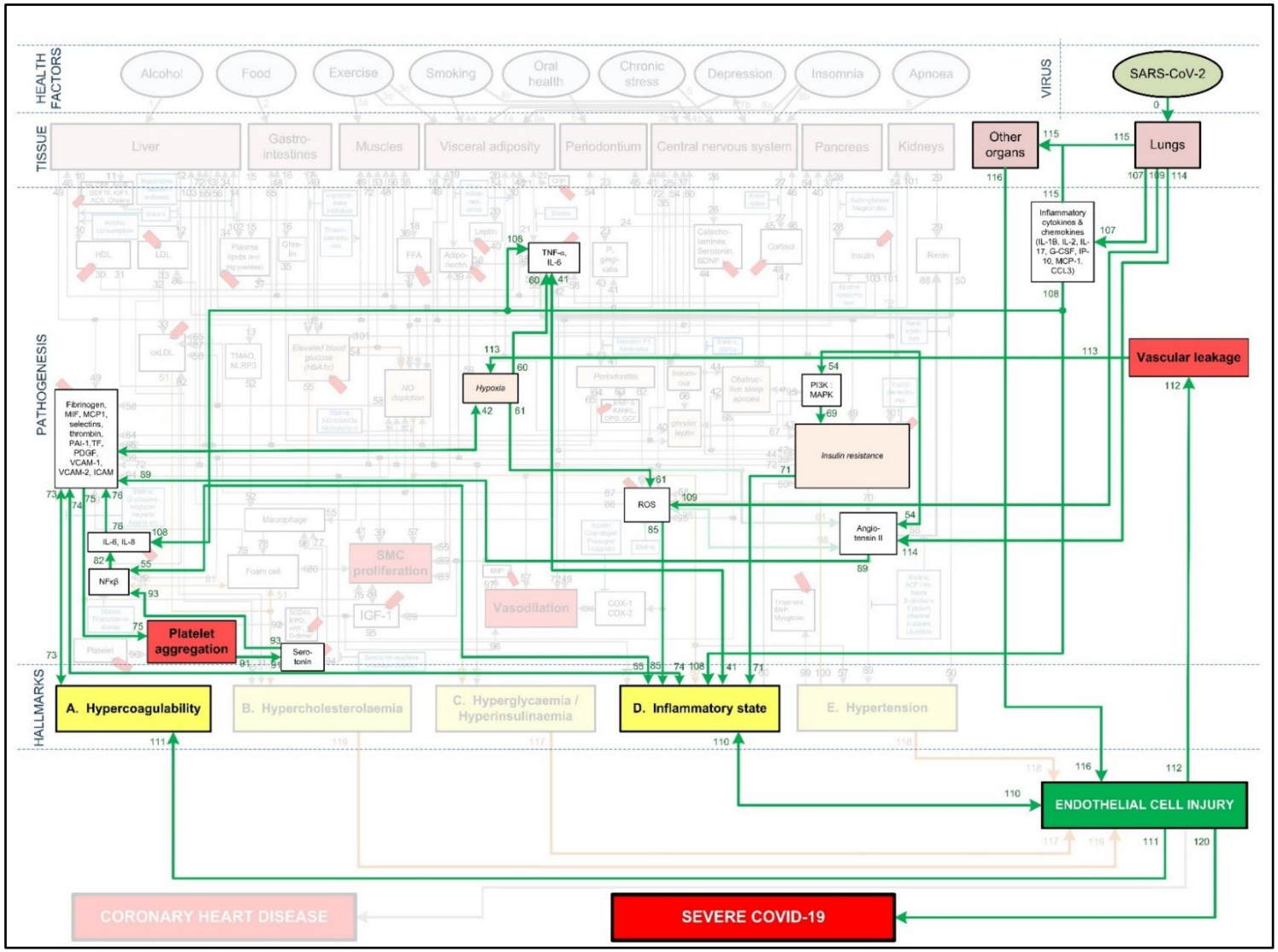

Figure 6.3. Integration of COVID-19 pathogenic pathways into the CHD model.

Phase 2: Iteration

For the iteration process in Phase 2, the following steps are conducted:

Step (6): The activated component (CHD hallmark, biomarker or trait) from Step (4), to which the green pathway from Step (4) leads, is further evaluated based on literature. If this component is a biomarker or trait, then Step (7) follows. If this component is rather a CHD hallmark, then Step (12) follows.

Step (7): In this step it is determined whether the CHD biomarker or trait has any outgoing (grey) CHD pathways. Most biomarkers and traits have outgoing CHD pathways. These grey CHD pathways are further assessed in Step (8). For the biomarkers and traits with no outgoing grey pathways (e.g., troponin for pathway 99 in Figure 6.3) Step (11) follows.

Step (8): In this step, it is determined whether the grey CHD pathway leads directly or indirectly to a CHD hallmark (yellow boxes in Figure 6.3). If the grey CHD pathway leads directly to a CHD hallmark then Step (9) follows, otherwise Step (10) follows.

Step (9): The CHD hallmark is further investigated to ensure its activation due to SARS-CoV-2 is relevant to severe COVID-19 patients. If it is reported in literature to be aggravated in severe COVID-19 patients then Step (12) follows (changing the grey pathway to a green pathway), otherwise Step (11) followes (keeping the pathway grey). These steps are explained in more detail in Phase 3.

Step (10): As determined in Step (8), the relevance to COVID-19 severity of the subsequent CHD biomarker or trait to which the grey CHD pathway led to is investigated. If relevance is found, then this CHD biomarker or trait is re-evaluated by following the same approach as in Step (7).

Phase 3: Outcome

This phase presents the two possible outcomes after integration and iteration of the identified biomarkers, traits, CHD hallmarks and their relevant pathways.

Step (11): This step is followed if the activated CHD biomarkers or traits have (i) no other outgoing CHD pathway, or (ii) the outgoing pathway leads to another biomarker or trait that has no relevance to severe COVID-19 patients. If one of these two conditions are met, then the biomarker, trait and the subsequent pathway are not evaluated further.

These biomarkers, traits and respective pathways e.g., oxidised low-density lipoprotein (oxLDL), nitric oxide (NO) depletion and cortisol, are made transparent as shown in Figure

6.3. Although these biomarkers or traits do not have a direct link to COVID-19 patients, they may influence COVID-19 severity indirectly by affecting one of the CHD hallmarks. This idea is discussed in more detail in Section 6.5.2.

Step (12): Step (12) is followed if the investigated biomarker, trait, CHD hallmark and respective pathways are relevant in most COVID-19 patients with severe disease and these are therefore prominently shown as green lines in Figure 6.3.

The COVID-19 pathways described in this section are shown as green lines in Figure 6.3. The final step is to show all the CHD pathways together with the COVID-19 pathways. The complete *integrated CHD/*COVID-19 *model,* is given in Figure 6.4*.*

6.4.3 Verification: Evaluation of health factors and pharmaceutical interventions

As previously defined, verification implies that the proposed solution is correctly implemented and thereby provides the expected results. The existing CHD model was developed by evaluating the pathogenic pathways of different *health factors* and their influence on the five CHD hallmarks [240]. Subsequently, *pharmaceutical interventions* were added onto the respective pathways on which they act and reduce CHD risk [240].

Therefore, to verify that the systems-based integration method was correctly implemented, the risk factors of each *health factor* and *pharmaceutical interventions* for CHD and COVID-19 were compared. It is expected that the *health factors* and *pharmaceutical interventions* risk factors will be similar. The *health factors* (blue ovals) in Figure 6.4 were defined as the following [240]:

- **Alcohol use:** Indicates moderate alcohol consumption (20g - 30g alcohol (ethanol) per day for men and half of that for women).
- **Food:** High glycaemic diets (HGD) (glycaemic load > 142).
- **Exercise:** Regular moderate exercise (550-3000 kcal/week).
- **Smoking:** Current smoker.
- **Oral Health:** Poor oral health in the form of periodontal disease.
- **Stress:** Chronic-level stress at work or home.
- **Depression:** Self-diagnosed, physician-diagnosed or use of antidepressants
- **Insomnia:** Inability to fall asleep or to maintain sleep.
- **Apnoea:** Obstructive sleep apnoea (apnoea-hypopnea index > 5 per hour).

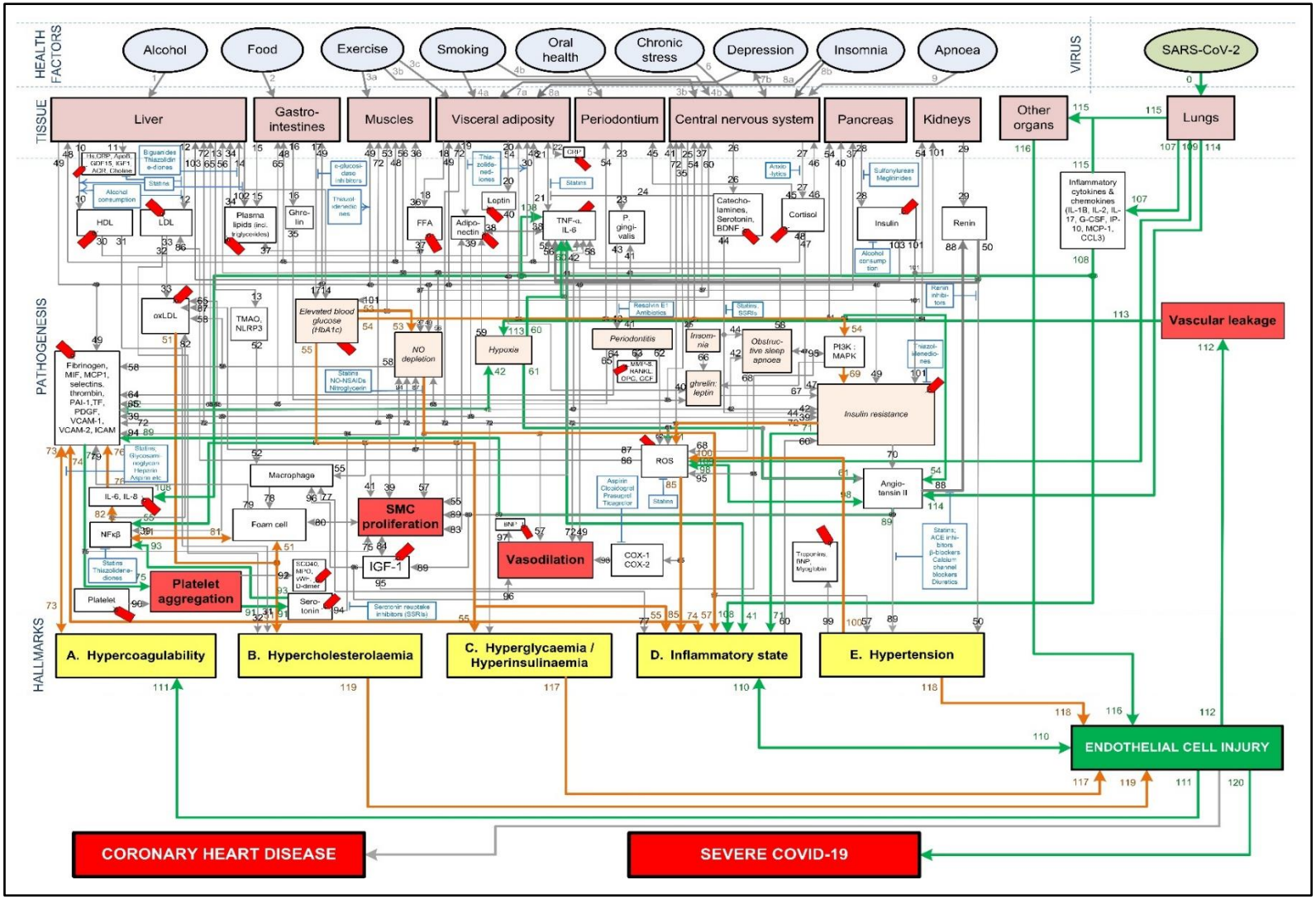

Figure 6.4. Proposed *integrated CHD/COVID-19 model*.

Section 6.5.3 discusses how a healthy vascular “baseline”, as a result of a healthy lifestyle, will influence COVID-19 severity.

The *pharmaceutical interventions* that were investigated were limited to those investigated in the original CHD model [240]. These include statins, salicylates (aspirin), indirect thrombin inhibitors (heparin), direct thrombin inhibitors (angiomax), Angiotensin-converting-enzyme (ACE) inhibitors, angiotensin-renin inhibitors, β-blockers, calcium channel blockers, diuretics, biguanides (metformin) and antidepressants. These are indicated in Figure 6.1 as blue boxes.

Although larger studies of how the *health factors* and *pharmaceutical interventions* influence a person’s risk for CHD are usually available, COVID-19 data are often limited. Nevertheless, several studies exist that evaluated the effect of many *health factors* and *pharmaceutical interventions* on COVID-19 severity. Limitations of these studies are that they vary in study size and design, i.e. some studies are case-control studies hence only reporting odds ratio (OR), whereas others are cohort studies or clinical trials that report on relative risks (RR) or hazard ratios (HR).

Unfortunately, RR, HR and OR are not the same and should only be compared in cases where the event being assessed is rare in the control group. In other words, the baseline risk of the control group should approximately be zero. However, at present it is the best information one has. Until better data becomes available, these studies were used as an initial indicative comparison between the effect what *health factors* and *pharmaceutical interventions* have on CHD risk and COVID-19 severity. This also applies to the data used to compare the risk between coagulation and COVID-19 severity in Section 6.5.1.3.

In this chapter the comparison of the data between CHD risk and COVID-19 severity was graphically reported using a non-traditional method [240], [241], [247]–[250]. The risks that indicate an increase in disease severity are displayed as reported, whereas the risk values that show a decrease in severity are presented as the inverse of the reported value.

This method presents a better visual illustration when comparing an increase and decreased risk. For example, a conventional RR = 3 constitutes to a three-fold increase in risk while a RR = 0.33 constitutes to a three-fold decrease in risk (1/0.33 = 3).

6.5 RESULTS AND DISCUSSION

Section 6.5.1 discusses the results of Figure 6.3, Figure 6.5 and Figure 6.6 in detail illustrating the detrimental interplay between inflammation, EC injury, coagulation and hypoxia. This visually explains the *death spiral* seen in some COVID-19 patients.

Section 6.5.2 discusses how each pre-existing CHD comorbidity or hallmark could further aggravate this *death spiral.* Figure 6.5, Figure 6.6, and Figure 6.8 to Figure 6.10 illustrate how patients with pre-existing *Hypercholesterolaemia* (Figure 6.8), *Hyperglycaemia/Hyperinsulinaemia* (Figure 6.9) or *Hypertension* (Figure 6.10) could aggravate this *death spiral.* Note that Figure 6.3, Figure 6.5, Figure 6.6, Figure 6.8, Figure 6.9 and Figure 6.10 are simplified versions of the fully *integrated CHD*/COVID-19 *model of* Figure 6.4. Only the prominent pathways, which are needed to explain a specific phenomenon, are shown in these Figures.

In Sections 6.5.3 and 6.5.4 the effects that *health factors* and *pharmaceutical interventions* have on developing severe COVID-19 are discussed with reference to the model in Figure 6.4.

6.5.1 Integrated CHD/COVID-19 model

6.5.1.1. EC injury from SARS-CoV-2 viral infection

Cell entry and pathologic effects of the SARS-CoV-2 virus mostly occur through two pathways, namely (i) the mucous membranes (primarily infecting the nasal epithelia) or (ii) the respiratory tract (infecting respiratory epithelial cells) [252]. This infection typically occurs *via* ACE2 [252], which partially decreases ACE2 function. This leads to an upregulation of angiotensin II effects, including amongst others, an enhanced *Inflammatory* response [234], [252], increased EC injury [253] and state of *Hypercoagulability* seen in severe COVID-19 patients [40]–[44].

These effects are illustrated in Figure 6.3 by following the relevant pathways (green lines with numbers) from SARS-CoV-2 (green oval) to the respective biomarkers (white boxes) or traits (orange boxes) and/or hallmarks (yellow boxes). For the rest of this chapter, the model is interpreted as follows:

(i) Evidence from literature describing the pathogenesis with the respective references.

(ii) These relevant pathways in Figure 6.3 to Figure 6.6, Figure 6.8 and Figure 6.9 are then given to illustrate the pathogenesis. Each pathway starts with the relevant tissue, biomarker or trait.

(iii) The relevant pathway (pw) numbers (#) are denoted as (pw#) e.g., pathway 112 (pw112) links EC injury with vascular leakage.

(iv) The upwards arrow (↑) represents an upregulation of the respective biomarker/trait/hallmark while the downwards arrow (↓) represents a downregulation.

Figure 6.3 illustrates how viral infection from SARS-CoV-2 may lead to an activation of a pro-inflammatory state, which causes EC injury *via* the following process:

- Angiotensin II can downregulate phosphoinositide 3-kinase (PI3K) pathway, which increases insulin resistance that directly effects inflammatory state [254]. The relevant pathways in Figure 6.3 are: SARS-CoV-2 viral infection within the lungs *via* (pw0), which through (pw114) upregulates angiotensin II. This follows a downregulation of biomarker PI3K *via* (pw54) that increases insulin resistance through (pw69). This leads to a pro-inflammatory state *via* (pw71), which, through (pw110), results in EC injury.
  The notation for this pathway and the rest of the chapter will be as follows: *SARS-CoV-2-(pw0)-Lungs-(pw114)-↑angiotensin II-(pw54)-↓PI3K-(pw69)-↑insulin resistance-(pw71)-↑inflammatory state-(pw110)-↑EC injury.*
- Angiotensin II can also upregulate various reactive oxygen species (ROS) at the site of infection, which causes a heightened inflammatory response [254]. See Figure 6.3 pathways: *SARS-CoV-2-(pw0)-Lungs-(pw114)-↑angiotensin II-(pw98)-↑ROS-(pw85)-↑inflammatory state-(pw110)-↑EC injury.*
- An upregulation of angiotensin II may increase platelet factors, which increases the risk for coagulability [254], [255]. Since hypercoagulation and inflammation are interrelated, an inflammatory state may be enhanced [255]. See Figure 6.3 pathways: *SARS-CoV-2-(pw0)-Lungs-(pw114)-↑angiotensin II-(pw89)-↑platelet factors-(pw73)-↑Hypercoagulability-(pw73)-(pw74)-↑inflammatory state-(pw110)-↑EC injury.*
- Furthermore, an increase in platelet factors can also upregulate platelet aggregation [254]. This could increase the inflammatory mediator nuclear factor-kappa-beta (NFκβ), aggregating inflammation [254]. See Figure 6.3 pathways: *SARS-CoV-2-(pw0)-Lungs-(pw114)-↑angiotensin II-(pw89)-↑platelet factors-(pw75)-↑platelet aggregation-(pw91)-serotonin-(pw93)-↑NFkβ-(pw55)-↑inflammatory state-(pw110)-↑EC injury.*

In addition to this pro-inflammatory state that causes EC injury, the virus can also directly cause EC injury in other organs. This could happen if the virus enters the bloodstream and binds to ACE2 receptors located in other organs [44]. Considerable evidence shows that the lungs of patients who died from COVID-19, have severe EC injury (endothelialitis) associated with the presence of intracellular viral infection [42]. The presence of viral particles were also

found in the ECs of the liver, kidneys and heart [44], [256]. This could then lead to inflammation and EC damage at the infected organ. See Figure 6.3 pathways: *SARS-CoV-2-(pw0)-Lungs-(pw115)-infect other organs via blood-(pw116)-↑EC injury.*

6.5.1.2. EC injury from a hyperimmune response to infection

Infection from SARS-CoV-2 causes damage-associated molecular patterns to occur, which can trigger a hyperimmune response. Most severe cases of patients with COVID-19 display a defective hyperinflammatory state with significantly increased serum levels of pro-inflammatory cytokines and chemokines [257]–[260].

This overproduction of pro-inflammatory cytokines and chemokines can damage lung infrastructure and further induce EC injury of pulmonary blood vessels [234], [237], [261], see Figure 6.3 pathways: *SARS-CoV-2-(pw0)-Lungs-(pw107)-↑pro-inflammatory cytokines & chemokines-(pw108)-↑inflammatory state-(pw110)-↑EC injury*.

Most critical cases show increased levels of, amongst others, the pro-inflammatory cytokines interleukin-6 (IL-6), interleukin-8 (IL-8) and tumour necrosis factor-α (TNF-α) [257]–[259]. These pro-inflammatory cytokines directly cause an upregulation of inflammation directly [261]. See Figure 6.3 pathways: *SARS-CoV-2-(pw0)-Lungs-(pw107)-↑pro-inflammatory cytokines-(pw108)-↑TNF-α, IL-6-(pw41)-↑inflammatory state-(pw110)-↑EC injury.*

These cytokines can also indirectly upregulate inflammation through dysregulation of platelet factors [262]. See Figure 6.3 pathways: *SARS-CoV-2-(pw0)-Lungs-(pw107)-↑pro-inflammatory cytokines-(pw108)-↑IL-6, IL-8-(pw76)-↑platelet factors-(pw74)-↑inflammatory state-(pw110)-↑EC injury*.

Furthermore, a hyperinflammatory state induced by an unmodulated immune response can also cause EC injury. This happens when neutrophils activate pathways that elevate reactive oxygen species (ROS) [239], [263]. See Figure 6.3 pathways: *SARS-CoV-2-(pw0)-Lungs-(pw109)-↑ROS-(pw85)-↑inflammatory state-(pw110)-↑EC injury*.

A hyperinflammatory response of cytokines can circulate to other organs. This could lead to acute inflammation such as septic shock and/or multiple organ damage, which may further cause EC injury [264]. See Figure 6.3 pathways: *SARS-CoV-2-(pw0)-Lungs-(pw107)-pro-inflammatory cytokines & chemokines-(pw115)-other organs-(pw116)-↑EC injury*.

6.5.1.3. *The death spiral: Inflammation, EC injury, coagulation, vascular leakage and hypoxia*

Hypoxia shown in Figure 6.1 and Figure 6.3 to Figure 6.6 includes hypoxemia. Although hypoxia might be respiratory related, vascular related EC injury could be one of the main factors fuelling this hypoxia [261], [265], [266]. This vascular related hypoxia may result from either hypercoagulation or vascular leakage, both stemming from EC injury [234], [239], [261], [262], [265], [266].

Vascular leakage from EC injury leads to an increase in leucocytes and platelets as well as vascular permeability [266]. This results in fluid from the blood to enter the alveoli, filling the alveolar space. In turn it decreases the efficiency of gas exchange in the lungs [266]. This prevents the body from taking in sufficient oxygen, leading to different severity levels of hypoxia [266]. These pathways are denoted in Figure 6.5 as: *EC injury-(pw112)-↑vascular leakage-(pw113)-↑hypoxia*.

On the other hand, coagulation stemming from EC injury articulates glycoproteins that are involved in haemostasis, to which platelets bind. This consequently upregulates the expression of platelets, which are the prime activators of a coagulation cascade [239], [267]. This leads to a high possibility of disseminated intravascular coagulation, congestion of the small capillaries by inflammatory cells and thrombosis in larger vessels [261].

Congestion or clogging of pulmonary blood vessels could increase hypoxemia *via* ventilation/perfusion mismatch and low level of mixed venous blood oxygen [265]. This build-up of blood clots in blood vessels within the lungs are commonly found in critically ill and non-surviving COVID-19 patients [43], [238], [268].

These pathways are denoted in Figure 6.5 as: *EC injury-(pw111)-↑Hypercoagulability-(pw73)-↑platelet factors-(pw42)-↑hypoxia.* Hypoxia also results in further upregulation of inflammation by activating IL-6 & TNF-α [269] or increasing ROS leading to further EC injury [270]. See Figure 6.5 pathways: *Hypoxia-(pw60)-↑TNF-α, IL*-6-*(pw41)-↑inflammatory state* or *Hypoxia-(pw61)-↑ROS-(pw85)-↑inflammatory state-(pw110)- EC injury*.

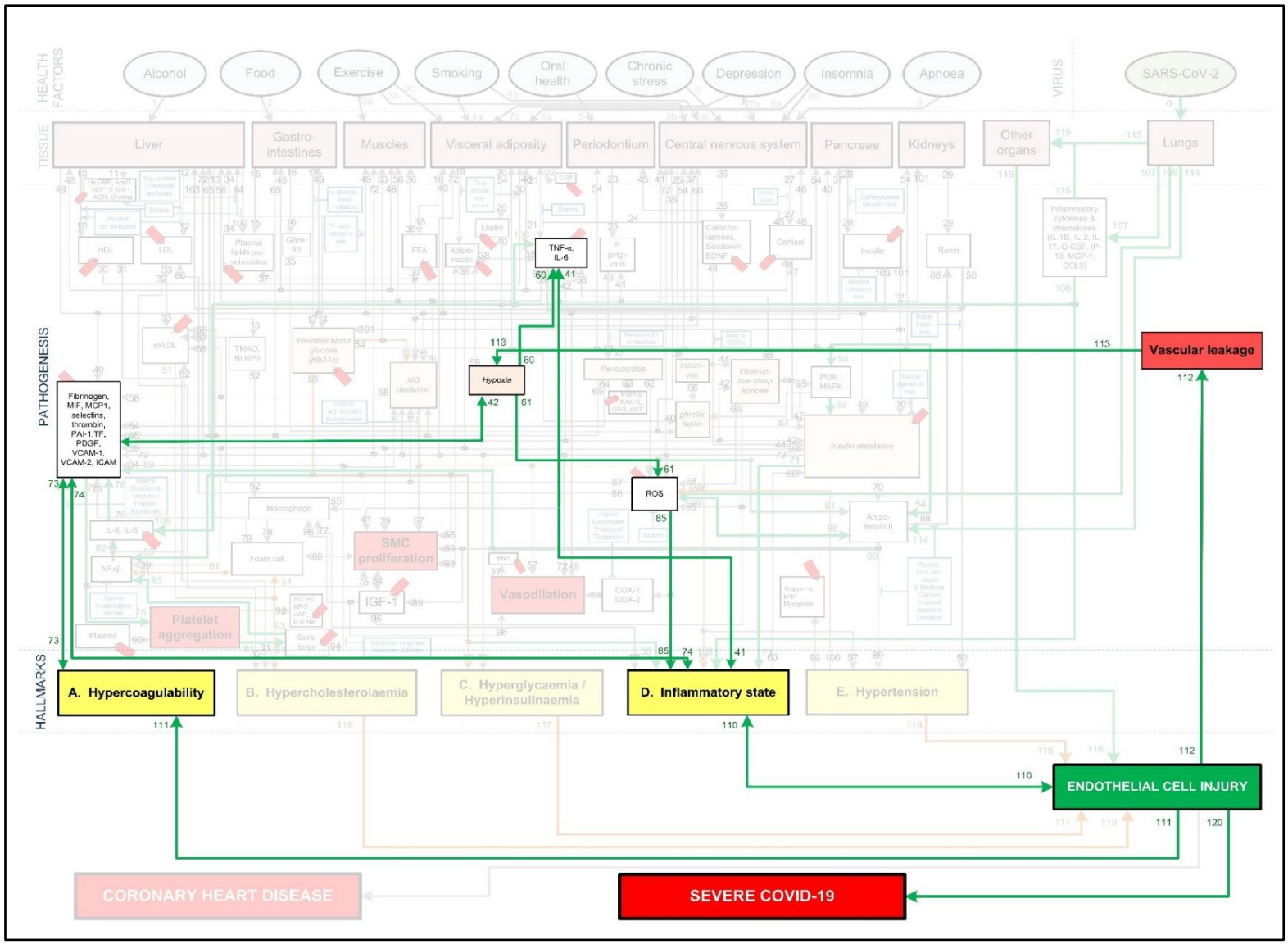

Figure 6.5. *Death spiral* evident in some critically ill COVID-19 patients.

With the aforementioned knowledge a summary of the main pathogeneses describing the *death spiral* are given. Note that inflammation has two different outgoing pathways (loops) that can lead to increased hypoxia. Both pathways are denoted in Figure 6.5 as follows:

1. **Hypercoagulability (positive feedback loop 1):** Inflammation from COVID-19 results in EC injury which may activate the coagulation cascade, forming microthrombi in the blood vessels near the alveoli [40]–[44]. This reduces oxygenation efficiency, see pathways: ↑*inflammatory state –(pw110)-EC injury-(pw111)-*↑*Hypercoagulability-(pw73)-*↑*platelet factors-(pw42)-*↑*hypoxia-(pw60)-*↑*TNF-α, IL-6-(pw41) AND/OR (pw61)-*↑*ROS-(pw85)-*↑*inflammatory state-(pw110)-Loop repeated-(pw120)-Severe* COVID-19*.*
2. **Vascular leakage (positive feedback loop 2):** Inflammation from COVID-19 results in EC injury. EC injury in blood vessels near the alveoli can lead to vascular leakage [239]. This causes fluid build-up within the alveoli [266], subsequently reducing oxygenation efficiency, see pathways: ↑*inflammatory state –(pw110)-EC injury-(pw112)-*↑*vascular leakage-(pw113)-*↑*hypoxia-(pw60)-*↑*TNF-α, IL-6-(pw41) AND/OR (pw61)-*↑*ROS-(pw85)-*↑*inflammatory state-(pw110)-Loop repeated-(pw120)-Severe* COVID-19*.*

A simplified schematic of the *death spiral* is illustrated in Figure 6.6, which shows the two closed positive feedback loops leading to hypoxia. If a COVID-19 patient becomes hypoxic, it is important to break these loops by administering supplemental oxygen. This is currently done in practice where supplemental oxygen reduces disease severity in hypoxic COVID-19 patients [271].

To reduce the risk of developing hypoxia one should focus on reducing inflammation that leads to the downstream effects, namely EC injury, coagulation and vascular leakage. This is also seen in practice where various pharmaceutical interventions that treat inflammation have shown promising results e.g. corticosteroid dexamethasone in later stage of illness [272] and anti-inflammatory drugs (Celebrex [273] and aspirin [274]).

If one focuses on loop 1 it is expected that people who have a higher risk of developing blood clots (coagulation) should have a higher risk of developing severe COVID-19. There are several uncontrollable factors that are known to increase a person's risk of developing blood clots, namely gender, age, ethnicity, blood type and pregnancy.

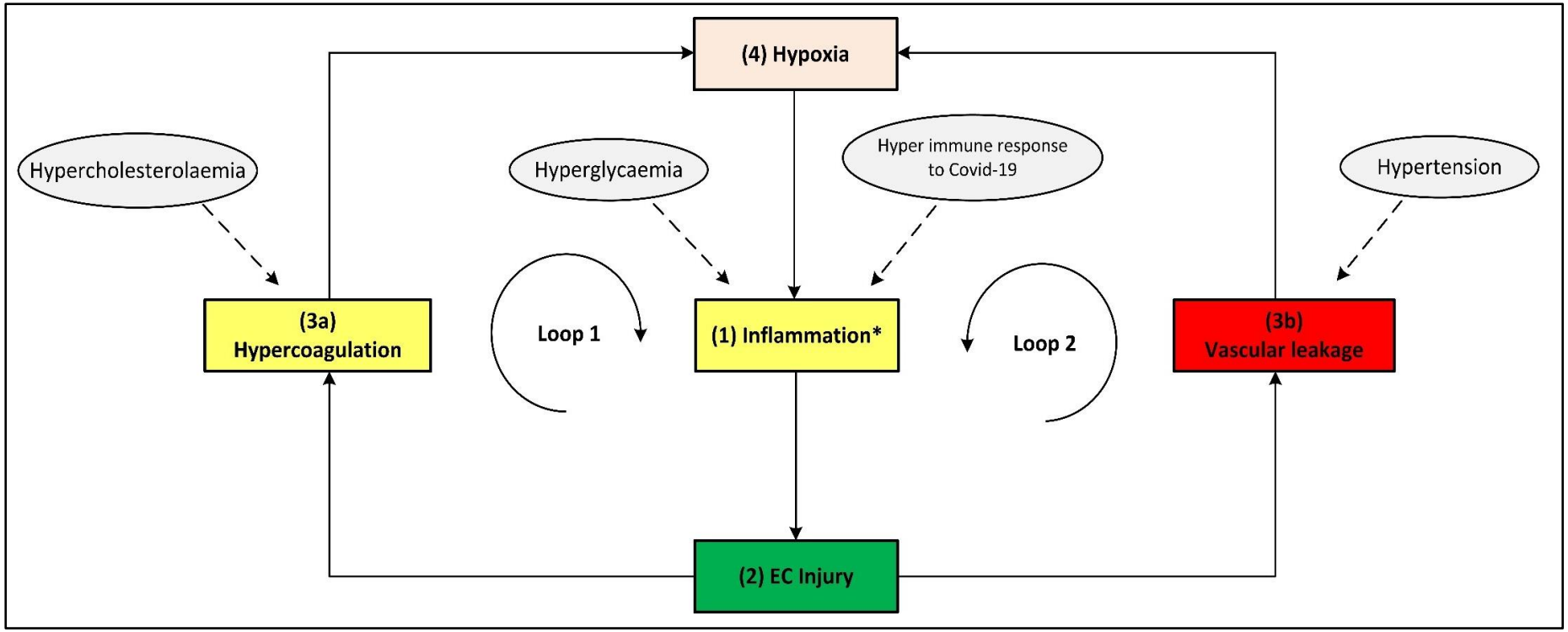

Note: The *death spiral* can be summarised as follows: Increased (1) inflammation at the lungs causes (2) EC injury, which can result in activation of the (3a) coagulation cascade and/or (3b) vascular leakage at the lungs, thereby causing (4) hypoxia which further increases inflammation, creating two closed positive feedback loops and causing severe COVID-19 through a *death spiral.* * As described in the text, this inflammation is initiated by various factors, primarily by a hyperimmune response to the infection of SARS-CoV-2 (cytokine storm) but also other factors such as *hyperinsulinaemia/hyperglycaemia* or *hypercholesterolaemia.*

Figure 6.6. Simplified *death spiral* evident in some critically ill COVID-19 patients.

Although this does not help the patient, it is of interest to help understand COVID-19 severity in these individuals. The data for the risk of coagulation (blood clots) and COVID-19 severity for these individuals are given in Table 6.1. A qualitative graphical comparison between the data for coagulation and COVID-19 severity from Table 6.1 is given in Figure 6.7.

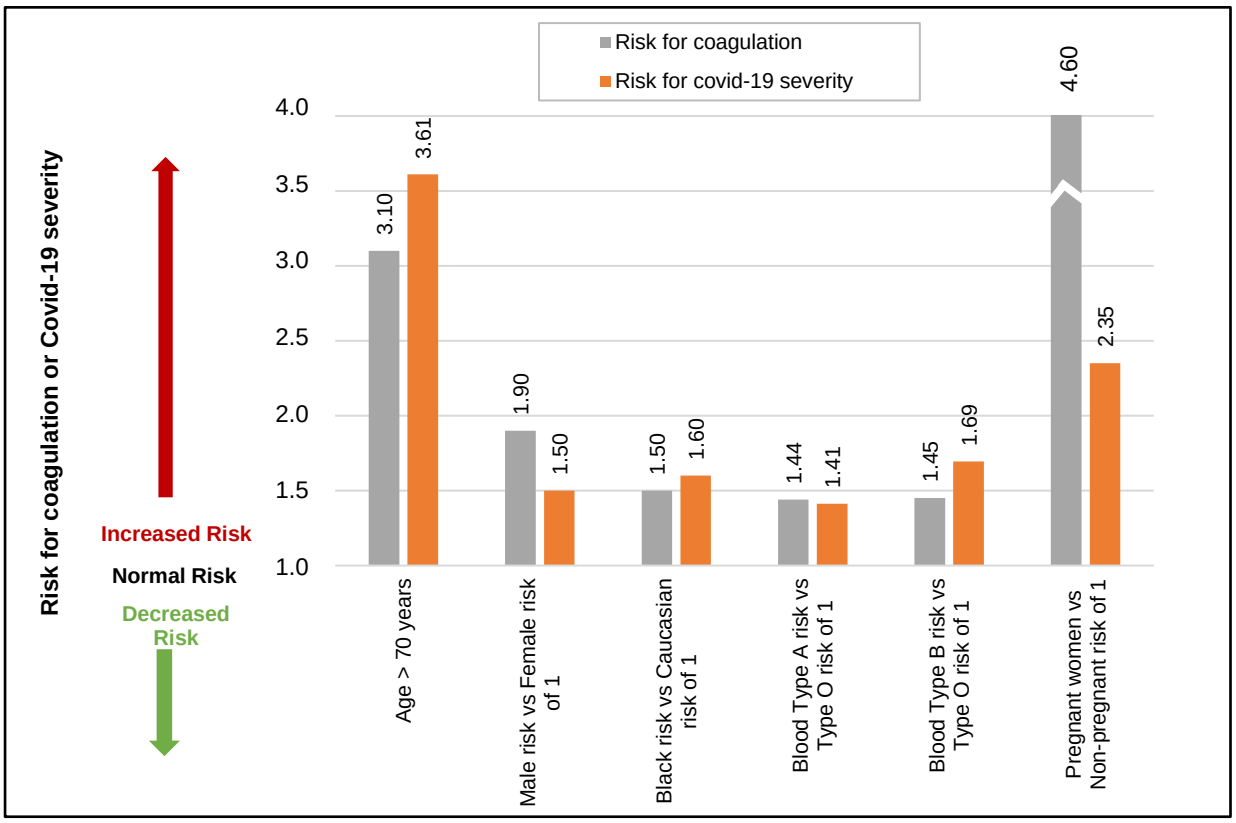

Note: An accurate quantitative comparison is not possible, mostly due to differences in study design and size.

Figure 6.7. Qualitative comparison of coagulation and COVID-19 severity risk.

(a) Age

Age is an independent risk factor of coagulation, with thrombotic incidences increasing rapidly in people older than 70 years [275]. The odds of venous thromboembolism in a person older than 70 years is three times higher than a person younger than 70 years, OR of 3.1 [275].

If one investigates COVID-19 mortality data, a similar trend is seen with age. Risk of mortality due to COVID-19 is much higher in older patients with a RR of 3.61 in patients older than 70 years [276], see Figure 6.7. The increased risk of coagulation due to older age could be one reason for this increased COVID-19 mortality.

Table 6.1. Qualitative risk comparison between coagulation and COVID-19.

Uncontrollable factors	Risk for coagulation					Risk of COVID-19 severity				
	Study size (n=no. of participants, N=no. of studies)	RR/OR	Value	95% CI	Ref	Study size (n=no. of participants, N=no. of studies)	RR/OR	Value	95% CI	Ref
Age > 70 years	n=607, N=1	OR	3.10	1.3-7.5	[275]	n=36 470, N=59	RR	3.61	2.70-4.84	[276]
Male vs Female	n=11 253, N=1	RR	1.90	1.9-2.4	[277]	n=36 470, N=59	RR	1.50	1.18-1.91	[276]
Black vs Caucasian	#	RR	1.50	#	[278]	n=505 992, N=1	OR	1.60	1.2-2.0	[279]
Blood Type A vs Type O	n=406 755, N=1	HR	1.44	1.39-1.50	[280]	n=31 100, N=4	OR	1.41	*	[281]
Blood Type B vs Type O	n=406 755, N=1	HR	1.45	1.37-1.54	[280]	n=31 100, N=4	OR	1.69	*	[281]
Pregnant vs Non-pregnant	n=1 142, N=1	OR	4.60	2.7-7.8	[282]	n=22 493, N=1	OR	2.35	1.48-3.74	[283]

Notes: 1. CI, Confidence Interval; HR, Hazard Ratio; OR, Odds Ratio; RR, Relative Risk. 2. (#) Denotes that the study did not provide this data. 3. (*) Study (66) only provides the 95% CI for each Blood Type separately and not the Blood Type vs Blood Type O. These individual 95% CI's for Blood Type A, B and O were (1.11-1.40), (0.99-1.21) and (0.63-0.77) respectively. These data were not included in the table since the OR's for each Blood Type were reported separately. Here the OR's of Blood Type A vs O and Blood Type B vs O were normalised.

(b) Gender

A 25-year population-based study showed that males have a higher risk to coagulate than females [284]. At younger ages (<45 years) females have a higher risk of coagulation than males, for various reproductive reasons [277]. However, since an increase in COVID-19 severity and mortality is typically seen in older patients (> 45 years) the focus was only on these older patients. Men have a 1.9-fold higher risk of developing venous thrombosis than women [277].

COVID-19 data also indicate that males have a higher risk of COVID-19 mortality than females, with a RR of 1.50 [276], see Figure 6.7. The increased risk of coagulation due to gender for individuals older than 45 years could be one reason for this increased COVID-19 mortality.

(c) Ethnicity

Ethnicity has also shown to be an independent risk factor for coagulation. The highest risk of thrombosis being in African Americans, with a RR of 1.5 compared to Europeans [278]. This is also seen in COVID-19 mortality data, which shows that African American's have a higher odds of death than Europeans, with an OR of 1.6 [279], see Figure 6.7. The increased risk of coagulation due to ethnicity could be one reason for this increased COVID-19 mortality.

(d) Blood Type

Another risk factor that seems to influence the odds of developing a thromboembolic event is a person's blood type. A single cohort study showed that blood types A&B vs O have higher risk of developing a thromboembolic event, with the following HRs: A vs O of 1.44, and B vs O of 1.45 [280], see Figure 6.7.

A similar trend is seen in the effect of different blood types on COVID-19 severity, with the following ORs: A of 1.06, B of 1.27, O of 0.75 [281]. If these values are normalised with respect to blood type O the ORs are the following: A vs O of 1.41, and B vs O of 1.69, see Figure 6.7.

None of the blood group values for COVID-19 severity were statistically significant [281]. It is however interesting that this limited study shows that patients with blood type O have lower odds of developing severe COVID-19 than blood types A and B. There is however still controversy regarding correlation between blood type and COVID-19 severity [285].

(e) Pregnancy

Pregnancy is not necessarily an uncontrollable factor, but for the duration of being pregnant it is. During pregnancy the risk of venous thrombosis is much higher than for non-pregnant women with an OR of 4.6 [282], see Figure 6.7.

Pregnant women are also at a higher risk of developing more severe COVID-19 complications than non-pregnant women, with an OR of 2.35 [283]. Fortunately, no significant association between pregnant and non-pregnant women was found for COVID-19 mortality risk [283]. This may be due to pregnant women seeking medical attention earlier than non-pregnant women. The higher severity risk could partially be due to the higher risk for coagulation during pregnancy. More research is however needed to validate this.

The abovementioned uncontrollable factors may contribute to the coagulation loop 1 of the *death spiral*. This could help explain why some patients experience accelerated disease severity. However, better studies for COVID-19, in especially different blood groups are needed.

The high mortality statistics in patients with pre-existing CHD comorbidities [45]–[47], [286] are discussed in more detail in the next section with reference to Figure 6.8 to Figure 6.10. This next section will show why a patient with a worse cardiovascular "baseline" before COVID-19 could potentially have a worse outcome than a patient with a healthy cardiovascular "baseline".

6.5.2 COVID-19 aggravation in patients with pre-existing CHD comorbidities

6.5.2.1. Severe COVID-19 patients with existing chronic Hypercholesterolemia

One of the risk factors for CHD is *Hypercholesterolaemia.* Chronic *Hypercholesterolaemia* may fuel the COVID-19 *death spiral* by increasing the risk of EC injury *via* an inflammatory state or plaque build-up. For EC injury induced by an inflammatory state see Figure 6.8 pathways: ↑*oxLDL-(pw51)-Hypercholesterolaemia-(pw51)-*↑*foam cell-(pw81)-*↑*NFkβ-(pw82)-*↑*IL-6, IL-8-(pw76)-*↑*platelet factors-(pw74)-*↑*inflammatory state-(pw110)-*↑*EC injury*. For EC injury induced by plaque build-up see Figure 6.8 pathways: ↑*oxLDL-(pw51)-Hypercholesterolaemia-(pw119)-*↑*EC injury*.

Hypercholesterolaemia could also have an impact on the severity of COVID-19 by increasing coagulation. This could happen by increased foam cell production and increased thrombin generation [242]. In turn increasing the platelet forming factors and reducing breakdown processes like fibrinolysis, increases coagulation [243]. See Figure 6.8 pathways: ↑*oxLDL-*

(pw51)-Hypercholesterolaemia-(pw51)-↑foam cell-(pw81)-↑NFkβ-(pw82)-↑IL-6, IL-8-(pw76)-↑platelet factors-(pw73)-↑Hypercoagulability.

The increased coagulation could aggravate thrombi within the lungs and lead to possible hypoxemia [265], potentially cascading the symptoms already experienced by a COVID-19 patient.

The above discussion partially explains why many patients with obesity have a high risk of developing severe COVID-19 complications [287], as obesity is associated with *Hypercholesterolaemia* [288], [289].

Interestingly it was also found that free cholesterol, as well as high-and low-density lipoprotein levels, are lower in end-stage COVID-19 patients than in patients with less severe COVID-19 [286], [290]. Why would cholesterol levels be lower in patients with more severe disease? Could this be explained by the ability of SARS-CoV-2 to use (“consume”) serum cholesterol for its entry into host cells [245].

If this is the case, then high cholesterol levels before infection might enhance viral infection *via* increased availability of serum cholesterol levels but as the virus “consumes” cholesterol the levels would decrease. These facts are however still controversial and further studies are warranted.

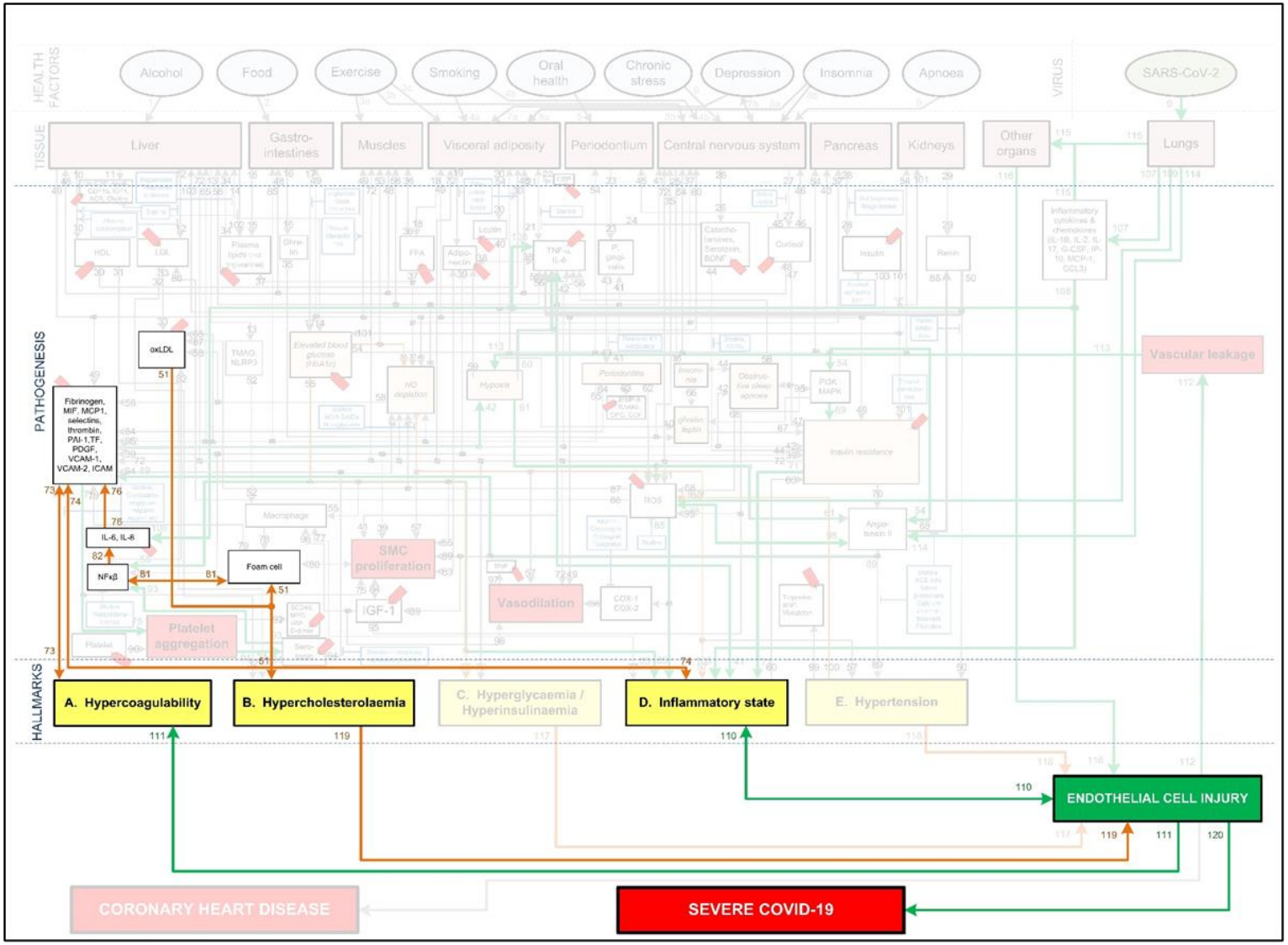

Figure 6.8. CHD related aggravation of COVID-19 in patients with high cholesterol.

6.5.2.2. Severe COVID-19 patients with existing chronic Hyperglycaemia or Hyperinsulinaemia

Elevated blood glucose aggravates COVID-19 severity and mortality risk irrespective of diabetes [291], [292]. One possible reason for this could be the indirect ability of blood glucose to induce EC injury.

Since glucose is the main energy source for cells, any change to its levels could have a direct effect on the cell's metabolism. Changes in blood glucose can cause ECs to undergo apoptosis (cell death or "suicide"), causing the ECs to detach and enter the bloodstream [293]. See Figure 6.9 pathways: *Elevated blood glucose (HbA1c)-(pw55)-Hyperglycaemia-(pw117)-↑EC injury*. This further leaves behind eroded arteries, which activate processes that lead to atherosclerosis, such as smooth cell proliferation [293].

Another pathway through which elevated blood glucose levels contribute to EC injury is through aggravated inflammation. This inflammation is caused by activating the insulin resistance and ROS producing pathways and impaired EC turnover. See Figure 6.9 pathways: *Elevated blood glucose (HbA1c)-(pw54)-PI3K:MAPK-(pw69)-↑Insulin resistance-(pw72)-↑ROS-(pw85)-↑inflammatory state-(pw110)-↑EC injury*. EC turnover is possibly impaired due to accelerated aging or reduced renewal of cells [294], [295]. This is most prominent in the microvascular and arterial ECs [296], which may be due to the differences in glucose uptake of cells.

A similar pathway also leads to increased inflammation due to a dysregulation of NO, which plays an important role in controlling the vascular tone and arterial pressure. A decrease in NO prevents ECs from responding to increased glucose stress, which may further accelerate cellular deterioration [295]. See Figure 6.9 pathways: *Elevated blood glucose (HbA1c)-(pw55)-Hyperglycaemia-(pw55)-↑inflammatory state-(pw110)-EC injury*.

These indirect impacts on EC injury could potentially explain why *Hyperglycaemia* is a significant co-morbidity and risk factor for severe COVID-19 patients [286]. It highlights the importance of ensuring that the glucose level of a diabetic patient remains within normal ranges. It may also be advantageous to reduce blood glucose levels in non-diabetic patients as elevated glucose in non-diabetic patients also increased COVID-19 severity [291], [292].

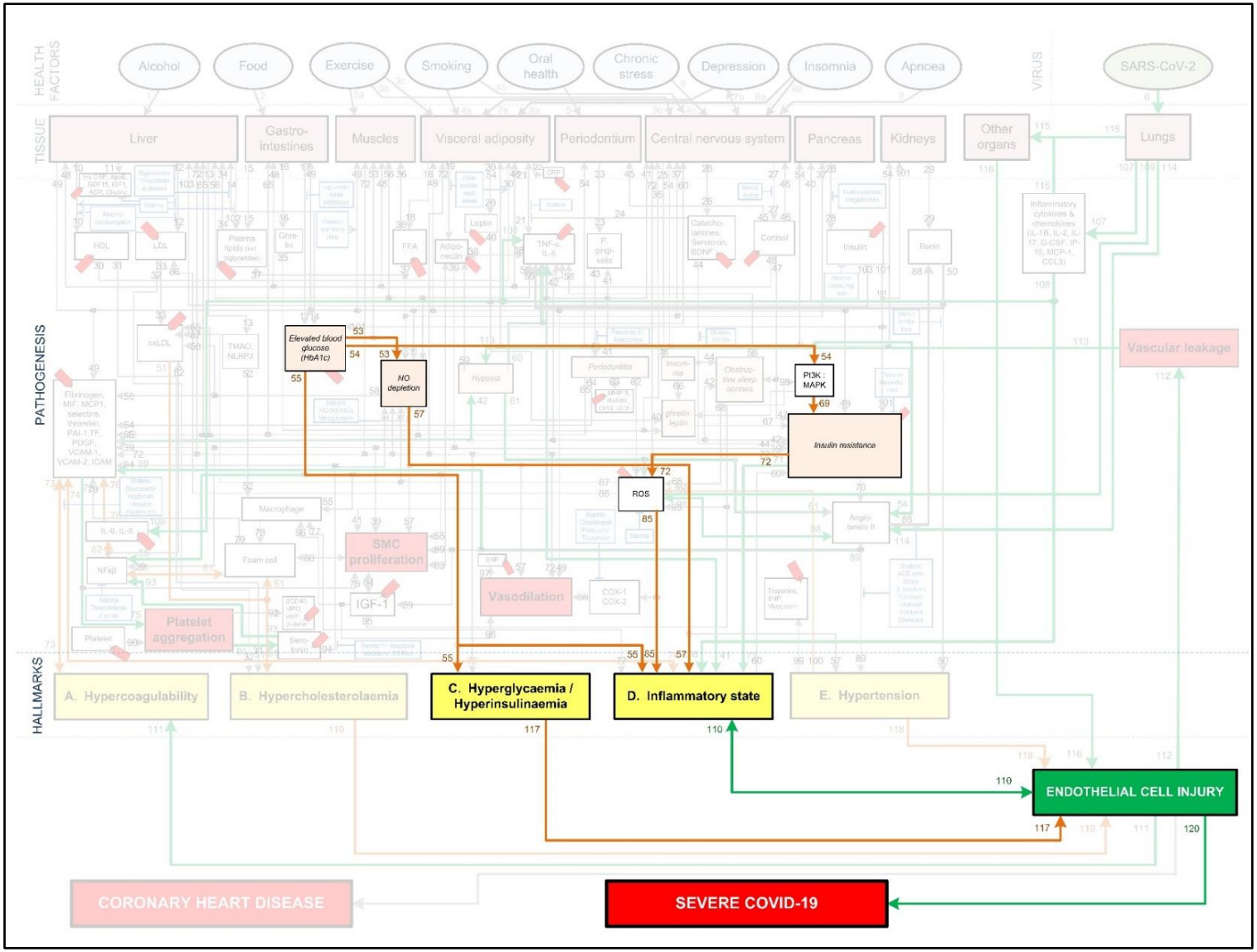

Figure 6.9. CHD related aggravation of COVID-19 in patients with high BG levels.

6.5.2.3. Severe COVID-19 patients with existing chronic hypertension

Hypertension is another common co-morbidity in COVID-19 related mortality [297]. This could be due to its indirect ability to increase inflammation or the direct injury caused to ECs [298], [299].

The indirect impact occurs through hypertension that increases the amount of ROS, especially from the oxidation of endothelial NO synthesis [299]. ROS can impact the inflammatory state and the ECs in several ways. It can, amongst others, cause EC death and increase the adhesion of inflammatory cells to the normally inert endothelium surface [299]. This could potentially exacerbate the response and symptoms related to EC injury. See Figure 6.10 pathways: *Hypertension-(pw100)-↑ROS-(pw85)-↑Inflammatory state-(pw110)-↑EC injury*.

Chronic hypertension can also directly cause damage to the microvascular ECs [298]. High blood pressure strains the ECs and could potentially cause ruptures in plaques that are adhered to the artery wall [298]. See Figure 6.10 pathways: *Hypertension-(pw118)-EC injury*. This creates additional areas that require attention and would probably also increase the inflammatory response.

Existing chronic hypertension can therefore possibly cause injury to the ECs through either the indirect or direct pathways. This injury could potentially contribute to the rapid worsening of health in COVID-19 patients with chronic hypertension [297].

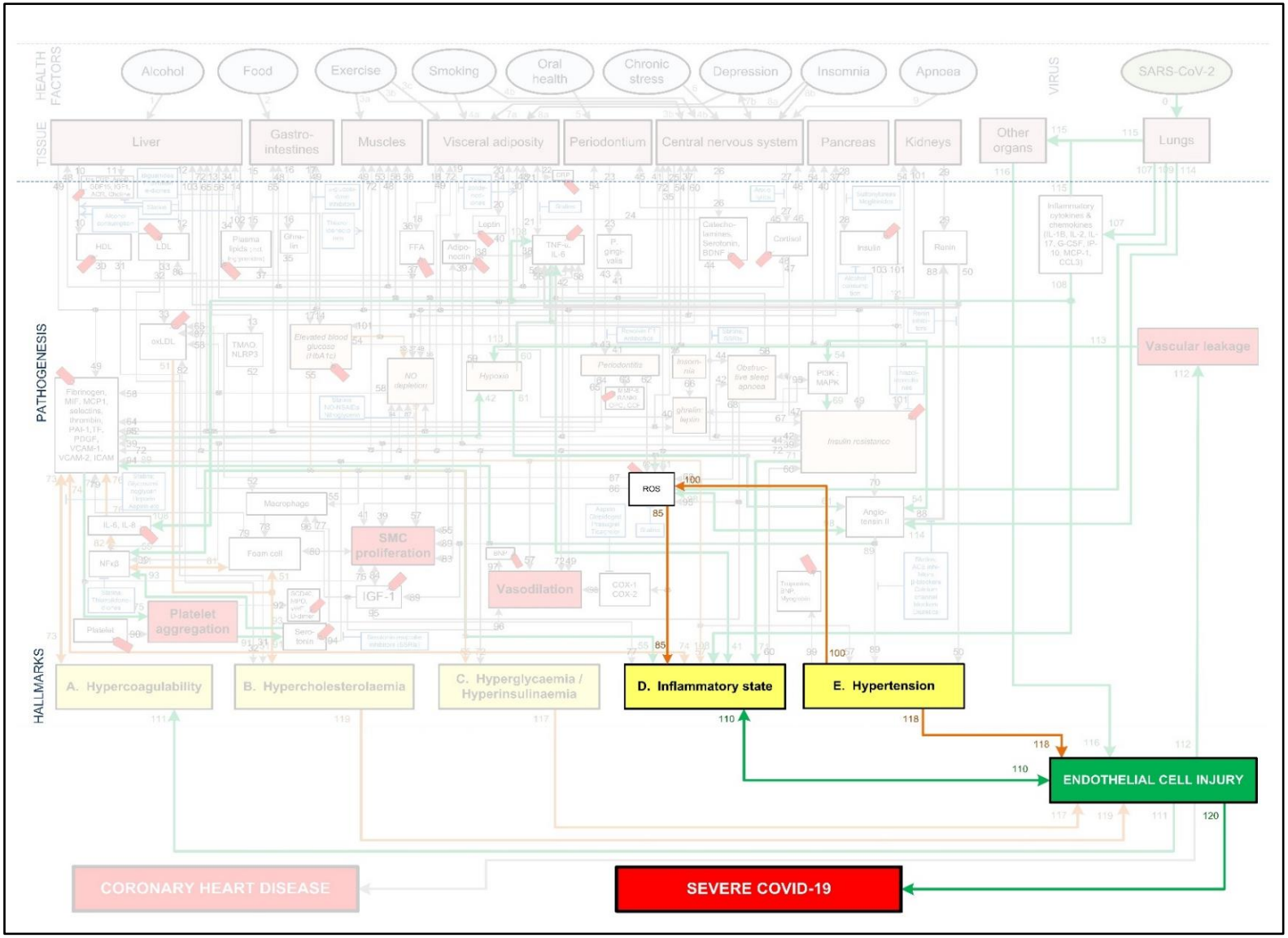

Figure 6.10. CHD related aggravation of COVID-19 in patients with hypertension.

6.5.3 Effects of different *health factors* on COVID-19 severity

The comparison between CHD and severe COVID-19 for different *health factors* with reference to Figure 6.4 are discussed. The definition of each *health factor* was given in Section 6.4.3.

Different *health factors* (pink ovals in Figure 6.4) were originally analysed in terms of their effects on CHD risk [240]. These *health factors* were either associated with an increase or decrease in risk for CHD [240], [241], [247]–[250]. The same *health factors* were investigated for COVID-19 severity. It will be shown to what extent a healthy CHD "baseline", as a result of a healthy lifestyle, will influence COVID-19 severity.

Table 6.2 summarises the CHD and COVID-19 data for the different *health factors* extracted from literature, namely study size (N), number of participants (n), risk type (RR/HR/OR), respective risk value, 95% confidence interval (CI), fold change (as calculated *via* the non-traditional method) and the respective references. Data not statistically significant are indicated with an (*) in Figure 6.11.

Where data were unavailable a hash (#) was inserted in Table 6.2, e.g., for the two *health factors*, alcohol use and food intake (high glycaemic diets). These *health factors* have not yet been fully investigated in COVID-19 patients. Despite no risk values being available for these *health factors,* their probable effects on COVID-19 severity are discussed in this section.

The *health factors* that increase or decrease a person's risk for CHD similarly increase or decrease a person's risk (RR/HR/OR) for developing severe COVID-19 (Figure 6.11). In the rest of this section the effects each *health factor* has on the CHD hallmarks are discussed in more detail, and hypothesise how this could affect COVID-19 severity.

(a) Moderate exercise

Based on the CHD model (Figure 6.1) a detailed description of the mechanism by which moderate exercise may reduce CHD risk has been published [250]. Only the salient features of the mechanism are described here.

Regular moderate exercise is universally accepted to reduce the risk of CHD [240], [250], [300] (the definition of moderate exercise was given in Section 6.4.3). Table 6.2 shows a decrease risk (RR) of 0.75 (n=645 087, N=33) [300]. This translates to a 1.33-fold decrease in CHD risk [240], [250] as illustrated in Figure 6.11.

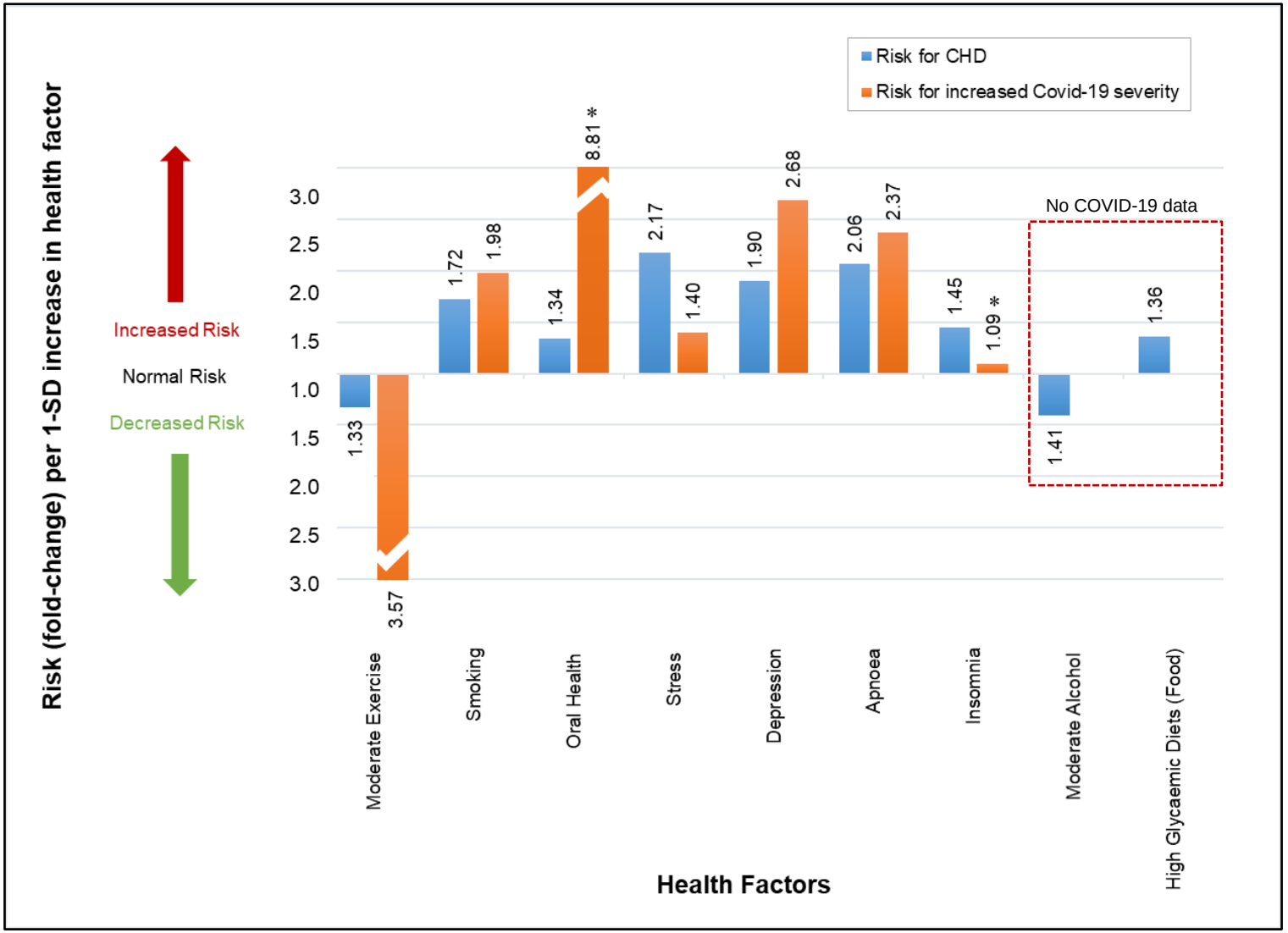

Note: An accurate quantitative comparison is not possible, mostly due to differences in study design and size.

Figure 6.11. Qualitative risk of different *health factors* on CHD and COVID-19.

Table 6.2. The effect of different *health factors* on CHD and COVID-19.

	Risk for CHD					Ref	Risk for increased COVID-19 severity					Ref
	Study size (n=no. of participants, N=no. of studies)	RR, HR or OR	Value	95% CI	Fold change as per definition		Study size (n=no. of participants, N=no. of studies)	RR, HR or OR	Value	95% CI	Fold change as per definition	
Moderate exercise	n=645 087, N=33	RR	0.75	(0.71-0.79)	-1.33	[240], [300]	n=260,N=1	OR	0.28	#	-3.57	[301]
Smoking	n=1 010 000, N=141	RR	1.72	(1.62-1.83)	1.74	[240], [302]	n=32 849, N=47	RR	1.98	(1.16-3.38)	1.98	[303]
Oral health	n=147 821, N=7	RR	1.34	(1.27-1.42)	1.34	[240], [249], [304]	n=568, N=1	OR	8.81	(1.00-77.70)	8.81	[305]
Stress	n=24 767, N=1	OR	2.17	(1.84-2.55)	2.17	[240], [306]	n=535, N=1	HR	1.40	(1.11-1.75)	1.40	[307]
Depression	n=124 509, N=21	RR	1.90	(1.49-2.42)	1.90	[240], [308]	n=421 014, N=1	OR	2.68	(2.03-3.54)	2.68	[309]
Apnoea	n=1 436, N=1	HR	2.06	(1.10-3.86)	2.06	[240], [310]	n=15 835, N=4	OR	2.37	(1.14-4.95)	2.37	[311]
Insomnia	n=122 501, N=13	RR	1.45	(1.29-1.62)	1.45	[240], [312]	n=568, N=1	OR	1.09	(0.44-2.71)	1.09	[313]
Moderate alcohol	n=504 651, N=29	RR	0.71	(0.66-0.77)	-1.41	[240], [248], [314]	#	#	#	#	#	#
Food (HGD)	n=220 050, N=8	RR	1.36	(1.13-1.63)	1.36	[240], [247], [315]	#	#	#	#	#	#

Note: CHD, Coronary Heart Disease; CI, Confidence Interval; COVID-19, Coronavirus Disease of 2019; HGD, High Glycaemic Diets; HR, Hazard Ratio; OR, Odds Ratio; RR, Relative Risk. A minus sign shows a reduction in risk. (#) denotes that the respective study did not provide this data. A small preliminary study [316] on the effect of the SSRI antidepressant, fluvoxamine, on COVID-19 has shown positive effects. Risk data were not given.

The effect of moderate exercise on COVID-19 was analysed in a small cross-sectional study (n=260) [301]. The authors concluded that moderate physical activity before onset of COVID-19 decreases the odds of developing severe COVID-19 (OR of 0.28) by 3.57 times [301], see Table 6.2 and Figure 6.11. Although this is only a small study, a larger study (n=48 440) substantiates the benefit of regular moderate exercise [317].

This larger study's results are not presented in Table 6.2 or Figure 6.11 since the study reported on inactivity. However, since being active helps reduce the odds of developing severe COVID-19, inactivity is expected to have an opposite effect. This is indeed the case as the study showed that patients who are consistently inactivate are 2.49 (OR) times more likely to die from COVID-19 [317].

Therefore, moderate exercise before the onset of disease decreases both the risk for CHD and COVID-19 severity. This could most likely be explained by the effect of moderate exercise on several CHD hallmarks. Moderate exercise largely influences, amongst others, glucose, cortisol and inflammatory mediator levels [240], [250], therefore reducing the risk of *Hyperglycaemia/Hyperinsulinaemia* and a heightened *Inflammatory state* [240], [250].

Regular exercise also reduces the accumulation of visceral fat, which reduces the risk of increased Low-density lipoprotein (LDL) levels, thus decreasing the risk for *Hypercholesterolaemia* [240], [250]. A decrease in visceral fat also reduces the risk of insulin resistance, which lowers one's risk for increased platelet factors and the potential for *Hypercoagulability* [240], [250].

The potential decrease of these CHD hallmarks could partially explain the benefit of moderate exercise on the reduced risk of COVID-19 severity. The respective CHD hallmark downregulated by exercise and the activated pathways are denoted in Figure 6.4 as follows:

- **Hyperglycaemia/Hyperinsulinaemia:** Moderate exercise-(pw3a)-muscles-(pw53)-↓blood glucose-(pw54)-↓PI3K:MAPK-(pw69)-↓insulin resistance-(pw72)-Hyperglycaemia/ Hyperinsulinaemia.
- **Inflammatory state:** Moderate exercise-(pw3b)-central nervous system-(pw27)-↓cortisol-(pw47)-↓insulin resistance-(pw70)-↓angiotensin II-(pw89)-↓hypertension-(pw100)-↓ROS-(pw85)-↓COX1/2-(pw85)-↓Inflammatory state.
- **Hypercholesterolaemia:** Moderate exercise-(pw3c)-visceral adiposity-(pw18)-↓FFA-(pw37)-↓plasma lipids-(pw34)-liver-(pw12)-↓LDL-(pw33)-↓oxLDL-(pw51)-↓Hypercholesterolaemia.

- **Hypercoagulability**: Moderate exercise-(pw3a)-muscles-(pw53)-↓blood glucose-(pw54)-↓PI3K:MAPK-(pw69)-↓insulin resistance-(pw72)-↓platelet factors-(pw73)-↓Hypercoagulability.

The potential decrease in four of the five CHD hallmarks due to moderate exercise before onset of COVID-19 (creating a healthier vascular system "baseline") could partially explain the decreased risk of COVID-19 severity. These beneficial effects of exercise are based on moderate exertion and not heavy exertion. Heavy exertion exercise has the following detrimental effects: transient immune dysfunction, elevated inflammatory biomarkers, and increased risk of upper respiratory tract infections [318]. Therefore, exercise exertion is an important factor to consider during the COVID-19 pandemic.

(b) Smoking

Smoking is a risk factor for CHD with a RR of 1.72 [302]. A recent systematic review and meta-analysis of 47 studies (32 849 hospitalised COVID-19 patients) showed that current smokers have an increased risk of developing severe or critical COVID-19, RR of 1.98 [303].

Most smokers develop insulin resistance and/or Hyperinsulinaemia as compared to non-smokers [319], [320]. This association may either be due to the lower adiponectin levels or higher cortisol secretion levels seen in current smokers compared to non-smokers [321], [322]. This increases a smoker's risk for *Hyperglycaemia/Hyperinsulinaemia.*

Moreover, most smokers also have higher plasma triglyceride and lower High-density lipoprotein (HDL) cholesterol concentrations than non-smokers [320], [323]. This increases a smoker's risk of *Hypercholesterolaemia.*

Another CHD hallmark that is upregulated in smokers is a heightened *Inflammatory state*. This is due to an upregulation of several inflammatory markers and cytokines such as TNF-α, granulocyte-macrophage colony-stimulating factor (GM-CSF) and monocyte chemoattractant protein (MCP-1) [324].

Smoking also induces an imbalance between various haemostatic molecules in the blood thereby increasing the state of *Hypercoagulability* [325]. This may be due to functional changes in clotting factors such as fibrinogen [325].

The associated pathways and respective CHD hallmarks increased by smoking are shown in Figure 6.4 as the following:

- **Hyperglycaemia/Hyperinsulinaemia:** Smoking-(pw4a)-visceral adiposity-(pw19)-↓adiponectin-(pw39)-↑insulin resistance-(pw72)- ↑Hyperglycaemia/Hyperinsulinaemia.

Smoking-(pw4b)-central nervous system-(pw27)-↑cortisol-(pw47)-↑insulin resistance-(pw72)- ↑Hyperglycaemia/Hyperinsulinaemia.

- **Hypercholesterolaemia:** Smoking-(pw4a)-visceral adiposity-(pw30)-↓HDL-(pw31)-↑ Hypercholesterolaemia.
- **Inflammatory state:** Smoking-(pw4b)-central nervous system-(pw41)-↑TNF-α-(pw41)-↑Inflammatory state.
- **Hypercoagulability:** Smoking-(pw4a)-visceral adiposity-(pw49)-↑Fibrinogen-(pw73)-↑Hypercoagulability.

The activation of these pathways and respective CHD hallmarks may explain some of the increased risk of smokers developing severe COVID-19 compared to non-smokers [303].

(c) Oral health

A paper on a detailed analysis of the mechanism by which oral health (in the form of periodontal disease) can influence CHD was published using the model of Figure 6.1 [249]. Important elements relevant to this study are discussed below.

Oral health in the form of periodontal disease is known to increase the risk of CHD by 1.34-fold [304] (Figure 6.11 and Table 6.2). COVID-19 patients with periodontitis have a much higher risk of mortality, OR of 8.81 (Figure 6.11 and Table 6.2) [305]. This value is quite large and could be overestimated. There are several reasons for potential overestimation, namely the small study size (n=568), the data is widely spread (95% CI of 1.00-77.7) and the data is not statistically significant (this statistical insignificance is illustrated on Figure 6.11 with an (*)) [305].

Nevertheless, the increased risk of COVID-19 severity due to periodontitis could partially be explained by the increase in several CHD hallmarks, namely *Inflammatory state, Hypercoagulability and Hypercholesterolaemia* [240], [249].

An increased risk of *Hypercoagulability* and *Inflammation* in these patients is through a common periodontitis associated bacteria, *p.gingivalis* [326]. This bacteria invades endothelial cells which concomitantly increases platelet activity and stimulates proinflammatory mediators/cytokines (CRP, TNF-α and IL-6) [326].

Inflammation can also be increased *via* ROS which is associated with periodontal disease [240], [249]. Subsequently, this also affects oxidised LDL levels pertaining to an increase in the risk for *Hypercholesterolaemia* [240], [249].

The associated pathways and respective CHD hallmarks increased by oral health in the form of periodontitis are shown in Figure 6.4 as the following:

- **Hypercoagulability:** Oral health-(pw5)-periodontium-(pw23)-↑P. gingivalis-(pw43)-↑periodontitis-(pw64)-↑platelet factors-(pw73)-↑Hypercoagulability.
- **Inflammatory state**: Oral health-(pw5)-periodontium-(pw23)-↑P. gingivalis-(pw43)-↑periodontitis-(pw41)-↑TNFα/IL6-(pw41)-↑inflammatory state.
  Oral health-(pw5)-periodontium-(pw23)-↑P. gingivalis-(pw43)-↑periodontitis-(pw62)-↑ROS-(pw85)-↑inflammatory state.
- **Hypercholesterolaemia:** Oral health-(pw5)-periodontium-(pw23)-↑P. gingivalis-(pw43)-↑periodontitis-(pw65)-↑oxLDL-(pw51)-↑Hypercholesterolaemia.

The potential increase of these CHD hallmarks due to periodontitis could partially explain the increased risk of COVID-19 severity.

(d) Chronic stress

Chronic stress (definition in Section 6.4.3) is also a common factor linked to an increased risk for CHD, with an OR of 2.17 [306], presented in Figure 6.11 and Table 6.2. COVID-19 severity is also increased by chronic stress with a HR of 1.4 [307], see Figure 6.11.

Chronic stress is known to elevate secretion of glucocorticoids in the form of cortisol. These high cortisol levels due to stress may elevate biomarkers such as blood glucose, TNF-α and insulin resistance [240]. These stress-related biomarkers are also upregulated in severe COVID-19 patients [240], [291], [292], [327]–[330].

The respective CHD hallmarks and activated pathways activated by chronic stress are denoted in Figure 6.4 as:

- **Hypercoagulability:** Chronic stress-(pw6)-central nervous system-(pw27)-↑cortisol-(pw48)-liver-(pw14)-↑blood glucose-(pw54)-PI3K:MAPK-(pw69)-↑insulin resistance-(pw72)-↑platelet factors-(pw73)-↑Hypercoagulability.
- **Hypercholesterolaemia:** Chronic stress-(pw6)-central nervous system-(pw27)-↑cortisol-(pw48)-liver-(pw12)-↑LDL-(pw33)-↑oxLDL-(pw51)-↑Hypercholesterolaemia.
- **Hyperglycaemia/Hyperinsulinaemia:** Chronic stress-(pw6)-central nervous system-(pw27)-↑cortisol-(pw48)-liver-(pw14)-↑blood glucose-(pw54)-PI3K:MAPK-(pw69)-↑insulin resistance-(pw72)-↑Hyperglycaemia/Hyperinsulinaemia.

- **Inflammatory state:** Chronic stress-(pw6)-central nervous system-(pw27)-↑cortisol-(pw48)-liver-(pw14)-↑blood glucose-(pw54)-PI3K:MAPK-(pw69)-↑insulin resistance-(pw70)-↑angiotensin II-(pw88)-renin-(pw50)-↑TNFα-(pw41)-↑Inflammatory state.
- **Hypertension:** Chronic stress-(pw6)-central nervous system-(pw27)-↑cortisol-(pw48)-liver-(pw14)-↑blood glucose-(pw54)-PI3K:MAPK-(pw69)-↑insulin resistance-(pw70)-↑angiotensin II-(pw89)- ↑Hypertension.

Although the COVID-19 study is small (n=535, see Table 6.2) stress affects all five CHD hallmarks. Future larger clinical studies are expected to emphasise the importance of stress management in patients with COVID-19.

(e) Depression

The effect of depression on CHD, using the CHD model in Figure 6.1, was described in detail in paper [241]. A summary of the potential effects of depression on COVID-19 are given in the rest of this section.

Depression increases one's risk for CHD by 1.90-fold (RR) [308], shown in Figure 6.11 and Table 6.2 This is also the case for COVID-19, where the odds of developing more severe disease in a person with pre-pandemic depression is 2.68-fold (OR) higher than without depression [309], see Figure 6.11.

Depression is thought to mediate, amongst others, over stimulation of the hypothalamic-pituitary-adrenocortical (HPA) axis induced by elevated levels of corticotropin-releasing factor and adrenocorticotropic hormone [240], [241]. Chronic dysregulation of the hypothalamic-pituitary-adrenal axis can lead to increased serum levels of cortisol. Similar to chronic stress, elevated cortisol levels can increase the risk of upregulating four CHD hallmarks, namely *Inflammatory state, Hypercholesterolaemia, Hypertension* and *Hyperglycaemia or Hyperinsulinaemia* [240], [241].

In addition to increased cortisol levels, the overstimulation of the hypothalamic-pituitary-adrenal axis may augment sympathoadrenal hyperactivity *via* central regulatory pathways. This results in increased plasma catecholamines [240], [241]. An increase of catecholamines can lead to abnormalities in insulin and platelet factors, thus also increasing another CHD hallmark, namely *Hypercoagulability* [240], [241].

The respective CHD hallmarks and activated pathways induced by depression are denoted in Figure 6.4 as the following:

- **Hypercholesterolaemia:** Depression-(pw7b)-central nervous system-(pw27)-↑cortisol-(pw48)-liver-(pw12)-↑LDL-(pw33)-↑oxLDL-(pw51)-↑Hypercholesterolaemia.
- **Inflammatory state:** Depression-(pw7b)-central nervous system-(pw27)-↑cortisol-(pw48)-liver-(pw14)-↑blood glucose-(pw54)-PI3K:MAPK-(pw69)-↑insulin resistance-(pw70)-↑angiotensin II-(pw88)-renin-(pw50)-↑TNFα-(pw41)-↑Inflammatory state.
- **Hypertension:** Depression-(pw7b)-central nervous system-(pw27)-↑cortisol-(pw48)-liver-(pw14)-↑blood glucose-(pw54)-PI3K:MAPK-(pw69)-↑insulin resistance-(pw70)-↑angiotensin II-(pw89)- ↑Hypertension.
- **Hyperglycaemia/Hyperinsulinaemia:** Depression-(pw7b)-central nervous system-(pw26)-↑catecholamines / ↓serotonin / ↓BDNF-(pw44)-↑insulin resistance-(pw72)-↑Hyperglycaemia / Hyperinsulinaemia.
- **Hypercoagulability:** Depression-(pw7b)-central nervous system-(pw26)-↑catecholamines / ↓serotonin / ↓BDNF-(pw44)-↑insulin resistance-(pw72)-↑platelet factors-(pw73)-↑Hypercoagulability.

Since depression can upregulate all five CHD hallmarks [240], [241], it may play a more important role in COVID-19 severity than expected.

(f) Apnoea

Figure 6.11 and Table 6.2 shows that obstructive sleep apnoea (OSA) is associated with an increased risk for CHD with an HR of 2.06 [310]. Amongst 15 835 COVID-19 patients, those with OSA have a 2.37-fold (OR) increased odds of developing severe COVID-19 [311].

Similar to depression, the effects of OSA may also include alterations of the hypothalamic-pituitary-adrenal axis and sympathetic nervous activity. This results in changes of catecholamine and cortisol secretion levels, which concomitantly serve to up-regulate two CHD hallmarks, namely *Inflammatory state* and *Hypertension* [240]. Subsequently, increased cortisol levels also increase the risk for elevated LDL and platelet factors, which influence the risk for two more CHD hallmarks, namely *Hypercholesterolaemia* and *Hypercoagulability* [240].

The respective CHD hallmarks and activated pathways induced by OSA are denoted in Figure 6.4 as the following:

- **Inflammatory state:** Apnoea-(pw9)-central nervous system-(pw27)-↑cortisol-OSA-(pw42)-hypoxia-(pw61)-↑ROS-(pw85)-↑Inflammatory state.
- **Hypertension:** Apnoea-(pw9)-central nervous system-(pw27)-↑cortisol-OSA-(pw42)-↑hypoxia-(pw42)-↑insulin resistance-(pw70)-↑angiotensin II-(pw89)-↑Hypertension.
- **Hypercholesterolaemia:** Apnoea-(pw9)-central nervous system-(pw27)-↑cortisol-(pw48)-visceral adiposity-(pw21)-↑TNF-α/IL-6-(pw56)-liver-(pw12)-↑LDL-(pw33)-↑oxLDL-(pw51)-↑Hypercholesterolaemia.
- **Hypercoagulability:** Apnoea-(pw9)-central nervous system-(pw27)-↑cortisol-(pw47)-↑insulin resistance-(pw42)-↑platelet factors-(pw73)-↑Hypercoagulability.

The activation of proinflammatory mediators, namely TNF-α, IL-6 and CRP induced by OSA are also elevated in severe COVID-19 patients without OSA [237]–[239]. Therefore, OSA could aggravate these mediators, leading to an increased risk of COVID-19 severity.

(g) Insomnia

Insomnia is another *health factor* that increases a person's risk for CHD with a RR of 1.45 [312], see Figure 6.11 and Table 6.2. The effect of insomnia on increased COVID-19 severity seems negligible with an OR of 1.09 [313], see Figure 6.11. Unfortunately, the study is small (n=568) and the data are statistically insignificant (95% CI of 0.44-2.71) [313], see Table 6.2 and Figure 6.11.

Nevertheless, insomnia affects several pathogenic pathways that may play an important role in COVID-19 severity [240]. Insomnia has shown to directly affect the levels of leptin (decreases) and ghrelin (increases), which are important hormones that regulate appetite. This could cause an increase in caloric consumption which, if left untreated, could negatively impact blood glucose levels and insulin sensitivity [240]. This would therefore result in an increased risk for *Hyperglycaemia/Hyperinsulinaemia* [240].

Subsequently, insulin resistance stemming from excessive caloric intake can stimulate pro-inflammatory mediators and cytokines such as TNF-α, IL-6 and CRP. This could result in a heightened *Inflammatory state*, which is common in severe COVID-19 patients [237]–[240]. Another CHD hallmark upregulated by insulin resistance through the regulation of platelet homeostasis is *Hypercoagulability* [240]. Coagulation is also a common risk factor in severe COVID-19 patients [40]–[44], [240].

The respective CHD hallmarks and activated pathways induced by insomnia are denoted in Figure 6.4 as the following:

- **Hyperglycaemia/Hyperinsulinaemia:** Insomnia-(pw8b)-central nervous system-(pw25)-(pw66)-↑ghrelin:leptin-(pw67)-↑insulin resistance-(pw72)-liver-(pw14)-↑blood glucose-(pw55)-↑Hyperglycaemia/Hyperinsulinaemia.
- **Inflammatory state:** Insomnia-(pw8b)-central nervous system-(pw25)-(pw66)-↑ghrelin:leptin-(pw67)-↑insulin resistance-(pw70)-↑angiotensin II-(pw88)-renin-(pw50)-↑TNF-α, IL-6-(pw41)-↑Inflammatory state.
- **Hypercoagulability:** Insomnia-(pw8b)-central nervous system-(pw25)-(pw66)-↑ghrelin:leptin-(pw67)-↑insulin resistance-(pw72)-↑platelet factors-(pw73)-↑Hypercoagulability.

Unfortunately, the clinical data on insomnia and its effect on COVID-19 severity are small. Its effect may be underestimated.

(h) Moderate alcohol use

The mechanism by which moderate alcohol consumption may influence CHD was described in detail in paper [248]. Moderate alcohol consumption is accepted to reduce the risk of CHD [240], [248], [314].

Table 6.2 shows a decrease risk (RR) of 0.75 (n=645 087, N=33) [314]. This translates to a 1.41-fold decrease in CHD risk [240], [248], illustrated in Figure 6.11. This decrease in CHD risk may be due to several pathways that decrease the risk for CHD hallmarks.

Moderate alcohol consumption may reduce fibrinogen levels, clotting factors, and platelet aggregation. Downregulation of these biomarkers reduces a state of *Hypercoagulability* [248]. In addition, it can also upregulate HDL and downregulate LDL, which decrease *Hypercholesterolaemia* [248].

Moreover, moderate alcohol consumption can reduce hepatic gluconeogenesis and concomitantly decrease plasma glucose levels, which decreases the incidence of *Hyperglycaemia* and *Hyperinsulinaemia* [248]. Lastly, it can serve to reduce chronic *Inflammation* through regulation of insulin resistance [248].

These respective CHD hallmarks and pathogenic pathways activated by moderate alcohol consumption [248], are denoted in Figure 6.4 as:

- **Hypercoagulability:** Alcohol-(pw1)-Liver-(pw49)- ↓fibrinogen/clotting factors-(pw73)-↓Hypercoagulability and Alcohol-(pw1)-Liver-(pw49)-↑fibrinogen/clotting factors-(pw75)-↓platelet aggregation.
- **Hypercholesterolaemia:** Alcohol-(pw1)-Liver-(pw10)-↑HDL-(pw31)-↓Hypercholesterolaemia and Alcohol-(pw1)-Liver-(pw12)-↓LDL-(pw33)- oxLDL-(pw51)-↓Hypercholesterolaemia.
- **Hyperglycaemia/Hyperinsulinaemia:** Alcohol-(pw1)-Liver-(pw14)-↓blood glucose-(pw55)-↓Hyperglycaemia/Hyperinsulinaemia.
- **Inflammation:** Alcohol-(pw1)-Liver-(pw14)-↓blood glucose-(pw54)-PI3K:MAPK-(pw69)-insulin resistance-(pw70)-Angiotensin II-(pw89)-↓Hypertension-(pw100)-↓ROS-(pw85)-↓Inflammatory state.

These pathways demonstrate an important role moderate alcohol consumption plays in four of the five CHD hallmarks. The argument whether moderate alcohol consumption before infection decreases or increases COVID-19 severity has not yet been thoroughly explored.

However, the prevailing point of view is that alcohol consumption during COVID-19 could increase COVID-19 severity [331]. This is due to alcohol increasing the risk of acute respiratory distress syndrome and admission to intensive care unit in patients with pneumonia [331], [332]. These are common risk factors in critical COVID-19 patients [331], [332].

Increased hypercoagulability, Hyperglycaemia and inflammation are common in severe COVID-19 patients [40]–[44], [46], [48], [49]. Therefore, the reduction of these CHD hallmarks by moderate alcohol consumption before infection of SARS-CoV-2 could be advantageous. It seems to create a better vascular “baseline” and could thus potentially reduce the risk of developing severe COVID-19 complications. These effects should, however, be studied in well-designed clinical trials.

(i) Food intake (high glycaemic diets)

It has previously been explained, with reference to Figure 6.1, how high glycaemic diets (HGDs) affect CHD [247]. Only a summary of the elements relevant to COVID-19 are given below.

A high glycaemic diet (HGD) increases the risk for CHD with a RR of 1.36 [315], see Figure 6.11 and Table 6.2. These diets could play an important role in COVID-19 severity through regulation of all five CHD hallmarks [240], [247].

HGDs influences glycaemic control by raising blood glucose levels *via* carbohydrate consumption. This may result in *Hyperglycaemia* [240], [247]. *Hyperglycaemia* resulting from HGDs can increase the risk of insulin resistance by upregulating the Phosphatidylinositol 3-kinase: Mitogen-activated protein kinase (PI3K:MAPK) ratio [240], [247]. Subsequently, an increased insulin resistance has been associated with increased levels of platelet factors that upregulate the potential for *Hypercoagulation* [240], [247].

Excessive intake of HGDs can result in increased adipose tissue, which enhances pro-inflammatory mediators such as CRP and TNF-α [240], [247]. These mediators are, amongst others, important to consider since they are upregulated in critical COVID-19 patients [328], [329], [333]–[339]. Macrophages, residing in adipose tissue, are also one of the most active secretory cells in the body that mediate activities of adipocytes and release a vast array of inflammatory mediators [240], [247]. This increases the risk for an *Inflammatory state.*

Moreover, excessive intake of HGDs can also increase visceral fat build-up and reduce the clearance of triglycerides, which leads to increased LDL and decreased HDL levels [240], [247]. This constitutes to a potential risk of *Hypercholesterolaemia* [240], [247]. Consequently, HGDs pertaining to visceral fat build-up also increases the risk of *Hypertension*. This happens through a build-up of excess adipose tissue, which increases the expression of angiotensinogen, thus leading to activation of the renin-angiotensin system [240], [247].

These respective CHD hallmarks and pathogenic pathways activated by HGD are denoted in Figure 6.4 as the following:

- **Hyperglycaemia:** Food-(pw2)-gastro-intestines-(pw17)-↑blood glucose-(pw55)-↑Hyperglycaemia.
- **Hypercoagulability:** Food-(pw2)-gastro-intestines-(pw17)-↑blood glucose-(pw54)-↑PI3K:MAPK-(pw69)-↑insulin resistance-(pw72)-↑platelet factors-(pw73)-↑Hypercoagulability.

- **Inflammatory state:** Food-(pw2)-gastro-intestines-(pw15)-plasma lipids-(pw34)-liver-(pw13)-TMAO/NLRP3-(pw52)-macrophage-(pw77)-↑Inflammatory state.
- **Hypercholesterolaemia:** Food-(pw2)-gastro-intestines-(pw15)-plasma lipids-(pw34)-liver-(pw12)-↑LDL-(pw33)-oxLDL-(pw51)-↑Hypercholesterolaemia.
- **Hypertension:** Food-(pw2)-gastro-intestines-(pw14)-blood glucose-(pw54)-↑angiotensin II-(pw89)-↑Hypertension.

These pathways demonstrate the detrimental effect HGDs may have on an individual's "baseline" vascular system before infection from SARS-CoV-2. It could potentially increase the risk of developing severe COVID-19 complications.

6.5.4 Effects of different CHD *pharmaceutical interventions* on COVID-19 severity

The *integrated CHD/*COVID-19 *model* shows that similar outcomes for different *health factors* are seen in CHD and COVID-19. The next question is: Since it is known that various *pharmaceutical interventions* decreases one's risk for CHD, will they also work for COVID-19? A positive outcome can build a stronger validity base for the proposed *integrated CHD/*COVID-19 *model.*

The *pharmaceutical interventions* are shown in Figure 6.4 as blue boxes, where blunted blue arrows *(* ⊣▭ *)* denote antagonise or inhibit and pointed blue arrows *(* ◁▭ *)* denote up-regulate or facilitate. The question is whether these pharmaceuticals would also decrease one's risk for severe COVID-19. This was investigated, despite the limited clinical data available for COVID-19.

Table 6.3 summarises the CHD and COVID-19 data for the different *pharmaceutical interventions* extracted from literature, namely study size (N), number of participants (n), risk type (RR/HR/OR), respective risk value, 95% confidence interval (CI), fold change (as calculated *via* the non-traditional method) and the respective references. Data not statistically significant are indicated with an (*) in Figure 6.12.

No risk value was available for antidepressants' effect on COVID-19 severity. However, its effect on COVID-19 severity is still discussed in this section as depression was shown to increase the odds of developing severe COVID-19 complications by 2.68 (Section 6.5.4, Table 6.3).

It is thus hypothesised that certain anti-depressants should have an important influence on COVID-19 severity. The effects each *pharmaceutical intervention* has on the CHD hallmarks, and how this could affect COVID-19 severity will be discussed, in more detail, in the rest of this section.

(a) Statins

The use of statins decreases the risk of CHD with a RR of 0.78 [340]. This translates to a 1.28-fold decrease in CHD risk [240], illustrated in Table 6.3. and Figure 6.12. Statins also decrease COVID-19 severity, with a HR of 0.58 (n=13 981) [341] (Table 6.3). This translates to a decrease of COVID-19 severity by 1.72-fold as shown in Figure 6.12. The effects statins have on all of the CHD hallmarks, which may partially explain the large reduction in COVID-19 severity with the use of statins, were evaluated.

Firstly, statins cholesterol lowering effect inhibits the following pathways in Figure 6.4: (pw11) and (pw12). Besides these cholesterol lowering effects, it also has an anti-inflammatory effect [240], [341]. The anti-inflammatory biomarkers and pathways on which inhibition is observed are denoted in Figure 6.4 as: NFκβ, ROS and (pw21), (pw57), (pw74).

In addition to their beneficial effects on cholesterol and inflammation, statins also have antihypertensive effects by reducing systolic, diastolic and mean arterial blood pressure [342]. The hypertensive pathways on which its actions are observed are denoted in Figure 6.4 as (pw88) and (pw89).

(b) Salicylates

Salicylates, such as aspirin is a common anti-inflammatory [343] and anti-thrombotic [344] medication that decreases the risk for CHD with a RR of 0.82 [345], see Table 6.3. This translates to a 1.22-fold decrease in CHD risk [240], illustrated in Figure 6.12. Its use in COVID-19 patients also showed a decrease in severity with HR of 0.53 [274]. This is shown in Figure 6.12 as a 1.89-fold decrease in COVID-19 severity [274].

This reduction in risk could be expected because of the detrimental effect of inflammation and coagulation seen in most severe COVID-19 patients [40]–[44], [237]–[239]. The pathways on which aspirin’s actions are observed are denoted in Figure 6.4 as (pw73) and (pw74).

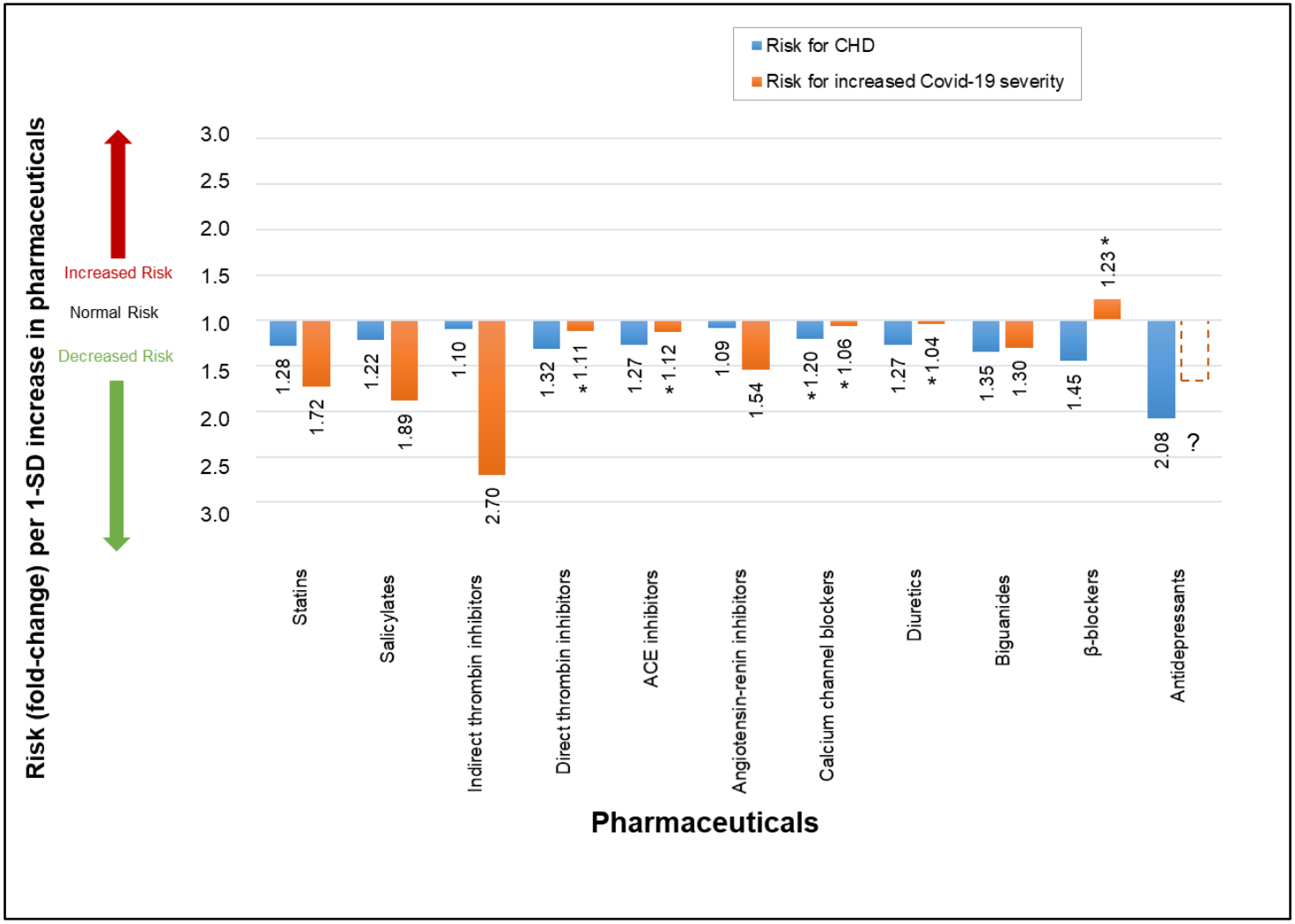

Note: An accurate quantitative comparison is not possible, mostly due to differences in study design and size.

Figure 6.12. Qualitative risk of different *pharmaceuticals* on CHD and COVID-19.

Table 6.3. The effect of different *pharmaceuticals* on CHD and COVID-19.

	Risk for CHD					Ref	Risk for increased COVID-19 severity					Ref
	Study size (n=no. of participants, N=no. of studies)	RR, HR or OR	Value	95% CI	Fold change as per definition		Study size (n=no. of participants, N=no. of studies)	RR, HR or OR	Value	95% CI	Fold change as per definition	
Statins	n=169 138, N=26	RR	0.78	(0.76-0.80)	-1.28	[240], [340]	n=13 981, N=1	HR	0.58	(0.43-0.80)	-1.72	[341]
Salicylates (Aspirin)	n=112 000, N=6	RR	0.82	(0.75-0.90)	-1.22	[240], [345]	n=412, N=1	HR	0.53	(0.31-0.90)	-1.89	[274]
Indirect thrombin inhibitors (Heparin)	n=31 402, N=6	OR	0.91	(0.84-0.98)	-1.10	[240], [346]	n=449, N=1	OR	0.37	(0.15-0.90)	-2.70	[347]
Direct thrombin inhibitors (Angiomax)	n=1 883, N=1	HR	0.76	(0.59-0.98)	-1.32	[240], [348]	n=103 703, N=1	HR	0.90	(0.71-1.15)	-1.11	[349]
ACE inhibitors	n=19 141, N=8	OR	0.79	(0.71-0.88)	-1.27	[240], [350]	n=19 486, N=1	HR	0.89	(0.75-1.06)	-1.12	[351]
Angiotensin-renin inhibitors	n=108 212, N=26	OR	0.92	(0.87-0.97)	-1.09	[240], [352]	n=2877, N=1	RR	0.65	(0.45-0.94)	-1.54	[353]
β-blockers	n=12 825, N=9	RR	0.69	(0.59-0.82)	-1.45	[240], [354]	n=101 141, N=8	OR	1.23	(0.74-2.04)	1.23	[355]
Calcium channel blockers	n=10 136, N=8	OR	0.83	(0.67-1.03)	-1.20	[240], [350]	n=106 566, N=8	OR	0.94	(0.8-1.10)	-1.06	[355]
Diuretics	n=192 478, N=42	RR	0.79	(0.69-0.92)	-1.27	[240], [356]	n=99 669, N=5	OR	0.96	(0.81-1.15)	-1.04	[355]
Biguanides (Metformin)	n=11 385, N=6	OR	0.74	(0.62-0.89)	-1.35	[240], [357]	n=1 800 005, N=1	HR	0.77	(0.73-0.81)	-1.30	[358]
Antidepressants	n=93 653, N=1	HR	0.48	(0.44-0.52)	-2.08	[240], [359]	#	#	#	#	#	#

Note: CHD, Coronary Heart Disease; CI, Confidence Interval; COVID-19, Coronavirus Disease of 2019; HR, Hazard Ratio; OR, Odds Ratio; RR, Relative Risk. A minus sign shows a reduction in risk. (#) denotes that the respective study did not provide this data. A small preliminary study [316] on the effect of the SSRI antidepressant, fluvoxamine, on COVID-19 has shown positive effects. Risk data were not given.

(c) Indirect thrombin inhibitors

Indirect thrombin inhibitors, such as heparin, are used as an anticoagulant, which decreases the odds of CHD with OR 0.91 [346], see Table 6.3. This translates to a 1.10-fold decrease in CHD risk [240] as shown in Figure 6.12. Since many severe cases of COVID-19 present venous thromboembolisms and microthrombi [40]–[44], indirect thrombin inhibitors should be of benefit to such cases.

Heparin was thus expected to reduce these thrombi and reduce COVID-19 severity. A small retrospective analysis (n=449) investigated heparin's effect in COVID-19 patients [347]. The study found an OR of 0.37 in COVID-19 mortality [347], see Table 6.3. This is illustrated in Figure 6.12 as a 2.7-fold decrease in odds of developing severe COVID-19 [347]. The coagulation pathway on which heparin's action is observed is shown in Figure 6.4 as (pw73).

Heparin also seems to have an anti-inflammatory effect [360], which is presented in Figure 6.4 as pathway (pw74). However, this effect is only seen at much higher concentrations, which could increase the risk of bleeding [360]. Therefore, heparin's anti-thrombotic effect would predominantly be the reason for lower COVID-19 severity.

(d) Direct thrombin inhibitors

Direct thrombin inhibitors have shown to decrease the risk of CHD with HR of 0.76 [348], see Table 6.3. This translates to a 1.32-fold decrease in CHD risk [240], illustrated in Figure 6.12. These pharmaceuticals' actions are also observed on the coagulation pathway (pw74) [240], see Figure 6.4.

For COVID-19, direct thrombin inhibitors are shown to slightly reduce the risk of developing severe disease with a HR of 0.90 [349], see Table 6.3. This translates to a 1.11-fold reduction in risk [349], illustrated in Figure 6.12. However, as shown in Figure 6.12 by an (*), this value is not statistically significant with the 95% CI of 0.71-1.15 presented in Table 6.3.

(e) Antihypertensive pharmaceuticals

The antihypertensive *pharmaceutical interventions* in Figure 6.4 are: ACE inhibitors, angiotensin-renin inhibitors, β-blockers, calcium channel blockers and diuretics. The pathways on which their actions are observed are shown in Figure 6.4 as (pw88), (pw89) and (pw50) [240].

The respective reduction of CHD risks for each pharmaceutical [240], [350], [352], [354], [356] is given in Figure 6.12 and Table 6.3 as the following:

- Angiotensin-renin inhibitors: 1.09 (OR of 0.92)
- Calcium channel blockers: 1.20 (OR of 0.83)
- ACE inhibitors: 1.27 (OR of 0.79)
- β-blockers: 1.46 (RR of 0.69)
- Diuretics: 1.27 (RR of 0.79)

The reduction in CHD risk is small for angiotensin-renin inhibitors with an OR close to one (0.92) [352]. However, angiotensin-renin inhibitors seem to be more beneficial for COVID-19 severity with a reduction in 1.54-fold [353], see Figure 6.12.

The risk data for calcium channel blockers (OR of 0.94) [355], ACE inhibitors (HR of 0.89) [351] and diuretics (OR of 0.96) [355] are currently not associated with COVID-19 severity. All risk values are close to one and the respective 95% CI's all show statistically insignificance (containing 1.0), see Table 6.3. This statistically insignificance is illustrated in Figure 6.12 with an (*).

The most interesting of the antihypertensive *pharmaceutical interventions* is β-blockers, which reduced the risk of CHD (RR of 0.69). However, its use increases ones odds of developing severe COVID-19 (OR of 1.23) [355], see Figure 6.12. The reason for this is unclear and further studies are warranted to investigate the mechanism of action involved. However, one explanation for this difference could be that the data is insignificant for COVID-19, with a 95% CI of 0.74-2.04 [355], see Table 6.3.

(f) Biguanides

Biguanides such as metformin has been used for many decades to treat type 2 diabetes and its use decreases the odds of developing CHD, with a OR of 0.74 [357], see Table 6.3. This translates to a 1.35-fold decrease in CHD risk [240], illustrated in Figure 6.12. Metformin's inhibition is observed on pathway (pw14) [240], see Figure 6.4.

Elevated blood glucose levels at admission is an independent predictor of COVID-19 severity irrespective of diabetes [291]. Therefore, glucose lowering agents are expected to reduce COVID-19 mortality. This is indeed the case since a large observational cohort study of type-2 diabetics (n=1 800 005) showed that the use of metformin decreased COVID-19-related mortality by 1.30-fold (HR of 0.77) [358], see Figure 6.12 and Table 6.3.

(g) Antidepressants

A detailed study of the mechanisms by which Selective serotonin uptake inhibitors (SSRIs) antidepressants may reduce CHD risk was published [241]. The study showed that SSRIs can influence most of the CHD hallmarks [241]. A summary, relevant to COVID-19, is given here.

SSRIs such as sertraline has shown to decrease the risk of CHD, with a HR of 0.48 [359], see Table 6.3. This translates to a 2.08-fold decrease in CHD risk [240], illustrated in Figure 6.12. Sertraline's actions are observed on the anti-inflammatory pathway (pw94), as shown in Figure 6.4.

A similar SSRI antidepressant, fluvoxamine's effect on COVID-19 severity is currently being investigated in a clinical trial (NCT04727424). This study was initiated by results from a small double-blind, randomised clinical trial of 152 COVID-19 positive patients treated with fluvoxamine [316]. The outcomes of this study showed that patients treated with fluvoxamine, compared with a placebo, had a lower likelihood of clinical deterioration (0% vs 8.3%) [316].

The study did not report any risk data. For this reason, the data could not be added to Figure 6.12 and Table 6.3. Nevertheless, since a therapeutic effect is seen in the small COVID-19 study, a dotted bar was added to Figure 6.12. It is hypothesised, based on the previous study [241], that most SSRIs will be beneficial.

6.5.5 Insights gained from the integrated CHD/COVID-19 model

6.5.5.1. Why do some patients with severe COVID-19 experience sudden death?

Although aspects of this have been proposed elsewhere [236], [239], [337], [361]–[364], here its integrated mechanism is systematically and visually shown with the relevant pathogenetic pathways with reference to CHD. This model further elucidates other underlying pathogenesis that may influence this *death spiral* before infection of SARS-CoV-2.

The *death spiral* was summarised as follows: Increased inflammation at the lungs causes EC injury, which can result in vascular leakage and/or activation of the coagulation cascade at the lungs, thereby causing hypoxia which can further increase inflammation, creating two closed positive feedback loops and causing severe COVID-19 through a *death spiral* (Figure 6.5).

6.5.5.2. How do CHD comorbidities influence this death spiral?

It is widely accepted that patients with pre-existing CHD comorbidities (thus a poor initial vascular "baseline") have a high risk of developing severe COVID-19 [46]–[49]. The detailed mechanisms of how these comorbidities may influence the *death spiral* was not fully integrated before.

This question was answered in this chapter by visually (Figure 6.8 to Figure 6.10) detailing the mechanisms of how three CHD comorbidities, namely *Hypercholesterolaemia, Hyperglycaemia/Hyperinsulinaemia* and *Hypertension* can fuel the *death spiral.*

6.5.5.3. How can an individual reduce the risk of developing severe COVID-19 from a cardiovascular point of view?

In literature different *health factors* [301], [303], [305], [307], [309], [311], [313] and CHD related *pharmaceuticals* [274], [341], [347], [349], [351], [353], [355], [358] present either a reduction or aggravation of COVID-19 severity. In this chapter the pathogenesis detailing the effect these *health factors* and *pharmaceuticals* may have on this *death spiral* was provided, especially for those with an increased risk for CHD.

It was shown that severe COVID-19 and CHD have similarities in underlying pathogenesis. Therefore, following a lifestyle that would decrease one's risk for CHD before onset of COVID-19 should also decrease the chances of developing severe COVID-19.

The remaining two research questions ((4) and (5)) have partially been answered by the model but future research is still needed. These are discussed in more detail in the following two sections.

6.6 VERIFICATION AND VALIDATION

6.6.1 Verification

As per definition, verification implies that the proposed solution is correctly implemented and thereby provides the expected results. Given the vast coverage of this extensive model, with multiple possibilities such as individualised predictions of COVID-19 severity, a more detailed verification would have been difficult. Therefore, research is needed to further investigate how the risk factors for CHD and COVID-19 can be verified.

Nevertheless, Figure 6.11 and Figure 6.12 clearly illustrate that the risk factors for CHD and COVID-19 are similar (except for β-blockers). Although COVID-19 data is still limited, this is aligned with the expected results. Therefore, one can conclude that the systems-based integration method used to develop the *integrated CHD/COVID-19 model* is partially verified.

6.6.2 Validation

As per definition, validation implies that the proposed method achieves the objectives and thereby solves the problem. The objectives of this chapter and the respective sections in which these objectives were achieved are the following:

1. To develop an *integrated CHD/COVID-19 model*, which explains the mechanisms of interaction of severe COVID-19 on the vascular system. This objective was achieved in Section 6.5.1 with the detailed model provided in Figure 6.4.
2. To use the integrated CHD/COVID-19 model to:
    (a) Investigate why some patients with severe COVID-19 experience sudden death. This objective was achieved in Section 6.5.1.3, refer to Figure 6.5 for the detailed *death spiral* and to Figure 6.6 for a simplified schematic.
    (b) Examine the effect of CHD comorbidities on COVID-19 severity. This objective was achieved in Section 6.5.2, refer to Figure 6.8, Figure 6.9 and Figure 6.10.
    (c) Examine how different *health factors* influence COVID-19 severity. This objective was achieved in Section 6.5.3, refer to Figure 6.11 and Table 6.2.
    (d) Explore how various CHD *pharmaceutical interventions* could help reduce an individual's risk of developing severe COVID-19. This objective was achieved in Section 6.5.4, refer to Figure 6.12 and Table 6.3.

Since all of the objectives were achieved in this chapter, after using the verified method, the proposed solution is validated.

6.7 CONCLUSIONS

COVID-19 data show that disease severity mostly occurs in patients with pre-existing cardiovascular comorbidities, i.e. in patients with poor initial vascular “baselines”. This chapter detailed how a systems approach can explore the mechanisms of cardiovascular complications in COVID-19.

Activated pathogenetic pathways of severe COVID-19 patients were integrated into an existing CHD model, thereby achieving the first objective detailed in Section 6.3. The resulting *integrated CHD/*COVID-19 *model,* depicted in Figure 6.4, addresses the remaining objectives of this study and gives insights into the following issues found in literature:

- The integrated CHD/COVID-19 pathogenesis of the *death spiral* seen in some critical COVID-19 patients.
- The comprehensive mechanisms of how underlying CHD comorbidities, namely *Hyperglycaemia/Hyperinsulinaemia, Hypercholesterolaemia* and/or *Hypertension* may fuel the *death spiral.*
- The detailed pathogeneses of different *health factors,* which affect CHD risk and COVID-19 severity.
- The mechanisms of how chronic CHD *pharmaceutical interventions* may influence COVID-19 severity.
- The proposed model shows many pathways that currently do not have pharmaceuticals which influence them. This information can be the focus of future drug discovery.
- Insights into the hallmarks of CHD, shown in the *integrated CHD/*COVID-19 *model,* also led to various research questions that can form the basis for future research. This includes potential repurposing of an existing drug for cardiovascular disease.

Although the details in this chapter are complex the message is simple. Studies such as this not only highlight the value of a cardiovascular healthy lifestyle in general but also specifically for COVID-19.

6.8 NOVEL CONTRIBUTIONS

6.8.1 Novel contributions of integrated CHD/COVID-19 model

COVID-19 data show that disease severity mainly occurs in patients with pre-existing cardiovascular comorbidities, i.e., poor initial vascular “baselines”. This chapter integrated the activated pathways of severe COVID-19 into an existing CHD model. The resulting integrated CHD/COVID-19 model provides the following novel insights:

- The *integrated CHD/COVID-19 model* presents the main pathogenesis activated during the *death spiral* seen in some critical COVID-19 patients.
- The comprehensive mechanisms of how underlying CHD comorbidities, namely *Hyperglycaemia*/*Hyperinsulinaemia*, *Hypercholesterolaemia* and/or *Hypertension* may fuel the *death spiral.*
- The *integrated CHD/COVID-19 model* provides the detailed pathogeneses of different *health factors*, which affect CHD risk and COVID-19 severity.
- The *integrated CHD/COVID-19 model provides* the mechanisms of how chronic CHD *pharmaceutical interventions* may influence COVID-19 severity.
- The *integrated CHD/COVID-19 model* shows many pathways that currently do not have pharmaceuticals that influence them. This information can be used to identify possible future therapeutic interventions.
- Insights into the hallmarks of CHD, shown in the integrated CHD/COVID-19 model, also led to various research questions that can form the basis for future research. This includes potential repurposing of an existing drug for cardiovascular disease.

6.8.2 Dissemination of results

This chapter has already been successfully published in a special edition research topic of Frontiers in Cardiovascular Medicine (impact factor 6.0 at the time of writing), namely “What do we know about COVID-19 implications for cardiovascular disease?”. The manuscript title: *Using a systems approach to explore the mechanisms of interaction between severe COVID-19 and its coronary heart disease complications.* DOI number: 10.3389/fcvm.2022.737592 (see Appendix D for the published manuscript).

CHAPTER 7
LIMITATIONS, RECOMMENDATIONS AND CONCLUSIONS

"You can't go back and change the beginning, but you can start where you are and change the ending."

C.S. Lewis[24]

[24]Goodreads, "C.S. Lewis Quotes." [Online]. Available: https://www.goodreads.com/quotes/10348517-you-can-t-go-back-and-change-the-beginning-but-you. [Accessed: 21-Nov-2021].

7.1 PREAMBLE

This chapter presents, in two separate sections, the limitations of the study, recommendations for future work and conclusions of Part A and B, respectively.

7.2 PART A: ENGINEERING EXPERIMENTAL MODELLING FOR IN VITRO CANCER MODELS

7.2.1 Limitations of the study

It is recognised that this study had some limitations. Identifying these limitations is essential to be able to make improvements for future work. This study had the following limitations:

- The experimental tests were limited to the available laboratory space and were subsequently only conducted on four available cell lines.
- Given the large amounts of accumulated data, only RCG were calculated from crystal violet staining and spectrophotometry. Whereas more detailed assays, which investigate the mechanism of action for the decrease in RCG, were not used.
- The glucose concentration used for the *in vitro* treatments to mimic those of typical cancer patients' glucose levels during long-term glucose deprivation was assumed.
- Constant values for both glucose and glutamine were assumed, which in reality would fluctuate throughout the day.
- It is still controversial whether *in vitro* chemotherapy dosages can be translated to *in vivo* pharmacokinetic values. Therefore, a limitation of this study is the chosen concentrations for both paclitaxel and carmustine, which were used for the non-metabolic *Pulses*.

7.2.2 Recommendations for future research

Chapters 2 to 4 demonstrate that each cancer cell line reacts differently to metabolic cancer treatments. One should ask why all three cancer cell lines respond differently to long-and short-term GD if glucose is a primary fuel for most cancer cells? To help answer this question, the following future research is proposed.

Firstly, the glucose uptake of the cancer cell lines needs to be quantified. Fortunately, this has been done before [365]–[367]. However, in these studies, the cells were cultured in much higher glucose concentrations (25.52 mmol/l) and not allowed to stabilise in typical cancer patients' glucose levels [365]–[367]. Therefore, a new method to measure cancer cells' glucose uptake at typical cancer patients' glucose concentrations should provide more replicable results.

Fortunately, a pilot study has recently been developed to test the glucose uptake of these three cancer cell lines at typical glucose concentrations of cancer patients. These tests are currently being conducted at South African Nuclear Energy Corporation's (NECSA) radiochemistry department. The study protocol is attached as Appendix E.

In short, the pilot study protocol can be summarised as follows:

1. Expose cells to typical glucose concentrations of cancer patients for 30 days. This ensures that the cells are stabilised at these new concentrations.

2. Expose cells to the glucose PET-tracer, namely FDG, for 1 hour. The FDG is metabolised by the cells in the same way as they would utilise glucose.

3. Measure the FDG uptake of these cells by using the following three different imaging techniques: gamma counter, phosphorimaging, and microPET imaging.

4. Calculate the respective glucose uptake value for each cell line. The most important of these values is the respective cell lines' SUV which is obtained from the microPET scanner (SUV_{cells}).

This protocol will, therefore, provide one with the SUV_{cells}. Once the SUV_{cells} are known for each cell line, they can be matched with the respective cell line's metabolic treatment efficacy (MTE_{cells}). This should thereby create a repository with each cell lines' SUV_{cells} and their respective (MTE_{cells}). Why would this be necessary? This is explained next.

PET scanners are commonly used in clinical practice to measure a cancer patient's tumour glucose uptake (SUV_{tumour}). With the availability of the cell line repository, the SUV_{tumour} could then be used to identify a cell line (of the same cancer type) with a similar SUV_{cells} , i.e., $SUV_{cells} = SUV_{tumour}$. This repository would then help the doctor predict whether metabolic treatment is viable for the patient or not.

This future research is illustrated in Figure 7.1 by the following example: A patient is diagnosed with cancer. The patient goes for a PET scan to determine the patient's tumour SUV_{tumour}. For this example, the SUV_{tumour} is assumed to be 12. The doctor then uses the repository (which consists of the SUV_{cells} and their respective MTE_{cells}) to identify a cell line with a similar SUV. Once a cell line with a similar SUV is found, the doctor is then able to see what the cell line's MTE_{cells} is (in this case 60%). The MTE_{cells} would then provide the doctor with a rough prediction of the patients metabolic treatment efficacy ($MTE_{patient}$), which in this case would be approximately 60%. This should help the doctor determine whether metabolic treatment would be viable for the patient.

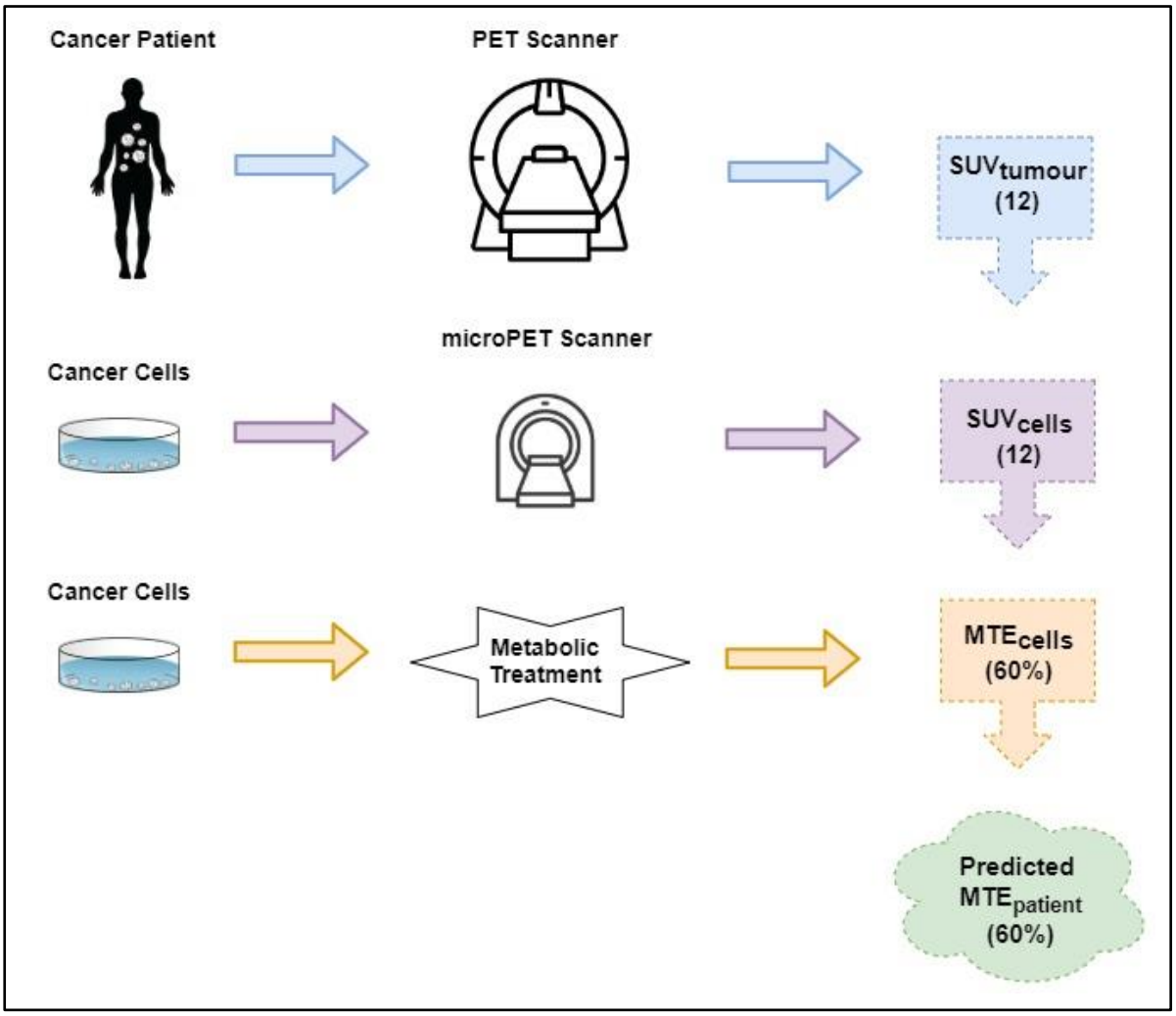

Note: PET, Positron Emission Tomography; SUV, Standard Uptake Value; MTE, Metabolic Treatment Efficacy.

Figure 7.1. Future work to predict metabolic treatment efficacy in cancer patients.

This work can further be improved by combining several cell lines, of the same cancer type, with similar SUV_{cells}. Therefore, the average efficacy of metabolic treatments of the combined cell lines should provide a more calculated estimation of the patient's $MTE_{patient}$.

Therefore, after considering the bigger picture, one can conclude that the novel *in vitro* cancer models developed in this study act as the stepping-stones to future personalised metabolic treatment. If one creates such a prediction model, the following considerations, amongst others, should be accounted for:

1. SUV is calculated based on volume. Therefore, the volume and number of cells should be kept constant. Therefore, a ratio of the patient's tumour (SUV_{tumour}) could be compared to the same non-tumour tissue ($SUV_{non\text{-}tumour}$). This would provide a normalised tumour-to-non-tumour SUV ratio. This method has been used to potentially characterise brain tumour FDG uptake [368], [369].

2. Several confounding factors influence SUV, namely scanner variability, region of interest, partial-volume and spill over effects, attenuation correction, reconstruction methods, time of SUV evaluation, etc. [84], [370]. Therefore, these factors should be accounted for to ensure that the SUV_{tumour} corresponds to the technique used to develop the SUV_{cells}.

Lastly, the proposed future research only considered glucose PET-tracers and could be expanded to other energy sources of cancer cells, namely glutamine, ketones, lactate and free fatty acids [15]. However, new cell culture media would first need to be developed since current cell culture media only contains glucose and glutamine [371]–[373]. Fortunately, new media known as *human plasma-like medium* has recently been developed and includes these other energy sources [374], [375].

In addition to the future work on FDG, another method could be used to further focus on determining the degree of dependency on both glucose (which provides the carbons for biomass synthesis) and glutamine (which provides the nitrogen and ATP synthesis through the glutaminolysis pathway) [376].

This may be done by growing cancer cells in basal media in the absence of added glucose, glutamine, and serum to determine their basal survival time. Thereafter, the control cells should be grown in basal media with glucose (12 mM) and glutamine (2 mM). The cells may then be grown in either glucose alone or glutamine alone to determine the degree of dependency on each fuel.

Furthermore, future work could also employ molecular studies that should help one understand the metabolic changes the cells undergo during long-term glucose deprivation. Recent research has shown that the expression of the (Pyruvate Kinase M2) PKM2 variant in the glycolytic pathway largely prevents ATP synthesis from glucose [377], [378].

Therefore, since the cells recovered from glucose deprivation, it is important to focus on new pathways that the cells may use for ATP synthesis. New information shows that cancer cells obtain their energy from mitochondrial substrate level phosphorylation in the glutaminolysis pathway [124]–[126].

Gene expressions can also be also be considered, namely the human Ki-67 protein that is associated with cell proliferation in tumourigenic cells *via* flow cytometry [379]. These findings can be supported *via* cell cycle progression experiments, which can be conducted by utilizing flow cytometry and propidium iodide staining [380].

Cell signalling should also be considered and can be evaluated by means of western blot and polymerase chain reaction for effects induced by the long-term *Press* deprivation conditions.

The following pathways should be the focus of this future work: phosphoinositide 3-kinases/protein kinase-b pathway (involved in cell survival, proliferation, protein synthesis and glucose metabolism), extracellular signal-regulated kinase (involved in cell survival and glucose metabolism), nuclear factor kappa-light-chain-enhancer of activated B-cells (which play a role in inflammation and cellular stress), lastly an energy status indicator and glucose cellular sensor, namely 5' AMP-activated protein kinase should also be evaluated since these pathways are essential for cell survival signalling [381]–[383].

Lastly, to evaluate cell death and not only relative cell growth, induction via autophagy and apoptosis can also be investigated by means of LC3II expression (western blot) and Annexin V-FITC and/or caspase activation (flow cytometry), respectively [384], [385].

7.2.3 Conclusions

The success rate for developing a new drug for cancer treatment is 3.4%, the lowest for all major diseases. Many have questioned the translatability of *in vitro* cancer models (the first step in novel drug development) to clinical outcomes.

This study identified problems with current *in vitro* cancer models, particularly used for metabolic treatments, using the principle of similarity (see Chapter 1, Section 1.2.1). This principle is commonly used in aerodynamics to ensure that the small-scale model is designed within the bounds of scaling validity, thereby accurately representing the full-scale model. Current metabolic treatments, tested on *in vitro* cancer models, present the following problems:

(i) The initial glucose and glutamine concentrations of metabolic treatments tested on cells are much higher than typical cancer patients' concentrations.

(ii) The glucose concentrations are then decreased to levels far below what is achievable in humans.

(iii) Metabolic treatment durations tested on *in vitro* cancer models do not mimic typical metabolic therapy durations of clinical practice.

These problems all indicate that current *in vitro* cancer models are designed outside of the bounds of scaling validity, i.e., not designed to mimic metabolic conditions of cancer patients during metabolic cancer treatments. Hence, Part A of this thesis aimed to address these problems by applying an engineering experimental modelling approach. This approach was used to mimic typical cancer patients' glucose and glutamine concentrations during metabolic treatments.

These new *in vitro* cancer models were achieved through seven specific research objectives:

1. To develop new *in vitro* cancer models that mimic typical cancer patients' glucose and glutamine levels.

2. To develop long-term GD tests that model GD concentrations of humans during metabolic treatments for investigating the effect on cancer and non-cancer cell growth.

3. To investigate the effect of additional very low, yet achievable, short-term GD on cancer and non-cancer cell growth combined with long-term GD.

4. To investigate the effect of chemotherapy on cancer and non-cancer cell growth when administered at typical cancer patients' glucose and glutamine concentrations.

5. To investigate the effect that additional non-metabolic chemotherapy treatment has on cancer and non-cancer cell growth when combined with long-term GD.

6. To determine if a lower chemotherapy dosage combined with GD will have a similar therapeutic effect compared to a higher chemotherapy dosage administered without GD.

7. To develop a non-toxic GD method that can be implemented in future clinical trials to investigate the effect of combined short- and long-term metabolic treatments.

The first two objectives were achieved by developing new *in vitro* cancer models that mimic normal (objective 1) and long-term GD (objective 2) conditions of typical cancer patients' glucose and glutamine levels during metabolic cancer treatments. The outcomes of these new methods provided the following valuable insights: (a) Long-term GD affects different cancer cell lines differently; (b) full cancer extinction is not possible with long-term GD deprivation alone, and (c) adjuvant therapies are needed to further reduce cell growth.

The third objective was achieved in Chapter 3 by developing new long-term GD (*Press* treatment) in combination with two different metabolic *Pulses.* The metabolic *Pulses* were the following: (i) short-term glucose-only *Pulses* (Treatment 1), and (ii) combined glucose and glutamine *Pulses* (Treatment 2). The results showed that only one of the three cancer cell lines presented a lower RCG after comparing the combined glucose and glutamine *Pulses* with the glucose-only *Pulses.* More importantly, the RCG of all cell lines were lower after the metabolic *Press-Pulse* treatments than after the *Press* only treatment.

In Chapter 4, objective four was achieved by developing new methods that expose cells to different chemotherapies (paclitaxel and carmustine) in combination with long-term GD. The results showed that the efficacy of chemotherapy is enhanced when combined with long-term

GD. However, the non-cancer cells' RCG also decreased further, which hints at increased toxicity.

In addition, objectives five and six were achieved by exposing cells to chemotherapy *Pulses* without GD, i.e., at typical cancer patients' glucose and glutamine concentrations. These results were compared to chemotherapy combined with GD. The comparison showed that lower doses of chemotherapy combined with GD achieved similar decreases in RCG rates in cells than at higher doses of chemotherapy without GD.

Insights gained from the above findings (Chapters 2 to 4) were used to achieve the last objective. A *Press-Pulse* method was developed that could be used to investigate the effect of future long-and short-term combined metabolic cancer treatments in clinical trials (Chapter 5). The use of this method would be feasible after further refinement and ethical clearance.

In conclusion, the novel metabolic *in vitro* cancer models developed in this study and their subsequent results provide evidence that the aim of Part A of this thesis, which was *to develop new long-term metabolic in vitro methods by applying an engineering experimental approach that models typical cancer patients' glucose and glutamine concentrations during metabolic treatments*, was achieved.

7.3 PART B: A SYSTEMS ENGINEERING APPROACH TO SEVERE COVID-19 AND ITS VASCULAR COMPLICATIONS

7.3.1 Limitations of the study

Given the novelty of COVID-19, this study has the following limitations:

- The integrated model only accounts for CHD and not other cardiovascular diseases such as stroke, heart failure, valvular, peripheral artery and cerebrovascular disease.
- Clinical data for the effect of the different *health factors* and *pharmaceutical interventions* on COVID-19 is limited. Therefore, due to the study designs and sizes of the available studies, a statistically significant comparison between these effects on COVID-19 and CHD could not be drawn.
- The model does not update automatically as new literature is published and could become outdated. This is due to the novelty of COVID-19, with new evidence published daily. This new research should be integrated into the model to ensure that its relevance is maintained.

7.3.2 Recommendations for future research

The resulting *integrated CHD/*COVID-19 *model* highlighted a number of research questions and could be used to provide some insight during future investigations.

7.3.2.1. How can computational analysis help to assess the risk of severity in COVID-19 in cardiovascular disease?

To explore how computational analysis can help to assess the risk of COVID-19 in cardiovascular disease the following can be done:

Step 1: Development of a fully integrated network model for the disease, accounting for all effects including cross linking.

Step 2: Characterisation of each interaction (typically at the nodes of the network in Step 1) is needed to solve the network.

The first attempt at Step 1 for severe COVID-19 in cardiovascular disease was conducted in Chapter 6 (Figure 6.4). The next step will be the characterisation of the network using Equation 7.1:

$$Out_{1\to n} = f_{1\to n} In_{1\to n} \tag{7.1}$$

where $In_{1\to n}$ are the inputs (1 to n) to a node, $out_{1\to n}$ are the outputs (1 to n) from the node, and f (1 to n) are the resulting transfer functions. The inputs and outputs are typically measured. More detail of this process is given in a previous study [240]. Fortunately, in engineering, it is easy to develop transfer functions (Equation 7.1) as it is relatively easy to do the required measurements. The challenge for medical networks is the measurements of all the relevant pathways in Figure 6.4.

A typical deep level mine simulation model (A) and a CHD simulation model (B) proposed in [240] are shown in Figure 7.2. If all the biomarkers can be measured for the proposed *integrated CHD/*COVID-19 *model*, it will be possible to individualise the network (Figure 6.4), thereby making it patient specific.

This is similar to individualising an engineering simulation to a specific mine. The risk for COVID-19 severity in CHD can thus be established for any specific individual by inputting the measured biomarkers of that person into the simulation model based on Figure 6.4. Step 1 has already been attempted. However, for Step 2, much work and data are still needed.

Fortunately, there are numerous clinical trials currently underway that focus on treatments for COVID-19 with respect to the CHD hallmarks, namely the following:

(a) *Hypercoagulation* (122 trials)

(b) *Hypercholesterolaemia* (23 trials)

(c) *Hyperglycaemia*/*Hyperinsulinaemia* (Diabetes) (84 trials)

(d) *Inflammation* (265 trials)

(e) *Hypertension* (68 trials)

The clinical trial numbers and respective treatments are available from the supplementary data of the published manuscript. The total number of registered clinical trials on CHD hallmarks effect on COVID-19 are 562. This also includes 94 duplicate studies that focus on more than one CHD hallmark.

Although this approach seems promising, it is unlikely that individual prediction will be feasible. The reason for this is that the data from these clinical trials are based on a large group of

patients, each with their own health complications. Therefore, future research should focus on evaluating studies that explore the risks of similar individuals to further explore this research question.

If such a model can be developed, one would hope that it may help identify optimal treatment strategies (pharmaceuticals) for each patient with Covid-19 or CHD. This approach would then be similar to identifying the optimum control strategies, routinely calculated in engineering, for each individual mine or industrial complexes.

7.3.3 Are there other opportunities in cardiovascular disease that can be derived from this study and the COVID-19 crisis?

This study showed that the late-stage consequences of severe COVID-19 seem to result in the form of accelerated cardiovascular disease. Furthermore, it was shown that most *pharmaceutical interventions* which mediate CHD also mediate the effects of COVID-19.

The question arises if the reverse is true. Are there any reported *pharmaceutical interventions* that reduced COVID-19 severity that could potentially be of value for vascular disease? This is an important question as approximately five times more people died during the past year from cardiovascular disease than from COVID-19.

Such a repurposed drug should preferably treat most of the hallmarks of cardiovascular disease. Such a drug was investigated, namely ivermectin [386]–[391]. Although ivermectin use is still controversial as a drug against COVID-19, studies over nearly three decades before COVID-19 have shown to reduce four of the five hallmarks of cardiovascular disease. These results and the publication dates are given below:

(a) *Hypercoagulability*: (1992) by increasing prothrombin time in 6.7% (ivermectin group) vs 1.4% (control group) of participants in vivo (humans) [392].

(b) *Hypercholesterolaemia*: cholesterol (2013) decreased by 1.5-fold in vivo (mice) [393].

(c) *Hyperglycaemia*: fasting blood glucose (2013) decreased by 1.4-fold in vivo (mice) [393].

(d) *Hyperinsulinaemia*: fasting insulin (2013) decreased by 2.0-fold in vivo (mice) [393].

(e) *Inflammation*: (2004) decreased IL-1β and TNF-α by 1.27-fold in vitro [394].

Except for the CHD hallmark *Inflammation* [395] the focus of ivermectin's proposed mechanism of action (MOA) for COVID-19 is currently on its anti-viral effect [386]–[389].

However, if ivermectin really shows promise for COVID-19 treatment, could the full vascular MOA for ivermectin be as important or even more important than its anti-viral effects?

This research question can only be answered fully by clinical trials, which measure the relevant vascular biomarkers for each CHD hallmark before and after ivermectin use. Side effects of chronic use such as mild elevation of serum aminotransferases should also be investigated [396].

The MOA of ivermectin for the prevention of COVID-19, reportedly seen in small studies [397], is also not clear to the authors. Why would the anti-viral MOA of ivermectin have a preventable effect if the patient has not been infected yet?

Suppose ivermectin really helps for the prevention of COVID-19. Could it rather help create a healthier vascular system (“baseline”) before the virus strikes, especially in vascular compromised individuals, rather than only help *via* its proposed anti-viral effect? Therefore, could ivermectin’s effect on the vascular system during severe COVID-19 be its most important MOA?

If well designed clinical trials show that ivermectin could be a potential cardiovascular drug, could it be an ideal, inexpensive drug for low- and middle-income countries where a high percentage of global cardiovascular-related deaths occur [398]?

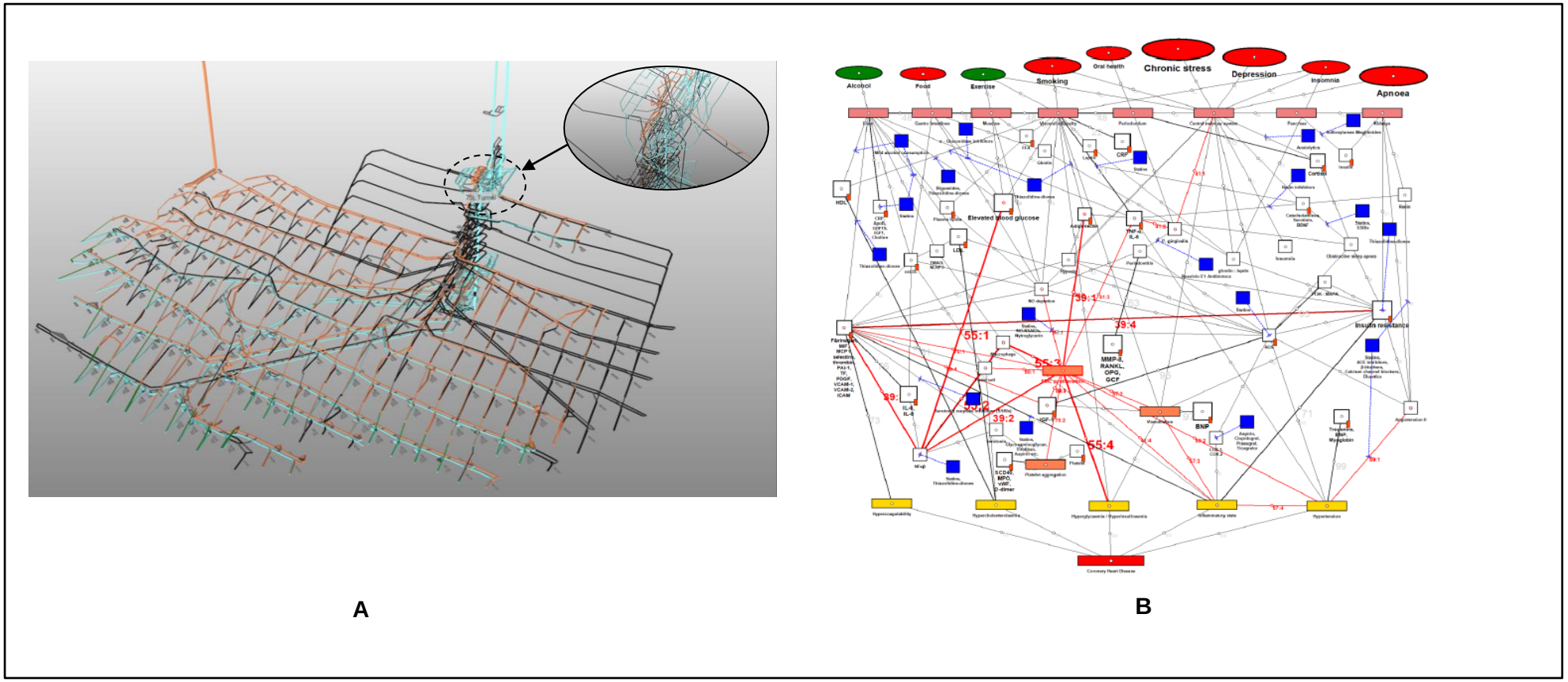

Note: Figure 7.2 A provides a small section of a computer model of a relatively complex deep mine. Figure 7.2B shows the initial computer model [240] developed from the existing CHD model in Figure 6.1 [240] using the simulation software developed for Figure 7.2A. The CHD computer model includes all the known interactions for *health factors,* measured elements (salient biomarkers) and controls (*pharmaceutical interventions).* Remember, it is the measured biomarkers that individualise a patient.

Figure 7.2. Simulation networks for engineering (A) and CHD (B) [240].

7.3.4 Other research questions emanating from this study

Other research questions that should be investigated in future research are the following:

1. Why would β -blockers have an opposite effect on COVID-19 severity than on CHD?
2. There exists an anomaly between statin's cholesterol-lowering effect and low cholesterol levels seen in end-stage COVID-19. How can this drug help decrease COVID-19 severity while it further decreases cholesterol? Can statin's anti-inflammatory effect be so large that it overrides its cholesterol-lowering effect? Would it then be better to drop statins and rather only use anti-inflammatory medication? Or does it depend on the stage of the disease, beneficial at first but not in the end-stage?
3. Does a high correlation of most CHD related *pharmaceutical interventions* and COVID-19 mean that other CHD pharmaceuticals not investigated in detail for COVID-19 could also help reduce COVID-19 severity?
4. Are there pathways shown in the proposed model (Figure 6.4) that do not have pharmaceuticals to regulate them? Could this be the focus of new drug discovery for COVID-19 and cardiovascular disease?
5. Could the model be extended to include cerebrovascular disease and other cardiac diseases such as heart failure, valvular heart disease and peripheral artery disease?

7.3.5 Conclusions

A traditional method used in medical research is based on a reductionistic approach, which entails dividing complex systems into smaller, simpler parts. Such an approach focuses on these smaller parts to either solve the problem or provide insight. As a result, this provides an in-depth understanding of only the smaller aspects and not the larger overall problem.

A reductionistic approach is seen in numerous medical studies of COVID-19, which showed that disease severity mostly occurs in patients with pre-existing cardiovascular comorbidities, i.e., patients with poor initial vascular "baselines". In contrast, complex problems in engineering are primarily solved using a different approach, namely a systems approach (see Chapter 1, Section 1.2.2). A systems approach rather focuses on the inputs and outputs of each element within the system and their effect on the entire system. This systems approach provides a more holistic and integrated understanding of each element's role within the system.

Therefore, in Part B of this thesis, a systems-based engineering approach was used to integrate the vascular complications into an existing model of CHD. This integration resulted in the development of a new *integrated CHD/COVID-19 model,* thereby achieving the first objective, which was:

1. To develop an *integrated CHD/COVID-19 model*, which explains the mechanisms of interaction of severe COVID-19 on the vascular system.

The *integrated CHD/COVID-19 model* was then further used to achieve the following research objectives:

2. To use the *integrated CHD/COVID-19 model* to
    (a) investigate why some patients with severe COVID-19 experience sudden death,
    (b) examine the effect of CHD comorbidities on COVID-19 severity,
    (c) examine how different *health factors* influence COVID-19 severity, and
    (d) explore how various CHD *pharmaceutical interventions* could help reduce an individual's risk of developing severe COVID-19.

The new model provides an integrative view of the pathogenesis of a *death spiral,* which is evident in some critically ill COVID-19 patients. This *death spiral* consists of two feedback loops: *Hypercoagulability* (feedback loop 1) and *Vascular leakage* (feedback loop 2). These feedback loops achieve objective 2 (a) and are described as the following:

- ***Hypercoagulability* (feedback loop 1):** *Inflammation* from COVID-19 results in *EC injury,* which may activate the *coagulation cascade*, forming blood clots in the blood vessels near the alveoli. These blood clots reduce oxygenation efficiency, resulting in *hypoxia* and further increasing *Inflammation,* and the *death spiral* continues.
- ***Vascular leakage* (feedback loop 2):** *Inflammation* from COVID-19 results in *EC injury* in blood vessels near the alveoli, which can lead to *vascular leakage*. This causes fluid build-up within the alveoli, which reduces oxygenation efficiency, resulting in *hypoxia.* The *hypoxia* further increases *Inflammation,* and the *death spiral* continues.

The new model illustrates the comprehensive mechanisms of how underlying CHD comorbidities, namely *Hyperglycaemia/Hyperinsulinaemia, Hypercholesterolaemia* and/or *Hypertension* may fuel the *death spiral.* The CHD comorbidities fuel the *death spiral* by either upregulating *Inflammation* and/or *Hypercoagulability. Hypercholesterolaemia* may upregulate both *Inflammation* and *Hypercoagulability;* whereas *Hyperglycaemia/Hyperinsulinaemia* and *Hypertension* mostly upregulate *Inflammation.* Therefore, objective 2 (b) was achieved.

The last two objectives, 2 (c) and 2 (d), were achieved using the new model to identify the pathogenesis of nine different *health factors* and eleven *pharmaceutical interventions* that affect the risk of CHD and COVID-19 severity. The available data showed that all *health factors* and most *pharmaceutical interventions* that increase CHD risk also increase one's risk for COVID-19 severity. Similarly, the *health factors* and most *pharmaceutical interventions* that decrease one's risk for CHD also reduce one's risk for COVID-19 severity

Insights into the hallmarks of CHD, shown in the *integrated CHD/*COVID-19 *model,* also led to various research questions that can form the basis for future research. This includes the following: (i) potential repurposing of an existing drug for cardiovascular disease, (ii) the development of a computational tool for both COVID-19 applications and cardiovascular disease, and (iii) the addition of new treatments for COVID-19, which could be identified by exploring the pathways that currently do not have *pharmaceuticals interventions* on them.

In conclusion, the *integrated CHD/COVID-19 model* and subsequent insights provide evidence that the aim of Part B in this thesis, which was *to apply a systems-based engineering approach to integrate an existing CHD model with the activated pathogenetic pathways seen in severe COVID-19 complications, to explain the mechanisms of interaction of severe COVID-19 on the vascular system,* was achieved.

GLOSSARY

ACE inhibitors: A class of medication that inhibits angiotensin-converting enzyme and used for the treatment of hypertension [350].

Adipose tissue: More commonly known as body fat, which is stored as reserve energy in a collection of adipocytes [399].

Angiotensinogen: A hormone that regulates fluid balances and blood pressure in the body *via* the renin-angiotensin system [400].

Apoptosis: The process whereby cells undergo programmed cell death [401].

Atherosclerosis: A disease that affects the inner wall of arteries, mostly due to chronic inflammation that leads to thrombosis (blood clots) [402].

α-blockers: A class of pharmaceutical agents that lowers blood pressure by blocking norepinephrine and relaxing muscles in small arteries and veins [403].

β-blockers: A class of pharmaceutical agents that also lowers blood pressure by blocking epinephrine (adrenaline) action, thereby affecting blood flow from the heart [403].

Biguanides: Pharmaceuticals used by type-2 diabetes mellitus and other insulin resistance diseases to reduce glucose production, the most common of these is metformin [404].

Biomarkers: These are biological measures that provide the objective medical state of a patient. They are also used to indicate the biological, pathogenic or pharmacologic responses to a therapeutic intervention [405].

Blood glucose: The concentration of glucose present in the blood (average concentration of 6 mmol/L), derived from the metabolism of foods and/or hepatic stores in the body [64].

Blood vessels: Veins and arteries.

Calcium channel blockers: Pharmaceuticals that are used as antihypertensive agents and for the treatment of chest pain and an irregular heartbeat [406].

Catecholamines: One of the main hormones released into the bloodstream during physical or psychological stress [407].

Cell proliferation: The process that defines cell growth and division [408].

Chemotherapy: A type of cancer treatment where chemotherapeutic drugs are used in the aim of curing, prolonging lifespan and/or reducing symptoms of cancer patients [128].

Cholesterol: An organic lipid molecule that helps maintain the integrity and fluidity of cell membranes. It also serves as a precursor for the synthesis of substances [409].

Coagulation: Also known as clotting, the process that leads to haemostasis, thereby preventing spontaneous bleeding [410].

Computed tomography: An imaging modality produced by a combination of X-ray measurements to develop cross-sectional images of a specified area in the human body [411].

Coronary heart disease: The incidence of atherosclerosis, coronary artery disease, or myocardial infarction [412].

Coronavirus disease: A disease caused by the infection of severe acute respiratory syndrome coronavirus 2 (SARS-CoV-2), which first emerged in Wuhan, China [229].

Cortisol: A glucocorticoid (stress hormone) that raises blood glucose levels by increasing gluconeogenesis when released into the blood [413].

Cytokines: Small proteins that facilitate an immune response to infection, also playing an important role in regulating inflammation [414].

Cytokin storm: An out of control immune response to infection, which results in an increase in pro-inflammatory cytokines [414].

C-reactive protein: A protein synthesised in the liver and its level increases in response to inflammation [415].

Diabetes mellitus: A metabolic disorder that affects the body’s ability to maintain glucose homeostasis due to defective insulin secretion [416].

Direct thrombin inhibitors: Pharmaceuticals that delay blood clot formation (anticoagulant) by directly inhibiting thrombin [417].

Diuretics: Mainly used to treat edema and hypertension, which primary physiologic function is to allow osmotic water abstraction [418].

Electrocardiography: A method used to record the electrical activity of the heart on the body surface [419].

Endothelial cells: Cells located on the inner walls of blood vessels, responsible for vascular elasticity (relaxation and contraction), control enzymes for coagulation and vascular permeability (fluid exchange between blood vessels and tissues) [267].

Endothelial cell injury: Damage of endothelial cells due to viral infection, inflammation, hyperlipidaemia, hypoxia and/or shear stress, etc., which can lead to, amongst others, uncontrolled vascular leakage and coagulation cascade [420].

Energy homeostasis: In biology, it involves the regulation of energy expenditure, food intake and storage [421].

Epinephrine: Also referred to as adrenaline, which is released *via* the adrenal glands. This release is usually activated by emotions such as fear or anger, which, amongst others, increases heart rate, blood pressure and sugar metabolism [407].

Fibrinogen: An essential protein in the blood that facilitates the coagulation process [422].

Fluorodeoxyglucose: A radioactive tracer that acts as a glucose analogue and is used for diagnostic purposes in conjunction with positron-emitting tomography (PET) to localise the tissues with altered glucose metabolism [423].

Free fatty acids: Unbound fatty acids that are metabolised and synthesised as a source of energy for biological processes [424].

Glucocorticoids: Steroid hormones that are used to treat acute inflammation [425].

Gluconeogenesis: The formation of glucose in the liver when the body's glucose storages are low [426].

Glucose: The primary nutrient for maintenance and promotion of cell function also known as sugar [195].

Glutamine: The most abundant free amino acid in the body with several important functions such as protein synthesis, muscle growth, acid-base balance and oxidative fuel for intestine and cells of the immune system [74].

Glycogen: A form of glucose that serves as a form of energy storage primarily stored in the muscles [195].

Glycolysis: The metabolic pathway in cells that convert glucose into energy [427].

Haemodialysis: Renal replacement modality that removes solutes from the bloodstream by diffusion [428].

Haemodiafiltration: A combination of haemodialysis and haemofiltration that removes both small and larger solutes *via* diffusion and enhanced convection [428].

Haemofiltration: Renal replacement modality that removes solutes from the bloodstream by convection [428].

Haemoglobin A_{1c}: The part of red blood cells that carries oxygen throughout your body, which can be used to measure the average level of blood sugar over the past 2 to 3 months [64].

Haemostasis: The mechanism that stops bleeding from a blood vessel *via* coagulation [429].

Health factors: External aspects such as food, stress, exercise that have either a positive or negative influence on CHD.

Highly glycolytic cancers: Cancers that have a much higher uptake of glucose for energy than other cancers.

Hypercholesterolaemia: Elevated cholesterol levels.

Hypercoagulability: An elevated state of coagulation.

Hyperbaric oxygen therapy: A therapy where patients are exposed to a partial pressure of oxygen greater than one atmosphere [430].

Hyperglycaemia: Elevated blood glucose levels.

Hyperinsulinaemia: Elevated levels of blood insulin.

Hypertension: High blood pressure.

Hypoglycaemia: Low blood glucose levels.

Hypothalamic-pituitary-adrenocortical axis: A complex neuroendocrine mechanism that helps maintain physiological homeostasis by regulating various processes such as metabolism, nervous system and immune response [431].

Hypoxemia: A decrease in the partial pressure of oxygen in the blood [265].

Hypoxia: A reduced level of tissue oxygenation [265].

Indirect thrombin inhibitors: Pharmaceuticals that delay blood clot formation (anticoagulant) by indirectly inhibiting thrombin and antithrombin [417].

Inflammation: The body's main biological response to injuries, which include increased blood flow to that area, increased vascular permeability, and cellular infiltration. This results in swelling, redness, pain and fever at the site of inflammation. Inflammation forms a crucial component of tissue repair [432].

Insomnia: A sleep disorder, i.e. difficulty initiating or maintaining sleep.

Insulin: A hormone secreted by the pancreas which is used to maintain normal circulating blood glucose levels. Its main functions include: assisting cellular uptake of glucose and regulating carbohydrate, lipid and protein metabolism [433]**.**

Insulin resistance: A state of irregular high insulin concentrations in the blood due to the body's inability to use insulin for glucose disposal [433]**.**

Insulin-like growth factor-1: An important growth hormone that facilitates the anabolic and linear growth promoting effects of growth hormone protein [434]**.**

Integrated model: A theoretical model of CHD and COVID-19 in which certain aspects of CHD pathogenesis, health factors, biomarkers and pharmaceuticals have been integrated with the pathogenesis of severe COVID-19 patients to show the interactions between the two.

Interleukin: A type of cytokine that facilitates the activation and differentiation of immune cells [435].

***In vitro*:** Tests, experiments or procedures conducted on cells in a controlled microenvironment, such as a test tube or petri dish.

***In vivo*:** Tests, experiments or procedures conducted in or on a living organism such as a human, animal or plant.

Ischemia: A condition that results in a reduction of blood flow (and thus oxygen) to a part of the body [436].

Ketogenic diet: A high fat and low carbohydrate diet, which was initially developed for the treatment of epilepsy. The diet consists of a typical ratio of fats to carbohydrates and protein is 3:1 or 4:1 [169].

Ketones: An alternative source of energy cells use when glucose is depleted due to prolonged fasting or ketogenic diets. Ketones are produced by the liver by breaking down fat [171].

Leptin: A hormone that is secreted mainly by white adipose tissue, which helps inhibit hunger and regulate energy balance [437].

Lipids: Insoluble water molecules, which include cholesterol, free fatty acids and triglycerides [409].

Lipoprotein: Complex biochemical particles that transport cholesterol and triglycerides [409].

Magnetic resonance imaging: A medical imaging technique used in radiology to produce pictures of the inside of the body, by means of a magnetic field and computer-generated radio waves [438].

Meta-analysis: A statistical analyses that combines the results of several scientific studies that address the same research question [439].

Metastases: The stage where cancer has spread from its primary state throughout the body *via* the blood and lymph system, forming new tumours in different parts of the body [440].

Mitochondria: An organelle that acts as the power plant of the cell, orchestrating cellular energy production [441].

Mitogen-activated protein kinase: A type of protein kinase that regulates cellular progams (cell differentiation, division and death) *via* cellular signal transduction pathways [442].

Myocardial infarction: More commonly known as a heart attack. Irreversible death of heart muscle, which happens when the heart muscles do not receive enough blood flow and thus not enough oxygen [443].

Nitric oxide: A molecule that modulates vascular tone, blood pressure and hemodynamics [444].

Norepinephrine: A hormone that increases heart rate, blood flow to muscles and glucose metabolism to provide the body with more energy [407].

Obstructive sleep apnoea: Repetitive narrowing or collapse of the throat during sleep, causing intermittent hypoxia [445].

Oxidative phosphorylation: The process in which energy is produced in the mitochondria of cells through electron transfer driven by substrate level oxidation [446].

Pandemic: A global outbreak of an infectious disease that can increase morbidity and mortality worldwide and disrupt economic, social and political sectors, in this case, COVID-19 pandemic [447].

Pathogenesis: The biological processes or pathways in which a disease develops [448].

Periodontal disease: An infection of the gum which causes severe damage through increased inflammation and, if left untreated, can destroy the bone that supports the teeth [449].

Plasma: Plasma of the blood is the liquid part of blood, consisting of 92% water and carries water, salts and enzymes, which assists, amongst others, blood clotting, osmotic pressure and fluid balance [450].

Platelets: Small blood cells that form clots and help prevent bleeding [451].

Positron emission tomography: An imaging technique that measures physiological functions such as metabolism using radiolabelled drugs [423].

Reactive oxygen species: Oxygen metabolites which are highly reactive chemicals formed from oxygen and mediate physiological and pathophysiological signal transduction [452].

Reductionistic: A research methodology that entails dividing complex systems into smaller parts and focusing on these smaller parts to solve the problem. This leads to an in-depth understanding of only the smaller aspects and not the larger overall problem.

Renin-angiotensin system: Plays an essential role in regulating sodium, water and blood pressure in the body [400].

Salicylates: Salicylates such as aspirin is a common anti-inflammatory [343] and anti-thrombotic [344] medication.

Severe acute respiratory syndrome coronavirus 2: The virus that causes coronavirus disease of 2019, which first emerged in Wuhan, China [229].

Selective serotonin reuptake inhibitors: A psychotropic medication used as an antidepressant, which inhibits serotonin uptake in the nervous system, thereby reducing depression symptoms [453].

Serotonin: A neurotransmitter that stabilises, amongst others, mood, appetite and sleep [454].

Statins: A lipid-lowering medication that inhibits hepatic cholesterol synthesis [342].

Stroke: Similar to myocardial infarction, the only difference is that it occurs in the brain and not the heart, i.e. when the brain does do not receive enough blood flow and thus not enough oxygen, causing lasting brain damage, long-term disability, or even death [455].

Systems approach: Integration of system elements by using a “black-box” method, which characterises each element in a system as a “black box”. It is important to understand the inputs and outputs of each element, rather than the internal detail of each element within the system. This provides a more holistic and integrated understanding of each element’s role in the system.

Thrombosis: A blood clot that blocks the flow of blood in blood vessels [429].

Tumour: An abnormal mass of cells in the body due to an abnormal increase in cell division and decrease in cell death [456].

Tumour necrosis factor: Multifunctional pro-inflammatory cytokine which effects cell survival, proliferation, and death [457].

Vascular: Vessels in the body that help circulate fluid, more specifically blood vessels.

Visceral fat: Adipose tissue stored throughout the body, such as in the abdomen, which plays an important role in maintaining lipid and glucose homeostasis [458].

REFERENCES

[1] S. Chien, R. Bashir, R. M. Nerem, and R. Pettigrew, “Engineering as a new frontier for translational medicine,” *Physiol. Behav.*, vol. 176, no. 1, pp. 1570–1573, 2018, doi: 10.1038/s41395-018-0061-4.

[2] F. M. White, “Dimensional Analysis and Similarity,” in *Fluid Mechanics*, McGraw-Hill Education, 2011, pp. 301–341.

[3] D. Bolster, R. E. Hershberger, and R. J. Donnelly, “Dynamic similarity, the dimensionless science,” *Phys. Today*, vol. 64, no. 9, pp. 42–47, 2011, doi: 10.1063/pt.3.1258.

[4] D. McLean, “Dynamic Similarity,” in *Understanding Aerodynamics: Arguing from the Real Physics*, 2012, pp. 63–65.

[5] M. Vahora, G. K. Ananda, and M. S. Selig, “Design methodology for aerodynamically scaling of a general aviation aircraft airfoil,” *AIAA Aerosp. Sci. Meet. 2018*, no. 210059, 2018, doi: 10.2514/6.2018-1277.

[6] J. A. DiMasi, H. G. Grabowski, and R. W. Hansen, “Innovation in the pharmaceutical industry: New estimates of R&D costs,” *J. Health Econ.*, vol. 47, pp. 20–33, 2016, doi: 10.1016/j.jhealeco.2016.01.012.

[7] C. H. Wong, K. W. Siah, and A. W. Lo, “Estimation of clinical trial success rates and related parameters,” *Biostatistics*, vol. 20, no. 2, pp. 273–286, 2019, doi: 10.1093/biostatistics/kxx069.

[8] A. Eastman, “Improving anticancer drug development begins with cell culture: misinformation perpetrated by the misuse of cytotoxicity assays,” *Oncotarget*, vol. 8, no. 5, pp. 8854–8866, 2017, doi: 10.18632/oncotarget.12673.

[9] D. R. Liston and M. Davis, “Clinically relevant concentrations of anticancer drugs: A guide for nonclinical studies,” *Clin. Cancer Res.*, vol. 23, no. 14, pp. 3489–3498, 2017, doi: 10.1016/j.physbeh.2017.03.040.

[10] T. Voskoglou-nomikos, J. L. Pater, and L. Seymour, “Clinical Predictive Value of the in Vitro Cell Line , Human Xenograft , and Mouse Allograft Preclinical Cancer Models Clinical Predictive Value of the in Vitro Cell Line , Human Xenograft , and Mouse Allograft Preclinical Cancer Models,” vol. 9, no. 613, pp. 4227–4239, 2003.

[11] D. G. Hackman and D. A. Redelmeier, “Translation of Research Evidence From Animals to Humans,” *J. Am. Med. Assoc.*, vol. 296, no. 14, pp. 1731–1732, 2006, doi: 10.3122/jabfm.19.6.648.

[12] I. W. Y. Mak, N. Evaniew, and M. Ghert, “Lost in translation: Animal models and clinical trials in cancer treatment,” *Am. J. Transl. Res.*, vol. 6, no. 2, pp. 114–118, 2014.

[13] M. E. Spilker *et al.*, “Found in translation: Maximizing the clinical relevance of nonclinical oncology studies,” *Clin. Cancer Res.*, vol. 23, no. 4, pp. 1080–1090, 2017, doi: 10.1158/1078-0432.CCR-16-1164.

[14] T. Takebe, R. Imai, and S. Ono, “The Current Status of Drug Discovery and Development as Originated in United States Academia: The Influence of Industrial and Academic Collaboration on Drug Discovery and Development,” *Clin. Transl. Sci.*, vol. 11, no. 6, pp. 597–606, 2018, doi: 10.1111/cts.12577.

[15] U. E. Martinez-Outschoorn, M. Peiris-Pagés, R. G. Pestell, F. Sotgia, and M. P. Lisanti, “Cancer metabolism: A therapeutic perspective,” *Nat. Rev. Clin. Oncol.*, vol. 14, no. 1, pp. 11–31, 2017, doi: 10.1038/nrclinonc.2016.60.

[16] Y. Zhuang, D. K. Chan, A. B. Haugrud, and W. K. Miskimins, “Mechanisms by which low glucose enhances the cytotoxicity of metformin to cancer cells both in vitro and in vivo,” *PLoS One*, vol. 9, no. 9, 2014, doi: 10.1371/journal.pone.0108444.

[17] N. Haga *et al.*, “Mitochondria regulate the unfolded protein response leading to cancer cell survival under glucose deprivation conditions,” *Cancer Sci.*, vol. 101, no. 5, pp. 1125–1132, 2010, doi: 10.1111/j.1349-7006.2010.01525.x.

[18] N. Aykin-Burns, I. M. Ahmad, Y. Zhu, L. W. Oberley, and D. R. Spitz, “Increased levels of superoxide and H2O2 mediate the differential susceptibility of cancer cells versus normal cells to glucose deprivation,” *Biochem. J.*, vol. 418, pp. 29–37, 2009, doi: 10.1042/bj20081258.

[19] A. Priebe *et al.*, “Glucose deprivation activates AMPK and induces cell death through modulation of Akt in ovarian cancer cells,” *Gynecol. Oncol.*, vol. 122, no. 2, pp. 389–395, 2011, doi: 10.1016/j.ygyno.2011.04.024.

[20] H.-R. Park *et al.*, “Effect on Tumor Cells of Blocking Survival Response to Glucose Deprivation,” *J. Natl. Cancer Inst.*, vol. 96, no. 17, pp. 1300–1310, 2004, doi: 10.1093/jnci/djh243.

[21] A. Garufi *et al.*, “Glucose restriction induces cell death in parental but not in homeodomain-interacting protein kinase 2-depleted RKO colon cancer cells: Molecular mechanisms and implications for tumor therapy,” *Cell Death Dis.*, vol. 4, no. 5, pp. 1–11, 2013, doi: 10.1038/cddis.2013.163.

[22] N. A. Graham *et al.*, “Glucose deprivation activates a metabolic and signaling amplification loop leading to cell death,” *Mol. Syst. Biol.*, vol. 8, no. 589, pp. 1–16, 2012, doi: 10.1038/msb.2012.20.

[23] R. Ampferl, H. P. Rodemann, C. Mayer, T. T. A. Höfling, and K. Dittmann, “Glucose starvation impairs DNA repair in tumour cells selectively by blocking histone acetylation,” *Radiother. Oncol.*, vol. 126, no. 3, pp. 465–470, 2018, doi: 10.1016/j.radonc.2017.10.020.

[24] S. K. Bardaweel, H. A. Alsalamat, S. M. Aleidi, and R. M. Bashatwah, “Glucose deprivation enhances the antiproliferative effects of oral hypoglycemic biguanides in different molecular subtypes of breast cancer : An in vitro study,” *Acta Pharm.*, vol. 68, pp. 517–524, 2018, doi: https://doi.org/10.2478/acph-2018-0031.

[25] J. R. Jangamreddy, M. V Jain, A. Hallbeck, K. Lotfi, and M. J. Łos, “Glucose starvation-mediated inhibition of salinomycin induced autophagy amplifies cancer cell specific cell death,” *Oncotarget*, vol. 6, no. 12, pp. 10134–10145, 2015.

[26] J. Yun *et al.*, “Glucose Deprivation Contributes to the Development of KRAS Pathway Mutations in Tumor Cells,” *Science.*, vol. 325, no. September, pp. 1555–1559, 2009, doi: 10.1126/science.1174229.Glucose.

[27] A. Pastò *et al.*, “Resistance to glucose starvation as metabolic trait of platinum- resistant human epithelial ovarian cancer cells,” *Oncotarget*, vol. 8, no. 4, pp. 6433–6445, 2017.

[28] G. Di Conza, S. Trusso Cafarello, X. Zheng, Q. Zhang, and M. Mazzone, “PHD2 Targeting Overcomes Breast Cancer Cell Death upon Glucose Starvation in a PP2A/B55α-Mediated Manner,” *Cell Rep.*, vol. 18, no. 12, pp. 2836–2844, Mar. 2017, doi: 10.1016/j.celrep.2017.02.081.

[29] H. Esumi, J. Lu, Y. Kurashima, and T. Hanaoka, “Antitumor activity of pyrvinium pamoate, 6-(dimethylamino)-2-[2-(2,5-dimethyl-1-phenyl-1H-pyrrol-3-yl)ethenyl]-1-methyl-quinolinium pamoate salt, showing preferential cytotoxicity during glucose starvation,” *Cancer Sci.*, vol. 95, no. 8, pp. 685–690, 2004, doi: doi.org/10.1111/j.1349-7006.2004.tb03330.x.

[30] M. Zhang *et al.*, “Pim1 supports human colorectal cancer growth during glucose deprivation by enhancing the Warburg effect,” *Cancer Sci.*, vol. 109, pp. 1468–1479, 2018, doi: 10.1111/cas.13562.

[31] R. Tomita *et al.*, “Assessment of Anticancer Drug Effects on Pancreatic Cancer Cells under Glucose-Depleted Conditions Using Intracellular and Extracellular Amino Acid Metabolomics,” *Biol. Pharm. Bull.*, vol. 41, no. 2, pp. 220–228, 2018.

[32] D. R. Spitz, J. E. Sim, L. A. Ridnour, S. S. Galoforo, and Y. J. Lee, “Glucose Deprivation-Induced Oxidative Stress in Human Tumor Cells: A Fundamental Defect in Metabolism?,” *Ann. N. Y. Acad. Sci.*, vol. 899, no. 1, pp. 349–362, 2000, doi: 10.1111/j.1749-6632.2000.tb06199.x.

[33] N. Jelluma, X. Yang, D. Stokoe, G. I. Evan, T. B. Dansen, and D. A. Haas-Kogan, “Glucose Withdrawal Induces Oxidative Stress followed by Apoptosis in Glioblastoma Cells but not in Normal Human Astrocytes,” *Mol. Cancer Res.*, vol. 4, no. 5, pp. 319–330, 2006, doi: 10.1158/1541-7786.mcr-05-0061.

[34] A. C. Ahn, M. Tewari, C. S. Poon, and R. S. Phillips, “The limits of reductionism in medicine: Could systems biology offer an alternative?,” *PLoS Med.*, vol. 3, no. 6, pp. 0709–0713, 2006, doi: 10.1371/journal.pmed.0030208.

[35] M. J. Beresford, “Medical reductionism: Lessons from the great philosophers,” *Qjm*, vol. 103, no. 9, pp. 721–724, 2010, doi: 10.1093/qjmed/hcq057.

[36] D. Vandamme, W. Fitzmaurice, B. Kholodenko, and W. Kolch, “Systems medicine: Helping us understand the complexity of disease,” *Qjm*, vol. 106, no. 10, pp. 891–895, 2013, doi: 10.1093/qjmed/hct163.

[37] M. Rajabalinejad, L. van Dongen, and M. Ramtahalsing, “Systems integration theory and fundamentals,” *Saf. Reliab.*, vol. 39, no. 1, pp. 83–113, 2020, doi: 10.1080/09617353.2020.1712918.

[38] D. N. Valencia, “Brief Review on COVID-19: The 2020 Pandemic Caused by SARS-CoV-2,” *Cureus*, vol. 12, no. 3, 2020, doi: 10.7759/cureus.7386.

[39] R. J. Klement, “The SARS-CoV-2 crisis : A crisis of reductionism ?,” *Public Health*, vol. 185, pp. 70–71, 2020, doi: doi.org/10.1016/j.puhe.2020.06.019.

[40] S. E. Fox, A. Akmatbekov, J. L. Harbert, G. Li, J. Quincy Brown, and R. S. Vander Heide, “Pulmonary and cardiac pathology in African American patients with COVID-19: an autopsy series from New Orleans,” *Lancet Respir. Med.*, vol. 8, no. 7, pp. 681–686, 2020, doi: 10.1016/S2213-2600(20)30243-5.

[41] S. F. Lax *et al.*, “Pulmonary Arterial Thrombosis in COVID-19 With Fatal Outcome: Results From a Prospective, Single-Center, Clinicopathologic Case Series,” *Ann. Intern. Med.*, vol. 173, no. May, pp. 330–361, 2020, doi: 10.7326/m20-2566.

[42] M. Ackermann *et al.*, “Pulmonary vascular endothelialitis, thrombosis, and angiogenesis in Covid-19,” *N. Engl. J. Med.*, vol. 383, no. 2, pp. 120–128, 2020, doi: 10.1056/NEJMoa2015432.

[43] D. Wichmann *et al.*, “Autopsy Findings and Venous Thromboembolism in Patients With COVID-19,” *Ann. Intern. Med.*, vol. 25, no. 4, 2020, doi: 10.7326/m20-2003.

[44] Z. Varga *et al.*, “Endothelial cell infection and endotheliitis in COVID-19,” *Lancet*, vol. 395, no. 10234, pp. 1417–1418, 2020, doi: 10.1016/S0140-6736(20)30937-5.

[45] A. Clark *et al.*, “Global, regional, and national estimates of the population at increased risk of severe COVID-19 due to underlying health conditions in 2020: a modelling study,” *Lancet Glob. Heal.*, no. 20, pp. 1–15, 2020, doi: 10.1016/S2214-109X(20)30264-3.

[46] Z. Zheng *et al.*, “Risk factors of critical & mortal COVID-19 cases: A systematic literature review and meta-analysis,” *J. Infect.*, 2020, doi: 10.1016/j.jinf.2020.04.021.

[47] F. Zhou *et al.*, “Clinical course and risk factors for mortality of adult inpatients with COVID-19 in Wuhan, China: a retrospective cohort study,” *Lancet*, vol. 395, no. 10229, pp. 1054–1062, 2020, doi: 10.1016/S0140-6736(20)30566-3.

[48] P. Ssentongo, A. E. Ssentongo, E. S. Heilbrunn, D. M. Ba, and V. M. Chinchilli, “Association of cardiovascular disease and 10 other pre-existing comorbidities with COVID-19 mortality: A systematic review and meta-analysis,” *PLoS One*, vol. 15, no. 8 August, pp. 1–16, 2020, doi: 10.1371/journal.pone.0238215.

[49] L. Luo *et al.*, “The potential association between common comorbidities and severity and mortality of coronavirus disease 2019: A pooled analysis,” *Clin. Cardiol.*, no. June, pp. 1–16, 2020, doi: 10.1002/clc.23465.

[50] M. Vander Heiden, L. Cantley, and C. Thompson, “Understanding the Warburg effect: The metabolic requirements of cell proliferation,” *Science.*, vol. 324, no. 5930, pp. 1029–1033, 2009, doi: 10.1126/science.1160809.

[51] S. F. Winter, F. Loebel, and J. Dietrich, “Role of ketogenic metabolic therapy in malignant glioma: A systematic review,” *Crit. Rev. Oncol. Hematol.*, vol. 112, pp. 41–58, 2017, doi: 10.1016/j.critrevonc.2017.02.016.

[52] V. D. Longo and M. P. Mattson, “Fasting: Molecular mechanisms and clinical applications,” *Cell Metab.*, vol. 19, no. 2, pp. 181–192, 2014, doi: 10.1016/j.cmet.2013.12.008.

[53] C. Lee and V. D. Longo, “Fasting vs dietary restriction in cellular protection and cancer treatment: From model organisms to patients,” *Oncogene*, vol. 30, no. 30, pp. 3305–3316, 2011, doi: 10.1038/onc.2011.91.

[54] C. H. O’Flanagan, L. A. Smith, S. B. McDonell, and S. D. Hursting, “When less may be more: Calorie restriction and response to cancer therapy,” *BMC Med.*, vol. 15, no. 1, pp. 1–10, 2017, doi: 10.1186/s12916-017-0873-x.

[55] C. J. d C. Harvey, G. M. Schofield, and M. Williden, “The use of nutritional supplements to induce ketosis and reduce symptoms associated with keto-induction: a narrative review,” *PeerJ*, vol. 6, p. e4488, 2018, doi: 10.7717/peerj.4488.

[56] B. G. Allen *et al.*, “Ketogenic diets as an adjuvant cancer therapy: History and potential mechanism,” *Redox Biol.*, vol. 2, no. 1, pp. 963–970, 2014, doi: 10.1016/j.redox.2014.08.002.

[57] R. J. Klement, “Fasting, Fats, and Physics: Combining Ketogenic and Radiation Therapy against Cancer,” *Complement. Med. Res.*, vol. 25, no. 2, pp. 102–113, 2018, doi: 10.1159/000484045.

[58] R. J. Klement, “Beneficial effects of ketogenic diets for cancer patients: a realist review with focus on evidence and confirmation,” *Med. Oncol.*, vol. 34, no. 8, pp. 1–34, 2017, doi: 10.1007/s12032-017-0991-5.

[59] A. Zahra *et al.*, “Consuming a Ketogenic Diet while Receiving Radiation and Chemotherapy for Locally Advanced Lung Cancer and Pancreatic Cancer: The University of Iowa Experience of Two Phase 1 Clinical Trials,” *Radiat. Res.*, vol. 187, no. 6, pp. 743–754, 2017, doi: 10.1667/RR14668.1.

[60] G. Zuccoli *et al.*, “Metabolic management of glioblastoma multiforme using standard therapy together with a restricted ketogenic diet: Case Report,” *Nutr. Metab.*, vol. 7, pp. 1–7, 2010, doi: 10.1186/1743-7075-7-33.

[61] A. M. A. Elsakka *et al.*, “Management of Glioblastoma Multiforme in a Patient Treated With Ketogenic Metabolic Therapy and Modified Standard of Care: A 24-Month Follow-Up,” *Front. Nutr.*, vol. 5, no. March, pp. 1–11, 2018, doi: 10.3389/fnut.2018.00020.

[62] D. D. Weber, S. Aminzadeh-Gohari, J. Tulipan, L. Catalano, R. G. Feichtinger, and B. Kofler, “Ketogenic diet in the treatment of cancer - where do we stand?,” *Mol. Metab.*, 2019, doi: 10.1016/j.molmet.2019.06.026.

[63] E. H. Mathews, M. H. Visagie, A. A. Meyer, A. M. Joubert, and G. E. Mathews, “In vitro quantification: Long-term effect of glucose deprivation on various cancer cell lines,” *Nutrition*, vol. 74, p. 110748, 2020, doi: 10.1016/j.nut.2020.110748.

[64] D. M. Nathan, J. Kuenen, R. Borg, H. Zheng, D. Schoenfeld, and R. J. Heine, “Translating the A1C assay into estimated average glucose values,” *Diabetes Care*, vol. 31, no. 8, pp. 1473–1478, 2008, doi: 10.2337/dc08-0545.

[65] M. Watanabe, “Internal environment in cancer patients and proposal that carcinogenesis is adaptive response of glycolysis to overcome adverse internal conditions,” *Health (Irvine. Calif).*, vol. 02, no. 07, pp. 781–788, 2010, doi: 10.4236/health.2010.27118.

[66] T. J. Mckee and S. V Komarova, “Is it time to reinvent basic cell culture medium?,” *Am. J. Physiol. - Cell Physiol.*, vol. 312, pp. 624–626, 2017, doi: 10.1038/483531a.5.

[67] P. Płudowski *et al.*, “Practical guidelines for the supplementation of vitamin D and the treatment of deficits in Central Europe - recommended vitamin D intakes in the general population and groups at risk of vitamin D deficiency.,” *Endokrynol. Pol.*, vol. 64, no. 4, pp. 319–27, 2013, doi: 10.5603/EP.

[68] M. Schmidt, N. Pfetzer, M. Schwab, I. Strauss, and U. Kämmerer, “Effects of a ketogenic diet on the quality of life in 16 patients with advanced cancer: A pilot trial,” *Nutr. Metab. (Lond).*, vol. 8, no. 1, p. 54, 2011, doi: 10.1186/1743-7075-8-54.

[69] E. H. Mathews and L. Liebenberg, “Improved rodent models of human brain metastases,” *Clin. Exp. Metastasis*, vol. 30, no. 7, pp. 949–950, 2013, doi: 10.1007/s10585-013-9588-3.

[70] E. H. Mathews and L. Liebenberg, “Revival of ‘unsuccessful’ chemotherapeutics for highly glycolytic cancers?,” *Med. Hypotheses*, vol. 77, no. 6, p. 1150, 2011, doi: https://doi.org/10.1016/j.mehy.2011.09.020.

[71] G. M. Kowalski and C. R. Bruce, “The regulation of glucose metabolism: implications and considerations for the assessment of glucose homeostasis in rodents,” *Am. J. Physiol. Metab.*, vol. 307, no. 10, pp. E859–E871, 2014, doi: 10.1152/ajpendo.00165.2014.

[72] M. Watanabe, “Internal environment for growth of cancer cells in mice: hypothermia, anemia and lymphocytopenia,” *Health (Irvine. Calif).*, vol. 03, no. 04, pp. 238–244, 2011, doi: 10.4236/health.2011.34042.

[73] W. Stewart and L. Flemming, “Features of a successful therapeutic fast of 382 days’ duration.,” *Postgrad. Med. J.*, vol. 49, pp. 203–209, 1973, doi: 10.1136/pgmj.49.569.203.

[74] R. Rajendram, V. R. Preedy, and V. B. Patel, “Combining Exercise with Glutamine Supplementation in Cancer-Cachexia Metabolism,” in *Glutamine in Clinical Nutrition*, Springer, 2015, p. 493.

[75] M. Gleeson, “Dosing and Efficacy of Glutamine Supplementation in Human Exercise and Sport Training,” *J. Nutr.*, vol. 138, no. 10, pp. 2045S-2049S, 2008, doi: 10.1093/jn/138.10.2045S.

[76] C. T. Hensley, A. T. Wasti, and R. J. Deberardinis, “Review series Glutamine and cancer : cell biology , physiology , and clinical opportunities,” *J. Clin. Invest.*, vol. 123, no. 9, pp. 3678–3684, 2013, doi: 10.1172/JCI69600.3678.

[77] M. H. Visagie, T. V. Mqoco, L. Liebenberg, E. H. Mathews, G. E. Mathews, and A. M. Joubert, “Influence of partial and complete glutamine-and glucose deprivation of breast- and cervical tumorigenic cell lines,” *Cell Biosci.*, vol. 5, no. 1, pp. 1–26, 2015, doi: 10.1186/s13578-015-0030-1.

[78] E. H. Mathews, B. A. Stander, A. M. Joubert, and L. Liebenberg, “Tumor cell culture survival following glucose and glutamine deprivation at typical physiological concentrations,” *Nutrition*, vol. 30, no. 2, pp. 218–227, 2013, doi: 10.1016/j.nut.2013.07.024.

[79] I. F. Robey, A. D. Lien, S. J. Welsh, B. K. Baggett, and R. J. Gillies, “Hypoxia-inducible factor-1α and the glycolytic phenotype in tumors,” *Neoplasia*, vol. 7, no. 4, pp. 324–330, 2005, doi: 10.1593/neo.04430.

[80] B. Liu *et al.*, “Metformin induces unique biological and molecular responses in triple negative breast cancer cells,” *Cell Cycle*, vol. 8, no. 13, pp. 2031–2040, 2009, doi: 10.4161/cc.8.13.8814.

[81] E. H. Mathews, G. E. Mathews, and A. A. Meyer, “A hypothetical method for controlling highly glycolytic cancers and metastases,” *Med. Hypotheses*, vol. 118, no. September, pp. 19–25, 2018, doi: 10.1016/j.anireprosci.2013.11.007.

[82] D. A. Mankoff and J. R. Bellon, “Positron-emission tomographic imaging of cancer: Glucose metabolism and beyond,” *Semin. Radiat. Oncol.*, vol. 11, no. 1, pp. 16–27, 2001, doi: 10.1053/srao.2001.18100.

[83] C. Leiva-salinas, D. Schiff, L. Flors, J. T. Patrie, and P. K. Rehm, “FDG PET/MR Imaging coregistration helps predict survival in patients with glioblastoma and radiologic progression after standard of care treatment,” *Radiology*, vol. 283, no. 2, 2017, doi: 10.1148/radiol.2016161172.

[84] J. A. Thie, “Understanding the standardized uptake value, its methods, and implications for usage.,” *J. Nucl. Med.*, vol. 45, no. 9, pp. 1431–4, 2004, [Online]. Available: http://www.ncbi.nlm.nih.gov/pubmed/15347707.

[85] D. Shi *et al.*, “The preoperative SUVmax for 18 F-FDG uptake predicts survival in patients with colorectal cancer,” *BMC Cancer*, vol. 15, pp. 1–8, 2015, doi: 10.1186/s12885-015-1991-5.

[86] E. H. Mathews and L. Liebenberg, “Is knowledge of brain metabolism the key to treating highly glycolytic cancers and metastases?,” *Neuro. Oncol.*, vol. 15(6), p. 649, 2013.

[87] R. Soffietti, R. Ruda, and R. Mutani, “Management of brain metastases,” *J. Neurol.*, vol. 249, no. 10, pp. 1357–1369, 2002, doi: 10.1007/s00415-002-0870-6.

[88] I. J. Fidler, “The role of the organ microenvironment in brain metastasis,” *Semin. Cancer Biol.*, vol. 21, no. 2, pp. 107–112, 2011, doi: 10.1016/j.semcancer.2010.12.009.

[89] I. J. Fidler, K. Balasubramanian, Q. Lin, S. W. Kim, and S. J. Kim, “The brain microenvironment and cancer metastasis,” *Mol. Cells*, vol. 30, no. 2, pp. 93–98, 2010, doi: 10.1007/s10059-010-0133-9.

[90] K. Herholz, K. Langen, C. Schiepers, and J. M. Mountz, “Brain Tumors,” *Semin. Nucl. Med.*, vol. 42, no. 6, pp. 356–370, 2012, doi: 10.1053/j.semnuclmed.2012.06.001.Brain.

[91] N. Kanarek, B. Petrova, and D. M. Sabatini, “Dietary modifications for enhanced cancer therapy,” *Nature*, vol. 579, no. March, pp. 507–517, 2020, doi: 10.1038/s41586-020-2124-0.

[92] Y. Zhang and J. M. Yang, “Altered energy metabolism in cancer: A unique opportunity for therapeutic intervention,” *Cancer Biol. Ther.*, vol. 14, no. 2, pp. 81–89, 2013, doi: 10.4161/cbt.22958.

[93] E. H. Mathews, L. Liebenberg, and R. Pelzer, “High-glycolytic cancers and their interplay with the body’s glucose demand and supply cycle,” *Med. Hypotheses*, vol. 76, no. 2, pp. 157–165, 2011, doi: 10.1016/j.mehy.2010.09.006.

[94] D. Hanahan and R. A. Weinberg, “Hallmarks of cancer: The next generation,” *Cell*, vol. 144, no. 5, pp. 646–674, 2011, doi: 10.1016/j.cell.2011.02.013.

[95] Y.-K. Choi and K.-G. Park, “Targeting Glutamine Metabolism for Cancer Treatment,” *Biomol. Ther. (Seoul).*, vol. 26, no. 1, pp. 19–28, 2017, doi: 10.4062/biomolther.2017.178.

[96] M. G. Vander Heiden, “Targeting cancer metabolism: A therapeutic window opens,” *Nat. Rev. Drug Discov.*, vol. 10, no. 9, pp. 671–684, 2011, doi: 10.1038/nrd3504.

[97] W. P. Katt, M. J. Lukey, and R. A. Cerione, “Starving the Devourer: Cutting Cancer Off from Its Favorite Foods.,” *Cell Chem. Biol.*, vol. 26, no. 9, pp. 1197–1199, 2019, doi: 10.1016/j.chembiol.2019.09.005.

[98] E. A. Bender, T. J. Case, and M. E. Giplin, “Perturbation Experiments in Community Ecology : Theory and Practice,” *Ecology*, vol. 65, no. 1, pp. 1–13, 1984.

[99] N. . C. Arens and I. . D. West, “Press-pulse: a general theory of mass extinction?,” *Paleobiology*, vol. 34, no. 4, pp. 456–471, 2008, doi: 10.1666/07034.1.

[100] Z. Ratajczak, P. D’Odorico, S. L. Collins, B. T. Bestelmeyer, F. I. Isbell, and J. B. Nippert, “The interactive effects of press/pulse intensity and duration on regime shifts at multiple scales,” *Ecol. Monogr.*, vol. 87, no. 2, pp. 198–218, 2017, doi: 10.1002/ecm.1249.

[101] N. C. Arens and I. D. West, “Press-pulse: a general theory of mass extinction?,” *Paleobiology*, vol. 34, no. 4, pp. 456–471, 2008, doi: 10.1666/07034.1.

[102] J. Cochero, M. Licursi, and N. Gómez, “Effects of pulse and press additions of salt on biofilms of nutrient-rich streams,” *Sci. Total Environ.*, pp. 1–8, 2016, doi: 10.1016/j.scitotenv.2016.11.152.

[103] T. N. Seyfried, G. Yu, J. C. Maroon, and D. P. D'Agostino, "Press-pulse: A novel therapeutic strategy for the metabolic management of cancer," *Nutr. Metab.*, vol. 14, no. 1, pp. 1–17, 2017, doi: 10.1186/s12986-017-0178-2.

[104] O. Warburg, "On the Origin of Cancer Cells," *Science.*, vol. 123, no. 3191, pp. 309–314, 1956.

[105] R. A. Gatenby and R. J. Gillies, "Why do cancers have high aerobic glycolysis?," *Nat. Rev. Cancer*, vol. 4, no. 11, pp. 891–899, 2004, doi: 10.1038/nrc1478.

[106] J. Son *et al.*, "Glutamine supports pancreatic cancer growth through a KRAS-regulated metabolic pathway," *Nature*, vol. 496, no. 7443, pp. 101–105, 2013, doi: 10.1038/nature12040.

[107] L. M. Shelton, L. C. Huysentruyt, and T. N. Seyfried, "Glutamine targeting inhibits systemic metastasis in the VM-M3 murine tumor model," *Int. J. Cancer*, vol. 127, no. 10, pp. 2478–2485, 2010, doi: 10.1002/ijc.25431.

[108] D. R. Wise and C. B. Thompson, "Glutamine Addiction: A New Therapeutic Target in Cancer," *Trends Biochem. Sci.*, vol. 35, no. 8, pp. 427–433, 2011, doi: 10.1016/j.tibs.2010.05.003.Glutamine.

[109] P. Mukherjee *et al.*, "Therapeutic benefit of combining calorie-restricted ketogenic diet and glutamine targeting in late-stage experimental glioblastoma," *Commun. Biol.*, vol. 2, no. 1, pp. 1–14, 2019, doi: 10.1038/s42003-019-0455-x.

[110] S. D. Stefanova, C. Cox, and M. Hill, "Hypoglycaemia: causes, risk factors and pathophysiology.," *Nurs. Stand.*, vol. 27, no. 42, pp. 42–8, 2013, doi: 10.7748/ns2013.06.27.42.42.e7615.

[111] M. A. Jackson *et al.*, "Occult hypoglycemia caused by hemodialysis.," *Clin. Nephrol.*, vol. 51, no. 4, pp. 242–247, 1999.

[112] J. E. Burmeister, A. Scapini, D. da R. Miltersteiner, M. G. da Costa, and B. M. Campos, "Glucose-added dialysis fluid prevents asymptomatic hypoglycaemia in regular haemodialysis," *Nephrol. Dial. Transplant.*, vol. 22, no. 4, pp. 1184–1189, 2007, doi: 10.1093/ndt/gfl710.

[113] S. S. Fajans, R. F. Knopf, J. C. Floyd, L. Power, and J. W. Conn, “The Experimental Induction in Man of Sensitivity to Leucine Hypoglycemia,” *JAMA J. Am. Med. Assoc.*, vol. 184, no. 11, p. 181, 1963, doi: 10.1001/jama.1963.03700240129142.

[114] R. a. Rizza, P. E. Cryer, and J. E. Gerich, “Role of Glucagon, Catecholamines, and Growth Hormone in Human Glucose Counterregulation,” *J. Clin. Invest.*, vol. 64, no. July, pp. 62–71, 1979, doi: 10.1172/JCI109464.

[115] E. J. Drenick, L. C. Alvarez, G. C. Tamasi, and A. S. Brickman, “Resistance to symptomatic insulin reactions after fasting.,” *J. Clin. Invest.*, vol. 51, no. 10, pp. 2757–2762, 1972, doi: 10.1172/JCI107095.

[116] J. M. Rosenthal *et al.*, “The Effect of Acute Hypoglycemia on Brain Function A Functional Magnetic Resonance Imaging Study,” *Diabetes*, vol. 50, no. July, 2001, doi: https://doi.org/10.2337/diabetes.50.7.1618.

[117] P. E. Cryer, “The barrier of hypoglycemia in diabetes,” *Diabetes*, vol. 57, no. 12, pp. 3169–3176, 2008, doi: 10.2337/db08-1084.

[118] R. Blaauw, D. G. Nel, and G. K. Schleicher, “Plasma glutamine levels in relation to intensive care unit patient outcome,” *Nutrients*, vol. 12, no. 2, pp. 1–15, 2020, doi: 10.3390/nu12020402.

[119] E. H. Mathews, L. Liebenberg, and R. Pelzer, “Haemodialysis machine retrofit and control installation and use thereof for the treatment of proliferative dsorders.,” 2012.

[120] E. A. Brooks, S. Galarza, M. F. Gencoglu, R. Chase Cornelison, J. M. Munson, and S. R. Peyton, “Applicability of drug response metrics for cancer studies using biomaterials,” *Philos. Trans. R. Soc. B Biol. Sci.*, vol. 374, no. 1779, 2019, doi: 10.1098/rstb.2018.0226.

[121] M. Hafner, M. Niepel, M. Chung, and P. K. Sorger, “Growth rate inhibition metrics correct for confounders in measuring sensitivity to cancer drugs,” *Nat. Methods*, vol. 13, no. 6, pp. 521–527, 2016, doi: 10.1038/nmeth.3853.

[122] A. Parekh *et al.*, “Bioimpedimetric analysis in conjunction with growth dynamics to differentiate aggressiveness of cancer cells,” *Sci. Rep.*, vol. 8, no. 1, pp. 1–10, 2018, doi: 10.1038/s41598-017-18965-9.

[123] H. Wu, M. Ying, and X. Hu, “Lactic acidosis switches cancer cells from aerobic glycolysis back to dominant oxidative phosphorylation,” *Oncotarget*, vol. 7, no. 26, pp. 36–38, 2016, doi: 10.18632/oncotarget.9746.

[124] T. N. Seyfried and C. Chinopoulos, “Can the mitochondrial metabolic theory explain better the origin and management of cancer than can the somatic mutation theory?,” *Metabolites*, vol. 11, no. 9, pp. 1–21, 2021, doi: 10.3390/metabo11090572.

[125] T. N. Seyfried, G. Arismendi-Morillo, P. Mukherjee, and C. Chinopoulos, “On the Origin of ATP Synthesis in Cancer,” *iScience*, vol. 23, p. 101761, 2020, doi: 10.1016/j.isci.2020.101761.

[126] T. Duraj, J. Carrión-Navarro, T. N. Seyfried, N. García-Romero, and A. Ayuso-Sacido, “Metabolic therapy and bioenergetic analysis: The missing piece of the puzzle,” *Mol. Metab.*, vol. 54, p. 101389, 2021, doi: 10.1016/j.molmet.2021.101389.

[127] T. Duraj, J. Carrión-Navarro, T. N. Seyfried, N. García-Romero, and A. Ayuso-Sacido, “Metabolic therapy and bioenergetic analysis: the missing piece of the puzzle,” *Mol. Metab.*, vol. 54, no. November, p. 101389, 2021, doi: 10.1016/j.molmet.2021.101389.

[128] V. T. DeVita and E. Chu, “A history of cancer chemotherapy,” *Cancer Res.*, vol. 68, no. 21, pp. 8643–8653, 2008, doi: 10.1158/0008-5472.CAN-07-6611.

[129] I. H. Plenderleith, “Treating the treatment: toxicity of cancer chemotherapy,” *Can. Fam. Physician*, vol. 36, no. Oct, pp. 1827–1830, 1990.

[130] L. Raffaghello *et al.*, “Starvation-dependent differential stress resistance protects normal but not cancer cells against high-dose chemotherapy,” *Proc. Natl. Acad. Sci.*, vol. 105, no. 24, pp. 8215–8220, 2008, doi: 10.1073/pnas.0708100105.

[131] R. Buono and V. D. Longo, “Starvation, Stress Resistance, and Cancer,” *Trends Endocrinol. Metab.*, vol. 29, no. 4, pp. 271–280, 2018, doi: 10.1016/j.tem.2018.01.008.

[132] S. Naveed, M. Aslam, and A. Ahmad, “Starvation Based Differential Chemotherapy: A Novel Approach for Cancer Treatment,” *Oman Med. J.*, vol. 29, no. 6, pp. 391–398, 2014, doi: 10.5001/omj.2014.107.

[133] C. Lee *et al.*, “Fasting Cycles Retard Growth of Tumors and Sensitize a Range of Cancer Cell Types to Chemotherapy,” *Sci. Transl. Med.*, vol. 4, no. 124, pp. 1–20, 2012, doi: 10.1126/scitranslmed.3003293.

[134] F. Safdie *et al.*, “Fasting Enhances the Response of Glioma to Chemo- and Radiotherapy,” *PLoS One*, vol. 7, no. 9, pp. 1–9, 2012, doi: 10.1371/journal.pone.0044603.

[135] J. Zhang, Y. Deng, and B. L. Khoo, “Fasting to enhance cancer treatment in models: the next steps,” *J. Biomed. Sci.*, vol. 27, no. 58, pp. 1–14, 2020.

[136] S. De Groot, H. Pijl, J. J. M. Van Der Hoeven, and J. R. Kroep, “Effects of short-term fasting on cancer treatment,” *J. Exp. Clin. Cancer Res.*, vol. 38, no. 1, pp. 1–14, 2019, doi: 10.1186/s13046-019-1189-9.

[137] National Institute of Health US and DailyMed, “Current medication information for BiCNU (carmustine).” 2019, [Online]. Available: https://dailymed.nlm.nih.gov/dailymed/drugInfo.cfm?setid=d6cbb63c-e0b1-43ee-ad6f-408da0772079.

[138] E. K. Rowinsky and R. C. Donehower, “Paclitaxel (taxol),” *N. Engl. J. Med.*, vol. 332, no. 15, pp. 1004–1014, Apr. 1995, doi: 10.1056/NEJM199504133321507.

[139] T. B. Stage, T. K. Bergmann, and D. L. Kroetz, “Clinical Pharmacokinetics of Paclitaxel Monotherapy: An Updated Literature Review,” *Clin. Pharmacokinet.*, vol. 57, no. 1, pp. 7–19, 2018, doi: 10.1007/s40262-017-0563-z.

[140] M. A. Smith and P. Houghton, “A Proposal Regarding Reporting of in Vitro Testing Results,” *Clin. Cancer Res.*, vol. 19, no. 11, pp. 2828–2833, 2013, doi: 10.1038/jid.2014.371.

[141] L. M. Zasadil *et al.*, “Cytotoxicity of paclitaxel in breast cancer is due to chromosome missegregation on multipolar spindles.,” *Sci. Transl. Med.*, vol. 6, no. 229, pp. 1–23, 2014, doi: 10.1126/scitranslmed.3007965.Cytotoxicity.

[142] A. G. Charles, T. Y. Han, Y. Y. Liu, N. Hansen, A. E. Giuliano, and M. C. Cabot, “Taxol-induced ceramide generation and apoptosis in human breast cancer cells,” *Cancer Chemother. Pharmacol.*, vol. 47, no. 5, pp. 444–450, 2001, doi: 10.1007/s002800000265.

[143] Z. Horvath *et al.*, “Synergistic cytotoxicity of the ribonucleotide reductase inhibitor didox (3,4-dihydroxy-benzohydroxamic acid) and the alkylating agent carmustine (BCNU) in 9L rat gliosarcoma cells and DAOY human medulloblastoma cells,” *Cancer Chemother. Pharmacol.*, vol. 54, no. 2, pp. 139–145, 2004, doi: 10.1007/s00280-004-0795-0.

[144] K. Hagihara *et al.*, “Promising Effect of a New Ketogenic Diet Regimen in Patients with Advanced Cancer,” *Nutrients*, vol. 12, no. 1473, pp. 1–13, 2020, doi: 10.3390/nu12051473.

[145] R. Velasco and J. Bruna, “Taxane-induced peripheral neurotoxicity,” *Toxics*, vol. 3, no. 2, pp. 152–169, 2015, doi: 10.3390/toxics3020152.

[146] M. Bhutani, P. M. Colucci, H. Laird-Fick, and B. A. Conley, “Management of paclitaxel-induced neurotoxicity,” *Oncol. Rev.*, vol. 4, no. 2, pp. 107–115, 2010, doi: 10.1007/s12156-010-0048-x.

[147] C. Scripture, W. Figg, and A. Sparreboom, “Peripheral Neuropathy Induced by Paclitaxel: Recent Insights and Future Perspectives,” *Curr. Neuropharmacol.*, vol. 4, no. 2, pp. 165–172, 2006.

[148] K. Kuroi and K. Shimozuma, “Neurotoxicity of taxanes: Symptoms and quality of life assessment,” *Breast Cancer*, vol. 11, no. 1, pp. 92–99, 2004, doi: 10.1007/BF02968010.

[149] S. Takeda *et al.*, “Bongkrekic acid as a warburg effect modulator in long-term estradiol-deprived mcf-7 breast cancer cells,” *Anticancer Res.*, vol. 36, no. 10, pp. 5171–5182, 2016, doi: 10.21873/anticanres.11087.

[150] Ş. Comşa, A. M. Cîmpean, and M. Raica, “The Story of MCF-7 Breast Cancer Cell Line: 40 years of Experience in Research,” *Anticancer Res.*, vol. 35, no. 6, pp. 3147–3154, 2015, [Online]. Available: http://ar.iiarjournals.org/content/35/6/3147.long.

[151] R. Robertson, M. S. Germanos, C. Li, G. S. Mitchell, S. R. Cherry, and M. D. Silva, “Optical imaging of Cerenkov light generation from positron-emitiing radiotracers,” *Phys Med Biol*, vol. 54, no. 16, pp. 355–365, 2009, doi: 10.1088/0031-9155/54/16/N01.Optical.

[152] C. Jose, N. Bellance, and R. Rossignol, “Choosing between glycolysis and oxidative phosphorylation: A tumor’s dilemma?,” *Biochim. Biophys. Acta - Bioenerg.*, vol. 1807, no. 6, pp. 552–561, 2011, doi: 10.1016/j.bbabio.2010.10.012.

[153] T. N. Seyfried and L. M. Shelton, “Cancer as a metabolic disease,” *Nutr. Metab. (Lond).*, vol. 7, no. 7, pp. 1–22, 2010, doi: 10.1097/CCO.0b013e32834e388a.

[154] M. Voss, N. I. Lorenz, A. L. Luger, J. P. Steinbach, J. Rieger, and M. W. Ronellenfitsch, “Rescue of 2-deoxyglucose side effects by ketogenic diet,” *Int. J. Mol. Sci.*, vol. 19, no. 8, pp. 1–12, 2018, doi: 10.3390/ijms19082462.

[155] L. Chen and H. Cui, “Targeting glutamine induces apoptosis: A cancer therapy approach,” *Int. J. Mol. Sci.*, vol. 16, no. 9, pp. 22830–22855, 2015, doi: 10.3390/ijmsl60922830.

[156] R. M. Wilder, “The effects of ketonemia on the course of epilepsy,” in *Mayo Clin Proc*, 1921, vol. 2, pp. 307–308.

[157] B. G. Allen *et al.*, “Ketogenic diets enhance oxidative stress and radio-chemo-therapy responses in lung cancer xenografts,” *Clin. Cancer Res.*, vol. 19, no. 14, pp. 3905–3913, 2013, doi: 10.1158/1078-0432.CCR-12-0287.

[158] M. S. İyikesici, A. K. Slocum, A. Slocum, F. B. Berkarda, M. Kalamian, and T. N. Seyfried, “Efficacy of Metabolically Supported Chemotherapy Combined with Ketogenic Diet, Hyperthermia, and Hyperbaric Oxygen Therapy for Stage IV Triple-Negative Breast Cancer,” *Cureus*, vol. 9, no. 7, pp. 1–14, 2017, doi: 10.7759/cureus.1445.

[159] R. J. Klement, “The emerging role of ketogenic diets in cancer treatment,” *Curr. Opin. Clin. Nutr. Metab. Care*, vol. 22, no. 2, pp. 129–134, 2019, doi: 10.1097/MCO.0000000000000540.

[160] M. Lv, X. Zhu, H. Wang, F. Wang, and W. Guan, “Roles of caloric restriction, ketogenic diet and intermittent fasting during initiation, progression and metastasis of cancer in animal models: A systematic review and meta-analysis,” *PLoS One*, vol. 9, no. 12, pp. 1–18, 2014, doi: 10.1371/journal.pone.0115147.

[161] G.-W. Hao, Y.-S. Chen, D.-M. He, H.-Y. Wang, G.-H. Wu, and B. Zhang, “Growth of human Colon cancer cells in nude mice is delayed by a ketogenic diet or without omega-3 fatty acids and medium-chain triglycerides,” *Asian Pacific J. Cancer Prev.*, vol. 16, no. 122, pp. 2061–2068, 2015, doi: 10.1186/1471-2407-8-122.

[162] C. Otto *et al.*, “Growth of human gastric cancer cells in nude mice is delayed by a ketogenic diet supplemented with omega-3 fatty acids and medium-chain triglycerides,” *BMC Cancer*, vol. 8, pp. 1–13, 2008, doi: 10.1186/1471-2407-8-122.

[163] R. J. Morscher *et al.*, “Inhibition of neuroblastoma tumor growth by ketogenic diet and/or calorie restriction in a CD1-nu mouse model,” *PLoS One*, vol. 10, no. 6, pp. 1–20, 2015, doi: 10.1371/journal.pone.0129802.

[164] S. Aminzadeh-Gohari *et al.*, “A ketogenic diet supplemented with medium-chain triglycerides enhances the anti-tumor and anti-angiogenic efficacy of chemotherapy on neuroblastoma xenografts in a CD1-nu mouse model,” *Oncotarget*, vol. 8, no. 39, pp. 64728–64744, 2017, doi: 10.18632/oncotarget.20041.

[165] S. K. Shukla *et al.*, “Metabolic reprogramming induced by ketone bodies diminishes pancreatic cancer cachexia,” *Cancer Metab.*, vol. 2, no. 1, p. 18, 2014, doi: 10.1186/2049-3002-2-18.

[166] J. C. Mavropoulos *et al.*, “The effects of varying dietary carbohydrate and fat content on survival in a murine LNCaP prostate cancer xenograft model,” *Cancer Prev. Res.*, vol. 2, no. 6, pp. 557–565, 2009, doi: 10.1158/1940-6207.CAPR-08-0188.

[167] H. S. Kim *et al.*, “Carbohydrate restriction and lactate transporter inhibition in a mouse xenograft model of human prostate cancer,” *BJU Int.*, vol. 110, no. 7, pp. 1062–1069, 2012, doi: 10.1111/j.1464-410X.2012.10971.x.

[168] J. Caso *et al.*, “The effect of carbohydrate restriction on prostate cancer tumor growth in a castrate mouse xenograft model,” *Prostate*, vol. 73, no. 5, pp. 449–454, 2013, doi: 10.1002/pros.22586.

[169] A. L. Hartman and E. P. G. Vining, “Clinical Aspects of the Ketogenic Diet,” *Epilepsia*, vol. 48, no. 1, pp. 31–42, 2007, doi: 10.1111/j.1528-1167.2007.00914.x.

[170] M. G. Vander Heiden, “Targeting cancer metabolism: A therapeutic window opens,” *Nat. Rev. Drug Discov.*, vol. 10, no. 9, pp. 671–684, 2011, doi: 10.1038/nrd3504.

[171] T. B. Vanitallie and T. H. Nufert, “Ketones : Metabolism ’ s Ugly Duckling,” *Nutr. Rev.*, vol. 61, no. 10, pp. 327–41, 2003, doi: 10.131/nr.2003.oct.327.

[172] F. M. Safdie *et al.*, “Fasting and cancer treatment in humans: A case series report.,” *Aging (Albany. NY).*, vol. 1, no. 12, pp. 988–1007, 2009, doi: 10.18632/aging.100114.

[173] L. B. A. Rojas and M. B. Gomes, “Metformin: an old but still the best treatment for type 2 diabetes,” *Diabetol. Metab. Syndr.*, vol. 5, no. 1, p. 6, 2013, doi: 10.1186/1758-5996-5-6.

[174] I. Ben Sahra, Y. Le Marchand-Brustel, J.-F. Tanti, and F. Bost, “Metformin in Cancer Therapy: A New Perspective for an Old Antidiabetic Drug?,” *Mol. Cancer Ther.*, vol. 9, no. 5, pp. 1092–1099, 2010, doi: 10.1158/1535-7163.mct-09-1186.

[175] M. B. Antonoff and J. D’cunha, “Teaching an Old Drug New Tricks: Metformin as a Targeted Therapy for Lung Cancer,” *Semin. Thorac. Cardiovasc. Surg.*, vol. 22, no. 3, pp. 195–196, 2010, doi: 10.1053/j.semtcvs.2010.10.015.

[176] H. A. Hirsch, D. Iliopoulos, P. N. Tsichlis, and K. Struhl, “Metformin selectively targets cancer stem cells, and acts together with chemotherapy to block tumor growth and prolong remission,” *Cancer Res.*, vol. 69, no. 19, pp. 7507–7511, 2009, doi: 10.1158/0008-5472.CAN-09-2994.

[177] C. W. Song *et al.*, “Metformin kills and radiosensitizes cancer cells and preferentially kills cancer stem cells,” *Sci. Rep.*, vol. 2, pp. 28–31, 2012, doi: 10.1038/srep00362.

[178] J. A. Menendez *et al.*, “Metformin is synthetically lethal with glucose withdrawal in cancer cells,” *Cell Cycle*, vol. 11, no. 15, pp. 2782–2792, 2012, doi: 10.4161/cc.20948.

[179] E. H. Mathews and L. Liebenberg, “A practical quantification of blood glucose production due to high-level chronic stress,” *Stress Heal.*, vol. 28, no. 4, pp. 327–332, 2012, doi: 10.1002/smi.2415.

[180] G. Shakhar and S. Ben-Eliyahu, “Potential prophylactic measures against postoperative immunosuppression: Could they reduce recurrence rates in oncological patients?,” *Ann. Surg. Oncol.*, vol. 10, no. 8, pp. 972–992, 2003, doi: 10.1245/ASO.2003.02.007.

[181] U. S. D. of H. and H. Services, F. and D. Administration, C. for D. E. and R. (CDER), and C. for B. E. and R. (CBER), “ICH Guideline for Good Clinical Practice: Consolidated Guidance (E6),” in *Human subject protection (HSP) and good clinical practice (GCP) regulations and guidelines*, Philadelphia: Clinical Research Resources, 1997, pp. 39–46.

[182] L. K. Shankar *et al.*, “Consensus Recommendations for the Use of 18 F- FDG PET as an Indicator of Therapeutic Response in Patients in National Cancer Institute Trials,” *J. Nucl. Med.*, vol. 47, no. 6, pp. 1059–1066, 2006.

[183] S. C. Huang, “Anatomy of SUV,” *Nucl. Med. Biol.*, vol. 27, no. 7, pp. 643–646, 2000, doi: 10.1016/S0969-8051(00)00155-4.

[184] R. L. Wahl, H. Jacene, Y. Kasamon, and M. A. Lodge, “From RECIST to PERCIST: Evolving Considerations for PET Response Criteria in Solid Tumors,” *J. Nucl. Med.*, vol. 50, no. Suppl_1, pp. 122S-150S, 2009, doi: 10.2967/jnumed.108.057307.

[185] W. Zhou, P. Mukherjee, M. A. Kiebish, W. T. Markis, J. G. Mantis, and T. N. Seyfried, “The calorically restricted ketogenic diet, an effective alternative therapy for malignant brain cancer.,” *Nutr. Metab. (Lond).*, vol. 4, p. 5, 2007, doi: 10.1186/1743-7075-4-5.

[186] J. J. Meidenbauer, P. Mukherjee, and T. N. Seyfried, “The glucose ketone index calculator: A simple tool to monitor therapeutic efficacy for metabolic management of brain cancer,” *Nutr. Metab.*, vol. 12, no. 1, pp. 1–8, 2015, doi: 10.1186/s12986-015-0009-2.

[187] L. Groop, K. J. Tötterman, K. Harno, and A. Gordin, “Influence of Beta-Blocking Drugs on Glucose Metabolism in Hypertensive, Non-Diabetic Patients,” *J. Intern. Med.*, vol. 213, no. 1, pp. 9–14, 1983.

[188] V. Vulpis, A. Antonacci, P. Prandi, D. Bokor, and A. Pirrelli, “The effects of bisoprolol and atenolol on glucose metabolism in hypertensive patients with non-insulin-dependent diabetes mellitus,” *Minerva Med.*, vol. 82, no. 4, pp. 189–193, 1991.

[189] G. Maartens *et al.*, “Cardiovascular System,” in *Standard Treatment Guidelines and Essential Medicines List for South Africa Hospital Level 2015 Edition*, 2015, pp. 3.6-3.16.

[190] D. A. Towler, C. E. Havlin, S. Craft, and P. Cryer, “Mechanism of awareness of hypoglycemia: Perception of neurogenic (predominantly cholinergic) rather than neuroglycopenic symptoms,” *Diabetes*, vol. 42, no. 12, pp. 1791–1798, 1993, doi: 10.2337/diab.42.12.1791.

[191] D. A. Popp, T. F. Tse, S. D. Shah, W. E. Clutter, and P. E. Cryer, “Oral propranolol and metoprolol both impair glucose recovery from insulin-induced hypoglycemia in insulin-dependent diabetes mellitus,” *Diabetes Care*, vol. 7, no. 3, pp. 243–247, 1984, doi: 10.2337/diacare.7.3.243.

[192] A. J. Garber, P. E. Cryer, J. V. Santiago, M. W. Haymond, A. S. Pagliara, and D. M. Kipnis, “The role of adrenergic mechanisms in the substrate and hormonal response to insulin induced hypoglycemia in man,” *J. Clin. Invest.*, vol. 58, no. 1, pp. 7–15, 1976, doi: 10.1172/JCI108460.

[193] L. R. Squire, D. Berg, F. Bloom, S. Du Lac, A. Ghosh, and N. Spitzer, “Fundamental neuroscience,” *Profesional Psychology*. Academic press, p. 261, 2012, doi: 10.1163/_q3_SIM_00374.

[194] G. Siegel, B. Agranoff, R. Albers, S. Fisher, and M. Uhler, *Basic neurochemistry: molecular, cellular and medical aspects.*, 6th ed. Philadelphia: Lippincott-Raven, 1999.

[195] D. H. Wasserman, “Four grams of glucose.,” *Am. J. Physiol. Endocrinol. Metab.*, vol. 296, no. 1, pp. E11-21, 2009, doi: 10.1152/ajpendo.90563.2008.

[196] A. Peters, “The selfish brain: Competition for energy resources,” *Am. J. Hum. Biol.*, vol. 23, no. 1, pp. 29–34, 2011, doi: 10.1002/ajhb.21106.

[197] P. E. Cryer, S. N. Davis, and H. Shamoon, “Hypoglycemia in Diabetes,” *Diabetes Care*, vol. 26, no. 6, pp. 1902–1912, 2003.

[198] P. E. Cryer, “Diverse Causes of Hypoglycemia-Associated Autonomic Failure in Diabetes,” *N. Engl. J. Med.*, vol. 350, no. 22, pp. 2272–2279, 2004, doi: 10.1056/NEJMra031354.

[199] American Diabetes Association, “Defining and Reporting Hypoglycemia in Diabetes,” *Diabetes Care*, vol. 28, no. 5, pp. 1245–1249, 2005, doi: 10.2337/diacare.28.5.1245.

[200] I. H. Study group, “Glucose Concentrations of Less Than 3.0 mmol/L (54 mg/dL) Should Be Reported in Clinical Trials: A Joint Position Statement of the American Diabetes Association and the European Association for the Study of Diabetes: Table 1,” *Diabetes Care*, vol. 40, no. 1, pp. 155–157, 2017, doi: 10.2337/dc16-2215.

[201] P. E. Cryer, “Hypoglycemia, functional brain failure, and brain death,” *J. Clin. Invest.*, vol. 117, no. 4, pp. 868–870, 2007, doi: 10.1172/JCI31669.

[202] A. Tameemm and H. Krovvidi, “Cerebral physiology,” *Contin. Educ. Anaesthesia, Crit. Care Pain*, vol. 13, no. 4, pp. 113–118, 2013, doi: 10.1093/bjaceaccp/mkt001.

[203] C. Moga and D. Chojechi, “Oxygen therapy in acute care settings,” 2016.

[204] P. E. Cryer *et al.*, “Evaluation and management of adult hypoglycemic disorders: An endocrine society clinical practice guideline,” *J. Clin. Endocrinol. Metab.*, vol. 94, no. 3, pp. 709–728, 2009, doi: 10.1210/jc.2008-1410.

[205] L. Shaashua *et al.*, “Perioperative COX-2 and β-adrenergic blockade improves metastatic biomarkers in breast cancer patients in a phase-II randomized trial,” *Clin. Cancer Res.*, vol. 23, no. 16, pp. 4651–4661, 2017, doi: 10.1158/1078-0432.CCR-17-0152.

[206] K. Guo *et al.*, “Norepinephrine-induced invasion by pancreatic cancer cells is inhibited by propranolol,” *Anticancer Res.*, vol. 22, pp. 825–830, 2009, doi: 10.3892/or.

[207] D. Palm *et al.*, “The norepinephrine-driven metastasis development of PC-3 human prostate cancer cells in BALB/c nude mice is inhibited by β-blockers,” *Int. J. Cancer*, vol. 118, no. 11, pp. 2744–2749, 2006, doi: 10.1002/ijc.21723.

[208] E. Botteri *et al.*, “Therapeutic effect of β-blockers in triple-negative breast cancer postmenopausal women,” *Breast Cancer Res. Treat.*, vol. 140, no. 3, pp. 567–575, 2013, doi: 10.1007/s10549-013-2654-3.

[209] T. I. Barron, R. M. Connolly, L. Sharp, K. Bennett, and K. Visvanathan, “Beta blockers and breast cancer mortality: a population-based study,” *J. Clin. Oncol.*, vol. 29, no. 19, pp. 2635–2644, 2011.

[210] H. H. Grytli, M. W. Fagerland, K. A. Tasken, S. D. Fossa, and L. L. Haheim, “Use of beta-blockers is associated with prostate cancer-specific survival in prostate cancer patients on androgen deprivation therapy,” *Prostate*, vol. 73, no. 3, pp. 250–260, 2013, doi: 10.1002/pros.22564.

[211] J. Tang, Z. Li, L. Lu, and C. H. Cho, “β-Adrenergic system, a backstage manipulator regulating tumour progression and drug target in cancer therapy,” *Semin. Cancer Biol.*, vol. 23, no. 6 PB, pp. 533–542, 2013, doi: 10.1016/j.semcancer.2013.08.009.

[212] S. W. Cole and A. K. Sood, “Molecular pathways: Beta-adrenergic signaling in cancer,” *Clin. Cancer Res.*, vol. 18, no. 5, pp. 1201–1206, 2012, doi: 10.1158/1078-0432.CCR-11-0641.

[213] C. Liebow, C. Reilly, M. Serrano, and a V Schally, “Somatostatin analogues inhibit growth of pancreatic cancer by stimulating tyrosine phosphatase.,” *Proc. Natl. Acad. Sci. U. S. A.*, vol. 86, no. 6, pp. 2003–2007, 1989, doi: 10.1073/pnas.86.6.2003.

[214] A. V Schally, “Oncological applications of somatostatin analogues,” *Cancer Res.*, vol. 48, pp. 6977–6985, 1988.

[215] A. Giustina, G. Mazziotti, V. Torri, M. Spinello, I. Floriani, and S. Melmed, “Meta-analysis on the effects of octreotide on tumor mass in acromegaly,” *PLoS One*, vol. 7, no. 5, 2012, doi: 10.1371/journal.pone.0036411.

[216] M. Yasukawa, K. Yasukawa, Y. Kamiizumi, and R. Yokoyama, “Intravenous phentolamine infusion alleviates the pain of abdominal visceral cancer, including pancreatic carcinoma,” *J. Anesth.*, vol. 21, no. 3, pp. 420–423, 2007, doi: 10.1007/s00540-007-0528-8.

[217] R. J. O. Dowling, P. J. Goodwin, and V. Stambolic, “Understanding the benefit of metformin use in cancer treatment.,” *BMC Med.*, vol. 9, no. 1, p. 33, 2011, doi: 10.1186/1741-7015-9-33.

[218] E. J. Fine *et al.*, “Targeting insulin inhibition as a metabolic therapy in advanced cancer: A pilot safety and feasibility dietary trial in 10 patients,” *Nutrition*, vol. 28, no. 10, pp. 1028–1035, 2012, doi: 10.1016/j.nut.2012.05.001.

[219] J. James, “Safety and insulin: Implementation of national guidance at a local level,” vol. 17, no. 5, pp. 180–186, 2013.

[220] M. F. Carroll, M. R. Burge, and D. S. Schade, “Severe hypoglycemia in adults,” *Rev. Endocr. Metab. Disord.*, vol. 4, no. 2, pp. 149–157, 2003, doi: 10.1023/A:1022990003161.

[221] M. S. Cairo and M. Bishop, “Tumour lysis syndrome: New therapeutic strategies and classification,” *Br. J. Haematol.*, vol. 127, no. 1, pp. 3–11, 2004, doi: 10.1111/j.1365-2141.2004.05094.x.

[222] K. Arrambide and R. D. Toto, “Tumor lysis syndrome.,” *Semin. Nephrol.*, vol. 13, no. 3, pp. 273–280, May 1993, [Online]. Available: http://nwulib.nwu.ac.za/login?url=http://search.ebscohost.com/login.aspx?direct=true&db=cmedm&AN=8321927&site=eds-live.

[223] S. C. Howard, D. P. Jones, and C.-H. Pui, “The Tumor Lysis Syndrome,” *N. Engl. J. Med.*, vol. 364, no. 19, pp. 1844–1854, 2011, doi: 10.1056/NEJMra0904569.

[224] B. Coiffier, A. Altman, C.-H. Pui, A. Younes, and M. S. Cairo, “Guidelines for the Management of Pediatric and Adult Tumor Lysis Syndrome: An Evidence-Based Review,” *J. Clin. Oncol.*, vol. 26, no. 16, pp. 2767–2778, 2008, doi: 10.1200/JCO.2007.15.0177.

[225] M. T. McCurdy and C. B. Shanholtz, “Oncologic emergencies,” *Crit. Care Med.*, vol. 40, no. 7, pp. 2212–2222, 2012, doi: 10.1097/CCM.0b013e31824e1865.

[226] W. R. Lu, J. Defilippi, and A. Braun, “Unleash Metformin: Reconsideration of the Contraindication in Patients with Renal Impairment,” *Ann. Pharmacother.*, vol. 47, no. 11, pp. 1488–1497, 2013, doi: 10.1177/1060028013505428.

[227] E. D. Michelakis, L. Webster, and J. R. Mackey, “Dichloroacetate (DCA) as a potential metabolic-targeting therapy for cancer,” *Br. J. Cancer*, vol. 99, no. 7, pp. 989–994, 2008, doi: 10.1038/sj.bjc.6604554.

[228] E. H. Mathews, M. H. Visagie, A. A. Meyer, A. M. Joubert, and G. E. Mathews, “In vitro quantification: Long-term effect of glucose deprivation on various cancer cell lines,” *Nutrition*, vol. 74, no. January, pp. 1–5, 2020, doi: 10.1016/j.nut.2020.110748.

[229] Y. C. Liu, R. L. Kuo, and S. R. Shih, “COVID-19: The first documented coronavirus pandemic in history,” *Biomed. J.*, pp. 1–6, 2020, doi: 10.1016/j.bj.2020.04.007.

[230] World Health Organization, “Weekly epidemiological update on COVID-19 - 10 August 2021,” 2021. [Online]. Available: https://www.who.int/publications/m/item/weekly-epidemiological-update-on-covid-19---10-august-2021.

[231] P. Martins-Filho, C. Santos, S. Tavares, and V. Antos, “Factors associated with mortality in patients with COVID-19. A quantitative evidence synthesis of clinical and laboratory data,” no. January, 2020, doi: doi.org/10.1016/j.ejim.2020.04.043.

[232] Y. Y. Zheng, Y. T. Ma, J. Y. Zhang, and X. Xie, “COVID-19 and the cardiovascular system,” *Nat. Rev. Cardiol.*, vol. 17, no. 5, pp. 259–260, 2020, doi: 10.1038/s41569-020-0360-5.

[233] B. Long, W. J. Brady, A. Koyfman, and M. Gottlieb, “Cardiovascular complications in COVID-19,” *Am. J. Emerg. Med.*, vol. 38, no. 7, pp. 1504–1507, 2020, doi: 10.1016/j.ajem.2020.04.048.

[234] P. P. Liu, A. Blet, D. Smyth, and H. Li, “The Science Underlying COVID-19: Implications for the Cardiovascular System,” *Circulation*, vol. 142, pp. 68–78, 2020, doi: 10.1161/CIRCULATIONAHA.120.047549.

[235] P. Libby, “The Heart in COVID-19: Primary Target or Secondary Bystander?,” *JACC Basic to Transl. Sci.*, vol. 5, no. 5, pp. 537–542, 2020, doi: 10.1016/j.jacbts.2020.04.001.

[236] D. Atri, H. K. Siddiqi, J. P. Lang, V. Nauffal, D. A. Morrow, and E. A. Bohula, “COVID-19 for the Cardiologist: Basic Virology, Epidemiology, Cardiac Manifestations, and Potential Therapeutic Strategies,” *JACC Basic to Transl. Sci.*, vol. 5, no. 5, pp. 518–536, 2020, doi: 10.1016/j.jacbts.2020.04.002.

[237] M. Z. Tay, C. M. Poh, L. Rénia, P. A. MacAry, and L. F. P. Ng, “The trinity of COVID-19: immunity, inflammation and intervention,” *Nat. Rev. Immunol.*, vol. 20, no. 6, pp. 363–374, 2020, doi: 10.1038/s41577-020-0311-8.

[238] L. M. Barton, E. J. Duval, E. Stroberg, S. Ghosh, and S. Mukhopadhyay, “COVID-19 Autopsies, Oklahoma, USA,” *Am. J. Clin. Pathol.*, vol. 153, no. 6, pp. 725–733, 2020, doi: 10.1093/ajcp/aqaa062.

[239] L. A. Teuwen, V. Geldhof, A. Pasut, and P. Carmeliet, “COVID-19: the vasculature unleashed,” *Nat. Rev. Immunol.*, vol. 20, no. 7, pp. 389–391, 2020, doi: 10.1038/s41577-020-0343-0.

[240] M. J. Mathews, “A systems engineering approach to coronary heart disease,” Doctor Philosophiae in Mechanical Engineering, North-West University, South Africa, 2015.

[241] M. J. Mathews, E. H. Mathews, and L. Liebenberg, “The mechanisms by which antidepressants may reduce coronary heart disease risk,” *BMC Cardiovasc. Disord.*, vol. 15, no. 1, pp. 1–12, 2015, doi: 10.1186/s12872-015-0074-5.

[242] L. Puccetti *et al.*, “Hypercoagulable state in hypercholesterolemic subjects assessed by platelet-dependent thrombin generation: In vitro effect of Cerivastatin,” *Eur. Rev. Med. Pharmacol. Sci.*, vol. 3, no. 5, pp. 197–204, 1999.

[243] P. Andersen, “Hypercoagulability and Reduced Fibrinolysis in Hyperlipidemia: Relationship to the Metabolic Cardiovascular Syndrome,” *J. Cardiovasc. Pharmacol.*, vol. 20, no. 8, pp. S29–S31, 1992.

[244] K. Tjaden, E. Pardali, and J. Waltenberger, “Hypercholesterolemia Induces Vascular Cell Dysfunction: Molecular Basis for Atherosclerosis,” *Austin J. Vasc. Med.*, vol. 2, no. 1, pp. 1–9, 2015.

[245] D. Radenkovic, S. Chawla, M. Pirro, A. Sahebkar, and M. Banach, “Cholesterol in Relation to COVID-19: Should We Care about It?,” *J. Clin. Med.*, vol. 9, no. 6, p. 1909, 2020, doi: 10.3390/jcm9061909.

[246] D. W. Sanders *et al.*, “Sars-cov-2 requires cholesterol for viral entry and pathological syncytia formation,” *Elife*, vol. 10, pp. 1–47, 2021, doi: 10.7554/ELIFE.65962.

[247] M. J. Mathews, L. Liebenberg, and E. H. Mathews, “How do high glycemic load diets influence coronary heart disease?,” *Nutr. Metab.*, vol. 12, no. 6, pp. 1–15, 2015, doi: 10.1186/s12986-015-0001-x.

[248] M. J. Mathews, L. Liebenberg, and E. H. Mathews, “The mechanism by which moderate alcohol consumption influences coronary heart disease,” *Nutr. J.*, vol. 14, no. 33, pp. 1–12, 2015, doi: 10.1186/s12937-015-0011-6.

[249] M. J. Mathews, E. H. Mathews, and G. E. Mathews, “Oral health and coronary heart disease,” *BMC Oral Health*, vol. 16, no. 122, pp. 1–10, 2016, doi: 10.1186/s12903-016-0316-7.

[250] M. J. Mathews, E. H. Mathews, and G. E. Mathews, “The integrated effect of moderate exercise on coronary heart disease,” *Cardiovasc. J. Afr.*, vol. 28, no. 2, pp. 125–133, 2017, doi: 10.5830/CVJA-2016-058.

[251] R. Pranata, I. Huang, M. A. Lim, E. J. Wahjoepramono, and J. July, “Impact of cerebrovascular and cardiovascular diseases on mortality and severity of COVID-19–systematic review, meta-analysis, and meta-regression,” *J. Stroke Cerebrovasc. Dis.*, vol. 29, no. 8, p. 104949, 2020, doi: 10.1016/j.jstrokecerebrovasdis.2020.104949.

[252] A. R. Bourgonje *et al.*, “Angiotensin-converting enzyme 2 (ACE2), SARS-CoV -2 and the pathophysiology of coronavirus disease 2019 (COVID -19),” *J. Pathol.*, vol. 251, pp. 228–248, 2020, doi: 10.1002/path.5471.

[253] A. Huertas *et al.*, “Endothelial cell dysfunction: a major player in SARS-CoV-2 infection (COVID-19)?,” *Eur. Respir. J.*, vol. 56, no. May, 2020, doi: 10.1183/13993003.01634-2020.

[254] P. Dandona, S. Dhindsa, H. Ghanim, and A. Chaudhuri, “Angiotensin II and inflammation: The effect of angiotensin-converting enzyme inhibition and angiotensin II receptor blockade,” *J. Hum. Hypertens.*, vol. 21, no. 1, pp. 20–27, 2007, doi: 10.1038/sj.jhh.1002101.

[255] C. T. Esmon, “The interactions between inflammation and coagulation,” *Br. J. Haematol.*, vol. 131, no. 4, pp. 417–430, 2005, doi: 10.1111/j.1365-2141.2005.05753.x.

[256] D. Lindner *et al.*, “Association of Cardiac Infection with SARS-CoV-2 in Confirmed COVID-19 Autopsy Cases,” *JAMA Cardiol.*, no. July, pp. 1–5, 2020, doi: 10.1001/jamacardio.2020.3551.

[257] M. Catanzaro, F. Fagiani, M. Racchi, E. Corsini, S. Govoni, and C. Lanni, “Immune response in COVID-19: addressing a pharmacological challenge by targeting pathways triggered by SARS-CoV-2,” *Signal Transduct. Target. Ther.*, vol. 5, no. 1, pp. 1–10, 2020, doi: 10.1038/s41392-020-0191-1.

[258] C. Qin *et al.*, “Dysregulation of immune response in patients with COVID-19 in Wuhan, China,” *Clin. Infect. Dis.*, vol. 71, no. 15, pp. 762–768, 2020, doi: 10.1093/cid/ciaa248.

[259] Q. Ruan, K. Yang, W. Wang, L. Jiang, and J. Song, “Clinical predictors of mortality due to COVID-19 based on an analysis of data of 150 patients from Wuhan, China,” *Intensive Care Med.*, vol. 46, no. 5, pp. 846–848, 2020, doi: 10.1007/s00134-020-05991-x.

[260] E. J. Giamarellos-Bourboulis *et al.*, “Complex Immune Dysregulation in COVID-19 Patients with Severe Respiratory Failure,” *Cell Host Microbe*, vol. 27, no. 6, pp. 992-1000.e3, 2020, doi: 10.1016/j.chom.2020.04.009.

[261] C. Zhang, “The role of inflammatory cytokines in endothelial dysfunction,” *Basic Res. Cardiol.*, vol. 103, no. 5, pp. 398–406, 2008, doi: 10.1007/s00395-008-0733-0.

[262] N. Leo *et al.*, “Immunothrombotic Dysregulation in COVID-19 Pneumonia is Associated with Respiratory Failure and Coagulopathy,” *Circulation*, 2020, doi: 10.1161/CIRCULATIONAHA.120.048488.

[263] C. C. Winterbourn, A. J. Kettle, and M. B. Hampton, “Reactive Oxygen Species and Neutrophil Function,” *Annu. Rev. Biochem.*, vol. 85, pp. 765–792, 2016, doi: 10.1146/annurev-biochem-060815-014442.

[264] H. Chaudhry *et al.*, “Role of Cytokines as a Double-edged Sword in Sepsis,” *vivo Int. J. Exp. Clin. Pathophysiol. Drug Res.*, vol. 27, no. 6, pp. 669–684, 2015.

[265] M. Sarkar, N. Niranjan, and P. K. Banyal, “Mechanisms of hypoxemia,” *Lung India*, vol. 34, no. 1, pp. 47–60, 2017, doi: 10.4103/0970-2113.197116.

[266] F. R. Millar, C. Summers, M. J. Griffiths, M. R. Toshner, and A. G. Proudfoot, “The pulmonary endothelium in acute respiratory distress syndrome: Insights and therapeutic opportunities,” *Thorax*, vol. 71, no. 5, pp. 462–473, 2016, doi: 10.1136/thoraxjnl-2015-207461.

[267] J. S. Pober and W. C. Sessa, “Evolving functions of endothelial cells in inflammation,” *Nat. Rev. Immunol.*, vol. 7, no. 10, pp. 803–815, 2007, doi: 10.1038/nri2171.

[268] B. Bikdeli *et al.*, “COVID-19 and Thrombotic or Thromboembolic Disease: Implications for Prevention, Antithrombotic Therapy, and Follow-Up: JACC State-of-the-Art Review,” *J. Am. Coll. Cardiol.*, vol. 75, no. 23, pp. 2950–2973, 2020, doi: 10.1016/j.jacc.2020.04.031.

[269] H. K. Eltzschig and P. Carmeliet, “Hypoxia and Inflammation,” *N. Engl. J. Med.*, vol. 364, no. 7, pp. 656–665, 2011, doi: 10.1056/NEJMra0910283.

[270] A. Görlach *et al.*, “Reactive oxygen species, nutrition, hypoxia and diseases: Problems solved?,” *Redox Biol.*, vol. 6, pp. 372–385, 2015, doi: 10.1016/j.redox.2015.08.016.

[271] R. Mellado-Artigas *et al.*, “High-flow nasal oxygen in patients with COVID-19-associated acute respiratory failure,” *Crit. Care*, vol. 25, no. 1, pp. 1–10, 2021, doi: 10.1186/s13054-021-03469-w.

[272] The RECOVERY Collaborative Group, “Dexamethasone in Hospitalized Patients with Covid-19 — Preliminary Report,” *N. Engl. J. Med.*, pp. 1–11, 2020, doi: 10.1056/NEJMoa2021436.

[273] W. Hong *et al.*, “Celebrex Adjuvant Therapy on Coronavirus Disease 2019: An Experimental Study,” *Front. Pharmacol.*, vol. 11, no. November, pp. 1–9, 2020, doi: 10.3389/fphar.2020.561674.

[274] J. H. Chow *et al.*, “Aspirin Use is Associated with Decreased Mechanical Ventilation, ICU Admission, and In-Hospital Mortality in Hospitalized Patients with COVID-19,” *Anesth. Analg.*, vol. 132, no. 4, pp. 930–941, 2021, doi: 10.1213/ane.0000000000005292.

[275] N. Bizien *et al.*, “Age is a major risk factor of venous thromboembolism (VTE),” *Eur. Respir. J.*, vol. 38, no. Suppl 55, p. p3936, Sep. 2011, [Online]. Available: http://erj.ersjournals.com/content/38/Suppl_55/p3936.abstract.

[276] B. G. Pijls *et al.*, “Demographic risk factors for COVID-19 infection, severity, ICU admission and death: A meta-analysis of 59 studies,” *BMJ Open*, vol. 11, no. 1, 2021, doi: 10.1136/bmjopen-2020-044640.

[277] R. E. J. Roach, S. C. Cannegieter, and W. M. Lijfering, “Differential risks in men and women for first and recurrent venous thrombosis: The role of genes and environment,” *J. Thromb. Haemost.*, vol. 12, no. 10, pp. 1593–1600, 2014, doi: 10.1111/jth.12678.

[278] N. A. Zakai and L. A. Mcclure, “Racial differences in venous thromboembolism,” *J. Thromb. Haemost.*, vol. 9, no. 10, pp. 1877–1882, 2011, doi: 10.1111/j.1538-7836.2011.04443.x.

[279] L. Golestaneh *et al.*, “The association of race and COVID-19 mortality,” *EClinicalMedicine*, vol. 25, p. 100455, 2020, doi: 10.1016/j.eclinm.2020.100455.

[280] H. E. Groot, L. E. V. Sierra, M. A. Said, E. Lipsic, J. C. Karper, and P. Van Der Harst, “Genetically determined ABO blood group and its associations with health and disease,” *Arterioscler. Thromb. Vasc. Biol.*, no. March, pp. 830–838, 2020, doi: 10.1161/ATVBAHA.119.313658.

[281] B. Wu, D. Gu, J. Yu, J. Yang, and W. Shen, “Association between ABO blood groups and COVID-19 infection, severity and demise: A systematic review and meta-analysis,” *Infect. Genet. Evol.*, vol. 84, p. 104485, 2020.

[282] E. R. Pomp, A. M. Lenselink, F. R. Rosendaal, and C. J. M. Doggen, “Pregnancy, the postpartum period and prothrombotic defects: Risk of venous thrombosis in the MEGA study,” *J. Thromb. Haemost.*, vol. 6, no. 4, pp. 632–637, 2008, doi: 10.1111/j.1538-7836.2008.02921.x.

[283] F. Qeadan, N. A. Mensah, B. Tingey, and J. B. Stanford, “The risk of clinical complications and death among pregnant women with COVID-19 in the Cerner COVID-19 cohort: a retrospective analysis,” *BMC Pregnancy Childbirth*, vol. 21, no. 1, pp. 1–14, 2021, doi: 10.1186/s12884-021-03772-y.

[284] M. D. Silverstein, J. A. Heit, D. N. Mohr, T. M. Petterson, W. M. O’Fallon, and J. Melton, “Trends in the Incidence of Deep Vein Thrombosis and Pulmonary Embolism,” *Arch. Intern. Med.*, vol. 158, pp. 585–593, 1998.

[285] L. Boudin and F. Dutasta, “Relationship Between ABO Blood Groups and Coronavirus Disease 2019: Study Design Matters,” *Clin. Infect. Dis.*, vol. 72, no. 11, pp. e927-8, 2021, doi: 10.1016/0196-6553(89)90009-6.

[286] N. Zaki, H. Alashwal, and S. Ibrahim, “Association of hypertension, diabetes, stroke, cancer, kidney disease, and high-cholesterol with COVID-19 disease severity and fatality: A systematic review,” *Diabetes Metab. Syndr. Clin. Res. Rev.*, vol. 14, no. January, pp. 1133–1142, 2020, doi: doi.org/10.1016/j.dsx.2020.07.005.

[287] Y. Chu, J. Yang, J. Shi, P. Zhang, and X. Wang, “Obesity is associated with increased severity of disease in COVID-19 pneumonia: a systematic review and meta-analysis,” *Eur. J. Med. Res.*, vol. 25, no. 64, pp. 1–15, 2020, doi: 10.1186/s40001-020-00464-9.

[288] G. Veghari *et al.*, “Obesity and risk of hypercholesterolemia in Iranian northern adults,” *ARYA Atheroscler.*, vol. 9, no. 1, pp. 2–6, 2013, doi: 10.22122/arya.v9i1.472.

[289] G. Veghari *et al.*, “The association between abdominal obesity and serum cholesterol level,” *Int. J. Appl. Basic Med. Res.*, vol. 5, no. 2, p. 83, 2015, doi: 10.4103/2229-516x.157150.

[290] X. Wei *et al.*, “Hypolipidemia is associated with the severity of COVID-19,” *J. Clin. Lipidol.*, vol. 14, no. January, pp. 297–304, 2020, doi: https://doi.org/10.1016/j.jacl.2020.04.008.

[291] S. Wang *et al.*, “Fasting blood glucose at admission is an independent predictor for 28-day mortality in patients with COVID-19 without previous diagnosis of diabetes: a multi-centre retrospective study,” *Diabetologia*, vol. 63, no. 10, pp. 2102–2111, 2020, doi: 10.1007/s00125-020-05209-1.

[292] J. Wu *et al.*, “Elevation of blood glucose level predicts worse outcomes in hospitalized patients with COVID-19: A retrospective cohort study,” *BMJ Open Diabetes Res. Care*, vol. 8, no. 1, pp. 1–7, 2020, doi: 10.1136/bmjdrc-2020-001476.

[293] A. Avogaro, M. Albiero, L. Menegazzo, S. De Kreutzenberg, and G. P. Fadini, “Endothelial dysfunction in diabetes: The role of reparatory mechanisms,” *Diabetes Care*, vol. 34, no. SUPPL. 2, pp. S285–S290, 2011, doi: 10.2337/dc11-s239.

[294] C. J. M. Loomans *et al.*, “Endothelial Progenitor Cell Dysfunction: A Novel Concept in the Pathogenesis of Vascular Complications of Type 1 Diabetes,” *Diabetes*, vol. 53, no. 1, pp. 195–199, 2004, doi: 10.2337/diabetes.53.1.195.

[295] S. C. Rogers, X. Zhang, G. Azhar, S. Luo, and J. Y. Wei, “Exposure to high or low glucose levels accelerates the appearance of markers of endothelial cell senescence and induces dysregulation of nitric oxide synthase,” *Journals Gerontol. - Ser. A Biol. Sci. Med. Sci.*, vol. 68, no. 12, pp. 1469–1481, 2013, doi: 10.1093/gerona/glt033.

[296] M. Brownlee, “The pathobiology of diabetic complications: A unifying mechanism,” *Diabetes*, vol. 54, no. 6, pp. 1615–1625, 2005, doi: 10.2337/diabetes.54.6.1615.

[297] M. Zuin, G. Rigatelli, G. Zuliani, A. Rigatelli, A. Mazza, and L. Roncon, “Arterial hypertension and risk of death in patients with COVID-19 infection: Systematic review and meta-analysis Dear,” *J. Infect.*, vol. 81, no. 1, pp. e84–e86, 2020, doi: 10.1016/j.jinf.2020.03.059.

[298] C. Bleakley, P. K. Hamilton, R. Pumb, M. Harbinson, and G. E. Mcveigh, “Endothelial Function in Hypertension: Victim or Culprit?,” *J. Clin. Hypertens.*, vol. 17, no. 8, pp. 651–654, 2015, doi: 10.1111/jch.12546.

[299] Y. Taniyama and K. K. Griendling, “Reactive Oxygen Species in the Vasculature: Molecular and Cellular Mechanisms,” *Hypertension*, vol. 42, no. 6, pp. 1075–1081, 2003, doi: 10.1161/01.HYP.0000100443.09293.4F.

[300] J. Sattelmair, J. Pertman, E. L. Ding, H. W. Kohl, W. Haskell, and I.-M. Lee, “Dose-Response Between Physical Activity and Risk of Coronary Heart Disease: A Meta-Analysis,” *Circulation*, vol. 124, no. 7, pp. 789–795, 2011, doi: doi:10.1161/CIRCULATIONAHA.110.010710.

[301] Z. Tavakol *et al.*, “Relationship between physical activity, healthy lifestyle and COVID-19 disease severity; a cross-sectional study,” *J. public Heal. From theory to Pract.*, pp. 1–9, 2021, doi: 10.1007/s10389-020-01468-9.

[302] A. Hackshaw, J. K. Morris, S. Boniface, J. L. Tang, and D. Milenkovi, “Low cigarette consumption and risk of coronary heart disease and stroke: Meta-analysis of 141 cohort studies in 55 study reports,” *BMJ*, vol. 360, p. j5855, 2018, doi: 10.1136/bmj.j5855.

[303] R. K. Reddy, W. N. Charles, A. Sklavounos, A. Dutt, P. T. Seed, and A. Khajuria, “The effect of smoking on COVID-19 symptom severity: Systematic review and meta-analysis,” *J. Med. Virol.*, pp. 1–12, 2020, doi: DOI: 10.1002/jmv.26389.

[304] A. Blaizot, J.-N. Vergnes, S. Nuwwareh, J. Amar, and M. Sixou, “Periodontal diseases and cardiovascular events: meta-analysis of observational studies.,” *Int. Dent. J.*, vol. 59, no. 4, pp. 197–209, Aug. 2009.

[305] N. Marouf *et al.*, “Association between periodontitis and severity of COVID-19 infection: A case–control study,” *J. Clin. Periodontol.*, vol. 0, pp. 1–9, 2021, doi: 10.1111/jcpe.13435.

[306] A. Rosengren *et al.*, “Association of psychosocial risk factors with risk of acute myocardial infarction in 11 119 cases and 13 648 controls from 52 countries (the INTERHEART study): Case-control study,” *Lancet*, vol. 364, pp. 953–962, 2004, doi: 10.1016/S0140-6736(04)17019-0.

[307] T. Tant *et al.*, “Association between high serum total cortisol concentrations and mortality from COVID-19,” *Lancet Diabetes Endocrinol.*, vol. 8, pp. 659–660, 2020, doi: 10.1016/ S2213-8587(20)30216-3.

[308] A. Nicholson, H. Kuper, and H. Hemingway, “Depression as an aetiologic and prognostic factor in coronary heart disease: A meta-analysis of 6362 events among 146 538 participants in 54 observational studies,” *Eur. Heart J.*, vol. 27, no. 23, pp. 2763–2774, 2006, doi: 10.1093/eurheartj/ehl338.

[309] H. Yang *et al.*, “Pre-pandemic psychiatric disorders and risk of COVID-19: a UK Biobank cohort analysis,” *Lancet Heal. Longev.*, vol. 1, no. 2, pp. e69–e79, 2020, doi: 10.1016/s2666-7568(20)30013-1.

[310] N. A. Shah, H. K. Yaggi, J. Concato, and V. Mohsenin, “Obstructive sleep apnea as a risk factor for coronary events or cardiovascular death,” *Sleep Breath.*, vol. 14, no. 2, pp. 131–136, 2010, doi: 10.1007/s11325-009-0298-7.

[311] S. Strausz *et al.*, “Sleep apnoea is a risk factor for severe COVID-19,” *BMJ Open Respir. Res.*, vol. 8, no. 1, pp. 6–11, 2021, doi: 10.1136/bmjresp-2020-000845.

[312] F. Sofi, F. Cesari, A. Casini, C. Macchi, R. Abbate, and G. F. Gensini, “Insomnia and risk of cardiovascular disease: A meta-analysis,” *Eur. J. Prev. Cardiol.*, vol. 21, no. 1, pp. 57–64, 2014, doi: 10.1177/2047487312460020.

[313] H. Kim *et al.*, “COVID-19 illness in relation to sleep and burnout,” *BMJ Nutr. Prev. Heal.*, pp. 1–8, 2021, doi: 10.1136/bmjnph-2021-000228.

[314] P. E. Ronksley, S. E. Brien, B. J. Turner, K. J. Mukamal, and W. A. Ghali, “Association of alcohol consumption with selected cardiovascular disease outcomes: A systematic review and meta-analysis,” *Bmj*, vol. 342, p. d671, 2011, doi: 10.1136/bmj.d671.

[315] J. Y. Dong, Y. H. Zhang, P. Wang, and L. Q. Qin, “Meta-analysis of dietary glycemic load and glycemic index in relation to risk of coronary heart disease,” *Am. J. Cardiol.*, vol. 109, no. 11, pp. 1608–1613, 2012, doi: 10.1016/j.amjcard.2012.01.385.

[316] E. J. Lenze *et al.*, “Fluvoxamine vs Placebo and Clinical Deterioration in Outpatients with Symptomatic COVID-19: A Randomized Clinical Trial,” *JAMA - J. Am. Med. Assoc.*, vol. 324, no. 22, pp. 2292–2300, 2020, doi: 10.1001/jama.2020.22760.

[317] R. Sallis *et al.*, “Physical inactivity is associated with a higher risk for severe COVID-19 outcomes: a study in 48 440 adult patients.,” *Br. J. Sports Med.*, vol. 0, pp. 1–8, 2021, doi: 10.1136/bjsports-2021-104080.

[318] D. C. Nieman and L. M. Wentz, “The compelling link between physical activity and the body’s defense system,” *J. Sport Heal. Sci.*, vol. 8, no. 3, pp. 201–217, 2019, doi: 10.1016/j.jshs.2018.09.009.

[319] F. S. Facchini, C. B. Hollenbeck, J. Jeppesen, Y. D. Ida Chen, and G. M. Reaven, “Insulin resistance and cigarette smoking,” *Lancet*, vol. 339, no. 8802, pp. 1128–1130, 1992, doi: 10.1016/0140-6736(92)90730-Q.

[320] G. Reaven and P. S. Tsao, “Insulin resistance and compensatory hyperinsulinemia: The key player between cigarette smoking and cardiovascular disease?,” *J. Am. Coll. Cardiol.*, vol. 41, no. 6, pp. 1044–1047, 2003, doi: 10.1016/S0735-1097(02)02982-0.

[321] S. Takefuji *et al.*, “Smoking status and adiponectin in healthy Japanese men and women,” *Prev. Med. (Baltim).*, vol. 45, no. 6, pp. 471–475, 2007, doi: 10.1016/j.ypmed.2007.07.001.

[322] E. Badrick, C. Kirschbaum, and M. Kumari, “The relationship between smoking status and cortisol secretion,” *J. Clin. Endocrinol. Metab.*, vol. 92, no. 3, pp. 819–824, 2007, doi: 10.1210/jc.2006-2155.

[323] W. Y. Craig, G. E. Palomaki, and J. E. Haddow, “Cigarette smoking and serum lipid and lipoprotein concentrations: an analysis of published data,” *BMJ*, vol. 298, pp. 784–788, 1989, doi: 10.1136/bmj.298.6683.1312-a.

[324] J. Lee, V. Taneja, and R. Vassallo, “Cigarette smoking and inflammation: Cellular and molecular mechanisms,” *J. Dent. Res.*, vol. 91, no. 2, pp. 142–149, 2012, doi: 10.1177/0022034511421200.

[325] R. S. Barua *et al.*, “Effects of cigarette smoke exposure on clot dynamics and fibrin structure: An ex vivo investigation,” *Arterioscler. Thromb. Vasc. Biol.*, vol. 30, no. 1, pp. 75–79, 2010, doi: 10.1161/ATVBAHA.109.195024.

[326] R. G. Deshpande, M. B. Khan, and C. A. Genco, “Invasion of aortic and heart endothelial cells by Porphyromonas gingivalis,” *Infect. Immun.*, vol. 66, no. 11, pp. 5337–5343, 1998, doi: 10.1128/iai.66.11.5337-5343.1998.

[327] X. Fan *et al.*, “Pre-diagnostic circulating concentrations of insulin-like growth factor-1 and risk of COVID-19 mortality: results from UK Biobank,” *Eur. J. Epidemiol.*, vol. 36, pp. 1–8, 2021, doi: 10.1007/s10654-020-00709-1.

[328] Y. Kong, J. Han, X. Wu, H. Zeng, J. Liu, and H. Zhang, “VEGF-D: A novel biomarker for detection of COVID-19 progression,” *Crit. Care*, vol. 24, no. 373, pp. 1–4, 2020, doi: 10.1186/s13054-020-03079-y.

[329] Y. Chen *et al.*, “IP-10 and MCP-1 as biomarkers associated with disease severity of COVID-19,” *Mol. Med.*, vol. 26, no. 97, pp. 1–12, 2020, doi: 10.1186/s10020-020-00230-x.

[330] E. Merzon *et al.*, “Haemoglobin A1c is a predictor of COVID-19 severity in patients with diabetes,” *Diabetes. Metab. Res. Rev.*, vol. 2019, no. June, pp. 1–6, 2020, doi: 10.1002/dmrr.3398.

[331] U. Saengow, S. Assanangkornchai, and S. Casswell, “Alcohol: a probable risk factor of COVID-19 severity,” *Addiction*, vol. 116, no. 1, pp. 202–208, 2021, doi: 10.1111/add.15194.

[332] E. Simou, J. Leonardi-Bee, and J. Britton, “The Effect of Alcohol Consumption on the Risk of ARDS: A Systematic Review and Meta-Analysis,” *Chest*, vol. 154, no. 1, pp. 58–68, 2018, doi: 10.1016/j.chest.2017.11.041.

[333] S. Keddie *et al.*, “Laboratory biomarkers associated with COVID-19 severity and management,” *Clin. Immunol.*, vol. 221, no. August, pp. 1–5, 2020, doi: 10.1016/j.clim.2020.108614.

[334] P. Malik *et al.*, “Biomarkers and outcomes of COVID-19 hospitalisations: systematic review and meta-analysis,” *BMJ Evidence-Based Med.*, pp. 1–12, 2020, doi: 10.1136/bmjebm-2020-111536.

[335] M. Jalali Nadoushan *et al.*, “Hematologic, biochemical and immune biomarker abnormalities associated with severe illness and mortality in coronavirus disease 2019 (COVID-19): a meta-analysis,” *Clin. Chem. Lab. Med.*, vol. 58, no. 7, pp. 1021–1028, 2020, doi: doi.org/10.1515/cclm-2020-0369.

[336] P. Ji *et al.*, “Association of elevated inflammatory markers and severe COVID-19: A meta-analysis,” *Medicine (Baltimore).*, vol. 99, no. 47, p. e23315, 2020, doi: 10.1097/MD.0000000000023315.

[337] A. Akhmerov and E. Marbán, “COVID-19 and the Heart,” *Circ. Res.*, pp. 1443–1455, 2020, doi: 10.1161/CIRCRESAHA.120.317055.

[338] O. J. Mcelvaney *et al.*, “Characterization of the Inflammatory Response to Severe COVID-19 Illness,” *Am. J. Respir. Crit. Care Med.*, vol. 202, no. 6, pp. 812–821, 2020, doi: 10.1164/rccm.202005-1583OC.

[339] R. Luis García de Guadiana *et al.*, “Circulating levels of GDF-15 and calprotectin for prediction of in-hospital mortality in COVID-19 patients: A case series,” *J. Infect.*, no. January, 2020, doi: 10.1016/j.jinf.2020.08.010.

[340] C. Baigent *et al.*, “Efficacy and safety of more intensive lowering of LDL cholesterol: A meta-analysis of data from 170 000 participants in 26 randomised trials,” *Lancet*, vol. 376, no. 9753, pp. 1670–1681, 2010, doi: 10.1016/S0140-6736(10)61350-5.

[341] X. J. Zhang *et al.*, “In-Hospital Use of Statins Is Associated with a Reduced Risk of Mortality among Individuals with COVID-19,” *Cell Metab.*, vol. 32, pp. 1–12, 2020, doi: 10.1016/j.cmet.2020.06.015.

[342] H. J. Milionis, E. N. Liberopoulos, A. Achimastos, M. S. Elisaf, and D. P. Mikhailidis, “Statins: Another class of antihypertensive agents?,” *J. Hum. Hypertens.*, vol. 20, no. 5, pp. 320–335, 2006, doi: 10.1038/sj.jhh.1002001.

[343] R. Amann and B. A. Peskar, “Anti-inflammatory effects of aspirin and sodium salicylate,” *Eur. J. Pharmacol.*, vol. 447, no. 1, pp. 1–9, 2002, doi: 10.1016/S0014-2999(02)01828-9.

[344] A. Undas, K. E. Brummel-Ziedins, and K. G. Mann, “Antithrombotic properties of aspirin and resistance to aspirin: Beyond strictly antiplatelet actions,” *Blood*, vol. 109, no. 6, pp. 2285–2292, 2007, doi: 10.1182/blood-2006-01-010645.

[345] R. Collins *et al.*, “Aspirin in the primary and secondary prevention of vascular disease: collaborative meta-analysis of individual participant data from randomised trials,” *Lancet*, vol. 373, no. 9678, pp. 1849–1860, 2009, doi: 10.1016/S0140-6736(09)60503-1.

[346] E. Boersma *et al.*, “Platelet glycoprotein IIb/IIIa inhibitors in acute coronary syndromes: A meta-analysis of all major randomised clinical trials,” *Lancet*, vol. 359, no. 9302, pp. 189–198, 2002, doi: 10.1016/S0140-6736(02)07442-1.

[347] N. Tang, H. Bai, X. Chen, J. Gong, D. Li, and Z. Sun, “Anticoagulant treatment is associated with decreased mortality in severe coronavirus disease 2019 patients with coagulopathy,” *J. Thromb. Haemost.*, no. March, 2020, doi: 10.1111/jth.14817.

[348] L. Wallentin *et al.*, “Oral ximelagatran for secondary prophylaxis after myocardial infarction: The ESTEEM randomised controlled trial,” *Lancet*, vol. 362, no. 9386, pp. 789–797, 2003, doi: 10.1016/S0140-6736(03)14287-0.

[349] B. Flam, V. Wintzell, J. F. Ludvigsson, J. Mårtensson, and B. Pasternak, “Direct oral anticoagulant use and risk of severe COVID-19,” *J. Intern. Med.*, vol. 289, no. 3, pp. 411–419, 2021, doi: 10.1111/joim.13205.

[350] P. Verdecchia *et al.*, “Angiotensin-converting enzyme inhibitors and calcium channel blockers for coronary heart disease and stroke prevention,” *Hypertension*, vol. 46, no. 2, pp. 386–392, 2005, doi: 10.1161/01.HYP.0000174591.42889.a2.

[351] J. Hippisley-Cox *et al.*, “Risk of severe COVID-19 disease with ACE inhibitors and angiotensin receptor blockers: Cohort study including 8.3 million people,” *Heart*, vol. 106, no. 19, pp. 1503–1511, 2020, doi: 10.1136/heartjnl-2020-317393.

[352] G. Savarese *et al.*, “A meta-analysis reporting effects of angiotensin-converting enzyme inhibitors and angiotensin receptor blockers in patients without heart failure,” *J. Am. Coll. Cardiol.*, vol. 61, no. 2, pp. 131–142, 2013, doi: 10.1016/j.jacc.2012.10.011.

[353] C. Gao *et al.*, “Association of hypertension and antihypertensive treatment with COVID-19 mortality: a retrospective observational study,” *Eur. Heart J.*, vol. 41, no. 22, pp. 2058–2066, 2020, doi: 10.1093/eurheartj/ehaa433.

[354] O. R. De Peuter, F. Lussana, R. J. G. Peters, H. R. Büller, and P. W. Kamphuisen, “A systematic review of selective and non-selective beta blockers for prevention of vascular events in patients with acute coronary syndrome or heart failure,” *Neth. J. Med.*, vol. 67, no. 9, pp. 284–294, 2009.

[355] L. Ren, S. Yu, W. Xu, J. L. Overton, N. Chiamvimonvat, and P. n. Thai, “Lack of association of antihypertensive drugs with the risk and severity of COVID-19: A meta-analysis,” *J. Cardiol.*, vol. 77, pp. 482–491, 2021, doi: doi.org/10.1016/j.jjcc.2020.10.015.

[356] B. M. Psaty *et al.*, “Health Outcomes Associated with Various Antihypertensive Therapies Used as First-Line Agents: A Network Meta-analysis,” *J. Am. Med. Assoc.*, vol. 289, no. 19, pp. 2534–2544, 2003, doi: 10.1001/jama.289.19.2534.

[357] E. Selvin *et al.*, “Cardiovascular outcomes in trials of oral diabetes medications: A systematic review,” *Arch. Intern. Med.*, vol. 168, no. 19, pp. 2070–2080, 2008, doi: 10.1001/archinte.168.19.2070.

[358] K. Khunti *et al.*, “Prescription of glucose-lowering therapies and risk of COVID-19 mortality in people with type 2 diabetes: a nationwide observational study in England,” *Lancet Diabetes Endocrinol.*, vol. 8587, no. 21, pp. 1–11, 2021, doi: 10.1016/S2213-8587(21)00050-4.

[359] J. F. Scherrer *et al.*, “Antidepressant drug compliance: Reduced risk of MI and mortality in depressed patients,” *Am. J. Med.*, vol. 124, no. 4, pp. 318–324, 2011, doi: 10.1016/j.amjmed.2010.11.015.

[360] E. Young, “The anti-inflammatory effects of heparin and related compounds,” *Thromb. Res.*, vol. 122, no. 6, pp. 743–752, 2008, doi: 10.1016/j.thromres.2006.10.026.

[361] H. K. Siddiqi, P. Libby, and P. M. Ridker, “COVID-19 - A vascular disease,” *Trends Cardiovasc. Med.*, no. January, pp. 1–5, 2021, doi: https://doi.org/10.1016/j.tcm.2020.10.005.

[362] M. Marchetti, “COVID-19-driven endothelial damage: complement, HIF-1, and ABL2 are potential pathways of damage and targets for cure,” *Ann. Hematol.*, vol. 99, no. 8, pp. 1701–1707, 2020, doi: 10.1007/s00277-020-04138-8.

[363] C. C. Danta, “SARS-CoV-2, Hypoxia, and Calcium Signaling: The Consequences and Therapeutic Options,” *ACS Pharmacol. Transl. Sci.*, vol. 4, no. 1, pp. 400–402, 2021, doi: 10.1021/acsptsci.0c00219.

[364] M. Jahani, S. Dokaneheifard, and K. Mansouri, “Hypoxia: A key feature of COVID-19 launching activation of HIF-1 and cytokine storm,” *J. Inflamm.*, vol. 17, no. 1, pp. 1–10, 2020, doi: 10.1186/s12950-020-00263-3.

[365] N. Matic, M. Ressner, E. Wiechec, and K. Roberg, “In vitro measurement of glucose uptake after radiation and cetuximab treatment in head and neck cancer cell lines using 18f-fdg, gamma spectrometry and pet/ct,” *Oncology Letters*, vol. 18, no. 5. pp. 5155–5162, 2019, doi: 10.3892/ol.2019.10916.

[366] F. Maddalena *et al.*, “Evaluation of glucose uptake in normal and cancer cell lines by positron emission tomography,” *Mol. Imaging*, vol. 14, no. 8, pp. 490–498, 2015, doi: 10.2310/7290.2015.00021.

[367] J. A. Chouinard, J. A. Rousseau, J. F. Beaudoin, P. Vermette, and R. Lecomte, “Positron emission tomography detection of human endothelial cell and fibroblast monolayers: Effect of pretreament and cell density on 18FDG uptake,” *Vasc. Cell*, vol. 4, no. 1, p. 5, 2012, doi: 10.1186/2045-824X-4-5.

[368] R. Hustinx, R. J. Smith, F. Benard, A. Bhatnagar, and A. Alavi, “Can the standardized uptake value characterize primary brain tumors on FDG-PET?,” *Eur. J. Nucl. Med.*, vol. 26, no. 11, pp. 1501–1509, 1999, [Online]. Available: http://www.embase.com/search/results?subaction=viewrecord&from=export&id=L29515616%5Cnhttp://dx.doi.org/10.1007/s002590050487%5Cnhttp://sfx.umd.edu/hs?sid=EMBASE&issn=03406997&id=doi:10.1007%2Fs002590050487&atitle=Can+the+standardized+uptake+value+charact.

[369] N. Kosaka, T. Tsuchida, H. Uematsu, H. Kimura, H. Okazawa, and H. Itoh, “18F-FDG PET of common enhancing malignant brain tumors,” *Am. J. Roentgenol.*, vol. 190, no. 6, pp. 365–369, 2008, doi: 10.2214/AJR.07.2660.

[370] M. C. Adams, T. G. Turkington, J. M. Wilson, and T. Z. Wong, “A systematic review of the factors affecting accuracy of SUV measurements,” *Am. J. Roentgenol.*, vol. 195, no. 2, pp. 310–320, 2010, doi: 10.2214/AJR.10.4923.

[371] Merck KGaA, “Sigma-Aldrich: L-Glutamine in Cell Culure,” 2019. https://www.sigmaaldrich.com/life-science/cell-culture/learning-center/media-expert/glutamine.html.

[372] Merck KGaA, “Sigma-Aldrich: Glucose in Cell Culture,” 2019. https://www.sigmaaldrich.com/life-science/cell-culture/learning-center/media-expert/glucose.html.

[373] S. Lagziel, E. Gottlieb, and T. Shlomi, “Mind your media,” *Nat. Metab.*, vol. 2, no. 12, pp. 1369–1372, 2020, doi: 10.1038/s42255-020-00299-y.

[374] J. R. Cantor *et al.*, “Physiologic medium rewires cellular metabolism and reveals uric acid as an endogenous inhibitor of UMP synthase,” *Cell*, vol. 169, no. 2, pp. 258–272, 2017, doi: 10.1016/j.cell.2017.03.023.Physiologic.

[375] T. Ackermann and S. Tardito, “Cell culture medium formulation and its implications in cancer metabolism,” *Trends in Cancer*, vol. 5, no. 6, pp. 329–332, 2019, doi: 10.1016/j.trecan.2019.05.004.

[376] T. N. Seyfried, G. Arismendi-Morillo, P. Mukherjee, and C. Chinopoulos, “On the Origin of ATP Synthesis in Cancer,” *iScience*, vol. 23, no. 11, pp. 1–21, 2020, doi: 10.1016/j.isci.2020.101761.

[377] C. Chinopoulos, “From Glucose to Lactate and Transiting Intermediates Through Mitochondria, Bypassing Pyruvate Kinase: Considerations for Cells Exhibiting Dimeric PKM2 or Otherwise Inhibited Kinase Activity,” *Front. Physiol.*, vol. 11, p. 543564, 2020, doi: 10.3389/fphys.2020.543564.

[378] W. J. Israelsen *et al.*, “PKM2 isoform-specific deletion reveals a differential requirement for pyruvate kinase in tumor cells,” *Cell*, vol. 155, no. 2, pp. 397–409, 2013, doi: 10.1016/j.cell.2013.09.025.

[379] T. Scholzen and J. Gerdes, “The Ki-67 protein: From the known and the unknown,” *J. Cell. Physiol.*, vol. 182, no. 3, pp. 311–322, 2000, doi: 10.1002/(SICI)1097-4652(200003)182:3<311::AID-JCP1>3.0.CO;2-9.

[380] K. H. Kim and J. M. Sederstrom, “Assaying cell cycle status using flow cytometry,” *Curr. Protoc. Mol. Biol.*, vol. 111, pp. 1–16, 2016, doi: 10.1002/0471142727.mb2806s111.

[381] H. Z. Long, Y. Cheng, Z. W. Zhou, H. Y. Luo, D. D. Wen, and L. C. Gao, “PI3K/AKT Signal Pathway: A Target of Natural Products in the Prevention and Treatment of Alzheimer’s Disease and Parkinson’s Disease,” *Front. Pharmacol.*, vol. 12, no. April, pp. 1–20, 2021, doi: 10.3389/fphar.2021.648636.

[382] P. Liu, H. Cheng, T. M. Roberts, and J. J. Zhao, “Targeting the phosphoinositide 3-kinase (PI3K) pathway in cancer,” *Nat. Rev. Drug Discov.*, vol. 8, no. 8, pp. 627–644, 2009, doi: 10.1038/nrd2926.

[383] S. C. Lin and D. G. Hardie, “AMPK: Sensing Glucose as well as Cellular Energy Status,” *Cell Metab.*, vol. 27, no. 2, pp. 299–313, 2018, doi: 10.1016/j.cmet.2017.10.009.

[384] M. M. Young *et al.*, “Autophagosomal membrane serves as platform for intracellular death-inducing signaling complex (iDISC)-mediated caspase-8 activation and apoptosis,” *J. Biol. Chem.*, vol. 287, no. 15, pp. 12455–12468, 2012, doi: 10.1074/jbc.M111.309104.

[385] Y. Li *et al.*, “Apoptin Regulates Apoptosis and Autophagy by Modulating Reactive Oxygen Species (ROS) Levels in Human Liver Cancer Cells,” *Front. Oncol.*, vol. 10, pp. 1–15, 2020, doi: 10.3389/fonc.2020.01026.

[386] L. Caly, J. D. Druce, M. G. Catton, D. A. Jans, and K. M. Wagstaff, “The FDA-approved drug ivermectin inhibits the replication of SARS-CoV-2 in vitro,” *Antiviral Res.*, vol. 178, no. March, pp. 3–6, 2020, doi: 10.1016/j.antiviral.2020.104787.

[387] V. Mody *et al.*, “Identification of 3-chymotrypsin like protease (3CLPro) inhibitors as potential anti-SARS-CoV-2 agents,” *Commun. Biol.*, vol. 4, no. 93, pp. 1–10, 2021, doi: 10.1038/s42003-020-01577-x.

[388] S. Lehrer and P. H. Rheinstein, “Ivermectin docks to the SARS-CoV-2 spike receptor-binding domain attached to ACE2,” *In Vivo (Brooklyn).*, vol. 34, no. 5, pp. 3023–3026, 2020, doi: 10.21873/invivo.12134.

[389] A. Swargiary, “Ivermectin as a promising RNA-dependent RNA polymerase inhibitor and a therapeutic drug against SARS-CoV2: Evidence from in silico studies,” *Res. Sq.*, 2020, [Online]. Available: https://doi.org/10.21203/rs.3.rs-73308/v1.

[390] P. Kory, G. U. Meduri, J. Varon, J. Iglesias, and P. E. Marik, “Review of the Emerging Evidence Demonstrating the Efficacy of Ivermectin in the Prophylaxis and Treatment of COVID-19,” *Am. J. Ther.*, vol. 28, no. 3, pp. e299–e318, 2021, doi: 10.1097/mjt.0000000000001377.

[391] A. Bryant, T. Lawrie, E. Fordham, M. Scott, S. Hill, and T. Tham, “Ivermectin for Prevention and Treatment of COVID-19 Infection: a Systematic Review and Meta-analysis,” *Am. J. Ther.*, vol. 27, pp. e1–e27, 2021, [Online]. Available: https://doi.org/10.21203/rs.3.rs-317485/v1.

[392] J. A. G. Whitworth, C. R. M. Hay, A. M. Nicholas, D. Morgan, G. H. Maude, and D. W. Taylor, “Coagulation abnormalities and ivermectin,” *Ann. Trop. Med. Parasitol.*, vol. 86, no. 3, pp. 301–305, 1992, doi: 10.1080/00034983.1992.11812667.

[393] L. Jin *et al.*, “The antiparasitic drug ivermectin is a novel FXR ligand that regulates metabolism,” *Nat. Commun.*, vol. 4, pp. 1–8, 2013, doi: 10.1038/ncomms2924.

[394] X. Ci *et al.*, “Avermectin exerts anti-inflammatory effect by downregulating the nuclear transcription factor kappa-B and mitogen-activated protein kinase activation pathway,” *Fundam. Clin. Pharmacol.*, vol. 23, no. 4, pp. 449–455, 2009, doi: 10.1111/j.1472-8206.2009.00684.x.

[395] J. J. DiNicolantonio, J. B.- Arranda, and M. McCarty, “Ivermectin may be a clinically useful anti-inflammatory agent for late-stage COVID-19,” *Open Hear.*, vol. 7, 2020, doi: 10.1136/openhrt-2020-001350corr1.

[396] A. E. Gracia-Ramos, J. O. Jaquez-Quintana, R. Contreras-Omaña, and M. Auron, “Liver dysfunction and SARS-CoV-2 infection,” *World J. Gastroenterol.*, vol. 27, no. 26, pp. 3951–3970, 2021, doi: 10.3748/wjg.v27.i26.3951.

[397] P. Kory *et al.*, “Review of the Emerging Evidence Demonstrating the Efficacy of Ivermectin in the Prophylaxis and Treatment of COVID-19,” *Front. Pharmacol.*, pp. 1–32, 2021, doi: 10.3389/fphar.2021.643369.

[398] G. A. Roth *et al.*, “Global, Regional, and National Burden of Cardiovascular Diseases for 10 Causes, 1990 to 2015,” *J. Am. Coll. Cardiol.*, vol. 70, no. 1, pp. 1–25, 2017, doi: 10.1016/j.jacc.2017.04.052.

[399] P. Bjorntorp, “Adipose tissue,” *Electron. J. Int. Fed. Clin. Chem. Lab. Med.*, vol. 12, no. 3, pp. 68–72, 2000, doi: eJIFCC2000Vol12No3pp068-072.

[400] H. Lu, L. A. Cassis, C. W. V. Kooi, and A. Daugherty, “Structure and functions of angiotensinogen,” *Hypertens. Res.*, vol. 39, no. 7, pp. 492–500, 2016, doi: 10.1038/hr.2016.17.

[401] S. Elmore, “Apoptosis: A Review of Programmed Cell Death,” *Toxicol. Pathol.*, vol. 35, no. 4, pp. 495–516, 2007, doi: 10.1080/01926230701320337.

[402] W. Insull, “The Pathology of Atherosclerosis: Plaque Development and Plaque Responses to Medical Treatment,” *Am. J. Med.*, vol. 122, pp. S3–S14, 2009, doi: 10.1016/j.amjmed.2008.10.013.

[403] P. A. Majid, M. K. Meeran, M. E. Benaim, B. Sharma, and S. H. Taylor, “Alpha- and beta-adrenergic receptor blockade in the treatment of hypertension,” *Br. Heart J.*, vol. 36, pp. 588–596, 1974.

[404] R. A. Miller, Q. Chu, J. Xie, M. Foretz, B. Viollet, and M. J. Birnbaum, “Biguanides suppress hepatic glucagon signaling by decreasing production production of cyclic AMP,” *Nature*, vol. 494, no. 7436, pp. 256–260, 2013, doi: 10.1038/nature11808.

[405] K. Strimbu and J. A. Tavel, “What are biomarkers?,” *Curr. Opin. HIV AIDS*, vol. 5, no. 6, pp. 463–466, 2010, doi: 10.1097/COH.0b013e32833ed177.

[406] M. J. Eisenberg, A. Brox, and A. N. Bestawros, “Calcium channel blockers: an update,” *Am. J. Med.*, vol. 116, no. 1, pp. 35–43, 2004, doi: https://doi.org/10.1016/j.amjmed.2003.08.027.

[407] D. S. Goldstein, “Catecholamines 101,” *Clin. Auton. Res.*, vol. 20, no. 6, pp. 331–352, 2010, doi: 10.1007/s10286-010-0065-7.

[408] R. J. Duronio and Y. Xiong, “Signaling pathways that control cell proliferation,” *Cold Spring Harb. Perspect. Biol.*, vol. 5, no. 3, 2013, doi: 10.1101/cshperspect.a008904.

[409] A. J. Brown, H. W. Coates, and L. Sharpe, *Biochemistry of Lipids, Lipoproteins and Membranes*, Seventh. Elsevier Science, 2021.

[410] S. Palta, R. Saroa, and A. Palta, “Overview of the coagulation system,” vol. 58, no. 5, 2014, doi: 10.4103/0019-5049.144643.

[411] H. Jung, “Basic Physical Principles and Clinical Applications of Computed Tomography,” *Prog. Med. Phys.*, vol. 32, no. 1, pp. 1–17, 2021, doi: 10.14316/pmp.2021.32.1.1.

[412] P. Libby and P. Theroux, “Pathophysiology of coronary artery disease,” *Circulation*, vol. 111, no. 25, pp. 3481–3488, 2005, doi: 10.1161/CIRCULATIONAHA.105.537878.

[413] S. Khani and J. A. Tayek, “Cortisol increases gluconeogenesis in humans: its role in the metabolic syndrome,” *Clin. Sci.*, vol. 101, pp. 739–747, 2001, doi: 10.1042/cs20010180.

[414] R. Karki and T. D. Kanneganti, “The ‘cytokine storm’: molecular mechanisms and therapeutic prospects,” *Trends Immunol.*, vol. 42, no. 8, pp. 681–705, 2021, doi: 10.1016/j.it.2021.06.001.

[415] P. M. Ridker, “C-reactive protein: A Simple Test to Help Predict Risk of Heart Attack and Stroke,” *Circulation*, vol. 108, pp. e81–e85, 2003, doi: 10.1161/01.CIR.0000093381.57779.67.

[416] American Diabetes Association, “Diagnosis and classification of diabetes mellitus,” *Diabetes Care*, vol. 33, no. SUPPL. 1, pp. S62–S69, 2010, doi: 10.2337/dc10-S062.

[417] C. J. Lee and J. E. Ansell, “Direct thrombin inhibitors,” *Br. J. Clin. Pharmacol.*, vol. 72, no. 4, pp. 581–592, 2011, doi: 10.1111/j.1365-2125.2011.03916.x.

[418] D. H. Ellison, “Clinical pharmacology in diuretic use,” *Clin. J. Am. Soc. Nephrol.*, vol. 14, no. 8, pp. 1248–1257, 2019, doi: 10.2215/CJN.09630818.

[419] J. D. Bronzino, D. R. Peterson, and E. J. Berbari, *Biomedical Egineering Principles*. Boca Raton: Taylor & Francis Group, 2014.

[420] D. Abraham and O. Distler, “How does endothelial cell injury start? The role of endothelin in systemic sclerosis,” *Arthritis Res. Ther.*, vol. 9, no. SUPPL. 2, pp. 1–8, 2007, doi: 10.1186/ar2186.

[421] R. E. Keesey and T. L. Powley, “Body energy homeostasis,” *Appetite*, vol. 51, no. 3, pp. 442–445, 2008, doi: 10.1016/j.appet.2008.06.009.

[422] P. Monagle, L. J. Stang, and L. G. Mitchell, *Haemostasis: Methods and Protocols, Methods in Molecular Biology*, vol. 992. New York: Springer Science, 2013.

[423] A. Berger, “Positron emission tomography,” *Br. Med. J.*, vol. 326, p. 1449, 2003.

[424] I. Kimura, A. Ichimura, R. Ohue-Kitano, and M. Igarashi, “Free fatty acid receptors in health and disease,” *Physiol. Rev.*, vol. 100, no. 1, pp. 171–210, 2020, doi: 10.1152/physrev.00041.2018.

[425] S. Timmermans, J. Souffriau, and C. Libert, “A general introduction to glucocorticoid biology,” *Front. Immunol.*, vol. 10, pp. 1–17, 2019, doi: 10.3389/fimmu.2019.01545.

[426] a C. Schoolwerth, B. C. Smith, and R. M. Culpepper, “Renal gluconeogenesis,” *Miner. Electrolyte Metab.*, vol. 14, no. 6, pp. 347–361, 1988, doi: 10.2337/diacare.24.2.382.

[427] A. Schurr, “Glycolysis paradigm shift dictates a reevaluation of glucose and oxygen metabolic rates of activated neural tissue,” *Front. Neurosci.*, vol. 12, no. OCT, pp. 1–12, 2018, doi: 10.3389/fnins.2018.00700.

[428] A. Jörres, “Hemofiltration or hemodialysis for acute kidney injury?,” *Crit. Care*, vol. 16, no. 147, pp. 1–2, 2012, doi: 10.1186/cc11450.

[429] B. Furie and B. C. Furie, “Mechanisms of thrombus formation.,” *N. Engl. J. Med.*, vol. 359, no. 9, pp. 938–49, 2008, [Online]. Available: http://www.ncbi.nlm.nih.gov/pubmed/18753650.

[430] J. Shah, “Hyperbaric oxygen therapy,” *J. Am. Col. Certif. Wound Spec.*, vol. 2, no. 1, pp. 9–13, 2010, doi: 10.1016/j.jcws.2010.04.001.

[431] J. A. Sheng *et al.*, “The Hypothalamic-Pituitary-Adrenal Axis: Development, Programming Actions of Hormones, and Maternal-Fetal Interactions,” *Front. Behav. Neurosci.*, vol. 14, pp. 1–21, 2021, doi: 10.3389/fnbeh.2020.601939.

[432] G. S. Hotamisligil, “Inflammation and metabolic disorders,” *Nature*, vol. 444, no. 7121, pp. 860–867, 2006, doi: 10.1038/nature05485.

[433] G. Wilcox, “Insulin and Insulin Resistance,” *Clin. Biochem. Rev.*, vol. 26, pp. 19–36, 2005.

[434] Z. Laron, “Insulin-like growth factor 1 (IGF-1): a growth hormone,” *Mol. Pathol.*, vol. 54, no. 5, pp. 311–316, 2001, doi: 10.1136/mp.54.5.311.

[435] C. Brocker, C. Carpenter, D. W. Nebert, and V. Vasiliou, “Evolutionary divergence and functions of the human acyl-CoA thioesterase gene (ACOT) family,” *Hum. Genomics*, vol. 5, no. 1, pp. 30–55, 2010, doi: 10.1186/1479-7364-4-6-411.

[436] R. B. Jennings, C. E. Ganote, and K. A. Reimer, “Ischemic tissue injury,” *Am. J. Pathol.*, vol. 81, no. 1, pp. 179–194, 1975.

[437] T. Kelesidis, I. Kelesidis, S. Chou, and C. S. Mantzoros, “Narrative review: The role of leptin in human physiology: Emerging clinical applications,” *Ann. Intern. Med.*, vol. 152, no. 2, pp. 93–100, 2010, doi: 10.7326/0003-4819-152-2-201001190-00008.

[438] R. P., P. P.M., and S. FA, “Principles of Magnetic Resonance Imaging and Magnetic Resonance Angiography,” in *Clinical MR Imaging*, Springer, Berlin, Heidelberg, 2006.

[439] H. AB, “Meta-analysis in medical research,” *Hippokratia*, vol. 14, pp. 29–37, 2010.

[440] S. Valastyan and R. A. Weinberg, “Tumor metastasis: Molecular insights and evolving paradigms,” *Cell*, vol. 147, no. 2, pp. 275–292, 2011, doi: 10.1016/j.cell.2011.09.024.

[441] L. D. Osellame, T. S. Blacker, and M. R. Duchen, “Cellular and molecular mechanisms of mitochondrial function,” *Best Pract. Res. Clin. Endocrinol. Metab.*, vol. 26, no. 6, pp. 711–723, 2012, doi: 10.1016/j.beem.2012.05.003.

[442] M. Soares-Silva, F. F. Diniz, G. N. Gomes, and D. Bahia, “The mitogen-activated protein kinase (MAPK) pathway: Role in immune evasion by trypanosomatids,” *Front. Microbiol.*, vol. 7, no. 183, pp. 1–9, 2016, doi: 10.3389/fmicb.2016.00183.

[443] K. Thygesen *et al.*, “Third universal definition of myocardial infarction,” *Eur. Heart J.*, vol. 33, no. 20, pp. 2551–2567, 2012, doi: 10.1093/eurheartj/ehs184.

[444] A. B. Levine, D. Punihaole, and T. B. Levine, “Characterization of the role of nitric oxide and its clinical applications,” *Cardiol.*, vol. 122, no. 1, pp. 55–68, 2012, doi: 10.1159/000338150.

[445] P. Lévy *et al.*, “Obstructive sleep apnoea syndrome,” *Nat. Rev. Dis. Prim.*, vol. 1, pp. 1–20, 2015, doi: 10.1038/nrdp.2015.15.

[446] B. JM, T. JL, and S. L, *Biochemistry*, 5th Additi. New York: W. H. Freeman and Company, 2002.

[447] N. Madhav, B. Oppenheim, M. Gallivan, P. Mulembakani, E. Rubin, and N. Wolfe, “Pandemics: Risks, Impacts, and Mitigation,” in *Disease Control Priorities: Improving Health and Reducing Poverty*, 3rd Editio., Washington (DC): The World Bank, 2017.

[448] J. W. Mcbride and D. H. Walker, “Pathogenesis of Infectious Diseases and Mechanisms of Immunity,” in *Vaccinology: An Essential Guide*, John Wiley & Sons Ltd, 2014, pp. 59–72.

[449] B. L. Pihlstrom, B. S. Michalowicz, and N. W. Johnson, “Periodontal diseases,” *Lancet*, vol. 366, no. 9499, pp. 1809–1820, 2005, doi: 10.1016/S0140-6736(05)67728-8.

[450] H. A. Krebs, “Chemical composition of blood plasma and serum.,” *Annu. Rev. Biochem.*, vol. 19, no. 12, pp. 409–430, 1950, doi: 10.1146/annurev.bi.19.070150.002205.

[451] K. R. Machlus, J. N. Thon, and J. E. Italiano, “Interpreting the developmental dance of the megakaryocyte: A review of the cellular and molecular processes mediating platelet formation,” *Br. J. Haematol.*, vol. 165, no. 2, pp. 227–236, 2014, doi: 10.1111/bjh.12758.

[452] S. J. Forrester, D. S. Kikuchi, M. S. Hernandes, Q. Xu, and K. K. Griendling, “Reactive oxygen species in metabolic and inflammatory signaling,” *Circ. Res.*, vol. 122, no. 6, pp. 877–902, 2018, doi: 10.1161/CIRCRESAHA.117.311401.

[453] M. Vaswani, F. K. Linda, and S. Ramesh, “Role of selective serotonin reuptake inhibitors in psychiatric disorders: A comprehensive review,” *Prog. Neuro-Psychopharmacology Biol. Psychiatry*, vol. 27, no. 1, pp. 85–102, 2003, doi: 10.1016/S0278-5846(02)00338-X.

[454] M. Berger, J. A. Gray, and B. L. Roth, “The expanded biology of serotonin,” *Annu. Rev. Med.*, vol. 60, pp. 355–366, 2009, doi: 10.1146/annurev.med.60.042307.110802.

[455] S. J. Murphy and D. J. Werring, “Stroke: causes and clinical features,” *Medicine (Baltimore).*, vol. 48, no. 9, pp. 561–566, 2020, doi: 10.1016/j.mpmed.2020.06.002.

[456] A. Patel, “Benign vs Malignant Tumors,” *JAMA Oncol.*, vol. 6, no. 9, p. 1488, 2020, doi: 10.1001/jamaoncol.2020.2592.

[457] X. Wang and Y. Lin, “Tumor necrosis factor and cancer, buddies or foes?,” *Acta Pharmacol. Sin.*, vol. 29, no. 11, pp. 1275–1288, 2008, doi: 10.1111/j.1745-7254.2008.00889.x.

[458] A. Chait and L. J. den Hartigh, “Adipose Tissue Distribution, Inflammation and Its Metabolic Consequences, Including Diabetes and Cardiovascular Disease,” *Front. Cardiovasc. Med.*, vol. 7, no. February, pp. 1–41, 2020, doi: 10.3389/fcvm.2020.00022.

APPENDICES

Appendix A: Author contributions to manuscripts and declarations

A1: Published manuscript 1

The author contributions to the published manuscript 1 of Chapter 2 in this thesis titled: **"In vitro quantification: Long-term effect of glucose deprivation on various cancer cell lines"** were the following:

Co-author	Affiliation	Contribution
Prof EH Mathews	Professor at North-West University, Department of Engineering.	Conceptualisation of the project and study design. He assisted in compiling the initial draft, detailed revisions and final approval of manuscript.
Prof AM Joubert	Professor and Head of Physiology Department at University of Pretoria.	Provided technical knowledge and approval of final manuscript. Supplied funding from research grants.
Dr. MH Visagie	Senior Technical Laboratory Assistant at University of Pretoria, Department of Physiology.	Laboratory experimental work and data accumulation and approval of final manuscript. Supplied funding from research grants.
Mr. GE Mathews	Centre for research and continued engineering development, North-West University.	Assisted in conceptualisation of the study design. Assisted in revisions and approval of the final manuscript.

According to the following statement, the co-authors confirm their role in this study and provide their permission that the manuscript may form part of this thesis:
"I declare that my above-mentioned contribution to the manuscript is correct and I hereby give my consent that it may be published as part of the PhD study of Albertus Abram Meyer."

Prof EH Mathews

Prof AM Joubert

Dr. MH Visagie

Mr. GE Mathews

A2: Published manuscript 2

The author contributions to the published manuscript 2 of Chapter 5 in this thesis titled: **"A hypothetical method for controlling highly glycolytic cancers and metastases"** were the following:

Author	Affiliation	Contribution
Prof EH Mathews	Professor at North-West University, Department of Engineering.	Conceptualisation of the project and study design. He assisted in compiling the initial draft, detailed revisions and final approval of manuscript.
Mr. GE Mathews	Centre for research and continued engineering development, North-West University.	Assisted in conceptualisation of the study design. Assisted in compiling the initial draft, revisions and final approval of the manuscript.

According to the following statement, the co-authors confirm their role in this study and provide their permission that the manuscript may form part of this thesis:

"I declare that my above-mentioned contribution to the manuscript is correct and I hereby give my consent that it may be published as part of the PhD study of Albertus Abram Meyer."

Prof EH Mathews

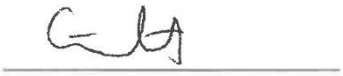

Mr. GE Mathews

A3: Published manuscript 3

The author contributions to the submitted manuscript 4 of Chapter 6 in this thesis titled: **"Using a systems approach to explore the mechanisms of interaction between severe COVID-19 and its coronary heart disease complications"** were the following:

Author	Affiliation	Contribution
Prof EH Mathews	Professor at North-West University, Department of Engineering and Professor extraordinaire of Physiology Department at University of Pretoria.	Initial review of COVID-19 literature. Envisaged the integration of COVID-19 into the CHD model. Assisted in detailed revisions and final approval of the manuscript.
Dr. AGS Gous	Lecturer extraordinaire at Stellenbosch University, Department of Industrial Engineering, South Africa.	Assisted in the development of the integrated CHD/Covid-19 model from literature. Helped compile the initial draft, reviewed and approved the final manuscript
Dr. MJ Mathews	Lecturer extraordinaire at Stellenbosch University, Department of Industrial Engineering, South Africa.	Developed the existing CHD model and provided expert opinion for the integration of the model with COVID-19. Review and approval of the final manuscript.

According to the following statement, the co-authors confirm their role in this study and provide their permission that the manuscript may form part of this thesis:

I declare that my above-mentioned contribution to the manuscript is correct and I hereby give my consent that it may be published as part of the PhD study of AA Meyer.

Prof EH Mathews

Dr. AGS Gous

Dr. MJ Mathews

A4: Accepted manuscript

The author contributions to the submitted manuscript 3 of Chapter 3 in this thesis titled: **"In vitro quantification: combined long and short-term metabolic effects on different cancer cell lines"** were the following:

Co-author	Affiliation	Contribution
Prof EH Mathews	Professor at North-West University, Department of Engineering and Professor extraordinaire of Physiology Department at University of Pretoria.	Conceptualisation of the project and study design. He assisted in compiling the initial draft, detailed revisions and final approval of manuscript.
Prof AM Joubert	Professor and Head of Physiology Department at University of Pretoria.	Provided technical knowledge and approval of final manuscript. Supplied funding from research grants.
Dr. MH Visagie	Senior Technical Laboratory Assistant at University of Pretoria, Department of Physiology.	Laboratory experimental work and data accumulation and approval of final manuscript. Supplied funding from research grants.
Mr. GE Mathews	Centre for research and continued engineering development, North-West University.	Assisted in compiling the initial draft, revisions and approval of the final manuscript.

According to the following statement, the co-authors confirm their role in this study and provide their permission that the manuscript may form part of this thesis:

"I declare that my above-mentioned contribution to the manuscript is correct and I hereby give my consent that it may be published as part of the PhD study of Albertus Abram Meyer."

Prof EH Mathews

Prof AM Joubert

Dr. MH Visagie

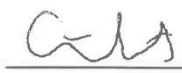

Mr. GE Mathews

Appendix B: Published manuscript 1 (Chapter 2)

Nutrition 74 (2020) 110748

Contents lists available at ScienceDirect

Nutrition

journal homepage: www.nutritionjrnl.com

Applied nutritional investigation

In vitro quantification: Long-term effect of glucose deprivation on various cancer cell lines

Edward Henry Mathews D.Eng. [a,b,*], Michelle Helen Visagie Ph.D. [c], Albertus Abram Meyer B.Eng. [a,b], Anna Margaretha Joubert Ph.D. [c], George Edward Mathews B.A. [a,b]

[a] Centre of Research and Continued Engineering Development, North-West University, Silver Lakes, South Africa
[b] TEMM International (Pty) Ltd, Pretoria, South Africa
[c] Department of Physiology, University of Pretoria, Pretoria, South Africa

ARTICLE INFO

Article History:
Received 27 February 2019
Received in revised form 10 January 2020
Accepted 19 January 2020

Keywords:
Cancer
Long-term glucose deprivation
In vitro
Metabolic treatment
Highly glycolytic cancers

ABSTRACT

Objective: Although metabolic treatment of highly glycolytic cancers and metastases is becoming an important research field, the effects of such treatments are not fully quantified yet. In this article we attempt to quantify the effect of long-term glucose deprivation (similar to ketogenic diets) on cancer cells using in vitro tests.
Methods: Two tumorigenic cell lines were used, namely a metastatic breast and a cervical cancer cell line. The non-tumorigenic control cell line was an immortalized breast cell line. All the cell lines were stabilized at a typical average human blood glucose level of 6 mmol/L. The cell lines were then exposed to the therapeutic blood glucose level of 3 mmol/L for 90 d.
Results: The tests indicated that glucose deprivation restricted the different cancer cell lines' growth more than that of non-tumorigenic cells. The different cell lines were also differentially affected, which suggests that long-term glucose deprivation will not be equally effective for different types of cancer.
The highly glycolytic breast cancer cell line was most adversely affected, with cell growth decreasing to 30% after 26 d. Cell growth was stable at this level for up to 22 d. Furthermore, all of the other cancer cell lines were similarly affected.
Conclusions: This in vitro data could help to direct future human in vivo tests to find the most therapeutic time (cancer cells at their most vulnerable) for additional short-term adjuvant therapies. Partial recovery of proliferation occurred after 90 d. Therefore, as expected, the results also indicated that without an adjuvant treatment, full extinction cannot be reached with the proposed long-term metabolic treatment. The need for more clinical data on long-term glucose deprivation treatments for cancer is well described in the literature. This paper attempts to add to the available pool of knowledge.

Introduction

There has been an increase in the understanding of the benefits of strict glucose control during the treatment of highly glycolytic cancers and metastases (HGCM) [1,2]. Various nutritional strategies are used to decrease circulating blood glucose (BG) levels and elevate ketone bodies for therapeutic purposes [3]. These nutritional strategies include fasting [4,5], restricted ketogenic diet (KD-R) [6], calorie restriction [6], and ketone supplementation [7] in combination with the use of diabetic medication (e.g., metformin).

The most established of these nutritional strategies, the KD-R, has been found to have therapeutic effects on various types of cancer when used in combination with adjuvant therapies [3,8–13]. Fasting, as used by anorexic patients, has been found to have a vastly reduced cooccurrence of HGCM [14].

These studies point to a therapeutic window created by the high glucose uptake of certain cancer cell types compared with that of non-cancer cells. Despite the large therapeutic evidence of the benefits of nutritional strategies, a very recent review (2017) by Winter et al. [3] stated that "nutritional strategies targeting

This study was supported by grants from the Cancer Association of South Africa, the Medical Research Council, the National Research Foundation, Struwig Germeshuysen Trust, and the School of Medicine Research Committee of the Faculty of Health Sciences, University of Pretoria. Some elements of the study were funded by E.H.Mathews and Human-Sim (Pty) Ltd. The authors declare that there is no conflict of interest.
*Corresponding author.
E-mail address: 10477438@nwu.ac.za (E.H. Mathews).

https://doi.org/10.1016/j.nut.2020.110748
0899-9007/

glycemic modulation to exploit the observed tumor glucose-dependency have not yet been thoroughly investigated in clinical trials and existing clinical data is limited."

We agree with Winter et al. [3]. Typical in vitro studies of glucose deprivation on cancer cells investigated the short-term effects, where glucose deprivation ranged from 5 h [15] to 2 d [16–18] to 7 d [19]. Because the effect of KD-R occurs over months, we need data for at least 90 d to see initial and longer-term effects.

More importantly, in previous studies [15–19] the following procedure was generally used: After initial cell growth in Dulbecco's modified Eagle medium (DMEM) at a glucose level of 25.52 mmol/L, the cells were exposed to severely low glucose levels (0–2.5 mmol/L) [15–19].

The glucose levels in DMEM are thus usually four times higher than the average human physiological BG concentration of approximately 6 mmol/L (glycated hemoglobin of 5.3% [20]). Therefore the cancer cells are not given adequate time to stabilize at typical human BG levels before being given the final push to the therapeutic BG level. A therapeutic level of 0 mmol/L is also not practical. Thus, the previously mentioned models are not appropriate for investigating practical long-term glucose deprivation effects.

In this paper we endeavor to add to the existing pool of in vitro clinical data for long-term glucose deprivation strategies. Some of the questions we intended to answer are the following:

1. Can we conduct in vitro tests with cancer cells at typical in vivo physiological BG concentrations? In vitro tests are usually done at four times higher BG levels [21]. Because the aim of the investigation is BG control, the BG baseline should be correct to have confidence in the results.
2. What is the effect of glucose deprivation on different cancer cell lines that possess varying glucose demands? We know that the ketogenic diet does not work for all cancer patients [10]. Therefore we want to investigate the effects in different models.
3. At what cell growth rate (for metabolic treatments) will cancer cell lines recover and after what treatment period?
4. When will the in vitro cancer line be at its most vulnerable, and thus when does a potential therapeutic window for short-term adjuvant therapies open? These in vitro data could direct future human in vivo tests regarding when cancer growths are at their most vulnerable.

We made a significant assumption in the present investigation that will need verification through additional research. We had to assume a minimum achievable BG level for a combination of KD-R, fasting, and the use of BG-lowering medication such as metformin.

An average BG level as low as 1 mmol/L has been reported for fasting [22]. BG levels as low as 4 mmol/L were reported for cancer patients on a KD [3]. Values for a combination of fasting, KD-R, and metformin use could not be found. For the present research a value of 3 mmol/L was assumed as a starting point.

The question may be asked why mouse models are not used for the present glycolytic study [23]. One important reason is the difference between the BG microenvironments between mice and humans [21,23,24].

Studies with cancer-bearing mice and humans indicate that in humans the BG environment increases by 1.15-fold [25], whereas in mice, very shortly after invasion by HGCM, BG decreases by 2.1-fold [26]. This can, inter alia, be attributed to the large difference in metabolic parameters between humans and mice [24].

For instance, mice have a 7.5-fold greater basal metabolic rate than humans [24], with a 10- to 15-fold higher relative basal glucose turnover rate [24]. This means that rodents are under much greater metabolic constraints than humans.

With such a high basal glucose demand in mice, together with the added high glucose demand of HGCM, it is important to either sustain adequate glycogen storages or to use very high levels of energy-expensive gluconeogenesis to provide for the upregulated glucose demand.

However, mice have 2-fold less liver and 4.5-fold less muscle glycogen stores than humans [24]. Furthermore, the mouse would have to eat excessively to supply the added BG demand of the cancer via gluconeogenesis [24], thus leading to the dramatic reported decrease in cancer-bearing mice's BG levels after invasion by highly glycolytic cancers.

Glucose availability to cancer cells (which is the effect we wanted to study) is thus much lower in mice compared with humans. Metabolic (glycolytic) effects on highly glycolytic cancers can therefore not always be accurately extrapolated to human responses from mice studies.

Furthermore, we would not have full control over BG levels in mice. On the other hand, we will have full control over the in vitro microenvironment. BG control in a cancer model is important because human BG control is much tighter than that of mice [21,23]. We thus hypothesize that properly formulated in vitro experiments could potentially be more relevant for obtaining long-term metabolic data for humans than using in vivo mice models.

Materials and methods

The average glucose microenvironment of healthy humans is approximately 5.8 mmol/L (glycated hemoglobin of 5.3% [20]). Because BG levels for cancer patients are usually higher [25], a value of 6 mmol/L was used as a starting point.

Standard cultivation of cancer cells is done in high-glucose DMEM at a glucose level of 25.52 mmol/L [15–17,19]. This represents a 4-fold higher concentration than physiological conditions, which could cast doubt over the validity of the proposed glucose treatment results. Furthermore, the glutamine level in standard cultivation of cancer cells is 4 mmol/L, which is also 4 to 8 times higher than human physiological plasma glutamine levels of 0.5 to 0.9 mmol/L [27–29].

Tumorigenic and non-tumorigenic cell lines were grown in DMEM before being exposed to physiological average glucose and glutamine levels of 6 mmol/L and 0.6 mmol/L, respectively, until cell growth stability was reached (experimental condition 1). Growth stability was regarded as a period of very little variation in relative cell growth. Thereafter, cells were exposed to low glucose levels of 3 mmol/L until cell growth stability was again reached (experimental condition 2).

Tests were conducted on four cell lines (i.e., three tumorigenic cell lines and one non-tumorigenic cell line). Of the tumorigenic cell lines, two were metastatic breast cancer cell lines—namely, the highly glycolytic MD Anderson metastasis breast cancer 231 (MDA-MB-231) and the less glycolytic Michigan Cancer Foundation 7 (MCF-7) cells. The third cancer cell line was the Henrietta Lacks (HeLa) cervical cancer cell line. The non-tumorigenic cell line used was a spontaneously immortalized non-tumorigenic breast cell line (MCF-10 A).

In this study we used the same methods as in previous studies, including morphology and proliferation experiments [30,31]. These methods were described in detail in previous reports [30,31]. Crystal violet staining and spectrophotometry [30,31] were again used here to interpret cell density, proliferation, and cell viability.

Cell culture procedure

Cells were grown and maintained in 25 cm^2 tissue culture flasks in a humidified atmosphere at 37°C, 5% CO_2, in a Forma water-jacketed incubator (Thermo Scientific, Cincinnati, OH, USA). Cells were cultured in DMEM with 25.52 mmol/L glucose, 4 mmol/L L-glutamine, and 1 mmol/L sodium pyruvate, supplemented with 10% dialyzed heat-inactivated fetal calf serum (FCS) (56°C, 30 min), 100 U/mL penicillin G, 100 μg/mL streptomycin, and 250 μg/L amphotericin B (Fungizone).

Negative control for tumorigenic cell lines

Negative control was cultured in DMEM with 25.52 mmol/L glucose and 4 mmol/L L-glutamine supplemented with 10% dialyzed heat-inactivated FCS (56°C, 30 min), 100 U/mL penicillin G, 100 μg/mL streptomycin, and 250 μg/L amphotericin B.

Negative control for the non-tumorigenic cell line

The non-tumorigenic breast cancer cell line was cultured in a ratio of 50% DMEM to 50% Ham's F-12 medium (HF12 M) containing with 17.56 mmol/L glucose and 2 mmol/L L-glutamine with the addition of 10% dialyzed FCS (56°C, 30 min), 500 ng/mL hydrocortisone, 20 ng/mL epidermal growth factor (EGF), 100 ng/mL cholera toxin, 10 μg/mL insulin, 100 U/mL penicillin G and 100 μg/mL streptomycin, and 250 μg/L amphotericin B.

Experimental conditions

Experimental condition 1 for tumorigenic cell lines

Experimental condition 1 for tumorigenic cell lines consisted of DMEM with 6 mmol/L glucose, 0.6 mmol/L L-glutamine, and 1 mmol/L sodium pyruvate supplemented with 10% dialyzed heat-inactivated FCS (56°C, 30 min), 100 U/mL penicillin G, 100 μg/mL streptomycin, and 250 μg/L amphotericin B.

Experimental condition 1 for non-tumorigenic cell line

Experimental condition 1 for the non-tumorigenic cell line consisted of a ratio of 50% DMEM to 50% HF12 M containing with 6 mmol/L glucose and 0.6 mmol/L L-glutamine with the addition of 10% dialyzed FCS (56°C, 30 min), 500 ng/mL hydrocortisone, 20 ng/mL EGF, 100 ng/mL cholera toxin, 10 μg/mL insulin, 100 U/mL penicillin G, and 100 μg/mL streptomycin, and 250 μg/L amphotericin B.

Experimental condition 2 for tumorigenic cell lines

Experimental condition 2 for tumorigenic cell lines consisted of DMEM with 3 mmol/L glucose, 0.6 mmol/L L-glutamine, and 1 mmol/L sodium pyruvate supplemented with 10% dialyzed heat-inactivated FCS (56°C, 30 min), 100 U/mL penicillin G, 100 μg/mL streptomycin, and 250 μg/L amphotericin B.

Experimental condition 2 for non-tumorigenic cell lines

Experimental condition 2 for the non-tumorigenic cell line consisted of a ratio of 50% DMEM to 50% HF12 M containing with 3 mmol/L glucose and 0.6 mmol/L L-glutamine with the addition of 10% dialyzed FCS (56°C, 30 min), 500 ng/mL hydrocortisone, 20 ng/mL EGF, 100 ng/mL cholera toxin, 10 μg/mL insulin, 100 U/mL penicillin G, 100 μg/mL streptomycin, and 250 μg/L amphotericin B.

Cell proliferation (crystal violet staining)

Cells were seeded in 96-well plates and incubated at 37°C and 5% CO_2 for 24 h in a complete growth medium containing DMEM with 25.52 mmol/L glucose, 4 mmol/L L-glutamine, and 1 mmol/L sodium pyruvate supplemented with 10% dialyzed heat-inactivated FCS (56°C, 30 min), 100 U/mL penicillin G, 100 μg/mL streptomycin, and 250 μg/L amphotericin B. Long-term proliferation studies were conducted in a 6-well plate.

Cells were then exposed to experimental condition 1. Cells were exposed to these conditions until cell growth stabilized (reached a plateau). After proliferation stabilized in these conditions, cells were exposed to experimental condition 2 until cell growth stabilized again (reached a plateau).

On termination of the experiment, cells were fixed with 1% glutaraldehyde (100 μL) at room temperature for 15 min. The glutaraldehyde was then replaced with 0.1% crystal violet (100 μL) at room temperature for 30 min. Plates were left to dry; thereafter, 0.2% triton X-100 (200 μL) was added to the plates and incubated overnight to solubilize the crystal violet. The plates were read on an Epoch Microplate Reader (BioTek Instruments, Inc., Winooski, VT, USA) at a wavelength of 570 nm thereafter.

Results and discussion

Quantitative data were collected via spectrophotometry from three independent repeats for all experiments. Figures 1 and 2 represent the calculated averages of percentage cell growth. The error bars illustrate the standard deviations compared with negative controls, which represent cells propagated in complete growth medium for the same period. (In some cases the standard deviations were so small that it is difficult to see them on the figures).

Figure 1 shows the response in percentage cell proliferation of all the tested cell lines when glucose concentration was reduced from 25.52 mmol/L to 6 mmol/L on day 0 (experimental condition 1). All cell lines were stable after approximately 30 d. (The non-tumorigenic cell line [MCF-10 A] remained stable from day 0).

Data indicate that tumorigenic cell lines can proliferate in physiological glucose cell culture media without long-term adverse effects on cell viability. This in vitro media condition is a more appropriate model for human in vivo conditions than the traditional DMEM conditions. It should thus yield improved confidence in the results of the next (glucose treatment) phase of the clinical trial.

After the cell growth of all cell lines stabilized, cells were exposed to the BG treatment phase (experimental condition 2). This was done at 3 mmol/L glucose to mimic a combination of fasting, KD-R, and metformin use. Figure 2 illustrates a decrease in cell growth of all cell lines compared with cells propagated in complete growth medium. All cell lines were stable at approximately 65 d of exposure.

Four important observations were made in this study, which will be investigated in the rest of this section:

1. Long-term glucose deprivation affects the investigated cancer cells more than non-cancer cells.
2. Different cancer cell lines are differentially affected by long-term glucose deprivation.
3. There is a period when the in vitro cancer cells are at their most vulnerable (lowest cell growth). Such information may be helpful to develop future cancer treatment protocols.
4. All cancer lines recover, but not fully. For full extinction of cancer cells, adjuvant therapies are needed.

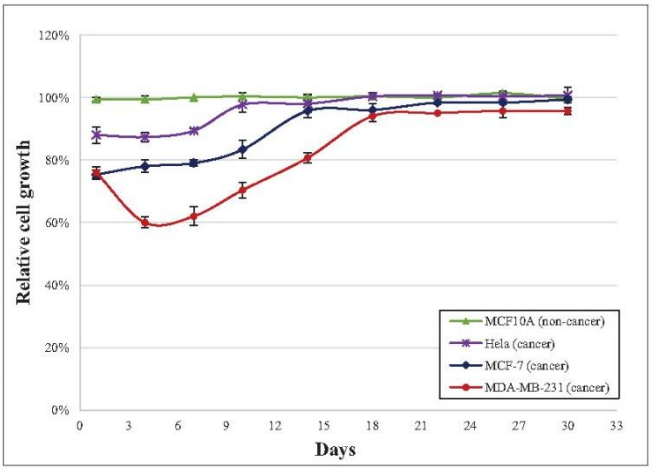

Fig. 1. Relative cell growth when cells were exposed to glucose concentration of 6 mmol/L and glutamine 0.6 mmol/L. (Glucose concentration was 25.52 mmol/L and glutamine 4 mmol/L before time zero.) Each data point is an average of three or more independent repeats. Cell growth was evaluated using crystal violet staining and spectrophotometry. HeLa, Henrietta Lacks; MCF, Michigan Cancer Foundation; MDA, MD Anderson.

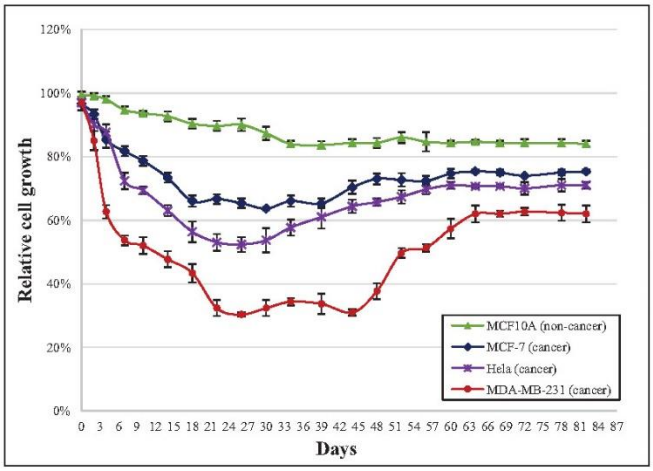

Fig. 2. Effects on cell lines with glucose concentration of 3 mmol/L after initial exposure to medium containing 6 mmol/L glucose and maintaining glutamine at 0.6 mmol/L. Each data point is an average of three or more independent repeats. Cell growth was evaluated using crystal violet staining and spectrophotometry. HeLa, Henrietta Lacks; MCF, Michigan Cancer Foundation; MDA, MD Anderson.

A summary of percentage cell growth recovery point, days until cell growth recovery point, percentage minimum cell growth, and days until minimum cell growth is given in Table 1. As expected, the highly glycolytic metastatic cell line (MDA-MB-231) was most affected, with a minimum cell growth of 30% (±0.58%) on day 26 and stabilization point at 62% (±2.65%).

Furthermore, the non-tumorigenic cell line (MCF-10 A) was affected the least, with cell growth remaining stable at 84% (±1.00%) after 34 d. This reduction in cell growth could be similar to the regular "weight loss" experienced during low glucose levels induced via restriction of dietary intake and metformin use. It may be concluded that metabolic glucose deprivation could be a well-tolerated therapy.

Figure 2 and Table 1 show that cancer cell growth increases again after the minimum levels were reached. This illustrates the need for adjuvant therapies, such as chemotherapy, radiation, and hyperbaric or other extrametabolic treatments [32].

The most therapeutic time to administer such an adjuvant therapy would be when the cancer is at its most vulnerable. This could be where the least cancer cells survive. Table 1 shows that for the three cell lines investigated, a potential time for an adjuvant therapy would be at around 26 d after reaching a BG level of 3 mmol/L. The most aggressive cancer stayed at its most vulnerable stage between days 22 and 44, which provides a wide adjuvant therapeutic window. However, the in vitro data have to be verified by future human in vivo tests.

Figure 2 also shows that the therapeutic effect is higher for the highly glycolytic cell line than for the less glycolytic ones. Future decisions on metabolic treatment should thus be done based on metabolic activity of the cancer (standard uptake values [SUVs]) rather than on the type of cancer. Glucose metabolic activity can be measured by [^{18}F]-fluorodeoxyglucose–based positron emission tomography scans and the cancer cells' respective SUVs [33].

Conclusions

The need for more clinical data on long-term glucose deprivation treatments for cancers (e.g., fasting, KD-R, etc.) is well described in literature. In this paper we attempted to add to the available pool of knowledge. The research indicated the following:

1. In vitro cancer tests can successfully be done at a human in vivo BG microenvironment of 6 mmol/L. This provides more confidence in results than the typically used in vitro BG microenvironment of 25.5 mmol/L.
2. Long-term metabolic treatment affects different cancer cell lines differently. It is suspected that the SUVs of cancers will be used in the future as standard practice to establish the usefulness of glucose deprivation treatment (e.g., nutritional, etc.). Future research should establish these SUVs.
3. Because full cancer extinction is not possible with long-term BG deprivation alone, adjuvant therapies are needed. Here we

Table 1
In vitro results after cells were exposure to 3 mmol/L glucose for 90 d

Cell line description	Cell growth recovery point (mean ± standard deviation)	Days until cell growth recovery point	Minimum cell growth (mean ± standard deviation)	Days until minimum cell growth
MCF-10 A (non-tumorigenic, breast cell line)	84 ± 1.00%	34	84 ± 1.00%	34
MCF-7 (metastatic luminal breast cell line)	75 ± 2.00%	60	65 ± 2.00%	26
HeLa (glycolytic cervical cancer cell line)	71 ± 1.00%	60	52.33 ± 2.31%	26
MDA-MB-231 (highly glycolytic metastatic breast cell line)	62 ± 2.65%	64	30 ± 0.58%	26
Average days until minimum cell growth (excluding non-tumorigenic cell line)				**26**

HeLa, Henrietta Lacks; MCF, Michigan Cancer Foundation; MDA, MD Anderson.

made a first in vitro attempt to establish the potentially best therapeutic time for any adjuvant therapy. For the cancer cell lines investigated, the 26-d period after a BG level of 3 mmol/L is reached seems to be a sensible adjuvant time target. This in vitro data could help direct future human in vivo studies to find the best therapeutic time for adjuvant therapies.

Acknowledgments

The work on the glucose cycle was initiated by C. Mathews. The angel investor was Dr. Arnold van Dyk.

References

[1] Vander Heiden M, Cantley L, Thompson C. Understanding the Warburg effect: the metabolic requirements of cell proliferation. Science 2009;324:1029–33.
[2] Martinez-Outschoorn UE, Peiris-Pagés M, Pestell RG, Sotgia F, Lisanti MP. Cancer metabolism: a therapeutic perspective. Nat Rev Clin Oncol 2017;14:11–31.
[3] Winter SF, Loebel F, Dietrich J. Role of ketogenic metabolic therapy in malignant glioma: a systematic review. Crit Rev Oncol Hematol 2017;112:41–58.
[4] Longo VD, Mattson MP. Fasting: molecular mechanisms and clinical applications. Cell Metab 2014;19:181–92.
[5] Lee C, Longo VD. Fasting vs dietary restriction in cellular protection and cancer treatment: from model organisms to patients. Oncogene 2011;30:3305–16.
[6] O'Flanagan CH, Smith LA, McDonell SB, Hursting SD. When less may be more: calorie restriction and response to cancer therapy. BMC Med 2017;15:1–10.
[7] Harvey CJDC, Schofield GM, Williden M. The use of nutritional supplements to induce ketosis and reduce symptoms associated with keto-induction: a narrative review. PeerJ 2018;6:e4488.
[8] Allen BG, Bhatia SK, Anderson CM, Eichenberger-Gilmore JM, Sibenaller ZA, Mapuskar KA, et al. Ketogenic diets as an adjuvant cancer therapy: history and potential mechanism. Redox Biol 2014;2:963–70.
[9] Klement RJ. Fasting, fats, and physics: combining ketogenic and radiation therapy against cancer. Complement Med Res 2018;25:102–13.
[10] Klement RJ. Beneficial effects of ketogenic diets for cancer patients: a realist review with focus on evidence and confirmation. Med Oncol 2017;34:1–34.
[11] Zahra A, Fath MA, Opat E, Mapuskar KA, Bhatia SK, Ma DC, et al. Consuming a ketogenic diet while receiving radiation and chemotherapy for locally advanced lung cancer and pancreatic cancer: the University of Iowa experience of two phase 1 clinical trials. Radiat Res 2017;187:743–54.
[12] Zuccoli G, Marcello N, Pisanello A, Servadei F, Vaccaro S, Mukherjee P, et al. Metabolic management of glioblastoma multiforme using standard therapy together with a restricted ketogenic diet: case report. Nutr Metab 2010;7:1–7.
[13] Elsakka AMA, Bary MA, Abdelzaher E, Elnaggar M, Kalamian M, Mukherjee P, et al. Management of glioblastoma multiforme in a patient treated with ketogenic metabolic therapy and modified standard of care: a 24-month follow-up. Front Nutr 2018;5:1–11.
[14] Mathews EH, Liebenberg L. Can successful cancer therapies build on what we learn from complex disorders? Med Hypotheses 2012;78:687.
[15] Graham NA, Tahmasian M, Kohli B, Komisopoulou E, Zhu M, Vivanco I, et al. Glucose deprivation activates a metabolic and signaling amplification loop leading to cell death. Mol Syst Biol 2012;8:1–16.
[16] Garufi A, Ricci A, Trisciuoglio D, Iorio E, Carpinelli G, Pistritto G, et al. Glucose restriction induces cell death in parental but not in homeodomain-interacting protein kinase 2-depleted RKO colon cancer cells: molecular mechanisms and implications for tumor therapy. Cell Death Dis 2013;4:1–11.
[17] Zhuang Y, Chan DK, Haugrud AB, Miskimins WK. Mechanisms by which low glucose enhances the cytotoxicity of metformin to cancer cells both in vitro and in vivo. PLoS One 2014;9.
[18] Bardaweel SK, Alsalamat HA, Aleidi SM, Bashatwah RM. Glucose deprivation enhances the antiproliferative effects of oral hypoglycemic biguanides in different molecular subtypes of breast cancer: an in vitro study. Acta Pharm 2018;68:517–24.
[19] Ampferl R, Rodemann HP, Mayer C, Höfling TTA, Dittmann K. Glucose starvation impairs DNA repair in tumour cells selectively by blocking histone acetylation. Radiother Oncol 2018;126:465–70.
[20] Nathan DM, Kuenen J, Borg R, Zheng H, Schoenfeld D, Heine RJ. Translating the A1C assay into estimated average glucose values. Diabetes Care 2008;31:1473–8.
[21] Mathews EH, Liebenberg L. Improved rodent models of human brain metastases. Clin Exp Metastasis 2013;30:949–50.
[22] Stewart W, Flemming L. Features of a successful therapeutic fast of 382 days' duration. Postgrad Med J 1973;49:203–9.
[23] Mathews EH, Liebenberg L. Revival of "unsuccessful" chemotherapeutics for highly glycolytic cancers? Med Hypotheses 2011;77:1150.
[24] Kowalski GM, Bruce CR. The regulation of glucose metabolism: implications and considerations for the assessment of glucose homeostasis in rodents. Am J Physiol Metab 2014;307:E859–71.
[25] Watanabe M. Internal environment in cancer patients and proposal that carcinogenesis is adaptive response of glycolysis to overcome adverse internal conditions. Health (Irvine Calif) 2010;02:781–8.
[26] Watanabe M. Internal environment for growth of cancer cells in mice: hypothermia, anemia and lymphocytopenia. Health (Irvine Calif) 2011;03:238–44.
[27] Rajendram R, Preedy VR, Patel VB, editors. Glutamine in clinical nutrition, New York: Springer; 2015.
[28] Gleeson M. Dosing and efficacy of glutamine supplementation in human exercise and sport training. J Nutr 2008;138:2045S–9S.
[29] Hensley CT, Wasti AT, Deberardinis RJ. Review series: glutamine and cancer: cell biology, physiology, and clinical opportunities. J Clin Invest 2013;123:3678–84.
[30] Visagie MH, Mqoco TV, Liebenberg L, Mathews EH, Mathews GE, Joubert AM. Influence of partial and complete glutamine-and glucose deprivation of breast-and cervical tumorigenic cell lines. Cell Biosci 2015;5:1–26.
[31] Mathews EH, Stander BA, Joubert AM, Liebenberg L. Tumor cell culture survival following glucose and glutamine deprivation at typical physiological concentrations. Nutrition 2013;30:218–27.
[32] Mathews EH, Mathews GE, Meyer AA. A hypothetical method for controlling highly glycolytic cancers and metastases. Med Hypotheses 2018;118:19–25.
[33] Maddalena F, Lettini G, Gallicchio R, Sisinni L, Simeon V, Nardelli A, et al. Evaluation of glucose uptake in normal and cancer cell lines by positron emission tomography. Mol Imaging 2015;14:490–8.

Appendix C: Published manuscript 2 (Chapter 5)

Medical Hypotheses 118 (2018) 19–25

Contents lists available at ScienceDirect

Medical Hypotheses

journal homepage: www.elsevier.com/locate/mehy

A hypothetical method for controlling highly glycolytic cancers and metastases

Edward H. Mathews[1], George E. Mathews[*,1], Albertus A. Meyer[1]

CRCED, North-West University, P.O. Box 11207, Silver Lakes 0054, South Africa

ABSTRACT

Most proliferating cancer cells and cancer-associated tumor stroma have an upregulated glucose energy demand in relation to normal cells. Cancer cells are further less metabolically flexible than normal cells. They can therefore not survive metabolic stress as well as normal cells can. Metabolic deprivation thus provides a potential therapeutic window.

Unfortunately, current glucose blockers have toxicity problems. An alternative way to reduce a cancer patient's blood glucose (BG), for a short-term period to very low levels, without the concomitant toxicity, is hypothesized in this paper.

In vitro tests have shown that short-term BG deprivation to 2 mmol/L for 180 min is an effective cancer treatment. This level of hypoglycaemia can be maintained *in vivo* with a combination of very low-dose insulin and the suppression of the glucose counter-regulation system. Such suppression can be safely achieved by the infusion of somatostatin and a combination of both α and β-blockers.

The proposed short-term *in vivo* method, was shown to be non-toxic and safe for non-cancer patients. The next step is to test the effect of the proposed method on cancer patients. It is also suggested to incorporate well-known, long-term BG deprivation treatments to achieve maximum effect.

Background

Preamble

The majority of cancer-associated deaths are due to solid metastatic, mostly glucose-addicted cancers [1]. The high glucose uptake by many cancer cells compared to normal cells, creates a therapeutic window [2–6].

Metabolic deprivation treatment has a different effect on normal healthy cells than on malignant cells [6,7]. Normal cells have metabolic flexibility in order to survive under metabolic stress. Malignant cells on the other hand lack this flexibility, due to cumulative genetic mutations [8]. This difference can be exploited in cancer treatment.

The research group has therefore previously published work on metabolic strategies to treat highly glycolytic cancers and metastases (HGCM) via lifestyle interventions, drugs and/or haemodialysis [6,9,10]. These hypothetical strategies proposed various levels of metabolic treatments for HGCM.

A recent article by Seyfried et al. proposed a series of similar strategies called a *Press-Pulse* metabolic cancer treatment [7]. The *Press-Pulse* treatment is based on an evolutionary concept dealing with evolutionary extinctions after gradual environmental changes (*Press*) or after acute disruptive events (*Pulse*) [7,11]. However, both *Press* and *Pulse* left some species alive, either through survival of the fittest in the *Press* or through the physical and biotic environments recovering to their pre-disturbance equilibria in the *Pulse*. It was thus only when both *Press* and *Pulse* occurred simultaneously that mass extinctions without recovery occurred [7,11].

The metabolic *Press* therapy for cancer treatment envisaged by Seyfried et al. *inter alia* entails the long-term management of blood glucose (BG) levels. This is done via a Ketogenic Diet as well as psychological stress reduction [7]. For the short-term metabolic *Pulse* therapy, glucose and glutamine inhibitors are *inter alia* suggested [7]. Other non-metabolic therapies i.e. hyperbaric oxygen, chemo and radiation therapy can also be used as a *Pulse* therapy [7]. The metabolic inhibitors have some problems with toxicity [7].

Abbreviations: BG, Blood Glucose; DCA, Dichloroacetate; ECG, Electrocardiography; EGFR, Estimated Glomerular Filtration Rate; FDG, Fluorodeoxyglucose; GKI, Glucose-Ketone Index; GKIC, Glucose-Ketone Index Calculator; HGCM, Highly Glycolytic Cancers and Metastases; KD-R, Restricted Ketogenic Diet; PET, Positron Emission Tomography; PERCIST, PET Response Criteria In Solid Tumors; SUV, Standardized Uptake Value

* Corresponding author.

E-mail addresses: 10477438@nwu.ac.za (E.H. Mathews), 20270046@nwu.ac.za (G.E. Mathews), 31554857@student.g.nwu.ac.za (A.A. Meyer).

[1] Consultants to TEMM International (Pty) Ltd.

https://doi.org/10.1016/j.mehy.2018.06.014

Received 5 April 2018; Accepted 15 June 2018

In this article the authors propose to add a non-toxic metabolic *Pulse* treatment to the work of Seyfried et al. [7]. The full strategy is also a *Press-Pulse* strategy. In the proposed strategy, the lifestyle intervention (Restricted Ketogenic Diet (KD-R)) [6,7] in combination with stress and blood glucose suppression [6] via *inter alia* atenolol and metformin act as the *Press*.

The hypothesized short-term, severe blood glucose restriction, is new for cancer treatment and is via a combination of pharmacological agents which act as the metabolic *Pulse* therapy. The patient's BG values can be dropped to very low levels, for short periods, in a safe manner. *In vitro* tests showed that BG reduction to 2 mmol/L for 180 min can be an effective cancer treatment [12].

Although BG is usually the main fuel for HGCM cells, glutamine is also an important fuel [4,6,13,14]. The authors have not yet found a similarly non-toxic method of reducing glutamine levels. The current hypothetical treatment methodology focuses solely on glucose deprivation and thus on HGCM treatment. Glutamine deprivation is however a large field to cover and as such deserves a more in-depth analysis. A non-toxic *Pulse* treatment for glutamine will therefore be the focus of a follow-up paper.

Current metabolic control strategies

Short-term (Pulse) pharmacological glucose and glutamine deprivation strategies

The currently recommended glycolysis inhibitor, 2-deoxyglucose (2-DG), has been shown to have therapeutic effects when used in combination with a Restricted Ketogenic Diet (KD-R). However, toxicity has been found with 2-DG [7].

Various compounds are also studied to inhibit the glutamine metabolism cycle by targeting either glutaminase, glutamine transporters or inhibiting glutamine directly [15]. A recent review reported that the three most studied inhibitors namely acivicin, 6-diazo-5-oxo-L-norleucine (DON), and azaserine all revealed degrees of gastrointestinal toxicity and neurotoxicity [16].

The current strategies for the short-term *(Pulse)* deprivation of both glucose and glutamine thus have some problems with the toxicity of the blockers used in the treatment. There is however potentially an alternative way to severely reduce a patient's blood glucose without the concomitant toxicity present in the use of glucose blockers. Such a new *Pulse* method for cancer treatment will be discussed in this paper. Short-term non-toxic glutamine deprivation will be discussed in a future paper.

Long-term (Press) glucose deprivation strategies

In 1921 Wilder developed the Ketogenic diet for the treatment of epilepsy [17]. In recent years the Ketogenic diet has also shown therapeutic effects as a cancer treatment when used in combination with various therapies [18].

These therapies are documented in preclinical studies for several cancers including; breast and ovarian [19,20], colon [21], gastric [22], lung [23,24], neuroblastoma [25,26], pancreatic [23,27] and prostate [28–30] cancers. The preclinical and clinical studies not only improve the treatment effectiveness of conventional therapies, but can safely be applied in cancer patients [23].

The KD-R consists of a standard Ketogenic diet combined with restricted calorie intake. A standard Ketogenic diet in turn consists of a high fat and low carbohydrate and protein diet, where the ratio of fats to carbohydrates and proteins is usually 3:1 or 4:1 [31]. Therefore, by decreasing carbohydrate and calorie intake, the KD-R acts as a long-term glucose deprivation therapy via the reduction of circulating glucose and insulin levels, while elevating ketone bodies [32].

With the reduction of glucose levels, cellular energy is reduced by decreasing glycolytic and pentose phosphate pathways [2,33]. The body makes up for this energy by generating water-soluble ketone bodies (D-β-hydroxybutyrate and acetoacetate) in the liver from adipocyte-derived fatty acids and ketogenic dietary fat. This state is known as nutritional ketosis.

Many types of peripheral cells, including brain cells, do not only use glucose to produce acetyl-CoA for the production of adenosine triphosphate, but can also use ketone bodies. The body is thus forced to burn fat instead of glucose for the generation of energy [33]. Nutritional ketosis can be maintained by the addition of exogenous ketone supplements, such as medium-chain triglycerides, ketone salts and/or esters [34].

Antidiabetic (BG reducing) medicines such as metformin could be used as a long-term *(Press)* BG deprivation strategy [6,7]. Metformin shows a reduced incidence of many different types of cancers, mimics aspects of nutritional deprivation and lowers cancer mortality [35]. Metformin decreases basal glucose by suppressing hepatic gluconeogenesis and glycogenolysis, as well as by increasing glucose uptake in muscle tissue [36]. It also increases free fatty acid utilization, insulin sensitivity and decreases blood insulin levels [36].

Stress is *inter alia* an important contributor to high levels of BG [6,37] as well as elevated levels of glucocorticoids, catecholamines and insulin-like growth factor (IGF-10) all of which promote tumorigenesis [7]. Successful long-term strategies should thus also include the stress management of cancer patients. Multiple stress management techniques such as exercise [6], yoga, music, etc. in addition to pharmacological methods may be used [7].

Methods

Preamble

The proposed metabolic treatment includes both long-term (*Press* [7]) and short-term (*Pulse* [7]) glucose deprivation strategies. Fig. 1 shows the treatment methodology schematically and will be described in more detail in the rest of the article.

All of the suggested procedures are standard, although some procedures are only standard in non-cancer patients. Therefore, in Fig. 1 the procedures are separated into two categories namely standard procedures in cancer patients and standard procedures in non-cancer patients. These two categories are denoted by different coloured check marks in the individual procedures. The important message is that all elements of the suggested treatment have already been proven to be safe for humans.

Cancer identification

Firstly, patients should undergo cancer identification in order to ensure that their cancer is sufficiently glucose avid for the treatment to have an effect. This should be done by using current glucose based positron emission tomography (PET), as shown for Visit 2 in Fig. 1. A non-metabolisable glucose analogue, fluorodeoxyglucose (FDG) is used [38].

A semi-quantitative method, namely standardized uptake value (SUV), should be used to determine the glucose analogue (FDG) uptake [39]. With the evidence of untreated solid tumors typically having a mean SUV value greater than 5.0 [6], it is suggested that only patients with a SUV higher than 5.0 should initially be included in this therapy. This will ensure a high probability that the treatment will show effect.

A modified version of the PET response criteria in solid tumors (PERCIST) evaluation criteria [40], should be used in combination with standard FDG-PET scanning. This will distinguish the metabolic and physical characteristics of the tumor, before and after the glucose-deprivation therapy (Visits 2 and 4 in Fig. 1).

Proposed long-term glucose deprivation (Press)

Long-term glucose deprivation should be done via dietary control and restriction as well as the use of metformin and stress reduction via

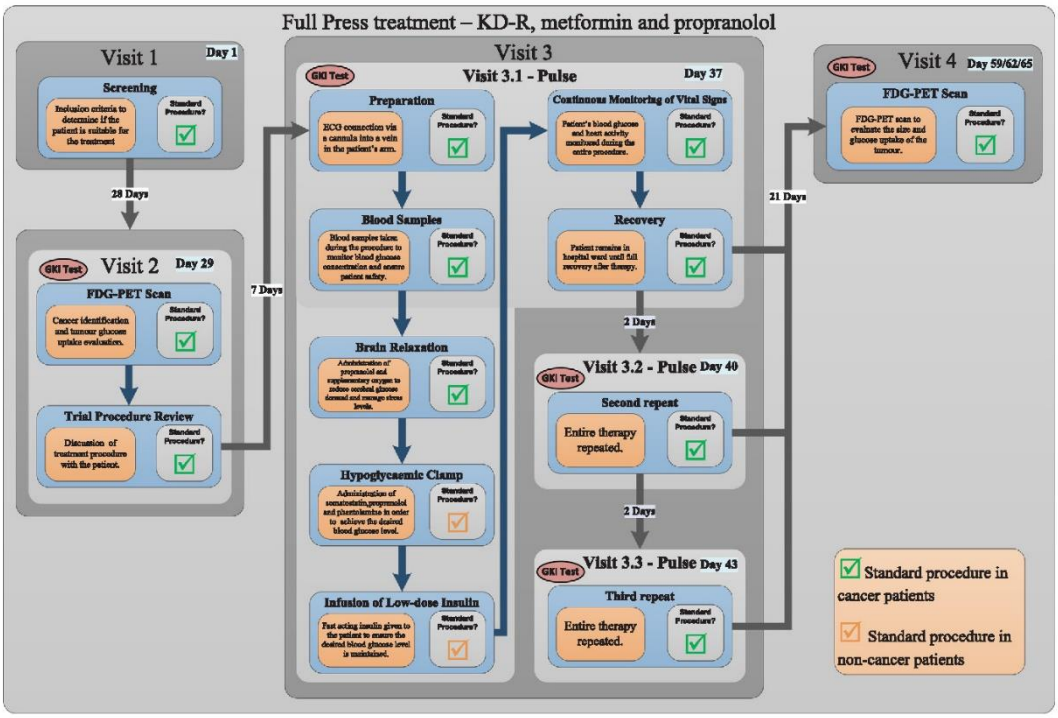

Fig. 1. Proposed *Press-Pulse* cancer treatment. Note: Fluorodeoxyglucose based Positron Emission Tomography (FDG-PET), Electrocardiography (ECG), Glucose Ketone Index (GKI), Restricted Ketogenic Diet (KD-R).

orally administered β-blockers. Metformin will be administered at a single dose of 500 mg per day as per nondiabetic patients. This will be adjusted according to the patients BG level [41].

A recent phase two clinical trial reported on the safety and efficacy of pharmacologically inhibiting β-adrenergic and cyclooxygenase-2 pathways in breast cancer patients via propranolol and etodolac [42]. It was concluded that these inhibitors provided a safe and effective strategy to inhibit multiple cellular and molecular pathways related to metastasis [42].

However, research shows that long-term use of the β-blocker propranolol slightly increases non-diabetic patients' BG levels [43]. Research also shows that propranolol reduces mitochondrial metabolism in healthy tissue [44]. Fortunately, a selective β_1-blocker, namely atenolol, has been shown not to have a significant effect on glucose metabolism [45]. It will therefore be administered to the patients to reduce stress levels. The dosage will be individualized based on the patients' response to an initial daily dosage of 50 mg [46]. The dosages of both metformin and atenolol will be adjusted in the weeks leading up to Visits 3.1–3.3 as seen in Fig. 1.

KD-R can act as a long-term glucose deprivation therapy, whereby circulating glucose and insulin levels reduce while ketone bodies are elevated [27,33,47]. The long-term glucose deprivation should start at Visit 1, in Fig. 1, with the screening visit.

Patients should follow a personalized KD-R throughout the entire treatment. In order to ensure efficacy of the therapeutic effects on HGCM patients, the glucose-ketone index (GKI) of each patient should be monitored via a glucose-ketone index calculator (GKIC) [48]. The patients will undergo a GKI test before each visit, as seen in Fig. 1. A GKI value of less than 2.0 (preferably 1.0) will ensure that the patient is in a manageable ketosis state [48], thus strictly adhering to the KD-R.

Hypothesized short-term glucose deprivation (Pulse)

A combination of *in vitro* studies [12,49] on short-term glucose-deprivation on cancer cells was used to deduce therapeutic periods and the desired blood glucose level required for the present *Pulse* treatment. The current target level of glycaemia is 2 mmol/L [12]. This can be achieved by a combination of low-dose insulin and suppression of the glucose counter-regulation system [50].

Such suppression can be safely done by continuous infusion of somatostatin (to suppress glucagon secretion) and a combination of both α and β-blockers (specifically the adrenergic antagonists, phentolamine and propranolol), to block epinephrine and norepinephrine actions [50,51]. Short-term use of the β-blocker propranolol has been shown to impair glucose recovery from insulin induced hypoglycaemia [52]. This will be beneficial for the short-term *(Pulse)* treatment.

The proposed procedure was successfully carried out in non-cancer patients by Rizza, Cryer and Gerich in 1979 [50]. It was clinically tested on human participants for an *inter alia* 90 min duration at 2 mmol/L blood glucose level.

The proposed short-term glucose deprivation will be a replication of the Rizza, Cryer and Gerich method [50] as the procedure already has ethical approval for non-cancer patients. The only suggested differences will be to firstly double the therapeutic time to 180 min, in order to coincide with our *in vitro* tests [12,49]. The second difference will be the addition of two or three repeating treatments separated by two days (as seen in Visits 3.2 and 3.3 in Fig. 1).

As it is known that cancer patients have unpredictable responses to various treatments, the short-term *(Pulse)* therapy could initially be tested for shorter time frames. Physiological and psychological responses to acute hypoglycaemia could then be assessed.

Although not part of the initial Rizza, Cryer and Gerich method, it should also be investigated to administer exogenous ketone supplements, such as a medium-chain triglycerides l, ketone salts and/or esters to the patients. This should elevate ketone levels to ensure further safety of the brain [33].

Suppression of glucose counter-regulation

In order to achieve blood glucose levels of approximately 2 mmol/L an initial administration of low-dose (0.04 IU/kg) rapid-acting insulin should be administered to the patient [50], illustrated in Fig. 1 as the "Infusion of Low-dose Insulin" step of Visit 3. Such a dose typically achieves blood glucose concentrations of 2 mmol/L within 15 min [50,53]. After the first dose of insulin, the patient should also be given a combination of drugs to suppress blood glucose counter-regulation levels for 180 min, referred to as the "Hypoglycaemic Clamp" step of Visit 3 in Fig. 1.

The suppression of glucose counter-regulation has previously been achieved by the combination of somatostatin, phentolamine and propranolol. The dosages for the respective drugs will be somatostatin at 250 μg/h, phentolamine at 500 μg/min and propranolol at 80 μg/min [50]. However, glucose slowly appears in the plasma during such infusion of these suppressors (which is an inherent safety feature). Therefore, in order to maintain blood glucose levels at 2 mmol/L, supplementary low-dose insulin (0.014 IU/kg) should be administered if necessary.

General effects of pharmacological agents

Glucose counter-regulation agents have various effects on the adrenergic system. The two adrenergic blockers that will be used in this treatment are α and β-blockers. Adrenergic blockers bind to adrenergic receptors, α receptors (located on nerves) or β receptors (located in smooth muscles of the heart, bronchioles, arterioles and visceral organs), but inhibit or block stimulation of the sympathetic nervous system [54].

For the sake of the proposed treatment, α-blockers and β-blockers cause inhibition of both glycogenolysis and gluconeogenesis with α-blockers also inhibiting glucagon release from the pancreas [54,55].

Somatostatin suppresses both glucagon and insulin secretion [56,57]. Although somatostatin is naturally secreted from pancreatic δ-cells (and in the hypothalamus) it is also available in synthetic form as somatostatin analogues [56,57].

Safety of pharmacological agents used in Pulse treatment

Propranolol is a β-blocker, and has been shown to inhibit development of metastases *in vitro* [58] and *in vivo* [59]. β-Clamps also significantly reduce resting energy expenditure in cancer patients [60]. The long-term use of propranolol is further associated with less advanced disease at diagnosis and lower breast cancer-specific mortality [61,62], improved prostate cancer survival and reduced metastases [63].

Up to 30% of women with breast cancer suffer from anxiety and depression, and a history of depression might predict cancer recurrence and overall survival [64]. Perioperative stress and anxiety stimulates the physiological stress response through the hypothalamic–pituitary–adrenocortical axis and the sympathetic nervous system. This leads to secretion of glucocorticoids, endogenous opioids, and catecholamines. These responses lead to immunosuppression, which could promote postoperative metastases [65]. Stress reduction should thus be beneficial for cancer patients, during *Pulse* and *Press* therapies.

A large amount of evidence shows that stress hormones (epinephrine and/or norepinephrine) induce a promoting effect on various tumors, including but not limited to, cancers of breast, colorectal, leukaemia, lung, melanoma, nasopharynx, oesophagus, ovary, pancreas, prostate, hemangioendotheliom and angiosarcoma [66]. Epinephrine and norepinephrine both bind to β_2-adrenoceptors and β_1-receptors respectively [66]. It has thus been proposed that β-adrenoceptor antagonists, such as propranolol and atenolol might inhibit some of the deleterious effects of stress [66,67].

Somatostatin analogues (e.g. octreotide/sandostatin or lanreotide) were found to inhibit growth of pancreatic and breast cancer cells *in vitro* [56]. Somatostatin is also used for treating pituitary tumors, insulinomas and carcinoid tumors [57,68]. Phentolamine has additionally been used for alleviation of pain in some cancer patients [69].

Insulin is a naturally occurring peptide hormone produced by the β-cells of the pancreatic islets. Although there are occasional problems with using insulin, these tend to be problems with dosage administration [70]. The insulin dosages and the patient's BG will thus be continuously monitored to ensure patient safety.

Unfortunately, insulin stimulates glycolysis. Also insulin receptors are overexpressed in cancer cells, which drives cancer growth and proliferation [6,71]. Although the insulin dose in this study is not excessive, similar to basal rates, the authors agree that the use of insulin is not ideal. However, the proposed method has already been ethically approved on non-cancer patients [50] and the authors will therefore not stray from this method for the current study. Future research should focus on alternative methods to reduce BG and simultaneously increase ketone bodies, such as administering ketogenic hypoglycaemic agent 1,3-butanediol [72].

All pharmacological agents used in the proposed procedure are safe for use by humans. It was further shown that most should also have a positive effect on cancer control.

Controlling of cerebral glucose demand

For patient safety it is important to downregulate cerebral glucose demand in a safe manner. This can be done by administering a relaxant [73,74]. In this case the β-blocker propranolol will be used, as discussed in Section "Suppression of glucose counter-regulation". In addition, supplemental oxygen will be administered via a cannula and two prongs in the nostrils, as illustrated in Fig. 1 by the "Brain Relaxation" step of Visit 3. This serves to reduce cerebral glucose metabolism by approximately 20% [75].

Although the proposed glucose deprivation therapy has been carried out previously on healthy patients without permanent adverse neurological effects [50], further caution will be taken with cancer patients. This is discussed in the next section.

Initial extra patient safety precautions

To ensure patient safety, each patient should undergo the short-term (*Pulse)* therapy in a controlled environment of a hospital ward setting. Furthermore, an oncologist and endocrinologist will continuously monitor the patient and oversee the short-term stage of the proposed glucose-deprivation therapy.

A patient undergoing the proposed glucose-deprivation therapy might experience slight hypoglycaemic symptoms. Awareness of hypoglycaemia is mainly the result of the perception of neurogenic symptoms [51], which are largely sympathetic-neural rather than adrenomedullary [76]. Some neurogenic symptoms such as palpitations, tremor, and anxiety are adrenergic whereas others such as sweating, hunger, and paraesthesia are cholinergic [51]. Neuroglycopenic symptoms range from behavioural changes, fatigue, and confusion to seizures and could result in loss of consciousness [51,77].

An important safety measure (as described earlier) is the reduction of the cerebral glucose demands by *inter alia* providing conventional supplementary oxygen. This would minimise possible hypoglycaemic-induced neurogenic symptoms, when blood glucose is reduced to 2 mmol/L. In general, recovery from any acute cognitive decrement after severe hypoglycaemia is complete by 1.5 days [78].

A value of 2 mmol/L was found to be safe by Rizza, Cryer and Gerich [50] without supplemental oxygen. We thus believe that blood glucose levels can safely be lowered to less than 2 mmol/L when supplementary oxygen is administered. This is however a subject for a future paper.

To further ensure safe treatment, emergency glucose infusion would be on hand to correct for excessive hypoglycaemia. Continuous monitoring of the following physiological parameters could also be done initially: blood glucose levels (via blood-gas monitoring), electrocardiography (ECG), blood pressure, heart rate, saturation oxygen, saturation carbon dioxide, arterial pH, Na^+, K^+, Ca^{2+} and Cl^-, as illustrated in Fig. 1 by the "Continuous Monitoring of Vital Signs" step of Visit 3.

In very successful cancer therapy it is possible that rapid cell death of tumorous cancer cells can occur. These dead cancer cells may enter autophagy ("self-eating"), apoptosis ("suicide"), or necrosis ("inflammatory cell death") [79]. It is thus prudent to investigate how the body will eliminate such dead cancer cells.

Acute tumour lysis syndrome results from rapid destruction of malignant cells and is characterized by hyperkalaemia, hyperphosphotaemia, hypercalcaemia, or hyperuricaemia [80,81]. The symptoms of hyperkalaemia, hyperphosphotaemia, hypercalcaemia or hyperuricaemia will continually be monitored during the proposed glucose-deprivation therapy, by taking regular blood samples for blood gas analysis of potassium, calcium, and phosphate.

If symptoms of hyperkalaemia (potassium > 6 mmol/L or 25% increase from baseline), hyperphosphotaemia (phosphorous > 2 mmol/L or 25% increase from baseline), hypercalcaemia (calcium > 1.75 mmol/L or 25% change from baseline), or hyperuricaemia (uric acid > 476 μmol/L or 25% increase from baseline) persist [80,82,83], the patient should be infused with intravenous fluid consisting of isotonic sodium bicarbonate to ensure normal levels of potassium, calcium and phosphate are reached [83,84]. To obtain normal levels of uric acid, rasburicase (or allopurinol) should be administered intravenously at 0.1–0.2 mg/kg over 30 min [80,83,84].

Regarding safety of the long-term *(Press)* therapy, the KD-R has been proven safe [23]. The safety of atenolol, for stress suppression, has been established in the more than 30 years it has been in use [85]. A potential risk factor in using metformin for long-term deprivation is metformin-associated lactic acidosis.

Although this is a potential risk, it is low even in patients with stable, mild to moderate renal impairment. Monitoring of estimated glomerular filtration rate (EGFR) is thus important to ensure metformin-associated lactic acidosis does not occur in patients. A reduction in the metformin dosage is recommended when EGFR is between 30 and 45 mL/min/1.73 m2 and discontinuation of metformin if EGFR is < 30 mL/min/1.73 m^2 [86].

If needed, this could also be mitigated by the administration of dichloroacetate (DCA), which has been used clinically as an investigational drug to treat lactic acidosis [87]. Substantial evidence in preclinical *in vitro* and *in vivo* models show that DCA might have an anticancer effect [88].

Discussion and conclusion

Normal cells have a much lower BG demand than most cancer cells. They are also more metabolically flexible as they can efficiently metabolize nutrients other than glucose (and glutamine). To capitalize on this therapeutic window a BG deprivation treatment method was proposed. (A non-toxic treatment to inhibit glutamine will be discussed in a follow-up paper).

The long-term *(Press)* BG therapy is well-known and was shown to be effective and safe [17,34]. For the hypothesized *Pulse* therapy the following: *In vitro* tests showed that highly glycolytic cancer cells can be severely affected if BG can be reduced to 2 mmol/L for 180 min [12]. It is hypothesized that if this *Pulse* therapy is used *in vivo* and repeated, the cancer cells should potentially receive a mortal blow. The proposed procedure has been safely applied to non-cancer patients [50]. A method to test the hypothetical treatment was also discussed.

The proposed *Pulse* metabolic treatment provides a method to severely reduce blood glucose supply in cancer patients without the toxic effects that posed problems in earlier works [7]. This methodology however only focuses on solving the problem of reducing the blood glucose supply and as such there is a large scope for further refinement of the methodology by combination with other non-metabolic factors.

Cancer cells are shown to be more vulnerable to chemotherapy and radiation, after their metabolic demands have been suppressed [7]; therefore further research of combination therapies is imperative [6,7]. This would identify potential targets for metabolic therapies in combination with chemotherapy, radiation and/or hyperbaric oxygen for the ongoing battle against cancer [6,7].

Ethics approval and consent to participate

Not applicable.

Consent for publication

Not applicable.

Availability of data and materials

All data used in this article were sourced from external sources. The relevant sources are referenced in text.

Competing interests

None.

Funding

The research was funded by the first author.

Authors' contributions

All of the authors have been involved in the writing of this manuscript and have read and approved the final text.

Conflicts of interest

None.

Acknowledgements

Prof Leon Liebenberg was involved in the initial research for this article and the work on the glucose cycle was initiated by C. Mathews. The angel investor was Dr Arnold van Dyk.

Appendix A. Supplementary data

Supplementary data associated with this article can be found, in the online version, at https://doi.org/10.1016/j.mehy.2018.06.014.

References

[1] Chaffer CL, Weinberg RA. A perspective on cancer cell metastasis. Science 2011;331:1559–64.
[2] Vander Heiden MG. Targeting cancer metabolism: a therapeutic window opens. Nat Rev Drug Discov 2011;10:671–84. http://dx.doi.org/10.1038/nrd3504.
[3] Seyfried TN, Flores RE, Poff AM, D'Agostino DP. Cancer as a metabolic disease: implications for novel therapeutics. Carcinogenesis 2014;35:515–27. http://dx.doi.org/10.1093/carcin/bgt480.
[4] Shelton LM, Huysentruyt LC, Seyfried TN. Glutamine targeting inhibits systemic

metastasis in the VM-M3 murine tumor model. Int J Cancer 2010;127:2478–85. http://dx.doi.org/10.1002/ijc.25431.
[5] Choi Y-K, Park K-G. Targeting glutamine metabolism for cancer treatment. Biomol Ther (Seoul) 2017;26:19–28. http://dx.doi.org/10.4062/biomolther.2017.178.
[6] Mathews EH, Liebenberg L, Pelzer R. High-glycolytic cancers and their interplay with the body's glucose demand and supply cycle. Med Hypotheses 2011;76:157–65. http://dx.doi.org/10.1016/j.mehy.2010.09.006.
[7] Seyfried TN, Yu G, Maroon JC, D'Agostino DP. Press-pulse: a novel therapeutic strategy for the metabolic management of cancer. Nutr Metab 2017;14:1–17. http://dx.doi.org/10.1186/s12986-017-0178-2.
[8] Seyfried TN, Shelton LM. Cancer as a metabolic disease. Nutr Metab (Lond) 2010. http://dx.doi.org/10.1097/CCO.0b013e32834e388a.
[9] Mathews EH, Liebenberg L. Is knowledge of brain metabolism the key to treating highly glycolytic cancers and metastases? Neuro-Oncology 2013;15(6):649.
[10] Mathews EH, Liebenberg L. Cancer control via glucose and glutamine deprivation. J Intern Med 2013;274:492. http://dx.doi.org/10.1111/joim.12068.
[11] Arens NC, West ID. Press-pulse: a general theory of mass extinction? Paleobiology 2008;34:456–71. http://dx.doi.org/10.1666/07034.1.
[12] Mathews EH, Stander BA, Joubert AM, Liebenberg L. Tumor cell culture survival following glucose and glutamine deprivation at typical physiological concentrations. Nutrition 2013;30:218–27. http://dx.doi.org/10.1016/j.nut.2013.07.024.
[13] Son J, Lyssiotis CA, Ying H, Wang X, Hua S, Ligorio M, et al. Glutamine supports pancreatic cancer growth through a KRAS-regulated metabolic pathway. Nature 2013;496:101–5. http://dx.doi.org/10.1038/nature12040.
[14] Wise DR, Thompson CB. Glutamine addiction: a new therapeutic target in cancer. Trends Biochem Sci 2011;35:427–33. http://dx.doi.org/10.1016/j.tibs.2010.05.003.Glutamine.
[15] Chen L, Cui H. Targeting glutamine induces apoptosis: a cancer therapy approach. Int J Mol Sci 2015;16:22830–55. http://dx.doi.org/10.3390/ijms160922830.
[16] Hensley CT, Wasti AT, Deberardinis RJ. Review series Glutamine and cancer : cell biology, physiology, and clinical opportunities. J Clin Invest 2013;123:3678–84. http://dx.doi.org/10.1172/JCI69600.3678.
[17] Wilder RM. The effects of ketonemia on the course of epilepsy. Mayo Clin Proc 1921;2:307–8.
[18] Allen BG, Bhatia SK, Anderson CM, Eichenberger-Gilmore JM, Sibenaller ZA, Mapuskar KA, et al. Ketogenic diets as an adjuvant cancer therapy: history and potential mechanism. Redox Biol 2014;2:963–70. http://dx.doi.org/10.1016/j.redox.2014.08.002.
[19] Lv M, Zhu X, Wang H, Wang F, Guan W. Roles of caloric restriction, ketogenic diet and intermittent fasting during initiation, progression and metastasis of cancer in animal models: a systematic review and meta-analysis. PLoS One 2014;9:1–18. http://dx.doi.org/10.1371/journal.pone.0115147.
[20] Zhuang Y, Chan DK, Haugrud AB, Miskimins WK. Mechanisms by which low glucose enhances the cytotoxicity of metformin to cancer cells both in vitro and in vivo. PLoS One 2014;9. http://dx.doi.org/10.1371/journal.pone.0108444.
[21] Hao G-W, Chen Y-S, He D-M, Wang H-Y, Wu G-H, Zhang B. Growth of human Colon cancer cells in nude mice is delayed by a ketogenic diet or without omega-3 fatty acids and medium-chain triglycerides. Asian Pacific J Cancer Prev 2015;16:2061–8. http://dx.doi.org/10.1186/1471-2407-8-122.
[22] Otto C, Kaemmerer U, Illert B, Muehling B, Pfetzer N, Wittig R, et al. Growth of human gastric cancer cells in nude mice is delayed by a ketogenic diet supplemented with omega-3 fatty acids and medium-chain triglycerides. BMC Cancer 2008;8:1–13. http://dx.doi.org/10.1186/1471-2407-8-122.
[23] Zahra A, Fath MA, Opat E, Mapuskar KA, Bhatia SK, Ma DC, et al. Consuming a ketogenic diet while receiving radiation and chemotherapy for locally advanced lung cancer and pancreatic cancer: the University of Iowa experience of two phase 1 clinical trials. Radiat Res 2017;187:743–54. http://dx.doi.org/10.1667/RR14668.1.
[24] Allen BG, Bhatia SK, Buatti JM, Brandt KE, Lindholm KE, Button AM, et al. Ketogenic diets enhance oxidative stress and radio-chemo-therapy responses in lung cancer xenografts. Clin Cancer Res 2013;19:3905–13. http://dx.doi.org/10.1158/1078-0432.CCR-12-0287.
[25] Morscher RJ, Aminzadeh-Gohari S, Feichtinger R, Mayr JA, Lang R, Neureiter D, et al. Inhibition of neuroblastoma tumor growth by ketogenic diet and/or calorie restriction in a CD1-nu mouse model. PLoS One 2015;10:1–20. http://dx.doi.org/10.1371/journal.pone.0129802.
[26] Aminzadeh-Gohari S, Feichtinger RG, Vidali S, Locker F, Rutherford T, O'Donnel M, et al. A ketogenic diet supplemented with medium-chain triglycerides enhances the anti-tumor and anti-angiogenic efficacy of chemotherapy on neuroblastoma xenografts in a CD1-nu mouse model. Oncotarget 2017;8:64728–44. http://dx.doi.org/10.18632/oncotarget.20041.
[27] Shukla SK, Gebregiworgis T, Purohit V, Chaika NV, Gunda V, Radhakrishnan P, et al. Metabolic reprogramming induced by ketone bodies diminishes pancreatic cancer cachexia. Cancer Metab 2014;2:18. http://dx.doi.org/10.1186/2049-3002-2-18.
[28] Mavropoulos JC, Buschemeyer WC, Tewari AK, Rokhfeld D, Pollak M, Zhao Y, et al. The effects of varying dietary carbohydrate and fat content on survival in a murine LNCaP prostate cancer xenograft model. Cancer Prev Res 2009;2:557–65. http://dx.doi.org/10.1158/1940-6207.CAPR-08-0188.
[29] Kim HS, Masko EM, Poulton SL, Kennedy KM, Pizzo SV, Dewhirst MW, et al. Carbohydrate restriction and lactate transporter inhibition in a mouse xenograft model of human prostate cancer. BJU Int 2012;110:1062–9. http://dx.doi.org/10.1111/j.1464-410X.2012.10971.x.
[30] Caso J, Masko EM, Ii JAT, Poulton SH, Dewhirst M, Pizzo SV, et al. The effect of carbohydrate restriction on prostate cancer tumor growth in a castrate mouse xenograft model. Prostate 2013;73:449–54. http://dx.doi.org/10.1002/pros.22586.
[31] Hartman AL, Vining EPG. Clinical aspects of the ketogenic diet. Epilepsia 2007;48:31–42. http://dx.doi.org/10.1111/j.1528-1167.2007.00914.x.
[32] O'Flanagan CH, Smith LA, McDonell SB, Hursting SD. When less may be more: Calorie restriction and response to cancer therapy. BMC Med 2017;15:1–10. http://dx.doi.org/10.1186/s12916-017-0873-x.
[33] Vanitallie TB, Nufert TH. Ketones: metabolism' s ugly duckling. Nutr Rev 2003;61:327–41. http://dx.doi.org/10.131/nr.2003.oct.327.
[34] Harvey CJdC, Schofield GM, Williden M. The use of nutritional supplements to induce ketosis and reduce symptoms associated with keto-induction: a narrative review. PeerJ 2018;6. http://dx.doi.org/10.7717/peerj.4488.
[35] Rojas LBA, Gomes MB. Metformin: an old but still the best treatment for type 2 diabetes. Diabetol Metab Syndr 2013;5:6. http://dx.doi.org/10.1186/1758-5996-5-6.
[36] Dowling RJO, Goodwin PJ, Stambolic V. Understanding the benefit of metformin use in cancer treatment. BMC Med 2011;9:33. http://dx.doi.org/10.1186/1741-7015-9-33.
[37] Mathews EH, Liebenberg L. A practical quantification of blood glucose production due to high-level chronic stress. Stress Heal 2012;28:327–32. http://dx.doi.org/10.1002/smi.2415.
[38] Shankar LK, Hoffman JM, Bacharach S, Graham MM, Karp J, Lammertsma AA, et al. Consensus recommendations for the use of 18 F- FDG PET as an indicator of therapeutic response in patients in national cancer institute trials. J Nucl Med 2006;47:1059–66.
[39] Huang SC. Anatomy of SUV. Nucl Med Biol 2000;27:643–6. http://dx.doi.org/10.1016/S0969-8051(00)00155-4.
[40] Wahl RL, Jacene H, Kasamon Y, Lodge MA. From RECIST to PERCIST: evolving considerations for PET response criteria in solid tumors. J Nucl Med 2009;50:122S–50S. http://dx.doi.org/10.2967/jnumed.108.057307.
[41] Drugs.com. Metformin – FDA Professional Drug Information 2018. https://www.drugs.com/pro/metformin.html#Table1 (accessed March 20, 2018).
[42] Shaashua L, Shabat-Simon M, Haldar R, Matzner P, Zmora O, Shabtai M, et al. Perioperative COX-2 and β-adrenergic blockade improves metastatic biomarkers in breast cancer patients in a phase-II randomized trial. Clin Cancer Res 2017;23:4651–61. http://dx.doi.org/10.1158/1078-0432.CCR-17-0152.
[43] Groop L, Tötterman KJ, Harno K, Gordin A. Influence of beta-blocking drugs on glucose metabolism in hypertensive, non-diabetic patients. J Intern Med 1983;213:9–14.
[44] Dreisbach AW, Greif RL, Lorenzo BJ, Reidenberg MM. Lipophilic beta-blockers inhibit rat skeletal muscle mitochondrial respiration. Pharmacology 1993;47:295–9.
[45] Vulpis V, Antonacci A, Prandi P, Bokor D, Pirrelli A. The effects of bisoprolol and atenolol on glucose metabolism in hypertensive patients with non-insulin-dependent diabetes mellitus. Minerva Med 1991;82:189–93.
[46] Maartens G, Benson F, Blockman M, Clark C, Bamford L, Bera R, et al. Standard treatment guidelines and essential medicines list for South Africa Hospital Level 2015 Edition. 2015.
[47] Zhou W, Mukherjee P, Kiebish MA, Markis WT, Mantis JG, Seyfried TN. The calorically restricted ketogenic diet, an effective alternative therapy for malignant brain cancer. Nutr Metab (Lond) 2007;4:5. http://dx.doi.org/10.1186/1743-7075-4-5.
[48] Meidenbauer JJ, Mukherjee P, Seyfried TN. The glucose ketone index calculator: a simple tool to monitor therapeutic efficacy for metabolic management of brain cancer. Nutr Metab 2015;12:1–8. http://dx.doi.org/10.1186/s12986-015-0009-2.
[49] Visagie MH, Mqoco TV, Liebenberg L, Mathews EH, Mathews GE, Joubert AM. Influence of partial and complete glutamine-and glucose deprivation of breast-and cervical tumorigenic cell lines. Cell Biosci 2015;5:1–26. http://dx.doi.org/10.1186/s13578-015-0030-1.
[50] Rizza RA, Cryer PE, Gerich JE. Role of glucagon, catecholamines, and growth hormone in human glucose counterregulation. J Clin Invest 1979;64:62–71. http://dx.doi.org/10.1172/JCI109464.
[51] Towler DA, Havlin CE, Craft S, Cryer P. Mechanism of awareness of hypoglycemia: Perception of neurogenic (predominantly cholinergic) rather than neuroglycopenic symptoms. Diabetes 1993;42:1791–8. http://dx.doi.org/10.2337/diab.42.12.1791.
[52] Popp DA, Tse TF, Shah SD, Clutter WE, Cryer PE. Oral propranolol and metoprolol both impair glucose recovery from insulin-induced hypoglycemia in insulin-dependent diabetes mellitus. Diabetes Care 1984;7:243–7. http://dx.doi.org/10.2337/diacare.7.3.243.
[53] Garber AJ, Cryer PE, Santiago JV, Haymond MW, Pagliara AS, Kipnis DM. The role of adrenergic mechanisms in the substrate and hormonal response to insulin-induced hypoglycemia in man. J Clin Invest 1976;58:7–15. http://dx.doi.org/10.1172/JCI108460.
[54] Squire LR, Berg D, Bloom F, Du Lac S, Ghosh A, Spitzer N. Fundamental neuroscience. Prof Psychol 2012;261. http://dx.doi.org/10.1163/_q3_SIM_00374.
[55] Propranolol (Cardiovascular). AHFS Consum Medicat Inf 2017:1.
[56] Liebow C, Reilly C, Serrano M, Schally AV. Somatostatin analogues inhibit growth of pancreatic cancer by stimulating tyrosine phosphatase. Proc Natl Acad Sci USA 1989;86:2003–7. http://dx.doi.org/10.1073/pnas.86.6.2003.
[57] Schally AV. Oncological applications of somatostatin analogues. Cancer Res 1988;48:6977–85.
[58] Guo K, Ma Q, Wang L, Hu H, Li J, Zhang D, et al. Norepinephrine-induced invasion by pancreatic cancer cells is inhibited by propranolol. Anticancer Res 2009;22:825–30. http://dx.doi.org/10.3892/or.
[59] Palm D, Lang K, Niggemann B, Drell IV TL, Masur K, Zaenker KS, et al. The norepinephrine-driven metastasis development of PC-3 human prostate cancer cells in BALB/c nude mice is inhibited by β-blockers. Int J Cancer 2006;118:2744–9. http://dx.doi.org/10.1002/ijc.21723.
[60] Hyltander A, Körner U, Lundholm KG. Evaluation of mechanisms behind elevated

energy expenditure in cancer patients with solid tumours. Eur J Clin Invest 1993;23:46–52.
[61] Botteri E, Munzone E, Rotmensz N, Cipolla C, De Giorgi V, Santillo B, et al. Therapeutic effect of β-blockers in triple-negative breast cancer postmenopausal women. Breast Cancer Res Treat 2013;140:567–75. http://dx.doi.org/10.1007/s10549-013-2654-3.
[62] Barron TI, Connolly RM, Sharp L, Bennett K, Visvanathan K. Beta blockers and breast cancer mortality: a population-based study. J Clin Oncol 2011;29:2635–44.
[63] Grytli HH, Fagerland MW, Tasken KA, Fossa SD, Haheim LL. Use of beta-blockers is associated with prostate cancer-specific survival in prostate cancer patients on androgen deprivation therapy. Prostate 2013;73:250–60. http://dx.doi.org/10.1002/pros.22564.
[64] Björneklett HG, Lindemalm C, Rosenblad A, Ojutkangas M-L, Letocha H, Strang P, et al. A randomised controlled trial of support group intervention after breast cancer treatment: results on anxiety and depression. Acta Oncol (Madr) 2012;51:198–207. http://dx.doi.org/10.3109/0284186X.2011.610352.
[65] Shakhar G, Ben-Eliyahu S. Potential prophylactic measures against postoperative immunosuppression: could they reduce recurrence rates in oncological patients? Ann Surg Oncol 2003;10:972–92. http://dx.doi.org/10.1245/ASO.2003.02.007.
[66] Tang J, Li Z, Lu L, Cho CH. β-Adrenergic system, a backstage manipulator regulating tumour progression and drug target in cancer therapy. Semin Cancer Biol 2013;23:533–42. http://dx.doi.org/10.1016/j.semcancer.2013.08.009.
[67] Cole SW, Sood AK. Molecular pathways: beta-adrenergic signaling in cancer. Clin Cancer Res 2012;18:1201–6. http://dx.doi.org/10.1158/1078-0432.CCR-11-0641.
[68] Giustina A, Mazziotti G, Torri V, Spinello M, Floriani I, Melmed S. Meta-analysis on the effects of octreotide on tumor mass in acromegaly. PLoS One 2012;7. http://dx.doi.org/10.1371/journal.pone.0036411.
[69] Yasukawa M, Yasukawa K, Kamiizumi Y, Yokoyama R. Intravenous phentolamine infusion alleviates the pain of abdominal visceral cancer, including pancreatic carcinoma. J Anesth 2007;21:420–3. http://dx.doi.org/10.1007/s00540-007-0528-8.
[70] James J. Implementation of national guidance at a local level. Safety Insulin 2013;17:180–6.
[71] Fine EJ, Segal-Isaacson CJ, Feinman RD, Herszkopf S, Romano MC, Tomuta N, et al. Targeting insulin inhibition as a metabolic therapy in advanced cancer: a pilot safety and feasibility dietary trial in 10 patients. Nutrition 2012;28:1028–35. http://dx.doi.org/10.1016/j.nut.2012.05.001.
[72] Poff AM, Ari C, Arnold P, Seyfried TN, D'Agostino DP. Ketone supplementation decreases tumor cell viability and prolongs survival of mice with metastatic cancer. Int J Cancer 2014;135:1711–20. http://dx.doi.org/10.1002/ijc.28809.
[73] Siegel GJ, Agranoff BW, Albers RW, Fisher SK, Uhler MD. Basic neurochemistry: molecular, cellular and medical aspects. 6th ed.Philadelphia: Lippincott-Raven; 1999.
[74] Cryer PE, Axelrod L, Grossman AB, Heller SR, Montori VM, Seaquist ER, et al. Evaluation and management of adult hypoglycemic disorders: an endocrine society clinical practice guideline. J Clin Endocrinol Metab 2009;94:709–28. http://dx.doi.org/10.1210/jc.2008-1410.
[75] Tolias C, Reinert M, Seiler R. Normobaric hyperoxia-induced improvement in cerebral metabolism and reduction in intracranial pressure in patients with severe head injury: a prospective historical. J Neurosurg 2004;101:435–44.
[76] DeRosa MA. Hypoglycemia and the sympathoadrenal system: neurogenic symptoms are largely the result of sympathetic neural, rather than adrenomedullary, activation. AJP Endocrinol Metab 2004;287:E32–41. http://dx.doi.org/10.1152/ajpendo.00539.2003.
[77] Cryer PE. Hypoglycemia, functional brain failure, and brain death. J Clin Invest 2007;117:868–70. http://dx.doi.org/10.1172/JCI31669.
[78] Carroll MF, Burge MR, Schade DS. Severe hypoglycemia in adults. Rev Endocr Metab Disord 2003;4:149–57. http://dx.doi.org/10.1023/A:1022990003161.
[79] Edinger AL, Thompson CB. Death by design: apoptosis, necrosis and autophagy. Curr Opin Cell Biol 2004;16:663–9. http://dx.doi.org/10.1016/j.ceb.2004.09.011.
[80] Cairo MS, Bishop M. Tumour lysis syndrome: new therapeutic strategies and classification. Br J Haematol 2004;127:3–11. http://dx.doi.org/10.1111/j.1365-2141.2004.05094.x.
[81] Arrambide K, Toto RD. Tumor lysis syndrome. Semin Nephrol 1993;13:273–80.
[82] Howard SC, Jones DP, Pui C-H. The tumor lysis syndrome. N Engl J Med 2011;364:1844–54. http://dx.doi.org/10.1056/NEJMra0904569.
[83] Coiffier B, Altman A, Pui C-H, Younes A, Cairo MS. Guidelines for the management of pediatric and adult tumor lysis syndrome: an evidence-based review. J Clin Oncol 2008;26:2767–78. http://dx.doi.org/10.1200/JCO.2007.15.0177.
[84] McCurdy MT, Shanholtz CB. Oncologic emergencies. Crit Care Med 2012;40:2212–22. http://dx.doi.org/10.1097/CCM.0b013e31824e1865.
[85] FDA. U.S. Food & Drug Administration 2018. https://www.accessdata.fda.gov/scripts/cder/ob/results_product.cfm?Appl_Type=A&Appl_No=072303 (accessed June 4, 2018).
[86] Lu WR, Defilippi J, Braun A. Unleash metformin: reconsideration of the contraindication in patients with renal impairment. Ann Pharmacother 2013;47:1488–97. http://dx.doi.org/10.1177/1060028013505428.
[87] National Institutes of Health. PubChem – Dichloroacetic Acid 2018. https://pubchem.ncbi.nlm.nih.gov/compound/6597#section=Information-Sources (accessed May 31, 2018).
[88] Michelakis ED, Webster L, Mackey JR. Dichloroacetate (DCA) as a potential metabolic-targeting therapy for cancer. Br J Cancer 2008;99:989–94. http://dx.doi.org/10.1038/sj.bjc.6604554.

Appendix D: Published manuscript 3 (Chapter 6)

frontiers in Cardiovascular Medicine

ORIGINAL RESEARCH
published: 16 February 2022
doi: 10.3389/fcvm.2022.737592

Using a Systems Approach to Explore the Mechanisms of Interaction Between Severe Covid-19 and Its Coronary Heart Disease Complications

Albertus A. Meyer[1], *Edward H. Mathews*[1,2,3*], *Andries G. S. Gous*[3] *and Marc J. Mathews*[3]

[1] *Centre for Research in Continued Engineering Development (CRCED), North-West University, Potchefstroom, South Africa,* [2] *Department of Physiology, Medical School, University of Pretoria, Pretoria, South Africa,* [3] *Department of Industrial Engineering, Stellenbosch University, Stellenbosch, South Africa*

OPEN ACCESS

Edited by:
Eric Sijbrands,
Erasmus Medical Center, Netherlands

Reviewed by:
Eric Sijbrands,
Erasmus Medical Center, Netherlands
Vladimir Uspenskiy,
Almazov National Medical Research Centre, Russia

***Correspondence:**
Edward H. Mathews
ehmathews@researchtoolbox.com

Specialty section:
This article was submitted to Cardiovascular Epidemiology and Prevention, a section of the journal Frontiers in Cardiovascular Medicine

Received: *07 July 2021*
Accepted: *24 January 2022*
Published: *16 February 2022*

Citation:
Meyer AA, Mathews EH, Gous AGS and Mathews MJ (2022) Using a Systems Approach to Explore the Mechanisms of Interaction Between Severe Covid-19 and Its Coronary Heart Disease Complications. Front. Cardiovasc. Med. 9:737592. doi: 10.3389/fcvm.2022.737592

Frontiers requested research on how a systems approach can explore the mechanisms of cardiovascular complications in Covid-19. The focus of this paper will thus be on these detailed mechanisms. It will elucidate the integrated pathogenic pathways based on an extensive review of literature. Many severe Covid-19 cases and deaths occur in patients with chronic cardiovascular comorbidities. To help understand all the mechanisms of this interaction, Covid-19 complications were integrated into a pre-existing systems-based coronary heart disease (CHD) model. Such a complete model could not be found in literature. A fully integrative view could be valuable in identifying new *pharmaceutical interventions*, help understand how *health factors* influence Covid-19 severity and give a fully integrated explanation for the Covid-19 *death spiral* phenomenon seen in some patients. Covid-19 data showed that CHD hallmarks namely, *Hypercoagulability, Hypercholesterolemia, Hyperglycemia/Hyperinsulinemia, Inflammation* and *Hypertension* have an important effect on disease severity. The pathogenic pathways that Covid-19 activate in CHD were integrated into the CHD model. This fully integrated model presents a visual explanation of the mechanism of interaction between CHD and Covid-19 complications. This includes a detailed integrated explanation of the death spiral as a result of interactions between *Inflammation*, endothelial cell injury, *Hypercoagulability* and hypoxia. Additionally, the model presents the aggravation of this *death spiral* through the other CHD hallmarks namely, *Hyperglycemia/Hyperinsulinemia, Hypercholesterolemia,* and/or *Hypertension*. The resulting model further suggests systematically how the pathogenesis of nine *health factors* (stress, exercise, smoking, etc.) and seven *pharmaceutical interventions* (statins, salicylates, thrombin inhibitors, etc.) may either aggravate or suppress Covid-19 severity. A strong association between CHD and Covid-19 for all the investigated *health factors* and *pharmaceutical interventions*, except for β-blockers, was found. It is further discussed how the proposed model can be extended in future to do computational analysis to help assess the risk of Covid-19 in cardiovascular disease. With insight gained from this study, recommendations are made

for future research in potential new pharmacotherapeutics. These recommendations could also be beneficial for cardiovascular disease, which killed five times more people in the past year than Covid-19.

Keywords: COVID-19, SARS-CoV-2, coronary heart disease, cardiovascular comorbidities, systems-approaches

INTRODUCTION

The coronavirus disease of 2019 (Covid-19) is caused by the infection of severe acute respiratory syndrome coronavirus 2 (SARS-CoV-2), which first emerged in December 2019 in Wuhan, China (1). In March 2020, the World Health Organization declared this disease a pandemic (2). As of 8 August 2021, the total number of confirmed global deaths were 4,285,421 (3).

It is widely accepted that Covid-19 severity is increased by respiratory complications such as hypoxia (4, 5). Critically ill patients developing hypoxia requires supplemental oxygen and/or mechanical ventilation (4, 5). Although this condition is respiratory related, this hypoxia is fueled by vascular complications which are documented in numerous autopsies (4, 6–9). Moreover, pre-existing cardiovascular related comorbidities are known risk factors that increase Covid-19 severity. These comorbidities include, among others, *Hypertension*, *Hyperglycemia/Hyperinsulinemia*, obesity and/or chronic cardiac disease (10–14).

Furthermore, hospitalized critically ill Covid-19 patients experience cardiovascular complications such as cardiac injury, thrombosis, arrhythmia, heart failure and myocardial dysfunction (15–19). This is again substantiated by autopsies that present various findings of vasculature damage that leads to a state of *Hypercoagulability* in deceased Covid-19 patients (4, 6–9).

Most severe Covid-19 patients also experience a chronic heightened *Inflammatory state*, especially within the alveoli and pulmonary capillaries (20–22). This may be as a result of the dysregulated hyperimmune response (20) and/or direct viral infection mediating inflammatory cell infiltration (11, 22).

Therefore, the prevailing viewpoints in literature are that most severe cases of Covid-19 (i) result in cardiovascular complications (4, 6–9) and/or (ii) are seen in patients with pre-existing cardiovascular comorbidities (10–14). A need therefore exists to further investigate the underlying mechanisms/pathogenesis between cardiovascular disease and Covid-19.

To fully investigate this, the pathogenesis of cardiovascular disease and Covid-19 needs to be integrated. Fortunately, most of the above mentioned vascular Covid-19 effects are included in an existing model of coronary heart disease (CHD) (**Figure 1**) (23, 24). These effects are depicted in **Figure 1** as the following CHD hallmarks (yellow boxes): *(A) Hypercoagulability, (B) Hypercholesterolemia, (C) Hyperglycemia/Hyperinsulinemia, (D) Inflammatory state* and *(E) Hypertension.*

Hypercholesterolemia is a common CHD risk factor, known to aggravate vascular cell dysfunction, aggravate coagulation and upregulate inflammation (29–31). *Hypercholesterolemia (B)*, depicted in **Figure 1**, has only been partially linked to Covid-19 through high circulating cholesterol levels that may make a person more susceptible to infection (32). Although this might still be controversial, a recent molecular study showed that SARS-CoV-2 requires cholesterol for viral entry (33). Subsequently, another molecular study (yet unpublished) showed how cholesterol optimally positions furin for priming SARS-CoV-2 (34). In other words, cholesterol improves binding to ACE2 receptor, while producing a more infectious virion (34).

We envisage another association between increased Covid-19 severity and *Hypercholesterolemia*, through vascular complications that arise from high cholesterol levels. Since both *Hypercoagulability* and *Inflammation* are known risk factors for Covid-19 and *Hypercholesterolemia* influences both these hallmarks (23), we also included *Hypercholesterolemia* in our *integrated CHD/Covid-19 model* (more detailed discussions are given in sections Severe Covid-19 Patients With Existing Chronic Hypercholesterolemia and Effects of Different CHD *Pharmaceutical Interventions* on Covid-19 Severity).

All of the CHD Hallmarks identified in the CHD model (**Figure 1**) play a significant role in Covid-19 severity. The question is, will it be possible to use this CHD model and integrate the pathogenesis of Covid-19 with it?

In this paper we will attempt to integrate the CHD pathogenic pathways with those of severe Covid-19 complications, using a systems-based approach. This CHD/Covid-19 integration should provide insight into the following questions, some of which were requested by *Frontiers*:

1. Why do some patients with severe Covid-19 experience sudden death? (Section The Death Spiral: Inflammation, EC Injury, Coagulation, Vascular Leakage and Hypoxia)
2. How do CHD comorbidities influence this *death spiral*? (Section Covid-19 Aggravation in Patients With Pre-existing CHD Comorbidities)
3. How can an individual reduce the risk of developing severe Covid-19 from a cardiovascular point of view? (Sections Effects of Different *Health Factors* on Covid-19 Severity and Effects of Different CHD *Pharmaceutical Interventions* on Covid-19 Severity)
4. How can computational analysis help to assess the risk of COVID-19 in cardiovascular disease? (Section How Can Computational Analysis Help to Assess the Risk of Severity in Covid-19 in Cardiovascular Disease?)
5. Are there other opportunities in cardiovascular disease that can be derived from this paper and the Covid-19 crisis? (Section Are There Other Opportunities in Cardiovascular Disease That Can Be Derived From This Paper and the Covid-19 Crisis?).

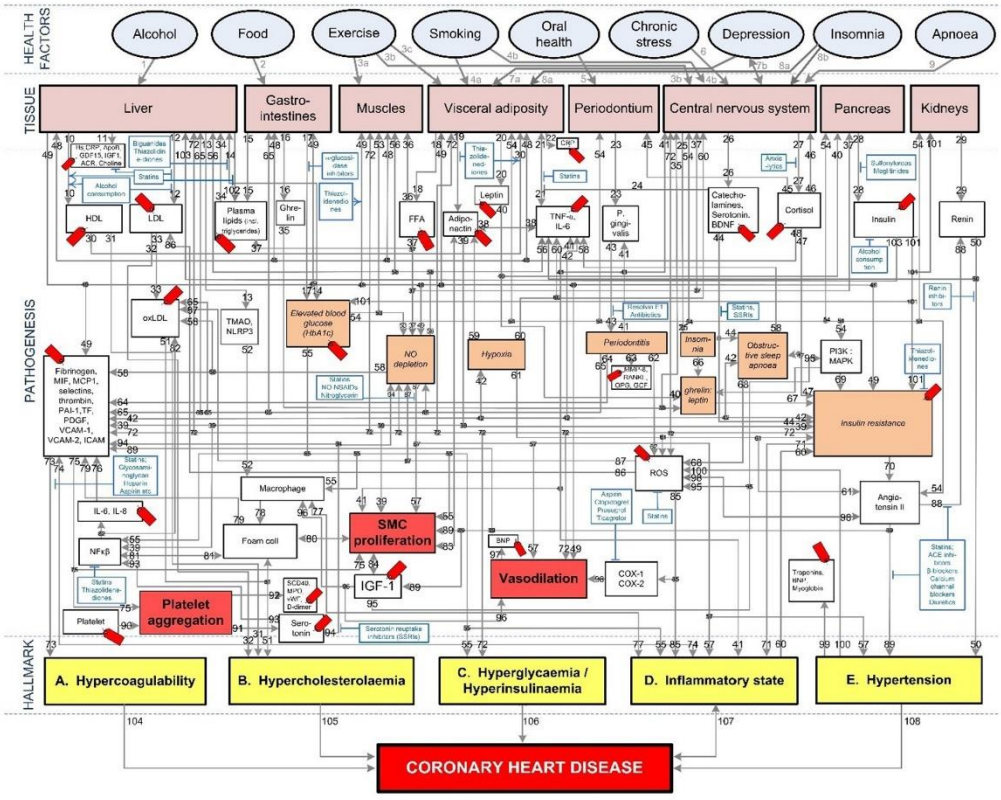

FIGURE 1 | Existing model showing the mechanisms of coronary heart disease (23–28). The affective pathway of pharmaceuticals, blue boxes, is shown in Figure and salient serological biomarkers are indicated by the red tags (🏷). The blunted blue arrows denote antagonize or inhibit and pointed blue arrows denote up-regulate or facilitate. ACE, angiotensin-converting-enzyme; β-blocker, beta-adrenergic antagonists; BDNF, brain-derived neurotrophic factor; BNP, B-type natriuretic peptide; OX, cyclooxygenase; CRP, C-reactive protein; D-dimer, fibrin degradation product D; FFA, free fatty acids; GCF, gingival crevicular fluid; HbA1c, glycated hemoglobin A1c; HDL, high-density lipoprotein; Hs, homocysteine; ICAM, intracellular adhesion molecule; IGF-1, insulin-like growth factor-1; IL, interleukin; LDL, low-density lipoprotein; MAPK, mitogen-activated protein (MAP) kinase; MCP, monocyte chemoattractant protein; MIF, macrophage migration inhibitory factor; MMP, matrix metalloproteinase; MPO, myeloperoxidase; NFκβ, nuclear factor-κβ; NLRP3, Inflammasome responsible for activation of inflammatory processes as well as epithelial cell regeneration and microflora; NO, nitric oxide; NO-NSAIDs, combinational NO-non-steroidal anti-inflammatory drug; OPG, osteoprotegerin; oxLDL, oxidized LDL; PAI, plasminogen activator inhibitor; PDGF, platelet-derived growth factor; P. gingivalis, Porphyromonas gingivalis; PI3K, phosphatidylinositol 3-kinase; RANKL, receptor activator of nuclear factor kappa-beta ligand; ROS, reactive oxygen species; SCD-40, recombinant human sCD40 ligand; SMC, smooth muscle cell; SSRI, serotonin reuptake inhibitors; TF, tissue factor; TMAO, an oxidation product of trimethylamine (TMA); TNF-α, tumor necrosis factor-α; VCAM, vascular cell adhesion molecule; vWF, von Willebrand factor.

We envisage that the proposed *integrated CHD/Covid-19 model* may help answer some of these questions, thereby potentially enhancing the future management of both Covid-19 and CHD.

METHOD

The methodology to develop the pathogenic pathways for the *integrated CHD/Covid-19 model* is divided into three parts namely the following:

1. Section Description of Existing CHD Model discribes the existing CHD model (23).
2. Section Systems-Based Integration of Covid-19 Factors Into the CHD Model discusses the systems-based method for integration (**Figure 2**) of Covid-19 factors into the CHD model (**Figure 1**). The outcome of this method is depicted in **Figures 3–6**, **8–10**. Its implications are discussed in the Results sections Integrated Covid-19/CHD Model and Covid-19 Aggravation in Patients With Pre-existing CHD Comorbidities.

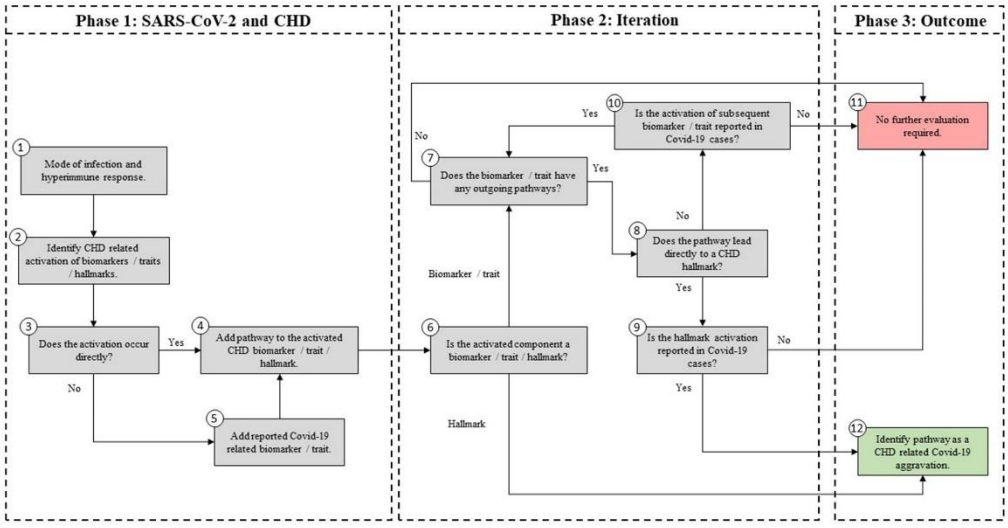

FIGURE 2 | Methodology used to develop an Integrated Covid-19/CHD model.

3. Section Evaluation of *Health Factors* and *Pharmaceutical Interventions* describes the method to evaluate the effects on Covid-19 severity of *health factors* (blue ovals) and *pharmaceutical interventions* (blue boxes) as depicted in **Figure 1**. The relevant pathogenic pathways that are activated are discussed in more detail in the Results sections Effects of Different *Health Factors* on Covid-19 Severity and Effects of Different CHD *Pharmaceutical Interventions* on Covid-19 Severity.

Description of Existing CHD Model

The existing CHD model (**Figure 1**) was developed as a PhD study and extensively described in (23). The model is available online from the university (23). Some results and implications of the model were published (24–28). Hence, we will only discuss the relevant salient elements here. The model defined CHD as the incidence of atherosclerosis, coronary artery disease, or myocardial infarction (23). Subsequently, where results were given for cardiovascular disease these were interpreted as CHD only in scenarios where the effect of stroke could be accounted for (23).

Although cerebrovascular disease is also a component of cardiovascular disease it was not addressed here. Our proposed *integrated CHD/Covid-19 model* is therefore based primarily on CHD attributes, with focus on vascular complications induced by the SARS-CoV-2 virus. We acknowledge that other pathogenic pathways may exist such as the cerebrovascular ones (35), which should warrant further research in an extended model.

The CHD model presented in **Figure 1**, was developed by analyzing the effect of different *health factors* (blue ovals) on *body tissues* (pink boxes) and investigating the respective *pathogenesis* (gray lines with numbers), *traits* (orange boxes) and activated *biomarkers* (white boxes) related to an increased risk of CHD (23–28).

Each gray line and respective number in the CHD model correspond to a certain pathogenesis pathway that could typically be present in a CHD patient. These pathways are visual representations of previously published literature, which link the effects of *health factors* (blue ovals) to the relevant *tissues* (pink boxes) and subsequently to the hallmarks of CHD (yellow boxes) (23–28).

The traits are represented in the lightly shaded orange boxes. Biomarkers are indicated as white boxes, with those that are typically measured, denoted with red tags (). The *pharmaceutical interventions*, acting on the respective pathways are indicated as blue boxes, where blunted blue arrows () denote antagonize or inhibit and pointed blue arrows () denote up-regulate or facilitate (23–28).

Systems-Based Integration of Covid-19 Factors Into the CHD Model

The systems-based integration methodology dicussed here is depicted as three phases in a flow chart in **Figure 2**. The iterative approach followed here is to ensure that only pathways discussed in literature, with substantial evidence, are included. We will use **Figure 3** to show the Covid-19 pathways in green, with all other pathways from the original model in **Figure 1** made transparent.

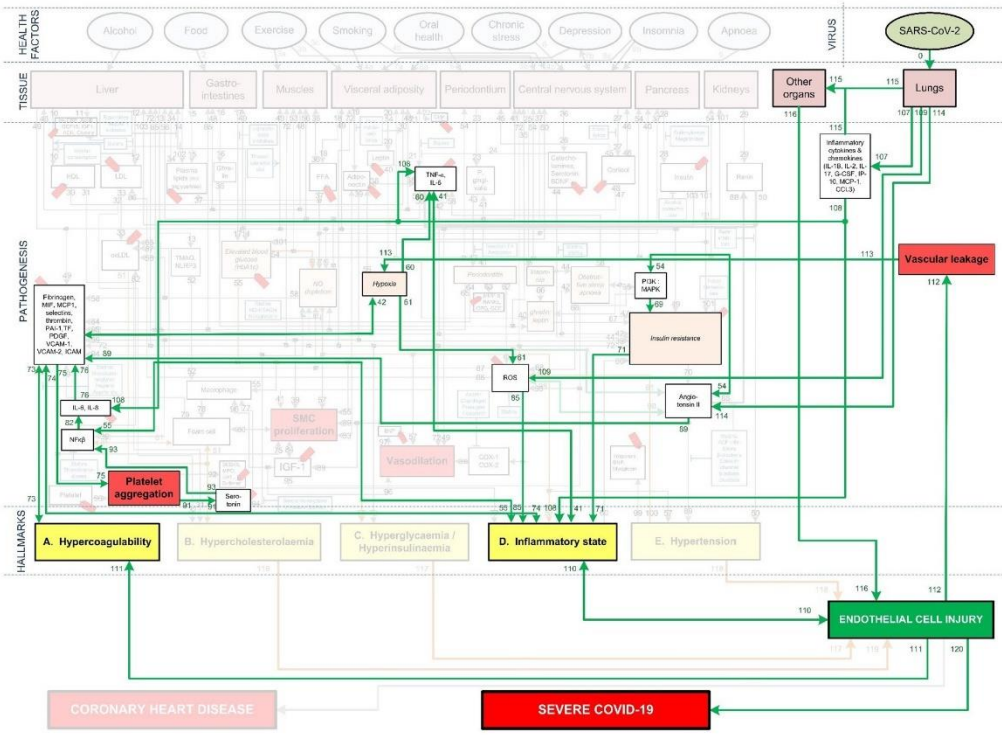

FIGURE 3 | Integration of Covid-19 pathogenic pathways into the pathways of CHD.

Phase 1: SARS-CoV-2 and CHD

SARS-CoV-2, which causes Covid-19, was incorporated into the existing CHD model by investigating pathogenic pathways and biomarkers reported in literature. These biomarkers and pathways were either included or excluded based on the following five steps, presented in **Figure 2** (Phase 1).

Step (1): Firstly, the relevant tissue (denoted as pink boxes in the right-hand corner of **Figure 3**) through which the SARS-CoV-2 virus (green oval in **Figure 3**) enters the body was evaluated. Although EC injury was discussed as the critical element in CHD in (23), it was not shown in **Figure 1**. Here we added EC injury as a green box between pathways 110, 111, 112, and 116 at the bottom of **Figure 3**.

Step (2): The activated CHD related biomarkers, traits or hallmarks, reported in severe Covid-19 patients were then identified from literature. These are, respectively, denoted as white, orange and yellow boxes in **Figure 3**.

Step (3): In this step we evaluated the identified CHD biomarkers, traits or hallmarks found in literature, in order to determine whether the activation of these occurs directly or indirectly as a result of the SARS-CoV-2 virus. Steps (4) and (5) describe the two possible outcomes of the identification process.

Step (4): If the activation occurs directly, as determined in step (3), then a new (green) pathway that led from the virus to the respective CHD biomarker, trait or hallmark was added to the integrated model as shown in **Figure 3**.

Step (5): If the activation occurs indirectly, as determined in step (3), then a new biomarker or trait was added to the model e.g., the inflammatory cytokines in the top, right-hand white box between pathways 107, 108, and 115 in **Figure 3**. A biomarker or trait was only added if its respective pathway eventually led to the activation of a CHD hallmark.

Phase 2: Iteration

For the iteration process in Phase 2, the following steps were conducted:

Step (6): The activated component (CHD hallmark, biomarker or trait) from step (4) to which the green pathway from step (4) leads was further evaluated based on literature. If this component is a biomarker or trait then step (7) was

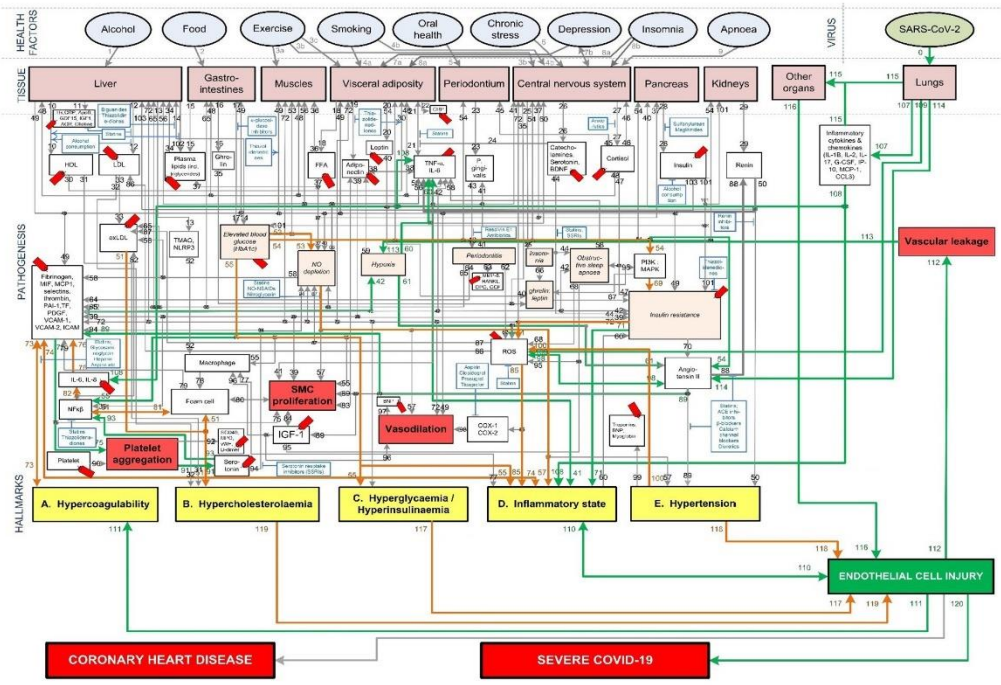

FIGURE 4 | Proposed integrated Covid-19/CHD model.

followed. If this component is rather a CHD hallmark, then step (12) was followed.

Step (7): In this step it was determined whether the CHD biomarker or trait has any outgoing (gray) CHD pathways. Most biomarkers and traits have outgoing CHD pathways. These gray CHD pathways were further assessed in Step (8). For the biomarkers and traits with no outgoing gray pathways (e.g., troponin for pathway 99 in **Figure 3**) step (11) was followed.

Step (8): In this step it was determined whether the gray CHD pathway leads directly or indirectly to a CHD hallmark (yellow boxes in **Figure 3**). If the gray CHD pathway leads directly to a CHD hallmark then step (9) was followed, otherwise step (10) was followed.

Step (9): The CHD hallmark was further investigated to ensure its activation due to SARS-CoV-2 was relevant to severe Covid-19 patients. If it was reported in literature to be aggravated in severe Covid-19 patients then step (12) was followed (changing the gray pathway to a green pathway) otherwise step (11) was followed (keeping the pathway gray). These steps are explained in more detail in phase 3.

Step (10): As determined in step (8), the relevance to Covid-19 severity of the subsequent CHD biomarker or trait to which the gray CHD pathway led to was investigated. If relevance was found, then this CHD biomarker or trait was re-evaluated by following the same approach as in step (7).

Phase 3: Outcome

This phase presents the two outcomes that were reached after integration and iteration of the identified biomarkers, traits, CHD hallmarks and their relevant pathways.

Step (11): This step was followed if the activated CHD biomarkers or traits had, (i) no other outgoing CHD pathway or (ii) the outgoing pathway led to another biomarker or trait that had no relevance to severe Covid-19 patients. If one of these two conditions were met then the biomarker, trait and the subsequent pathway was not evaluated further.

These biomarkers, traits and respective pathways e.g., oxidized low-density lipoprotein (oxLDL), nitric oxide (NO) depletion and cortisol were made transparent, as shown in **Figure 3**. Although these biomarkers or traits do not have a direct link to Covid-19 patients, they may influence Covid-19 severity indirectly by affecting one of the CHD hallmarks. This idea is discussed in more detail in section Covid-19 Aggravation in Patients With Pre-existing CHD Comorbidities.

Step (12): Step (12) was followed if the investigated biomarker, trait, CHD hallmark and respective pathways were relevant

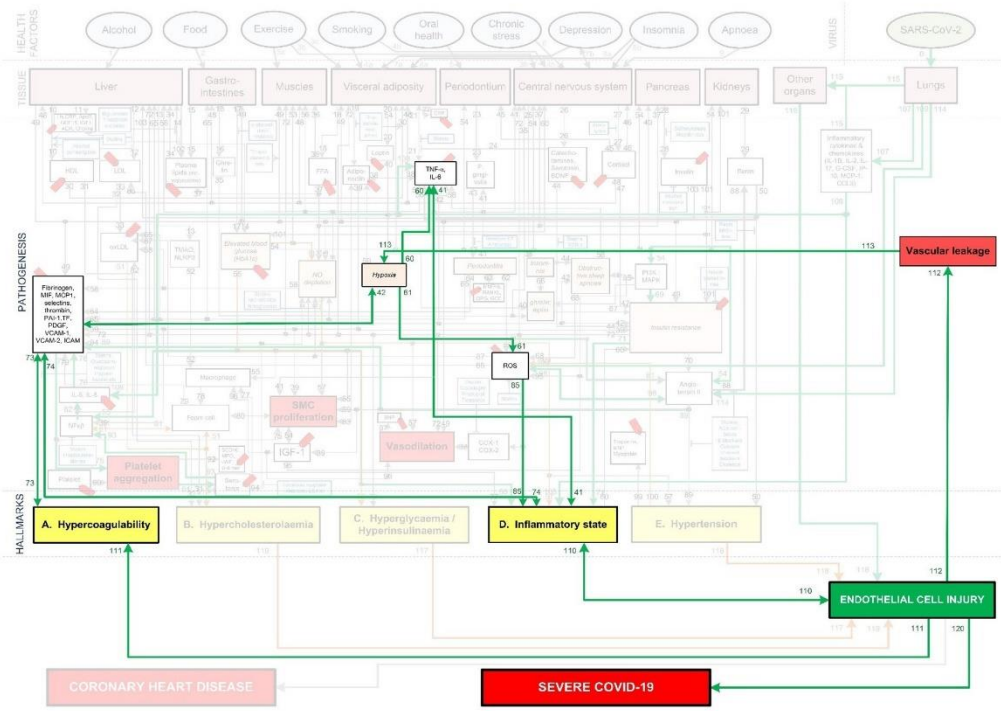

FIGURE 5 | *Death spiral* evident in some critical Covid-19 patients.

in most Covid-19 patients with severe disease and these are therefore prominently shown as green lines in **Figure 3**.

The Covid-19 pathways were described in this section and shown as green lines in **Figure 3**. The final step is to show all the CHD pathways together with the Covid-19 pathways. The complete *integrated CHD/Covid-19 model* is given in **Figure 4**.

Evaluation of *Health Factors* and *Pharmaceutical Interventions*

The mechanisms of interaction between CHD and Covid-19 (**Figure 4**) can help to compare the few factors a patient can control namely, *health factors* (before infection with SARS-CoV-2) and *pharmaceutical interventions* (after infection). Only the *health factors* and *pharmaceutical interventions* investigated in (23) for CHD risk are investigated here for Covid-19.

The *health factors* (blue ovals) in **Figure 4** were defined as the following (23):

- Alcohol use: Indicates moderate alcohol consumption (20–30 g alcohol (ethanol) per day for men and half of that for women).
- Food: High glycemic diets (HGD) (glycemic load > 142).
- Exercise: Regular moderate exercise (550–3,000 kcal/week).
- Smoking: Current smoker.
- Oral Health: oor oral health in the form of periodontal disease.
- Stress: Chronic-level stress at work or home.
- Depression: Self-diagnosed, physician diagnosed or use of antidepressant medication.
- Insomnia: Inability to fall asleep or to maintain sleep or the perception of disturbed sleep.
- Apnoea: Obstructive sleep apnoea or hypopnoea (apnoea-hypopnea index>5/h).

We will discuss in Results section Effects of Different *Health Factors* on Covid-19 Severity to what extent a healthy vascular "baseline," as a result of a healthy lifestyle, will influence Covid-19 severity.

The *pharmaceutical interventions* that were investigated were limited to those investigated in the original CHD model (23). These include statins, salicylates (aspirin), indirect thrombin inhibitors (heparin), direct thrombin inhibitors (angiomax), Angiotensin-Converting-Enzyme (ACE) inhibitors, angiotensin-renin inhibitors, β-blockers, calcium channel blockers, diuretics,

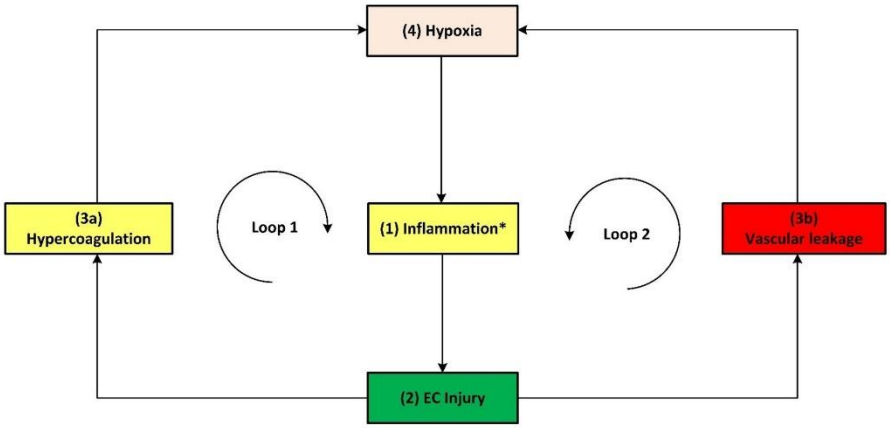

FIGURE 6 | Simplified schematic of the *death spiral* evident in some critical Covid-19 patients. The *death spiral* can be summarized as follows: Increased (1) inflammation at the lungs causes (2) EC injury, which can result in activation of the (3a) coagulation cascade and/or (3b) vascular leakage at the lungs, thereby causing (4) hypoxia which further increases inflammation, creating two closed positive feedback loops and causing severe Covid-19 through a *death spiral*. *As described in the text, this inflammation is initiated by various factors, primarily by a hyperimmune response to infection of SARS-CoV-2 (cytokine storm) but also other factors such as hyperinsulinaemia/hyperglycaemia or hypercholesterolaemia.

biguanides (metformin) and antidepressants. They are indicated in **Figure 1** as blue boxes, where blunted blue arrows (⊣) denote antagonize or inhibit and pointed blue arrows (⇐) denote up-regulate or facilitate.

Although larger studies of how the *health factors* and *pharmaceutical interventions* influence a person's risk for CHD are usually available, Covid-19 data are often limited. Nevertheless, several studies exist that evaluated the effect of many *health factors* and *pharmaceutical interventions* on Covid-19 severity. Limitations of these studies are that they vary in study size and design i.e., some studies are case-control studies hence only reporting odds ratio (OR), whereas others are cohort studies or clinical trials that report on relative risks (RR) or hazard ratios (HR).

Unfortunately, RR, HR and OR are not the same and should only be compared in cases where the event being assessed is rare in the control group. In other words, the baseline risk of the control group should approximately be zero. However, at present it is the best information we have. Until better data becomes available, these studies were used as an initial indicative comparison between the effect what *health factors* and *pharmaceutical interventions* have on CHD risk and Covid-19 severity. This also applies to the data used to compare the risk between coagulation and Covid-19 severity in section The Death Spiral: Inflammation, EC Injury, Coagulation, Vascular Leakage and Hypoxia.

In this paper the comparison of the data between CHD risk and Covid-19 severity was graphically reported using a non-traditional method (23–28). The risks that indicate an increase in disease severity are displayed as reported, whereas the risk values that show a decrease in severity are presented as the inverse of the reported value.

This method presents a better visual illustration when comparing an increase and decreased risk. For example, a conventional RR = 3 constitutes to a 3-fold increase in risk while a RR = 0.33 constitutes to a 3-fold decrease in risk (1/0.33 = 3). The method has also been used in previous papers (24–28).

RESULTS

Section Integrated Covid-19/CHD Model discusses **Figures 3**, **5**, **6** in detail illustrating the detrimental interplay between inflammation, EC injury, coagulation and hypoxia. This visually explains the *death spiral* seen in some Covid-19 patients.

Section Covid-19 Aggravation in Patients With Pre-existing CHD Comorbidities discusses how each pre-existing CHD comorbidity/hallmark could further aggravate this *death spiral*. *Five* figures are provided (**Figures 5**, **6**, **8–10**). These figures illustrate how patients with pre-existing *Hypercholesterolemia* (**Figure 8**), *Hyperglycemia/Hyperinsulinemia* (**Figure 9**) or *Hypertension* (**Figure 10**) could aggravate this *death spiral*. Note that **Figures 3**, **5**, **6**, **8–10** are simplified versions of **Figure 4** (the fully *integrated CHD/Covid-19 model*). Only the prominent pathways, which are needed to explain a specific phenomenon, are shown in these Figures.

In sections Effects of Different *Health Factors* on Covid-19 Severity and Effects of Different CHD *Pharmaceutical Interventions* on Covid-19 Severity the effects that *health factors*

and *pharmaceutical interventions* have on developing severe Covid-19 are discussed with reference to the model in **Figure 4**.

Integrated Covid-19/CHD Model

EC Injury From SARS-CoV-2 Viral Infection

Cell entry and pathologic effects of the SARS-CoV-2 virus mostly occur through two pathways namely, (i) the mucous membranes (primarily infecting the nasal epithelia) or (ii) the respiratory tract (infecting respiratory epithelial cells) (36). This infection typically occurs *via* ACE2 (36), which partially decreases ACE2 function. This leads to an upregulation of angiotensin II effects, including among others an enhanced *Inflammatory* response (17, 36), increased EC injury (37) and state of *Hypercoagulability* seen in severe Covid-19 patients (4, 6–9).

These effects are illustrated in **Figure 3** by following the relevant pathways (green lines with numbers) from SARS-CoV-2 (green oval) to the respective biomarkers (white boxes) or traits (orange boxes) and/or hallmarks (yellow boxes). The model will be interpreted in the following way for the rest of this paper:

a) Evidence from literature describing the pathogenesis with the respective (references).
b) These relevant pathways in **Figures 3**–**6**, **8**, **9** are then given to illustrate the pathogenesis. Each pathway starts with the relevant tissue, biomarker or trait.
c) The relevant pathway (pw) numbers (#) are denoted as (pw#) e.g., pathway 112 (pw112) links EC injury with vascular leakage.
d) The upwards arrow (↑) represents an upregulation of the respective biomarker/trait/hallmark while the downwards arrow (↓) represents a downregulation.

Figure 3 illustrates how viral infection from SARS-CoV-2 may lead to an activation of a pro-inflammatory state, which causes EC injury *via* the following process:

- Angiotensin II can downregulate phosphoinositide 3-kinase (PI3K) pathway, which increases insulin resistance that directly effects inflammatory state (38). The relevant pathways in **Figure 3** are: SARS-CoV-2 viral infection within the lungs *via* (pw0), which through (pw114) upregulates angiotensin II. This follows a downregulation of biomarker PI3K *via* (pw54) that increases insulin resistance through (pw69). This leads to a pro-inflammatory state *via* (pw71), which, through (pw110), results in EC injury. The notation for this pathway and the rest of the paper will be as follows: *SARS-CoV-2-(pw0)-Lungs-(pw114)-↑angiotensin II-(pw54)-↓PI3K-(pw69)-↑insulin resistance-(pw71)-↑inflammatory state-(pw110)-↑EC injury.*
- Angiotensin II can also upregulate various reactive oxygen species (ROS) at the site of infection, which causes a heightened inflammatory response (38). See **Figure 3** pathways: *SARS-CoV-2-(pw0)-Lungs-(pw114)-↑angiotensin II-(pw98)-↑ROS-(pw85)-↑inflammatory state-(pw110)-↑EC injury.*
- An upregulation of angiotensin II may increase platelet factors, which increases the risk for coagulability (38, 39). Since hypercoagulation and inflammation are interrelated, an inflammatory state may be enhanced (39). See **Figure 3** pathways: *SARS-CoV-2-(pw0)-Lungs-(pw114)-↑angiotensin II-(pw89)-↑platelet factors-(pw73)-↑Hypercoagulability-(pw73)-(pw74)-↑inflammatory state-(pw110)-↑EC injury.*
- Furthermore, an increase in platelet factors can also upregulate platelet aggregation (38). This could increase the inflammatory mediator nuclear factor-kappa-beta (NFκβ), aggregating inflammation (38). See **Figure 3** pathways: *SARS-CoV-2-(pw0)-Lungs-(pw114)-↑angiotensin II-(pw89)-↑platelet factors-(pw75)-↑platelet aggregation-(pw91)-serotonin-(pw93)-↑NFkβ-(pw55)-↑inflammatory state-(pw110)-↑EC injury.*

In addition to this pro-inflammatory state that causes EC injury, the virus can also directly cause EC injury in other organs. This could happen if the virus enters the bloodstream and binds to ACE2 receptors located in other organs (9). Considerable evidence shows that the lungs of patients who died from Covid-19, have severe EC injury (endothelialitis) associated with the presence of intracellular viral infection (4). The presence of viral particles were also found in the ECs of the liver, kidneys and heart (9, 40). This could then lead to inflammation and EC damage at the infected organ. See **Figure 3** pathways: *SARS-CoV-2-(pw0)-Lungs-(pw115)-infect other organs via blood-(pw116)-↑EC injury.*

EC Injury From a Hyperimmune Response to Infection

Infection from SARS-CoV-2 causes damage-associated molecular patterns to occur, which can trigger a hyperimmune response. Most severe cases of patients with Covid-19 display a defective hyperinflammatory state with significantly increased serum levels of pro-inflammatory cytokines and chemokines (41–44).

This overproduction of pro-inflammatory cytokines and chemokines can damage lung infrastructure and further induce EC injury of pulmonary blood vessels (17, 20, 45), see **Figure 3** pathways: *SARS-CoV-2-(pw0)-Lungs-(pw107)-↑pro-inflammatory cytokines & chemokines-(pw108)-↑inflammatory state-(pw110)-↑EC injury.*

Most critical cases show increased levels of, among others, the pro-inflammatory cytokines interleukin-6 (IL-6), interleukin-8 (IL-8) and tumor necrosis factor-α (TNF-α) (41–43). These pro-inflammatory cytokines directly cause an upregulation of inflammation (45). See **Figure 3** pathways: *SARS-CoV-2-(pw0)-Lungs-(pw107)-↑pro-inflammatory cytokines-(pw108)-↑TNF-α, IL-6-(pw41)-↑inflammatory state-(pw110)-↑EC injury.*

These cytokines can also indirectly upregulate inflammation through dysregulation of platelet factors (46). See **Figure 3** pathways: *SARS-CoV-2-(pw0)-Lungs-(pw107)-↑pro-inflammatory cytokines-(pw108)-↑IL-6, IL-8-(pw76)-↑platelet factors-(pw74)-↑inflammatory state-(pw110)-↑EC injury.*

Furthermore, a hyperinflammatory state induced by an unmodulated immune response can also cause EC injury. This happens when neutrophils activate pathways that elevate reactive oxygen species (ROS) (22, 47). See **Figure 3** pathways: *SARS-CoV-2-(pw0)-Lungs-(pw109)-↑ROS-(pw85)-↑inflammatory state-(pw110)-↑EC injury.*

A hyperinflammatory response of cytokines can circulate to other organs. This could lead to acute inflammation such as

septic shock and/or multiple organ damage, which may further cause EC injury (48). See **Figure 3** pathways: *SARS-CoV-2-(pw0)-Lungs-(pw107)-pro-inflammatory cytokines & chemokines-(pw115)-other organs-(pw116)-↑EC injury.*

The Death Spiral: Inflammation, EC Injury, Coagulation, Vascular Leakage and Hypoxia

Note that *hypoxia* shown in **Figures 1**, **3**–**6** includes hypoxemia. Although hypoxia might be respiratory related, vascular related EC injury could be one of the main factors fueling this hypoxia (45, 49, 50). This vascular related hypoxia may result from either hypercoagulation or vascular leakage, both stemming from EC injury (17, 22, 45, 46, 49, 50).

Vascular leakage from EC injury leads to an increase in leucocytes and platelets as well as vascular permeability (50). This results in fluid from the blood to enter the alveoli, filling the alveolar space. In turn it decreases the efficiency of gas exchange in the lungs (50). This prevents the body from taking in sufficient oxygen, leading to different severity levels of hypoxia (50). These pathways are denoted in **Figure 5** as: *EC injury-(pw112)-↑vascular leakage-(pw113)-↑hypoxia.*

On the other hand, coagulation stemming from EC injury articulates glycoproteins that are involved in hemostasis, to which platelets bind. This consequently upregulates the expression of platelet tissue factors, which are the prime activators of a coagulation cascade (22, 51). This leads to a high possibility of disseminated intravascular coagulation, congestion of the small capillaries by inflammatory cells and thrombosis in larger vessels (45).

Congestion or clogging of pulmonary blood vessels could increase hypoxemia *via* ventilation/perfusion mismatch and low level of mixed venous blood oxygen (49). This build-up of blood clots in blood vessels within the lungs are commonly found in critically ill and non-surviving Covid-19 patients (6, 21, 52). These pathways are denoted in **Figure 5** as: *EC injury-(pw111)-↑Hypercoagulability-(pw73)-↑platelet factors-(pw42)-↑hypoxia.* Hypoxia also results in further upregulation of inflammation by activating IL-6 & TNF-α (53) or increasing ROS leading to further EC injury (54). See **Figure 5** pathways: *Hypoxia-(pw60)-↑TNF-α, IL-6-(pw41)-↑inflammatory state* or *Hypoxia-(pw61)-↑ROS-(pw85)-↑inflammatory state-(pw110)- EC injury.*

With the aforementioned knowledge a summary of the main pathogeneses describing the *death spiral* are given. Note that inflammation has two different outgoing pathways (loops) that can lead to increased hypoxia. Both pathways are denoted in **Figure 5** as follows:

1. **Hypercoagulability (positive feedback loop 1):** Inflammation from Covid-19 results in EC injury which may activate the coagulation cascade, forming microthrombi in the blood vessels near the alveoli (4, 6–9). This reduces oxygenation efficiency, see pathways: *↑inflammatory state –(pw110)-EC injury-(pw111)-↑Hypercoagulability-(pw73)-↑platelet factors-(pw42)-↑hypoxia-(pw60)-↑TNF-α, IL-6-(pw41) AND/OR (pw61)-↑ROS-(pw85)-↑inflammatory state-(pw110)-Loop repeated-(pw120)-Severe Covid-19.*
2. **Vascular leakage (positive feedback loop 2):** Inflammation from Covid-19 results in EC injury. EC injury in blood vessels near the alveoli can lead to vascular leakage (22). This causes fluid build-up within the alveoli (50), subsequently reducing oxygenation efficiency, see pathways: *↑inflammatory state –(pw110)-EC injury-(pw112)-↑vascular leakage-(pw113)-↑hypoxia-(pw60)-↑TNF-α, IL-6-(pw41) AND/OR (pw61)-↑ROS-(pw85)-↑inflammatory state-(pw110)-Loop repeated-(pw120)-Severe Covid-19.*

A simplified schematic of the *death spiral* is illustrated in **Figure 6**, which shows the two closed positive feedback loops leading to hypoxia. If a Covid-19 patient becomes hypoxic, it is important to break these loops by administering supplemental oxygen. This is currently done in practice where supplemental oxygen reduces disease severity in hypoxic Covid-19 patients (55).

To reduce the risk of developing hypoxia one should focus on reducing inflammation that leads to the downstream effects namely EC injury, coagulation and vascular leakage. This is also seen in practice where various pharmaceutical interventions that treat inflammation have shown promising results e.g., corticosteroid dexamethasone in later stage of illness (56) and anti-inflammatory drugs [Celebrex (57) and aspirin (58)].

If we focus on loop 1 it is expected that people who have a higher risk of developing blood clots (coagulation) should have a higher risk of developing severe Covid-19. There are several uncontrollable factors that are known to increase a person's risk of developing blood clots namely, gender, age, ethnicity, blood type and pregnancy.

Although this does not help the patient, it is of interest to help understand Covid-19 severity in these individuals. The data for the risk of coagulation (blood clots) and Covid-19 severity for these individuals are given in **Table 1**. A qualitative graphical comparison between the data for coagulation and Covid-19 severity from **Table 1** is given in **Figure 7**.

Age

Age is an independent risk factor of coagulation, with thrombotic incidences increasing rapidly in people older than 70 years (59). The odds of venous thromboembolism in a person older than 70 years is three times higher than a person young than 70 years, OR of 3.1 (59).

If we investigate Covid-19 mortality data, a similar trend is seen with age. Risk of mortality due to Covid-19 is much higher in older patients with a RR of 3.61 in patients older than 70 years (60), see **Figure 7**. The increased risk of coagulation due to older age could be one reason for this increased Covid-19 mortality.

Gender

A 25-year population-based study showed that males have a higher risk to coagulate than females (68). At younger ages (<45 years) females have a higher risk of coagulation than males, for various reproductive reasons (61). However, since an increase in Covid-19 severity and mortality is typically seen in older patients (> 45 years) we only focused on these older patients. Men have a 1.9-fold higher risk of developing venous thrombosis than women (61).

TABLE 1 | Data for the qualitative comparison of risk factors between coagulation and Covid-19 severity.

Uncontrollable factor	Risk for coagulation					Risk of covid-19 severity				
	Study size (n = no. of participants, N = no. of studies)	RR/OR	Value	95% CI	References	Study size (n = no. of participants, N = no. of studies)	RR/OR	Value	95% CI	References
Age > 70 years	$n = 607$, $N = 1$	OR	3.10	1.3–7.5	(59)	$n = 36\,470$, $N = 59$	RR	3.61	2.70–4.84	(60)
Male vs. Female	$n = 11\,253$, $N = 1$	RR	1.90	1.9–2.4	(61)	$n = 36\,470$, $N = 59$	RR	1.50	1.18–1.91	(60)
Black vs. Caucasian	#	RR	1.50	#	(62)	$n = 505\,992$, $N = 1$	OR	1.60	1.2–2.0	(63)
Blood Type A vs. Type O	$n = 406\,755$, $N = 1$	HR	1.44	1.39–1.50	(64)	$n = 31\,100$, $N = 4$	OR	1.41	*	(65)
Blood Type B vs. Type O	$n = 406\,755$, $N = 1$	HR	1.45	1.37–1.54	(64)	$n = 31\,100$, $N = 4$	OR	1.69	*	(65)
Pregnant vs. Non-pregnant	$n = 1\,142$, $N = 1$	OR	4.60	2.7–7.8	(66)	$n = 22\,493$, $N = 1$	OR	2.35	1.48–3.74	(67)

1. CI, Confidence Interval; HR, Hazard Ratio; OR, Odds Ratio; RR, Relative Risk.
2. (#) Denotes that the study did not provide this data.
3. (*) Study (65) only provides the 95% CI for each Blood Type separately and not the Blood Type vs. Blood Type O. These individual 95% CI's for Blood Type A, B, and O were (1.11–1.40), (0.99–1.21), and (0.63–0.77), respectively. These data were not included in the table since the OR's for each Blood Type were reported separately. Here we normalized the OR's of Blood Type A vs. O and Blood Type B vs. O.

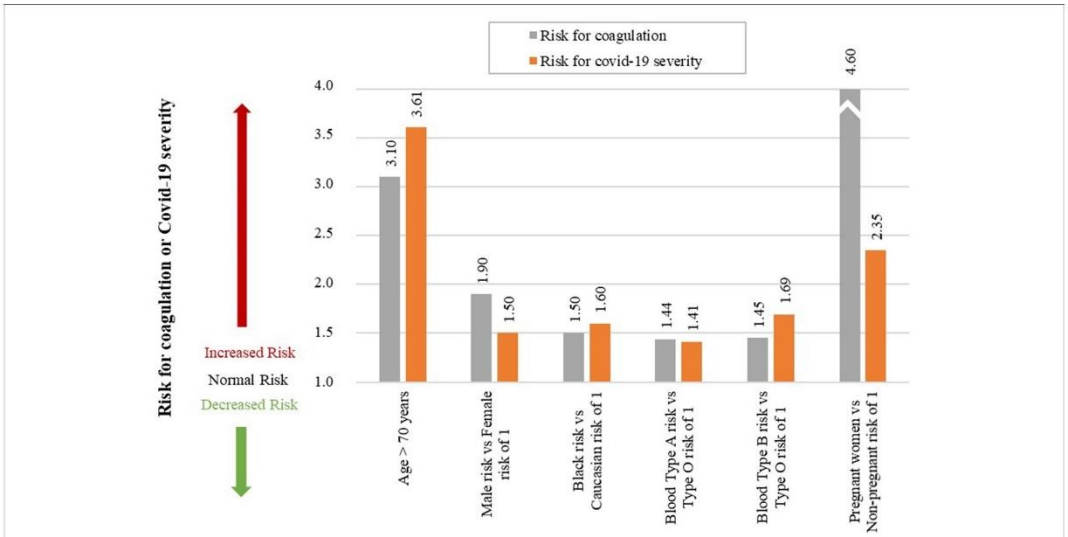

FIGURE 7 | Qualitative comparison of risk factors between coagulation and Covid-19 severity. (An accurate quantitative comparison is not possible, mostly due to differences in study design and size).

Covid-19 data also indicate that males have a higher risk of Covid-19 mortality than females, with a RR of 1.50 (60), see **Figure 7**. The increased risk of coagulation due to gender for individuals older than 45 years could be one reason for this increased Covid-19 mortality.

Ethnicity

Ethnicity has also shown to be an independent risk factor for coagulation. The highest risk of thrombosis being in African Americans, with a RR of 1.5 compared to Europeans (62). This is also seen in Covid-19 mortality data, which shows that African American's have a higher odds of death than Europeans, with an OR of 1.6 (63), see **Figure 7**. The increased risk of coagulation due to ethnicity could be one reason for this increased Covid-19 mortality.

Blood Type

Another risk factor that seems to influence the odds of developing a thromboembolic event is a person's blood type. A single cohort study showed that blood types A&B vs. O have higher risk of developing a thromboembolic event, with the following HRs: A vs. O of 1.44, and B vs. O of 1.45 (64), see **Figure 7**.

A similar trend is seen in the effect of different blood types on Covid-19 severity, with the following ORs: A of 1.06, B of 1.27, O of 0.75 (65). If these values are normalized with respect to blood type O the ORs are the following: A vs. O of 1.41, and B vs. O of 1.69, see **Figure 7**.

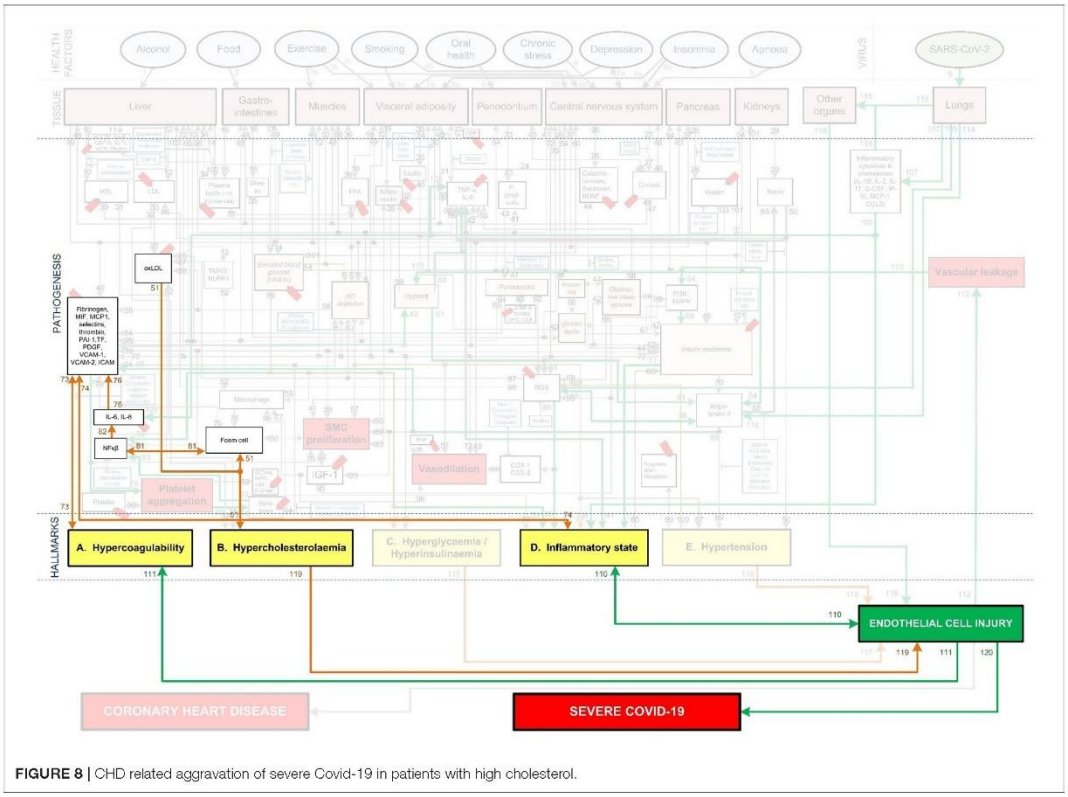

FIGURE 8 | CHD related aggravation of severe Covid-19 in patients with high cholesterol.

None of the blood group values for Covid-19 severity were statistically significant (65). It is however interesting that this limited study shows that patients with blood type O have lower odds of developing severe Covid-19 than blood types A and B. There is however still controversy regarding correlation between blood type and Covid-19 severity (69).

Pregnancy

Pregnancy is not necessarily an uncontrollable factor, but for the duration of being pregnant it is. During pregnancy the risk of venous thrombosis is much higher than for non-pregnant women, with an OR of 4.6 (66), see **Figure 7**.

Pregnant women are also at a higher risk of developing more severe Covid-19 complications than non-pregnant women, with an OR of 2.35 (67). Fortunately, no significant association between pregnant and non-pregnant women was found for Covid-19 mortality risk (67). This may be due to pregnant women seeking medical attention earlier than non-pregnant women. The higher severity risk could partially be due to the higher risk for coagulation during pregnancy. More research is however needed to validate this.

The above mentioned uncontrollable factors may contribute to the coagulation loop 1 of the *death spiral*. This could help explain why some patients experience accelerated disease severity. However, better studies for Covid-19 in especially different blood groups are needed.

The high mortality statistics in patients with pre-existing CHD comorbidities (10–12, 70) are discussed in more detail in the next Section with reference to **Figures 8–10**. We will show why a patient with a worse cardiovascular "baseline" before Covid-19 could potentially have a worse outcome than a patient with a healthy cardiovascular "baseline."

Covid-19 Aggravation in Patients With Pre-existing CHD Comorbidities

Severe Covid-19 Patients With Existing Chronic Hypercholesterolemia

One of the risk factors for CHD is *Hypercholesterolemia*. Chronic *Hypercholesterolemia* may fuel the Covid-19 *death spiral* by increasing the risk of EC injury *via* an inflammatory state or plaque buildup. For EC injury induced by an inflammatory state see **Figure 8** pathways: *↑oxLDL-(pw51)-Hypercholesterolemia-(pw51)-↑foam cell-(pw81)-↑NFkβ-(pw82)-↑IL-6, IL-8-(pw76)-↑platelet factors-(pw74)-↑inflammatory state-(pw110)-↑EC injury*. For EC injury induced by

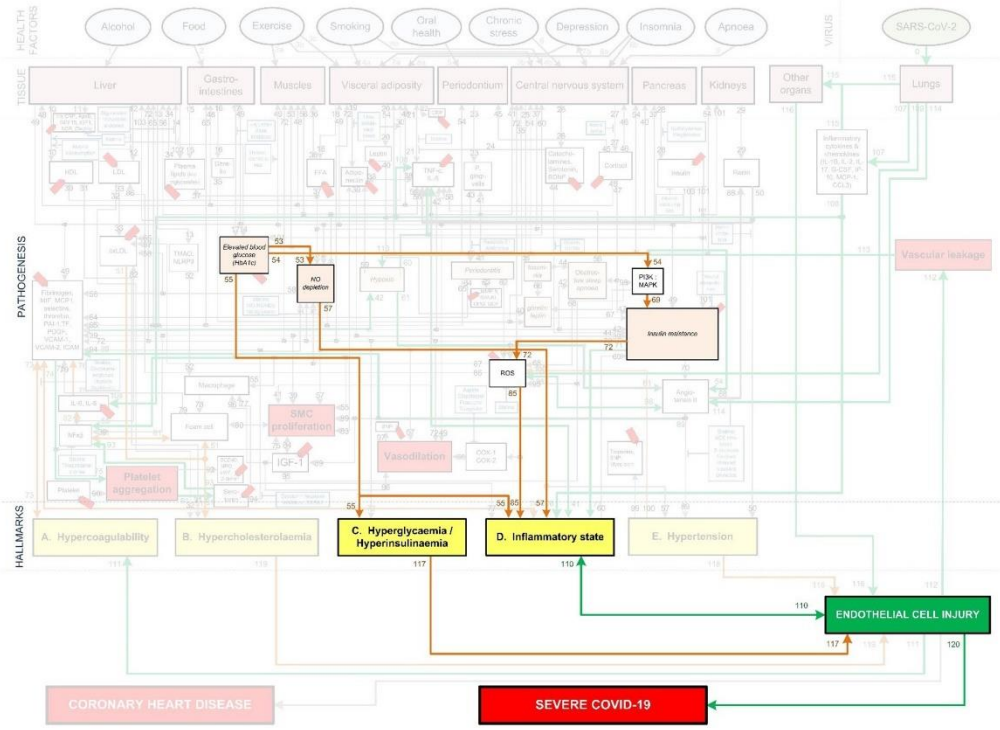

FIGURE 9 | CHD related aggravation of severe Covid-19 in patients with high blood glucose levels.

plaque buildup see **Figure 8** pathways: *↑oxLDL-(pw51)-Hypercholesterolemia-(pw119)-↑EC injury.*

Hypercholesterolemia could also have an impact on the severity of Covid-19 by increasing coagulation. This could happen by increased foam cell production and increased thrombin generation (29). In turn increasing the platelet forming factors and reducing breakdown processes like fibrinolysis, increases coagulation (30). See **Figure 8** pathways: *↑oxLDL-(pw51)-Hypercholesterolemia-(pw51)-↑foam cell-(pw81)-↑NFkβ-(pw82)-↑IL-6, IL-8-(pw76)-↑platelet factors-(pw73)-↑Hypercoagulability.*

The increased coagulation could aggravate thrombi within the lungs and lead to possible hypoxemia (49), potentially cascading the symptoms already experienced by a Covid-19 patient.

The above discussion partially explains why many patients with obesity have a high risk of developing severe Covid-19 complications (71) as obesity is associated with *Hypercholesterolemia* (72, 73).

Interestingly it was also found that free cholesterol, as well as high-and low-density lipoprotein levels are lower in end-stage Covid-19 patients than in patients with less severe Covid-19 (70, 74). Why would cholesterol levels be lower in patients with more severe disease? Could this be explained by the ability of SARS-CoV-2 to use ("consume") serum cholesterol for its entry into host cells (32).

If this is the case, then high cholesterol levels before infection might enhance viral infection *via* increased availability of serum cholesterol levels but as the virus "consumes" cholesterol the levels would decrease. These facts are however still controversial and further studies are warranted.

Severe Covid-19 Patients With Existing Chronic Hyperglycemia or Hyperinsulinemia

Elevated blood glucose aggravates Covid-19 severity and mortality risk irrespective of diabetes (75, 76). One possible reason for this could be the indirect ability of blood glucose to induce EC injury.

Since glucose is the main energy source for cells, any change to its levels could have a direct effect on the cell's metabolism. Changes in blood glucose can cause ECs to undergo apoptosis (cell death or "suicide"), causing the ECs to detach and enter the bloodstream (77). See **Figure 9** pathways:

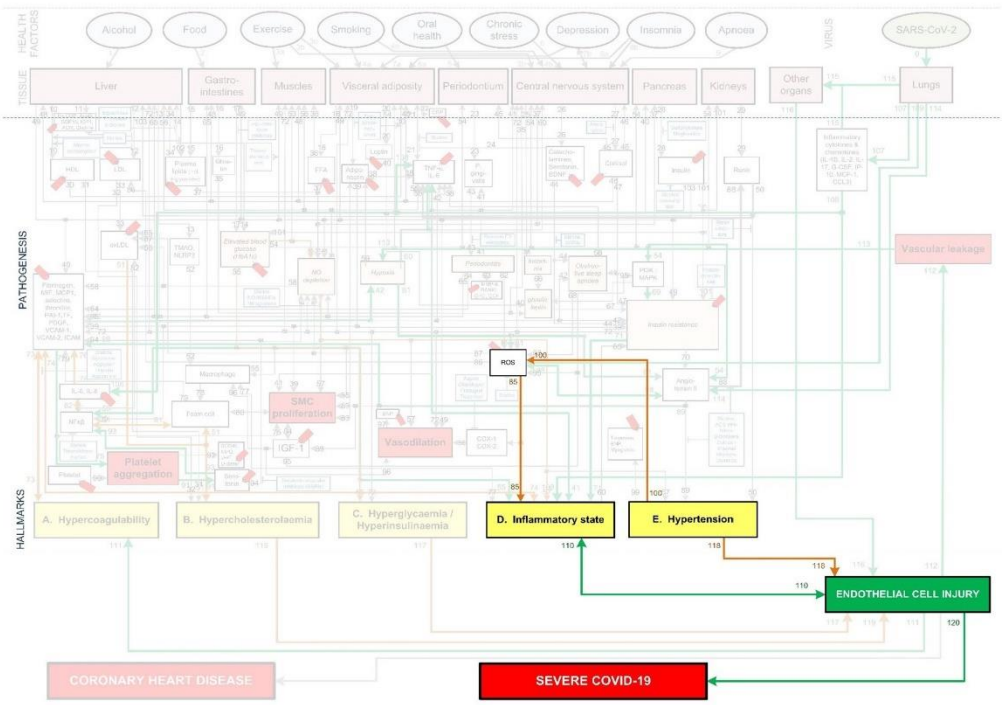

FIGURE 10 | CHD related aggravation of severe Covid-19 in patients with chronic hypertension.

Elevated blood glucose (HbA1c)-(pw55)-Hyperglycemia-(pw117)-↑EC injury. This further leaves behind eroded arteries which activate processes that lead to atherosclerosis, such as smooth cell proliferation (77).

Another pathway through which elevated blood glucose levels contribute to EC injury is through aggravated inflammation. This inflammation is caused by activating the insulin resistance and ROS producing pathways and impaired EC turnover. See **Figure 9** pathways: *Elevated blood glucose (HbA1c)-(pw54)-PI3K:MAPK-(pw69)-↑Insulin resistance-(pw72)-↑ROS-(pw85)-↑inflammatory state-(pw110)-↑EC injury*. EC turnover is possibly impaired due to accelerated aging or reduced renewal of cells (78, 79). This is most prominent in the microvascular and arterial ECs (80), which may be due to the differences in glucose uptake of cells.

A similar pathway also leads to increased inflammation due to a dysregulation of NO, which plays an important role in controlling the vascular tone and arterial pressure. A decrease in NO prevents ECs from responding to increased glucose stress, which may further accelerate cellular deterioration (79). See **Figure 9** pathways: *Elevated blood glucose (HbA1c)-(pw55)-Hyperglycemia-(pw55)-↑inflammatory state-(pw110)-EC injury*.

These indirect impacts on EC injury could potentially explain why *Hyperglycemia* is a significant co-morbidity and risk factor for severe Covid-19 patients (70). It highlights the importance of ensuring that the glucose level of a diabetic patient remains within normal ranges. It may also be advantageous to reduce blood glucose levels in non-diabetic patients as elevated glucose in non-diabetic patients also increased Covid-19 severity (75, 76).

Severe Covid-19 Patients With Existing Chronic Hypertension

Hypertension is another common co-morbidity in Covid-19 related mortality (81). This could be due to its indirect ability to increase inflammation or the direct injury caused to ECs (82, 83).

The indirect impact occurs through hypertension that increases the amount of ROS, especially from the oxidation of endothelial NO synthesis (83). ROS can impact the inflammatory state and the ECs in several ways. It can, among others, cause EC death and increase the adhesion of inflammatory cells to the normally inert endothelium surface (83). This could potentially exacerbate the response and symptoms related to EC injury. See **Figure 10** pathways: *Hypertension-(pw100)-↑ROS-(pw85)-↑Inflammatory state-(pw110)-↑EC injury*.

Chronic hypertension can also directly cause damage to the microvascular ECs (82). High blood pressure strains the ECs and could potentially cause ruptures in plaques that are adhered to the artery wall (82). See **Figure 10** pathways: *Hypertension-(pw118)-EC injury*. This creates additional areas that require attention and would probably also increase the inflammatory response.

Existing chronic hypertension can therefore possibly cause injury to the ECs through either the indirect or direct pathways. This injury could potentially contribute to the rapid worsening of health in Covid-19 patients with chronic hypertension (81).

Effects of Different *Health Factors* on Covid-19 Severity

We discuss the comparison between CHD and severe Covid-19 for different *health factors* with reference to **Figure 4**. The definition of each *health factor* was given in section Evaluation of *Health Factors* and *Pharmaceutical Interventions*.

Different *health factors* (pink ovals in **Figure 4**) were originally analyzed in terms of their effects on CHD risk (23). These *health factors* were either associated with an increase or decrease in risk for CHD (23–28). The same *health factors* were investigated for Covid-19 severity. We will show to what extent a healthy CHD "baseline," as a result of a healthy lifestyle, will influence Covid-19 severity.

Table 2 summarizes the CHD and Covid-19 data extracted from literature namely, study size (N), number of participants (n), risk type (RR/HR/OR), respective risk value, 95% confidence interval (CI), fold change (as calculated *via* the non-traditional method) and the respective references. Data not statistically significant are indicated with an (*) in **Figure 11**.

Where data were unavailable a hash (#) was inserted in **Table 2** e.g., for the two *health factors*, alcohol use and food intake (high glycemic diets). These *health factors* have not yet been fully investigated in Covid-19 patients. Despite no risk values being available for these *health factors*, their probable effects on Covid-19 severity are discussed in this section.

The *health factors* that increase/decrease a person's risk for CHD similarly increase/decrease a person's risk (RR/HR/OR) for developing severe Covid-19 (**Figure 11**). In the rest of this section we will discuss, in more detail, the effects each *health factor* has on the CHD hallmarks, and hypothesize how this could affect Covid-19 severity.

Moderate Exercise

Based on the CHD model (**Figure 1**) our research group has published a detailed description of the mechanism by which moderate exercise may reduce CHD risk (28). Only the salient features of the mechanism will be described here.

Regular moderate exercise is universally accepted to reduce the risk of CHD (23, 28, 84) (the definition of moderate exercise was given in section Evaluation of *Health Factors* and *Pharmaceutical Interventions*). **Table 2** shows a decrease risk (RR) of 0.75 (n = 645 087, N = 33) (84). This translates to a 1.33-fold decrease in CHD risk (23, 28) as illustrated in **Figure 11**.

The effect of moderate exercise on Covid-19 was analyzed in a small cross-sectional study (n = 260) (85). The authors concluded that moderate physical activity before onset of Covid-19 decreases the odds of developing severe Covid-19 (OR of 0.28) by 3.57 times (85), see **Table 2** and **Figure 11**. Although this is only a small study, a larger study (n = 48 440) substantiates the benefit of regular moderate exercise (118).

This larger study's results are not presented in **Table 2** or **Figure 11** since the study reported on inactivity. However, since being active helps reduce the odds of developing severe Covid-19, inactivity is expected to have an opposite effect. This is indeed the case as the study showed that patients who are consistently inactivate are 2.49 (OR) times more likely to die from Covid-19 (118).

Therefore, moderate exercise before the onset of disease decreases both the risk for CHD and Covid-19 severity. This could most likely be explained by the effect of moderate exercise on several CHD hallmarks. Moderate exercise largely influences, among others, glucose, cortisol and inflammatory mediator levels (23, 28), therefore reducing the risk of *Hyperglycemia/Hyperinsulinemia* and a heightened *Inflammatory state* (23, 28).

Regular exercise also reduces the accumulation of visceral fat, which reduces the risk of increased Low-Density Lipoprotein (LDL) levels thus decreasing the risk for *Hypercholesterolemia* (23, 28). A decrease of visceral fat also reduces the risk of insulin resistance, which lowers one's risk for increased platelet factors and the potential for *Hypercoagulability* (23, 28).

The potential decrease of these CHD hallmarks could partially explain the benefit of moderate exercise on the reduced risk of Covid-19 severity. The respective CHD hallmark downregulated by exercise and the activated pathways are denoted in **Figure 4** as follows:

- **Hyperglycemia/Hyperinsulinemia**: *Moderate exercise-(pw3a)-muscles-(pw53)-↓blood glucose-(pw54)-↓PI3K:MAPK-(pw69)-↓insulin resistance-(pw72)-Hyperglycemia/ Hyperinsulinemia.*
- **Inflammatory state**: *Moderate exercise-(pw3b)-central nervous system-(pw27)-↓cortisol-(pw47)-↓insulin resistance-(pw70)-↓angiotensin II-(pw89)-↓hypertension-(pw100)-↓ROS-(pw85)-↓COX1/2-(pw85)-↓Inflammatory state.*
- **Hypercholesterolemia**: *Moderate exercise-(pw3c)-visceral adiposity-(pw18)-↓FFA-(pw37)-↓plasma lipids-(pw34)-liver-(pw12)-↓LDL-(pw33)-↓oxLDL-(pw51)-↓Hypercholesterolemia.*
- **Hypercoagulability**: *Moderate exercise-(pw3a)-muscles-(pw53)-↓blood glucose-(pw54)-↓PI3K:MAPK-(pw69)-↓insulin resistance-(pw72)-↓platelet factors-(pw73)-↓Hypercoagulability.*

The potential decrease in four of the five CHD hallmarks due to moderate exercise before onset of Covid-19 (creating a healthier vascular system "baseline") could partially explain the decreased risk of Covid-19 severity. These beneficial effects of exercise are based on moderate exertion and not heavy exertion. Heavy exertion exercise has the following detrimental effects: transient

TABLE 2 | The effect which different health factors and pharmaceuticals have on CHD risk and Covid-19 severity.

	Risk for CHD					References	Risk for increased COVID-19 severity					References
	Study size (*n* = no. of participants, *N* = no. of studies)	**RR, HR or OR**	**Value**	**95% CI**	**Fold change as per our definition**		**Study size (*n* = no. of participants, *N* = no. of studies)**	**RR, HR or OR**	**Value**	**95% CI**	**Fold change as per our definition**	
HEALTH FACTORS												
Moderate exercise	*n* = 645 087, *N* = 33	RR	0.75	(0.71–0.79)	−1.33	(23, 84)	*n* = 260, *N* = 1	OR	0.28	#	−3.57	(85)
Smoking	*n* = 1 010 000, *N* = 141	RR	1.72	(1.62–1.83)	1.74	(23, 86)	*n* = 32 849, *N* = 47	RR	1.98	(1.16–3.38)	1.98	(87)
Oral health	*n* = 147 821, *N* = 7	RR	1.34	(1.27–1.42)	1.34	(23, 27, 88)	*n* = 568, *N* = 1	OR	8.81	(1.00–77.70)	8.81	(89)
Stress	*n* = 24 767, *N* = 1	OR	2.17	(1.84–2.55)	2.17	(23, 90)	*n* = 535, *N* = 1	HR	1.40	(1.11–1.75)	1.40	(91)
Depression	*n* = 124 509, *N* = 21	RR	1.90	(1.49–2.42)	1.90	(23, 92)	*n* = 421 014, *N* = 1	OR	2.68	(2.03–3.54)	2.68	(93)
Apnoea	*n* = 1 436, *N* = 1	HR	2.06	(1.10–3.86)	2.06	(23, 94)	*n* = 15 835, *N* = 4	OR	2.37	(1.14–4.95)	2.37	(95)
Insomnia	*n* = 122 501, *N* = 13	RR	1.45	(1.29–1.62)	1.45	(23, 96)	*n* = 568, *N* = 1	OR	1.09	(0.44–2.71)	1.09	(97)
Moderate alcohol	*n* = 504 651, *N* = 29	RR	0.71	(0.66–0.77)	−1.41	(23, 26, 98)	#	#	#	#	#	#
Food (HGD)	*n* = 220 050, *N* = 8	RR	1.36	(1.13–1.63)	1.36	(23, 25, 99)	#	#	#	#	#	#
PHARMACEUTICALS												
Statins	*n* = 169 138, *N* = 26	RR	0.78	(0.76–0.80)	−1.28	(23, 100)	*n* = 13 981, *N* = 1	HR	0.58	(0.43–0.80)	−1.72	(101)
Salicylates (Aspirin)	*n* = 112 000, *N* = 6	RR	0.82	(0.75–0.90)	−1.22	(23, 102)	*n* = 412, *N* = 1	HR	0.53	(0.31–0.90)	−1.89	(58)
Indirect thrombin inhibitors (Heparin)	*n* = 31 402, *N* = 6	OR	0.91	(0.84–0.98)	−1.10	(23, 103)	*n* = 449, *N* = 1	OR	0.37	(0.15–0.90)	−2.70	(104)
Direct thrombin inhibitors (Angiomax)	*n* = 1 883, *N* = 1	HR	0.76	(0.59–0.98)	−1.32	(23, 105)	*n* = 103 703, *N* = 1	HR	0.90	(0.71–1.15)	−1.11	(106)
ACE inhibitors	*n* = 19 141, *N* = 8	OR	0.79	(0.71–0.88)	−1.27	(23, 107)	*n* = 19 486, *N* = 1	HR	0.89	(0.75–1.06)	−1.12	(108)
Angiotensin-renin inhibitors	*n* = 108 212, *N* = 26	OR	0.92	(0.87–0.97)	−1.09	(23, 109)	*n* = 2,877, *N* = 1	RR	0.65	(0.45–0.94)	−1.54	(110)
β-blockers	*n* = 12 825, *N* = 9	RR	0.69	(0.59–0.82)	−1.45	(23, 111)	*n* = 101 141, *N* = 8	OR	1.23	(0.74–2.04)	1.23	(112)
Calcium channel blockers	*n* = 10 136, *N* = 8	OR	0.83	(0.67–1.03)	−1.20	(23, 107)	*n* = 106 566, *N* = 8	OR	0.94	(0.8–1.10)	−1.06	(112)
Diuretics	*n* = 192 478, *N* = 42	RR	0.79	(0.69–0.92)	−1.27	(23, 113)	*n* = 99 669, *N* = 5	OR	0.96	(0.81–1.15)	−1.04	(112)
Biguanides (Metformin)	*n* = 11 385, *N* = 6	OR	0.74	(0.62–0.89)	−1.35	(23, 114)	*n* = 1 800 005, *N* = 1	HR	0.77	(0.73–0.81)	−1.30	(115)
Antidepressants	*n* = 93 653, *N* = 1	HR	0.48	(0.44–0.52)	−2.08	(23, 116)	#	#	#	#	#	#

CHD, Coronary Heart Disease; CI, Confidence Interval; Covid-19, Coronavirus Disease of 2019; HGD, High Glycemic Diets; HR, Hazard Ratio; OR, Odds Ratio; RR, Relative Risk. A minus sign shows a reduction in risk. (#) denotes that the respective study did not provide this data. A small preliminary study (117) on the effect of the SSRI antidepressant, fluvoxamine, on Covid-19 has shown positive effects. Risk data were not given.

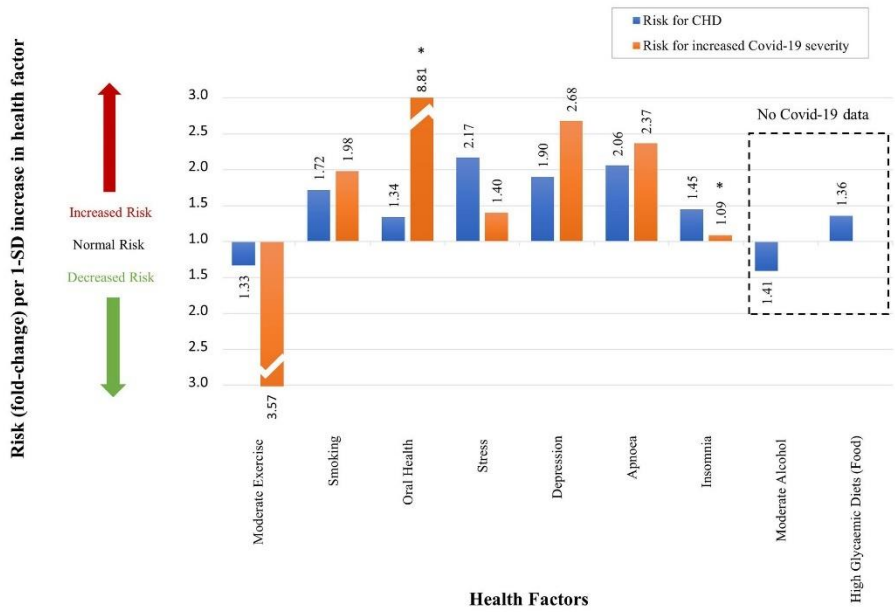

FIGURE 11 | The qualitative effect which different health factors have on CHD risk and Covid-19 severity. (An accurate quantitative comparison is not possible, mostly due to differences in study design and size).

immune dysfunction, elevated inflammatory biomarkers, and increased risk of upper respiratory tract infections (119). Therefore, exercise exertion is an important factor to consider during the Covid-19 pandemic.

Smoking

Smoking is a risk factor for CHD with a RR of 1.72 (86). A recent systematic review and meta-analysis of 47 studies (32 849 hospitalized Covid-19 patients) showed that current smokers have an increased risk of developing severe or critical Covid-19, RR of 1.98 (87).

Most smokers develop insulin resistance and/or Hyperinsulinemia as compared to non-smokers (120, 121). This association may either be due to the lower adiponectin levels or higher cortisol secretion levels seen in current smokers compared to non-smokers (122, 123). This increases a smoker's risk for *Hyperglycemia/Hyperinsulinemia.*

Moreover, most smokers also have higher plasma triglyceride and lower High-Density Lipoprotein (HDL) cholesterol concentrations than non-smokers (121, 124). This increases a smoker's risk of *Hypercholesterolemia.*

Another CHD hallmark that is upregulated in smokers is a heightened *Inflammatory state.* This is due to an upregulation of several inflammatory markers and cytokines such as TNF-α, granulocyte-macrophage colony-stimulating factor (GM-CSF) and monocyte chemoattractant protein (MCP-1) (125).

Smoking also induces an imbalance between various hemostatic molecules in the blood thereby increasing the state of *Hypercoagulability* (126). This may be due to functional changes in clotting factors such as fibrinogen (126).

The associated pathways and respective CHD hallmarks increased by smoking are shown in **Figure 4** as the following:

- **Hyperglycemia/Hyperinsulinemia:** *Smoking-(pw4a)-visceral adiposity-(pw19)-↓adiponectin-(pw39)-↑insulin resistance-(pw72)- ↑Hyperglycemia/Hyperinsulinemia. Smoking-(pw4b)-central nervous system-(pw27)-↑cortisol-(pw47)-↑insulin resistance-(pw72)- ↑Hyperglycemia/Hyperinsulinemia.*
- **Hypercholesterolemia:** *Smoking-(pw4a)-visceral adiposity-(pw30)-↓HDL-(pw31)-↑ Hypercholesterolemia.*
- **Inflammatory state:** *Smoking-(pw4b)-central nervous system-(pw41)-↑TNF-α-(pw41)-↑Inflammatory state.*
- **Hypercoagulability:** *Smoking-(pw4a)-visceral adiposity-(pw49)-↑Fibrinogen-(pw73)-↑Hypercoagulability.*

The activation of these pathways and respective CHD hallmarks may explain some of the increased risk of smokers developing severe Covid-19 compared to non-smokers (87).

Oral Health

Using **Figure 1**, we published a detailed analysis of the mechanism by which oral health (in the form of periodontal disease) can influence CHD (27). Important elements relevant to this study are discussed below.

Oral health in the form of periodontal disease is known to increase the risk of CHD by 1.34-fold (88) (**Figure 11** and **Table 2**). Covid-19 patients with periodontitis have a much

higher risk of mortality, OR of 8.81 (**Figure 11** and **Table 2**) (89). This value is quite large and could be overestimated. There are several reasons for potential overestimation namely, the small study size ($n = 568$), the data is widely spread (95% CI of 1.00–77.7) and the data is not statistically significant [this statistical insignificance is illustrated on **Figure 11** with an (*)] (89).

Nevertheless, the increased risk of Covid-19 severity due to periodontitis could partially be explained by the increase in several CHD hallmarks namely, *Inflammatory state, Hypercoagulability and Hypercholesterolemia* (23, 27).

An increased risk of *Hypercoagulability* and *Inflammation* in these patients is through a common periodontitis associated bacteria, porphyromonas gingivalis (p.gingivalis) (127). This bacteria invades endothelial cells which concomitantly increases platelet activity and stimulates proinflammatory mediators/cytokines (CRP, TNF-α, and IL-6) (127).

Inflammation can also be increased *via* reactive oxygen species (ROS) which is associated with periodontal disease (23, 27). Subsequently, this also affects oxidized LDL levels pertaining to an increase in the risk for *Hypercholesterolemia* (23, 27).

The associated pathways and respective CHD hallmarks increased by oral health in the form of periodontitis are shown in **Figure 4** as the following:

- **Hypercoagulability:** *Oral health-(pw5)-periodontium-(pw23)-↑P. gingivalis-(pw43)-↑periodontitis-(pw64)-↑platelet factors-(pw73)-↑Hypercoagulability.*
- **Inflammatory state:** *Oral health-(pw5)-periodontium-(pw23)-↑P. gingivalis-(pw43)-↑periodontitis-(pw41)-↑TNFα/IL6-(pw41)-↑inflammatory state. Oral health-(pw5)-periodontium-(pw23)-↑P. gingivalis-(pw43)-↑periodontitis-(pw62)-↑ROS-(pw85)-↑inflammatory state.*
- **Hypercholesterolemia:** *Oral health-(pw5)-periodontium-(pw23)-↑P. gingivalis-(pw43)-↑periodontitis-(pw65)-↑oxLDL-(pw51)-↑Hypercholesterolemia.*

The potential increase of these CHD hallmarks due to periodontitis could partially explain the increased risk of Covid-19 severity.

Chronic Stress

Chronic stress (definition in section Evaluation of *Health Factors* and *Pharmaceutical Interventions*) is also a common factor linked to an increased risk for CHD, with an OR of 2.17 (90), presented in **Figure 11** and **Table 2.** Covid-19 severity is also increased by chronic stress with a HR of 1.4 (91), see **Figure 11.**

Chronic stress is known to elevate secretion of glucocorticoids in the form of cortisol. These high cortisol levels due to stress may elevate biomarkers such as blood glucose, TNF-α and insulin resistance (23). These stress related biomarkers are also upregulated in severe Covid-19 patients (23, 75, 76, 128–131).

The respective CHD hallmarks and activated pathways activated by chronic stress are denoted in **Figure 4** as:

- **Hypercoagulability:** *Chronic stress-(pw6)-central nervous system-(pw27)-↑cortisol-(pw48)-liver-(pw14)-↑blood glucose-(pw54)-PI3K:MAPK-(pw69)-↑insulin resistance-(pw72)-↑platelet factors-(pw73)-↑Hypercoagulability.*
- **Hypercholesterolemia:** *Chronic stress-(pw6)-central nervous system-(pw27)-↑cortisol-(pw48)-liver-(pw12)-↑LDL-(pw33)-↑oxLDL-(pw51)-↑Hypercholesterolemia.*
- **Hyperglycemia/Hyperinsulinemia:** *Chronic stress-(pw6)-central nervous system-(pw27)-↑cortisol-(pw48)-liver-(pw14)-↑blood glucose-(pw54)-PI3K:MAPK-(pw69)-↑insulin resistance-(pw72)-↑Hyperglycemia/Hyperinsulinemia.*
- **Inflammatory state:** *Chronic stress-(pw6)-central nervous system-(pw27)-↑cortisol-(pw48)-liver-(pw14)-↑blood glucose-(pw54)-PI3K:MAPK-(pw69)-↑insulin resistance-(pw70)-↑angiotensin II-(pw88)-renin-(pw50)-↑TNFα-(pw41)-↑Inflammatory state.*
- **Hypertension:** *Chronic stress-(pw6)-central nervous system-(pw27)-↑cortisol-(pw48)-liver-(pw14)-↑blood glucose-(pw54)-PI3K:MAPK-(pw69)-↑insulin resistance-(pw70)-↑angiotensin II-(pw89)- ↑Hypertension.*

Although the Covid-19 study is small ($n = 535$, see **Table 2**) stress affects all five CHD hallmarks. Future larger clinical studies are expected to emphasize the importance of stress management in patients with Covid-19.

Depression

The effect of depression on CHD, using the CHD model in **Figure 1**, was described in detail in a previous paper (24). A summary of the potential effects of depression on Covid-19 are given in the rest of this section.

Depression increases one's risk for CHD by 1.90-fold (RR) (92), shown in **Figure 11** and **Table 2.** This is also the case for Covid-19, where the odds of developing more severe disease in a person with pre-pandemic depression is 2.68-fold (OR) higher that without depression (93), see **Figure 11.**

Depression is thought to mediate, among others, over stimulation of the hypothalamic-pituitary-adrenocortical (HPA) axis induced by elevated levels of corticotropin-releasing factor and adrenocorticotropic hormone (23, 24). Chronic dysregulation of the hypothalamic-pituitary-adrenal axis can lead to increased serum levels of cortisol. Similar to chronic stress, elevated cortisol levels can increase the risk of upregulating four CHD hallmarks namely, *Inflammatory state, Hypercholesterolemia, Hypertension* and *Hyperglycemia/Hyperinsulinemia* (23, 24).

In addition to increased cortisol levels, the overstimulation of the hypothalamic-pituitary-adrenal axis may augment sympathoadrenal hyperactivity *via* central regulatory pathways. This results in increased plasma catecholamines (23, 24). An increase of catecholamines can lead to abnormalities in insulin and platelet factors thus also increasing another CHD hallmark namely, *Hypercoagulability* (23, 24).

The respective CHD hallmarks and activated pathways induced by depression are denoted in **Figure 4** as the following:

- **Hypercholesterolemia:** *Depression-(pw7b)-central nervous system-(pw27)-↑cortisol-(pw48)-liver-(pw12)-↑LDL-(pw33)-↑oxLDL-(pw51)-↑Hypercholesterolemia.*
- **Inflammatory state:** *Depression-(pw7b)-central nervous system-(pw27)-↑cortisol-(pw48)-liver-(pw14)-↑blood*

glucose-(pw54)-PI3K:MAPK-(pw69)-↑insulin resistance-(pw70)-↑angiotensin II-(pw88)-renin-(pw50)-↑TNFα-(pw41)-↑Inflammatory state.

- **Hypertension:** *Depression-(pw7b)-central nervous system-(pw27)-↑cortisol-(pw48)-liver-(pw14)-↑blood glucose-(pw54)-PI3K:MAPK-(pw69)-↑insulin resistance-(pw70)-↑angiotensin II-(pw89)- ↑Hypertension.*
- **Hyperglycemia/Hyperinsulinemia:** *Depression-(pw7b)-central nervous system-(pw26)-↑catecholamines / ↓serotonin / ↓BDNF-(pw44)-↑insulin resistance-(pw72)- ↑Hyperglycemia / Hyperinsulinemia.*
- **Hypercoagulability:** *Depression-(pw7b)-central nervous system-(pw26)-↑catecholamines / ↓serotonin / ↓BDNF-(pw44)-↑insulin resistance-(pw72)-↑platelet factors-(pw73)-↑Hypercoagulability.*

Since depression can upregulate all five CHD hallmarks (23, 24), it may play a more important role in Covid-19 severity than expected.

Apnoea

Figure 11 and **Table 2** show that obstructive sleep apnoea (OSA) is associated with an increased risk for CHD with a HR of 2.06 (94). Among 15 835 Covid-19 patients, those with OSA have a 2.37-fold (OR) increased odds of developing severe Covid-19 (95).

Similar to depression, the effects of OSA may also include alterations of the hypothalamic-pituitary-adrenal axis and sympathetic nervous activity. This results in changes of catecholamine and cortisol secretion levels, which concomitantly serve to up-regulate two CHD hallmarks namely, *Inflammatory state* and *Hypertension* (23). Subsequently, increased cortisol levels also increases the risk for elevated LDL and platelet factors, which influence the risk for two more CHD hallmarks namely, *Hypercholesterolemia* and *Hypercoagulability* (23).

The respective CHD hallmarks and activated pathways induced by OSA are denoted in **Figure 4** as the following:

- **Inflammatory state:** *Apnoea-(pw9)-central nervous system-(pw27)-↑cortisol-OSA-(pw42)-hypoxia-(pw61)-↑ROS-(pw85)-↑Inflammatory state.*
- **Hypertension:** *Apnoea-(pw9)-central nervous system-(pw27)-↑cortisol-OSA-(pw42)-↑hypoxia-(pw42)-↑)-oxia-(pSA-(pus systw70)-↑angiotensin II-(pw89)-↑Hypertension.*
- **Hypercholesterolemia:** *Apnoea-(pw9)-central nervous system-(pw27)-↑cortisol-(pw48)-visceral adiposity-(pw21)-↑TNF-α/IL-6-(pw56)-liver-(pw12)-↑LDL-(pw33)-↑oxLDL-(pw51)-↑Hypercholesterolemia.*
- **Hypercoagulability:** *Apnoea-(pw9)-central nervous system-(pw27)-↑cortisol-(pw47)-↑insulin resistance-(pw42)-↑platelet factors-(pw73)-↑Hypercoagulability.*

The activation of proinflammatory mediators namely, TNF-α, IL-6 and CRP induced by OSA are also elevated in severe Covid-19 patients without OSA (20–22). Therefore, OSA could aggravate these mediators, leading to an increased risk of Covid-19 severity.

Insomnia

Insomnia is another *health factor* that increases a person's risk for CHD with a RR of 1.45 (96), see **Figure 11** and **Table 2.** The effect of insomnia on increased Covid-19 severity seems negligible with an OR of 1.09 (97), see **Figure 11.** Unfortunately the study is small ($n = 568$) and the data are statistically insignificant (95% CI of 0.44–2.71) (97), see **Table 2** and **Figure 11.**

Nevertheless, insomnia affects several pathogenic pathways that may play an important role in Covid-19 severity (23). Insomnia has shown to directly affect the levels of leptin (decreases) and ghrelin (increases), which are important hormones that regulate appetite. This could cause an increase in caloric consumption which, if left untreated, could negatively impact blood glucose levels and insulin sensitivity (23). This would therefore result in an increased risk for *Hyperglycemia/Hyperinsulinemia* (23).

Subsequently, insulin resistance stemming from excessive caloric intake can stimulate proinflammatory mediators and cytokines such as TNF-α, IL-6 and CRP. This could result in a heightened *Inflammatory state*, which is common in severe Covid-19 patients (20–23). Another CHD hallmark upregulated by insulin resistance through the regulation of platelet homeostasis is *Hypercoagulability* (23). Coagulation is also a common risk factor in severe Covid-19 patients (4, 6–9, 23).

The respective CHD hallmarks and activated pathways induced by insomnia are denoted in **Figure 4** as the following:

- **Hyperglycemia/Hyperinsulinemia:** *Insomnia-(pw8b)-central nervous system-(pw25)-(pw66)-↑ghrelin:leptin-(pw67)-↑insulin resistance-(pw72)-liver-(pw14)-↑blood glucose-(pw55)-↑Hyperglycemia/Hyperinsulinemia.*
- **Inflammatory state:** *Insomnia-(pw8b)-central nervous system-(pw25)-(pw66)-↑ghrelin:leptin-(pw67)-↑insulin resistance-(pw70)-↑angiotensin II-(pw88)-renin-(pw50)-↑TNF-α, IL-6-(pw41)-↑Inflammatory state.*
- **Hypercoagulability:** *Insomnia-(pw8b)-central nervous system-(pw25)-(pw66)-↑ghrelin:leptin-(pw67)-↑insulin resistance-(pw72)-↑platelet factors-(pw73)-↑Hypercoagulability.*

Unfortunately, the clinical data on insomnia and its effect on Covid-19 severity are small. Its effect may be underestimated.

Moderate Alcohol Use

The mechanism by which moderate alcohol consumption may influence CHD was described in detail in our previous paper (26). Moderate alcohol consumption is accepted to reduce the risk of CHD (23, 26, 98). **Table 2** shows a decrease risk (RR) of 0.75 ($n = 645\,087$, $N = 33$) (98). This translates to a 1.41-fold decrease in CHD risk (23, 26), illustrated in **Figure 11.** This decrease in CHD risk may be due to several pathways that decrease the risk for CHD hallmarks.

Moderate alcohol consumption may reduce fibrinogen levels, clotting factors, and platelet aggregation. Downregulation of these biomarkers reduces a state of *Hypercoagulability* (26). In addition, it can also upregulate HDL and downregulate LDL, which decrease *Hypercholesterolemia* (26).

Moreover, moderate alcohol consumption can reduce hepatic gluconeogenesis and concomitantly decrease plasma glucose levels, which decreases the incidence of *Hyperglycemia* and *Hyperinsulinemia* (26). Lastly, it can serve

to reduce chronic *Inflammation* through regulation of insulin resistance (26).

These respective CHD hallmarks and pathogenic pathways activated by moderate alcohol consumption (26), are denoted in **Figure 4** as:

- **Hypercoagulability:** *Alcohol-(pw1)-Liver-(pw49)-↓fibrinogen/clotting factors-(pw73)- ↓Hypercoagulability* and *Alcohol-(pw1)-Liver-(pw49)-↑fibrinogen/clotting factors-(pw75)- ↓platelet aggregation.*
- **Hypercholesterolemia:** *Alcohol-(pw1)-Liver-(pw10)-↑HDL-(pw31)-↓Hypercholesterolemia* and *Alcohol-(pw1)-Liver-(pw12)-↓LDL-(pw33)- oxLDL-(pw51)-↓Hypercholesterolemia.*
- **Hyperglycemia/Hyperinsulinemia:** *Alcohol-(pw1)-Liver-(pw14)-↓blood glucose-(pw55)-↓Hyperglycemia/Hyperinsulinemia.*
- **Inflammation:** *Alcohol-(pw1)-Liver-(pw14)-↓blood glucose-(pw54)-PI3K:MAPK-(pw69)-insulin resistance-(pw70)-Angiotensin II-(pw89)-↓Hypertension-(pw100)-↓ROS-(pw85)-↓Inflammatory state.*

These pathways demonstrate an important role moderate alcohol consumption plays in four of the five CHD hallmarks. The argument whether moderate alcohol consumption before infection decreases or increases Covid-19 severity has not yet been thoroughly explored.

However, the prevailing point of view is that alcohol consumption during Covid-19 could increase Covid-19 severity (132). This is due to alcohol increasing the risk of acute respiratory distress syndrome and admission to intensive care unit in patients with pneumonia (132, 133). These are common risk factors in critical Covid-19 patients (132, 133).

Increased hypercoagulability, Hyperglycemia and inflammation are common in severe Covid-19 patients (4, 6–9, 11, 13, 14). Therefore, the reduction of these CHD hallmarks by moderate alcohol consumption before infection of SARS-CoV-2 could be advantageous. It seems to create a better vascular "baseline" and could thus potentially reduce the risk of developing severe Covid-19 complications. These effects should however be studied in well-designed clinical trials.

Food Intake (High Glycemic Diets)

We have previously explained, with reference to **Figure 1**, how high glycemic diets (HGDs) affect CHD (25). Only a summary of the elements relevant to Covid-19 are given below.

A high glycemic diet (HGD) increases the risk for CHD with a RR of 1.36 (99), see **Figure 11** and **Table 2.** These diets could play an important role in Covid-19 severity through regulation of all five CHD hallmarks (23, 25).

HGDs influences glycemic control by raising blood glucose levels *via* carbohydrate consumption. This may result in *Hyperglycemia* (23, 25). *Hyperglycemia* resulting from HGDs can increase the risk of insulin resistance by upregulating the Phosphatidylinositol 3-kinase : Mitogen-activated protein kinase (PI3K:MAPK) ratio (23, 25). Subsequently, an increased insulin resistance has been associated with increased levels of platelet factors that upregulate the potential for *Hypercoagulation* (23, 25).

Excessive intake of HGDs can result in increased adipose tissue, which enhances pro-inflammatory mediators such as CRP and TNF-α (23, 25). These mediators are, among others, important to consider since they are upregulated in critical Covid-19 patients (129, 130, 134–140). Macrophages, residing in adipose tissue, are also one of the most active secretory cells in the body that mediate activities of adipocytes and release a vast array of inflammatory mediators (23, 25). This increases the risk for an *Inflammatory state.*

Moreover, excessive intake of HGDs can also increase visceral fat build up and reduce clearance of triglycerides, which leads to increased LDL and decreased HDL levels (23, 25). This constitutes to a potential risk of *Hypercholesterolemia* (23, 25). Consequently, HGDs pertaining to visceral fat build up also increases the risk of *Hypertension.* This happens through build-up of excess adipose tissue, which increases the expression of angiotensinogen thus leading to activation of the renin-angiotensin system (23, 25).

These respective CHD hallmarks and pathogenic pathways activated by HGD are denoted in **Figure 4** as the following:

- **Hyperglycemia:** *Food-(pw2)-gastro-intestines-(pw17)-↑blood glucose-(pw55)-↑Hyperglycemia.*
- **Hypercoagulability:** *Food-(pw2)-gastro-intestines-(pw17)-↑blood glucose-(pw54)-↑PI3K:MAPK-(pw69)-↑insulin resistance-(pw72)-↑platelet factors-(pw73)-↑Hypercoagulability.*
- **Inflammatory state:** *Food-(pw2)-gastro-intestines-(pw15)-plasma lipids-(pw34)-liver-(pw13)-TMAO/NLRP3-(pw52)-macrophage-(pw77)-↑Inflammatory state.*
- **Hypercholesterolemia:** *Food-(pw2)-gastro-intestines-(pw15)-plasma lipids-(pw34)-liver-(pw12)-↑LDL-(pw33)-oxLDL-(pw51)-↑Hypercholesterolemia.*
- **Hypertension:** *Food-(pw2)-gastro-intestines-(pw14)-blood glucose-(pw54)-↑angiotensin II-(pw89)-↑Hypertension.*

These pathways demonstrate the detrimental effect HGDs may have on an individual's "baseline" vascular system before infection from SARS-CoV-2. It could potentially increase the risk of developing severe Covid-19 complications.

Effects of Different CHD *Pharmaceutical Interventions* on Covid-19 Severity

The *integrated CHD/Covid-19 model* shows that similar outcomes for different *health factors* are seen in CHD and Covid-19. The next question is: Since we know that various *pharmaceutical interventions* decreases one's risk for CHD, will they also work for Covid-19? If they do then this will further show validity of the proposed *integrated CHD/Covid-19 model.*

The *pharmaceutical interventions* are shown in **Figure 4** as blue boxes, where blunted blue arrows (⊣) denote antagonize or inhibit and pointed blue arrows (→) denote up-regulate or facilitate. The question is whether these pharmaceuticals would also decrease one's risk for severe Covid-19. This was investigated, despite the limited clinical data available for Covid-19. The data were extracted from literature and are summarized in **Table 2.**

No risk value was available for antidepressants' effect on Covid-19 severity. However, its effect on Covid-19 severity is still discussed in this section as depression was shown to increase the odds of developing severe Covid-19 complications by 2.68 (Section Effects of Different CHD *Pharmaceutical Interventions* on Covid-19 Severity, **Table 2**). It is thus hypothesized that certain anti-depressants should have an important influence on Covid-19 severity.

In the rest of this section we will discuss, in more detail, the effects each *pharmaceutical intervention* has on the CHD hallmarks, and how this could affect Covid-19 severity.

Statins

The use of statins decreases the risk of CHD with a RR of 0.78 (100). This translates to a 1.28-fold decrease in CHD risk (23), illustrated in **Table 2** and **Figure 12**. Statins also decrease Covid-19 severity, with a HR of 0.58 ($n = 13\,981$) (101) (**Table 2**). This translates to a decrease of Covid-19 severity by 1.72-fold as shown in **Figure 12**. We evaluated the effects statins has on all of the CHD hallmarks, which may partially explain the large reduction in Covid-19 severity with the use of statins.

Firstly, statins cholesterol lowering effect inhibits the following pathways in **Figure 4**: (pw11) and (pw12). Besides these cholesterol lowering effects, it also has an anti-inflammatory effect (23, 101). The anti-inflammatory biomarkers and pathways on which inhibition is observed are denoted in **Figure 4** as: NFκβ, ROS and (pw21), (pw57), (pw74).

In addition to their beneficial effects on cholesterol and inflammation, statins also have antihypertensive effects by reducing systolic, diastolic and mean arterial blood pressure (141). The hypertensive pathways on which its actions are observed are denoted in **Figure 4** as (pw88) and (pw89).

Salicylates

Salicylates such as aspirin is a common anti-inflammatory (142) and anti-thrombotic (143) medication that decreases the risk for CHD with a RR of 0.82 (102), see **Table 2**. This translates to a 1.22-fold decrease in CHD risk (23), illustrated in **Figure 12**. Its use in Covid-19 patients also showed a decrease in severity with HR of 0.53 (58). This is shown in **Figure 12** as a 1.89-fold decrease in Covid-19 severity (58).

This reduction in risk could be expected because of the detrimental effect of inflammation and coagulation seen in most severe Covid-19 patients (4, 6–9, 20–22). The pathways on which aspirin's actions are observed are denoted in **Figure 4** as (pw73) and (pw74).

Indirect Thrombin Inhibitors

Indirect thrombin inhibitors such as heparin is used as an anticoagulant, which decreases the odds of CHD with OR 0.91 (103), see **Table 2**. This translates to a 1.10-fold decrease in CHD risk (23) as shown in **Figure 12**. Since many severe cases of Covid-19 present venous thromboembolisms and microthrombi (4, 6–9), indirect thrombin inhibitors should be of benefit to such cases.

Heparin was thus expected to reduce these thrombi and reduce Covid-19 severity. A small retrospective analysis ($n = 449$) investigated heparin's effect in Covid-19 patients (104). The study found an OR of 0.37 in Covid-19 mortality (104), see **Table 2**. This is illustrated in **Figure 12** as a 2.7-fold decrease in odds of developing severe Covid-19 (104). The coagulation pathway on which heparin's action is observed is shown in **Figure 4** as (pw73).

Heparin also seems to have an anti-inflammatory effect (144), which is presented in **Figure 4** as pathway (pw74). This effect is however only seen at much higher concentrations which could increase the risk of bleeding (144). Therefore, heparin's anti-thrombotic effect would predominantly be the reason for lower Covid-19 severity.

Direct Thrombin Inhibitors

Direct thrombin inhibitors have shown to decrease the risk of CHD with HR of 0.76 (105), see **Table 2**. This translates to a 1.32-fold decrease in CHD risk (23), illustrated in **Figure 12**. These pharmaceuticals' actions are also observed on the coagulation pathway (pw74) (23), see **Figure 4**.

For Covid-19, direct thrombin inhibitors are shown to slightly reduce the risk of developing severe disease with a HR of 0.90 (106), see **Table 2**. This translates to a 1.11-fold reduction in risk (106), illustrated in **Figure 12**. However, as shown in **Figure 12** by an (*), this value is not statistically significant with the 95% CI of 0.71–1.15 presented in **Table 2**.

Antihypertensive Pharmaceuticals

The antihypertensive *pharmaceutical interventions* in **Figure 4** are: ACE inhibitors, angiotensin-renin inhibitors, β-blockers, calcium channel blockers and diuretics. The pathways on which their actions are observed are shown in **Figure 4** as (pw88), (pw89), and (pw50) (23).

The respective reduction of CHD risks for each pharmaceutical (23, 107, 109, 111, 113) is given in **Figure 12** and **Table 2** as the following:

- Angiotensin-renin inhibitors: 1.09 (OR of 0.92)
- Calcium channel blockers: 1.20 (OR of 0.83)
- ACE inhibitors: 1.27 (OR of 0.79)
- β-blockers: 1.46 (RR of 0.69)
- Diuretics: 1.27 (RR of 0.79)

The reduction in CHD risk is small for angiotensin-renin inhibitors with an OR close to one (0.92) (109). However, angiotensin-renin inhibitors seem to be more beneficial for Covid-19 severity with a reduction in 1.54-fold (110), see **Figure 12**.

The risk data for calcium channel blockers (OR of 0.94) (112), ACE inhibitors (HR of 0.89) (108) and diuretics (OR of 0.96) (112) are currently not associated with Covid-19 severity. All risk values are close to one and the respective 95% CI's all show statistically insignificance (containing 1.0), see **Table 2**. This statistically insignificance is illustrated in **Figure 12** with an (*).

The most interesting of the antihypertensive *pharmaceutical interventions* is β-blockers, which reduced the risk of CHD (RR of 0.69). However, its use increases ones odds of developing severe Covid-19 (OR of 1.23) (112), see **Figure 12**. The reason for this is unclear and further studies are warranted to investigate the

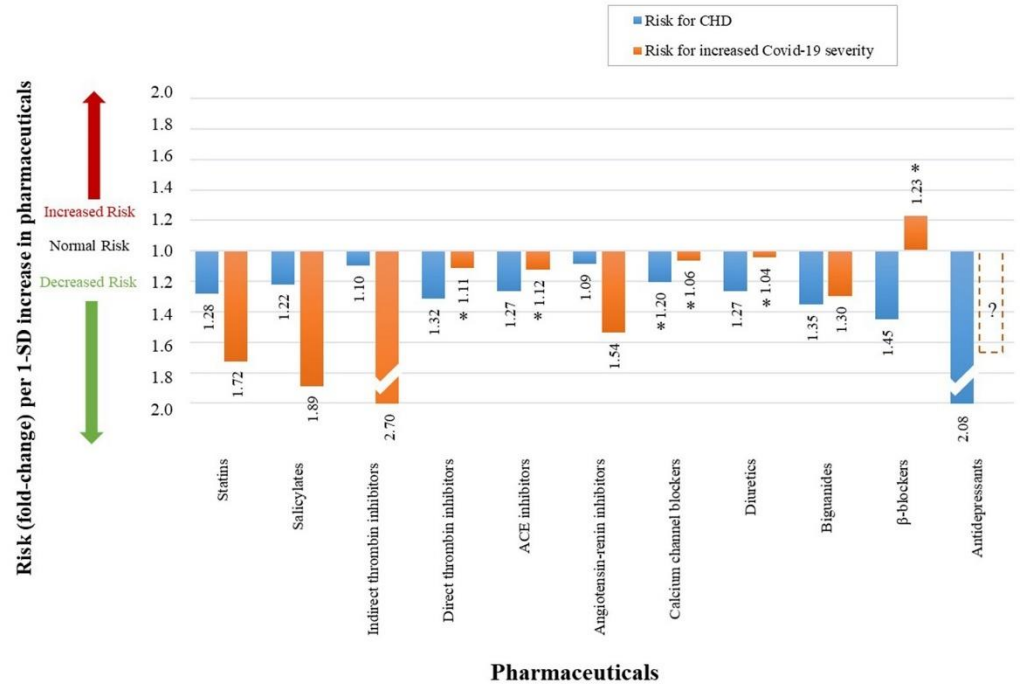

FIGURE 12 | The qualitative effect that different pharmaceuticals have on CHD risk and Covid-19 severity. (An accurate quantitative comparison is not possible, mostly due to differences in study design and size).

mechanism of action involved. However, one explanation for this difference could be that the data is insignificant for Covid-19, with a 95% CI of 0.74-2.04 (112), see **Table 2**.

Biguanides

Biguanides such as metformin has been used for many decades to treat type 2 diabetes and its use decreases the odds of developing CHD, with a OR of 0.74 (114), see **Table 2**. This translates to a 1.35-fold decrease in CHD risk (23), illustrated in **Figure 12**. Metformin's inhibition is observed on pathway (pw14) (23), see **Figure 4**.

Elevated blood glucose levels at admission is an independent predictor of Covid-19 severity irrespective of diabetes (75). Therefore, glucose lowering agents are expected to reduce Covid-19 mortality. This is indeed the case since a large observational cohort study of type-2 diabetics ($n = 1\ 800\ 005$) showed that the use of metformin decreased Covid-19-related mortality by 1.30-fold (HR of 0.77) (115), see **Figure 12** and **Table 2**.

Antidepressants (SSRIs)

We have done a detailed study of the mechanisms by which SSRI antidepressants may reduce CHD risk (24). We showed that SSRIs can influence most of the CHD hallmarks (24). A summary, relevant to Covid-19, is given below.

Selective serotonin uptake inhibitors (SSRIs) such as sertraline has shown to decrease the risk of CHD, with a HR of 0.48 (116), see **Table 2**. This translates to a 2.08-fold decrease in CHD risk (23), illustrated in **Figure 12**. Sertraline's actions are observed on the anti-inflammatory pathway (pw94), as shown in **Figure 4**.

A similar SSRI antidepressant, fluvoxamine's effect on Covid-19 severity is currently being investigated in a clinical trial (NCT04727424). This study was initiated by results from a small double-blind, randomized clinical trial of 152 Covid-19 positive patients treated with fluvoxamine (117). The outcomes of this study showed that patients treated with fluvoxamine, compared with a placebo, had a lower likelihood of clinical deterioration (0% vs. 8.3%) (117).

The study did not report any risk data. For this reason, the data could not be added to **Figure 12** and **Table 2**. Nevertheless, since a therapeutic effect is seen in the small Covid-19 study, a dotted bar was added to **Figure 12**. We hypothesize, based on our previous studies (24), that most SSRIs will be beneficial.

DISCUSSION AND FUTURE RESEARCH

The aim of this paper was to use a systems approach to explore the mechanisms between severe Covid-19 and its cardiovascular complications, as requested by *Frontiers*. The resulting *integrated*

CHD/Covid-19 model may provide insight into the various research questions, some also requested by *Frontiers*.

Why Do Some Patients With Severe Covid-19 Experience Sudden Death?

Although aspects of this has been proposed elsewhere (19, 22, 138, 145–148), here its integrated mechanism is systematically and visually shown with the relevant pathogenetic pathways with reference to CHD. This model further elucidates other underlying pathogenesis that may influence this *death spiral* before infection of SARS-CoV-2.

The *death spiral* was summarized as follows: Increased inflammation at the lungs causes EC injury, which can result in vascular leakage and/or activation of the coagulation cascade at the lungs, thereby causing hypoxia which can further increase inflammation, creating two closed positive feedback loops and causing severe Covid-19 through a *death spiral* (**Figure 5**).

How Do CHD Comorbidities Influence This *Death Spiral*?

It is widely accepted that patients with pre-existing CHD comorbidities (thus a poor initial vascular "baseline") have a high risk of developing severe Covid-19 (11–14). The detailed mechanisms of how these comorbidities may influence the *death spiral* was not fully integrated before.

This question was answered in this paper by visually (**Figures 8–10**) detailing the mechanisms of how three CHD comorbidities namely *Hypercholesterolemia, Hyperglycemia/Hyperinsulinemia* and *Hypertension* can fuel the *death spiral.*

How Can an Individual Reduce the Risk of Developing Severe Covid-19 From a Cardiovascular Point of View?

In literature different *health factors* (85, 87, 89, 91, 93, 95, 97) and CHD related *pharmaceuticals* (58, 101, 104, 106, 108, 110, 112, 115) present either a reduction or aggravation of Covid-19 severity. In this paper we provide the pathogenesis detailing the effect these *health factors* and *pharmaceuticals* may have on this *death spiral,* especially for those with an increased risk for CHD.

We have shown that severe Covid-19 and CHD have similarities in underlying pathogenesis. Therefore, following a lifestyle that would decrease one's risk for CHD before onset of Covid-19 should also decrease the chances of developing severe Covid-19.

The remaining two research questions [(4) and (5)] have partially been answered by the model but future research is still needed. These are discussed in more detail in the following two Sections.

How Can Computational Analysis Help to Assess the Risk of Severity in Covid-19 in Cardiovascular Disease?

One of the research questions posed by *Frontiers* in their request for papers was the following: *"How can computational analysis help to assess the risk of COVID-19 in cardiovascular disease?"* We speculate that to achieve such an outcome, at least the following must be done:

Step 1: Development of a fully integrated network model for the disease, accounting for all effects including cross linking.

Step 2: Characterization of each interaction (typically at the nodes of the network in Step 1) is needed to solve the network.

A first attempt at Step 1 for severe Covid-19 in cardiovascular disease was done in this paper (**Figure 4**). The next step is characterization of the network using the following equation:

$$Out_{1\to n} = f_{1\to n} In_{1\to n} \quad (1)$$

where $In_{1\to n}$ are the inputs (1 to n) to a node and $out_{1\to n}$ are the outputs (1 to n) from the node and f (1 to n) are the resulting transfer functions. The inputs and outputs are typically measured. More detail of this process is given in (23).

Using this process we have developed, over the past four decades, simulation software to solve complex engineering networks e.g., in deep mines and industrial complexes (149). Fortunately, in engineering it is easy to develop transfer functions (Equation 1) as it is relatively easy to do the required measurements. The challenge for medical networks is the measurements of all the relevant pathways in **Figure 4**.

A typical deep level mine simulation model (A) and a CHD simulation model (B) proposed in (23) are shown in **Figure 13**. The following has to be investigated in the future: if all the biomarkers can be measured for the proposed *integrated CHD/Covid-19 model*, will it be possible to individualize the network (**Figure 4**), thereby making it patient specific? This could be similar to us individualizing our engineering simulations to a specific mine.

The question is: can the risk for Covid-19 severity in CHD then be established for any specific individual by inputting the measured biomarkers of that person into the simulation model based on **Figure 4**? We have already attempted Step 1. However, for Step 2 much work and data are still needed.

Fortunately, there are numerous clinical trials currently underway that focus on treatments for Covid-19 with respect to the CHD hallmarks, namely the following:

(A) *Hypercoagulation* (122 trials)
(B) *Hypercholesterolemia* (23 trials)
(C) *Hyperglycemia /Hyperinsulinemia (Diabetes)* (84 trials)
(D) *Inflammation* (265 trials)
(E) *Hypertension* (68 trials)

The clinical trial numbers and respective treatments are available as **Supplementary Data**. The total number of registered clinical trials on CHD hallmarks effect on Covid-19 are 562. This also includes 94 duplicate studies that focus on more than one CHD hallmark.

If we can successfully develop a simulation model, could the best control strategy (pharmaceuticals) be calculated for each individual Covid-19 or CHD patient? This would be similar to identifying the optimum control strategies, which we

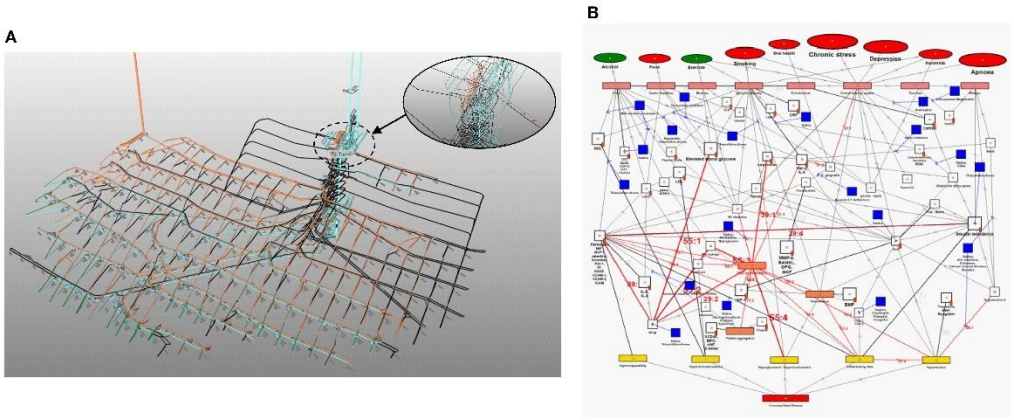

FIGURE 13 | Schematics of typical simulation networks for **(A)** engineering and **(B)** CHD (23). **(A)** provides a small section of computer model of a relatively complex deep mine. **(B)** shows the initial computer model (23) developed from the existing CHD model in **Figure 1** (23) using the simulation software developed for **(A)**. The CHD computer model includes all the known interactions for *health factors*, measured elements (salient biomarkers) and controls (*pharmaceutical interventions*). Remember it is the measured biomarkers that individualize a patient.

routinely calculate in engineering, for each individual mine or industrial complex.

However, we acknowledge that there are many assumptions and restrictions relevant to a CHD/Covid-19 computational analysis, which is completely speculative at present. For example, research is needed to investigate how individualized predictions will be feasible. The full details on the research question of computational analysis will be the purpose of future papers.

Are There Other Opportunities in Cardiovascular Disease That Can Be Derived From This Paper and the Covid-19 Crisis?

We have shown in this paper that the late-stage consequences of severe Covid-19 is often accelerated cardiovascular disease. We have also shown that most *pharmaceutical interventions* which mediate CHD also mediate the effects of Covid-19.

The question arises if the reverse is true. Are there any reported *pharmaceutical interventions* that reduced Covid-19 severity which could potentially be of value for vascular disease? This is an important question as approximately five times more people died during the past year from cardiovascular disease than from Covid-19.

Such a repurposed drug should preferably treat most of the hallmarks of cardiovascular disease. We investigated such a drug namely, ivermectin (150–155). Although ivermectin use is still controversial as a drug against Covid-19, studies over nearly three decades before Covid-19, has shown to reduce four of the five hallmarks of cardiovascular disease. These results and the publication dates are given below:

(A) *Hypercoagulability:* (1992) by increasing prothrombin time in 6.7% (ivermectin group) vs. 1.4% (control group) of participants *in vivo* (humans) (156).
(B) *Hypercholesterolemia:* cholesterol (2013) decreased by 1.5-fold *in vivo* (mice) (157).
(C) *Hyperglycemia:* fasting blood glucose (2013) decreased by 1.4-fold *in vivo* (mice) (157).
(D) *Hyperinsulinemia:* fasting insulin (2013) decreased by 2.0-fold *in vivo* (mice) (157).
(E) *Inflammation:* (2004) decreased IL-1β and TNF-α by 1.27-fold *in vitro* (158).

Except for the CHD hallmark *Inflammation* (159) the focus of ivermectin's proposed mechanism of action (MOA) for Covid-19 is currently on its anti-viral effect (150–153). However, if ivermectin really shows promise for Covid-19 treatment, could the full vascular MOA for ivermectin be as important or even more important than its anti-viral effects?

This research question can only be answered fully by clinical trials, which measure the relevant vascular biomarkers for each CHD hallmark before and after ivermectin use. Side effects of chronic use such as mild elevation of serum aminotransferases should also be investigated (160).

The MOA of ivermectin for prevention of Covid-19, reportedly seen in small studies (161), is also not clear to the authors. Why would the anti-viral MOA of ivermectin have a preventable effect if the patient has not been infected yet?

If ivermectin really helps for prevention of Covid-19, could it rather help create a healthier vascular system ("baseline") before the virus strikes, especially in vascular compromised individuals, rather than only help *via* its proposed anti-viral effect? Therefore,

could ivermectin's effect on the vascular system during severe Covid-19 be its most important MOA?

If well-designed clinical trials show that ivermectin could be a potential cardiovascular drug, could it be an ideal, inexpensive, drug for low- and middle-income countries where a high percentage of global cardiovascular related deaths occur (162)?

Other Research Questions Emanating From This Study

Other research questions that should be investigated in future research are the following:

1. Why would β -blockers have an opposite effect on Covid-19 severity than on CHD?
2. There exists an anomaly between statin's cholesterol lowering effect and low cholesterol levels seen in end-stage Covid-19. How can this drug help decrease Covid-19 severity while it further decreases cholesterol? Can statin's anti-inflammatory effect be so large that it overrides its cholesterol lowering effect? Would it then be better to drop statins and rather only use anti-inflammatory medication? Or does it depend on the stage of the disease, beneficial at first but not in the end stage?
3. Does a high correlation of most CHD related *pharmaceutical interventions* and Covid-19 mean that other CHD pharmaceuticals not investigated in detail for Covid-19 could also help reduce Covid-19 severity?
4. Are there pathways shown in the proposed model (**Figure 4**) that do not have pharmaceuticals to regulate them? Could this be the focus of new drug discovery for Covid-19 and cardiovascular disease?
5. Could the model be extended to include cerebrovascular disease and other cardiac diseases such as heart failure, valvular heart disease and peripheral artery disease?

CONCLUSION

Covid-19 data show that disease severity mostly occurs in patients with pre-existing cardiovascular comorbidities i.e., in patients with poor initial vascular "baselines." *Frontiers* therefore requested papers on how a systems approach can explore the mechanisms of cardiovascular complications in Covid-19.

This study attempted to fulfill this request by integrating pathways for severe Covid-19 into an existing coronary heart disease (CHD) model. The resulting *integrated CHD/Covid-19 model*, depicted in **Figure 4**, gives insights into the following issues, some also raised in the *Frontiers* request for research:

- The integrated CHD/Covid-19 pathogenesis of the *death spiral* seen in some critical Covid-19 patients.
- The comprehensive mechanisms of how underlying CHD comorbidities namely, *Hyperglycemia/Hyperinsulinemia, Hypercholesterolemia* and/or *Hypertension* may fuel the *death spiral.*
- The detailed pathogeneses of different *health factors*, which effect CHD risk and Covid-19 severity.
- The mechanisms of how chronic CHD *pharmaceutical interventions* may influence Covid-19 severity.
- The proposed model shows many pathways that currently do not have pharmaceuticals which influence them. This information can be the focus of future drug discovery.
- The proposed model can be further developed as a computational tool not only for Covid-19 application but also for cardiovascular disease.
- Insights into the hallmarks of CHD, shown in the *integrated CHD/Covid-19 model*, also led to various research questions that can form the basis for future research. This includes potential repurposing of an existing drug for cardiovascular disease.

Although the details in this study are complex the message is simple. Studies such as this one not only highlight the value of a cardiovascular healthy lifestyle in general but also specifically for Covid-19. With the sharp focus on Covid-19 we hope that this "healthy living" message will be intensified, thus help to reduce cardiovascular deaths, the prime killer of man.

DATA AVAILABILITY STATEMENT

The original contributions presented in the study are included in the article/**Supplementary Material**, further inquiries can be directed to the corresponding author/s.

AUTHOR CONTRIBUTIONS

AM developed the first draft (of more than 30) of the manuscript and compiled and analyzed the Covid-19 risk factor data. EM was the principal investigator. During level 5 Lockdown in May 2020 he initiated the original ideas and research including the *death spiral* and potential use of ivermectin for CHD based on MM's Ph.D. AM and AG developed the integrated CHD/Covid-19 model from literature. MM developed the CHD-based model and provided expert opinion for the integration of the model with Covid-19. All authors have assisted in revisions and have approved the final manuscript.

FUNDING

The research was funded by EM and HumanSim (Pty) Ltd.

ACKNOWLEDGMENTS

Kristy Nell compiled the clinical trial data presented in the manuscript as **Supplementary Information**. C. Mathews helped with the initial CHD Covid-19 link and provided funding *via* HumanSim (Pty) Ltd. We thank her for her continuous inputs. The initial angel investor was Dr. Arnold van Dyk.

SUPPLEMENTARY MATERIAL

The Supplementary Material for this article can be found online at: https://www.frontiersin.org/articles/10.3389/fcvm.2022.737592/full#supplementary-material

REFERENCES

1. Liu YC, Kuo RL, Shih SR. COVID-19: the first documented coronavirus pandemic in history. *Biomed J.* (2020) 43:328–33. doi: 10.1016/j.bj.2020.04.007
2. Valencia DN. Brief review on COVID-19: the 2020 pandemic caused by SARS-CoV-2. *Cureus.* (2020) 12:e7386. doi: 10.7759/cureus.7386
3. World Health Organization. *Weekly Epidemiological Update on COVID-19 - 10 August 2021* (2021). Available online at: https://www.who.int/publications/m/item/weekly-epidemiological-update-on-covid-19 (accessed August 10, 2021).
4. Ackermann M, Verleden SE, Kuehnel M, Haverich A, Welte T, Laenger F, et al. Pulmonary vascular endothelialitis, thrombosis, and angiogenesis in Covid-19. *N Engl J Med.* (2020) 383:120–8. doi: 10.1056/NEJMoa2015432
5. Martins-Filho P, Santos C, Tavares S, Antos V. Factors associated with mortality in patients with COVID-19. A quantitative evidence synthesis of clinical and laboratory data. *Eur J Intern Med.* (2020) 76:97–9. doi: 10.1016/j.ejim.2020.04.043
6. Wichmann D, Sperhake J-P, Lütgehetmann M, Steurer S, Edler C, Heinemann A, et al. Autopsy findings and venous thromboembolism in patients with COVID-19. *Ann Intern Med.* (2020) 173:1030. doi: 10.7326/L20-1206
7. Fox SE, Akmatbekov A, Harbert JL, Li G, Quincy Brown J, Vander Heide RS. Pulmonary and cardiac pathology in African American patients with COVID-19: an autopsy series from New Orleans. *Lancet Respir Med.* (2020) 8:681–6. doi: 10.1016/S2213-2600(20)30243-5
8. Lax SF, Skok K, Zechner P, Kessler HH, Kaufmann N, Koelblinger C, et al. Pulmonary arterial thrombosis in COVID-19 with fatal outcome: results from a prospective, single-center, clinicopathologic case series. *Ann Intern Med.* (2020) 173:330–61. doi: 10.2139/ssrn.3586685
9. Varga Z, Flammer AJ, Steiger P, Haberecker M, Andermatt R, Zinkernagel AS, et al. Endothelial cell infection and endotheliitis in COVID-19. *Lancet.* (2020) 395:1417–8. doi: 10.1016/S0140-6736(20)30937-5
10. Clark A, Jit M, Warren-gash C, Guthrie B, Wang HHX, Mercer SW, et al. Global, regional, and national estimates of the population at increased risk of severe COVID-19 due to underlying health conditions in 2020: a modelling study. *Lancet Glob Heal.* (2020) 8:e1003–17. doi: 10.1016/S2214-109X(20)30264-3
11. Zheng Z, Peng F, Xu B, Zhao J, Liu H, Peng J, et al. Risk factors of critical & mortal COVID-19 cases: a systematic literature review and meta-analysis. *J Infect.* (2020) 81:e16–25. doi: 10.1016/j.jinf.2020.04.021
12. Zhou F, Yu T, Du R, Fan G, Liu Y, Liu Z, et al. Clinical course and risk factors for mortality of adult inpatients with COVID-19 in Wuhan, China: a retrospective cohort study. *Lancet.* (2020) 395:1054–62. doi: 10.1016/S0140-6736(20)30566-3
13. Ssentongo P, Ssentongo AE, Heilbrunn ES, Ba DM, Chinchilli VM. Association of cardiovascular disease and 10 other pre-existing comorbidities with COVID-19 mortality: a systematic review and meta-analysis. *PLoS ONE.* (2020) 15:1–16. doi: 10.1371/journal.pone.0238215
14. Luo L, Fu M, Li Y, Hu S, Luo J, Chen Z, et al. The potential association between common comorbidities and severity and mortality of coronavirus disease 2019: a pooled analysis. *Clin Cardiol.* (2020) 43:1478–93. doi: 10.1002/clc.23465
15. Zheng YY, Ma YT, Zhang JY, Xie X. COVID-19 and the cardiovascular system. *Nat Rev Cardiol.* (2020) 17:259–60. doi: 10.1038/s41569-020-0360-5
16. Long B, Brady WJ, Koyfman A, Gottlieb M. Cardiovascular complications in COVID-19. *Am J Emerg Med.* (2020) 38:1504–7. doi: 10.1016/j.ajem.2020.04.048
17. Liu PP, Blet A, Smyth D, Li H. The science underlying COVID-19: implications for the cardiovascular system. *Circulation.* (2020) 142:68–78. doi: 10.1161/CIRCULATIONAHA.120.047549
18. Libby P. The heart in COVID-19: primary target or secondary bystander? *JACC Basic Transl Sci.* (2020) 5:537–42. doi: 10.1016/j.jacbts.2020.04.001
19. Atri D, Siddiqi HK, Lang JP, Nauffal V, Morrow DA, Bohula EA. COVID-19 for the cardiologist: basic virology, epidemiology, cardiac manifestations, and potential therapeutic strategies. *JACC Basic to Transl Sci.* (2020) 5:518–36. doi: 10.1016/j.jacbts.2020.04.002
20. Tay MZ, Poh CM, Rénia L, MacAry PA, Ng LFP. The trinity of COVID-19: immunity, inflammation and intervention. *Nat Rev Immunol.* (2020) 20:363–74. doi: 10.1038/s41577-020-0311-8
21. Barton LM, Duval EJ, Stroberg E, Ghosh S, Mukhopadhyay S. COVID-19 autopsies, Oklahoma, USA. *Am J Clin Pathol.* (2020) 153:725–33. doi: 10.1093/ajcp/aqaa062
22. Teuwen LA, Geldhof V, Pasut A, Carmeliet P. COVID-19: the vasculature unleashed. *Nat Rev Immunol.* (2020) 20:389–91. doi: 10.1038/s41577-020-0343-0
23. Mathews MJ. A systems engineering approach to coronary heart disease. *Philos Mech Eng North West Univ South Africa.* (2015). Available online at: https://repository.nwu.ac.za/handle/10394/18953
24. Mathews MJ, Mathews EH, Liebenberg L. The mechanisms by which antidepressants may reduce coronary heart disease risk. *BMC Cardiovasc Disord.* (2015) 15:1–12. doi: 10.1186/s12872-015-0074-5
25. Mathews MJ, Liebenberg L, Mathews EH. How do high glycemic load diets influence coronary heart disease? *Nutr Metab.* (2015) 12:1–15. doi: 10.1186/s12986-015-0001-x
26. Mathews MJ, Liebenberg L, Mathews EH. The mechanism by which moderate alcohol consumption influences coronary heart disease. *Nutr J.* (2015) 14:1–12. doi: 10.1186/s12937-015-0011-6
27. Mathews MJ, Mathews EH, Mathews GE. Oral health and coronary heart disease. *BMC Oral Health.* (2016) 16:1–10. doi: 10.1186/s12903-016-0316-7
28. Mathews MJ, Mathews EH, Mathews GE. The integrated effect of moderate exercise on coronary heart disease. *Cardiovasc J Afr.* (2017) 28:125–33. doi: 10.5830/CVJA-2016-058
29. Puccetti L, Bruni F, Di Renzo M, Bova G, Cercignani M, Iadanza A, et al. Hypercoagulable state in hypercholesterolemic subjects assessed by platelet-dependent thrombin generation: *in vitro* effect of Cerivastatin. *Eur Rev Med Pharmacol Sci.* (1999) 3:197–204.
30. Andersen P. Hypercoagulability and reduced fibrinolysis in hyperlipidemia: relationship to the metabolic cardiovascular syndrome. *J Cardiovasc Pharmacol.* (1992) 20:S29–31. doi: 10.1097/00005344-199200208-00007
31. Tjaden K, Pardali E, Waltenberger J. Hypercholesterolemia induces vascular cell dysfunction: molecular basis for atherosclerosis. *Austin J Vasc Med.* (2015) 2:1–9. Available online at: https://austinpublishinggroup.com/vascular-medicine/fulltext/ajvm-v2-id1011.php
32. Radenkovic D, Chawla S, Pirro M, Sahebkar A, Banach M. Cholesterol in relation to COVID-19: should we care about it? *J Clin Med.* (2020) 9:1909. doi: 10.3390/jcm9061909
33. Sanders DW, Jumper CC, Ackerman PJ, Bracha D, Donlic A, Kim H, et al. Sars-cov-2 requires cholesterol for viral entry and pathological syncytia formation. *Elife.* (2021) 10:1–47. doi: 10.7554/eLife.65962
34. Wang H, Yuan Z, Pavel MA, Hansen SB. The role of high cholesterol in age-related COVID19 lethality. *bioRxiv [Preprint].* (2020) 1–17. doi: 10.1101/2020.05.09.086249
35. Pranata R, Huang I, Lim MA, Wahjoepramono EJ, July J. Impact of cerebrovascular and cardiovascular diseases on mortality and severity of COVID-19–systematic review, meta-analysis, and meta-regression. *J Stroke Cerebrovasc Dis.* (2020) 29:104949. doi: 10.1016/j.jstrokecerebrovasdis.2020.104949
36. Bourgonje AR, Abdulle AE, Timens W, Hillebrands J-L, Navis GJ, Gordijn SJ, et al. Angiotensin-converting enzyme 2 (ACE2), SARS-CoV−2 and the pathophysiology of coronavirus disease 2019 (COVID-19). *J Pathol.* (2020) 251:228–48. doi: 10.1002/path.5471
37. Huertas A, Montani D, Savale L, Pichon J, Tu L, Parent F, et al. Endothelial cell dysfunction: a major player in SARS-CoV-2 infection (COVID-19)? *Eur Respir J.* (2020) 56:2001634. doi: 10.1183/13993003.01634-2020
38. Dandona P, Dhindsa S, Ghanim H, Chaudhuri A. Angiotensin II and inflammation: the effect of angiotensin-converting enzyme inhibition and angiotensin II receptor blockade. *J Hum Hypertens.* (2007) 21:20–27. doi: 10.1038/sj.jhh.1002101
39. Esmon CT. The interactions between inflammation and coagulation. *Br J Haematol.* (2005) 131:417–30. doi: 10.1111/j.1365-2141.2005.05753.x
40. Lindner D, Fitzek A, Bräuninger H, Aleshcheva G, Edler C, Meissner K, et al. Association of cardiac infection with SARS-CoV-2 in confirmed COVID-19 autopsy cases. *JAMA Cardiol.* (2020) 5:1281–5. doi: 10.1001/jamacardio.2020.3551

41. Catanzaro M, Fagiani F, Racchi M, Corsini E, Govoni S, Lanni C. Immune response in COVID-19: addressing a pharmacological challenge by targeting pathways triggered by SARS-CoV-2. *Signal Transduct Target Ther.* (2020) 5:1–10. doi: 10.1038/s41392-020-0191-1
42. Qin C, Zhou L, Hu Z, Zhang S, Yang S, Tao Y, et al. Dysregulation of immune response in patients with COVID-19 in Wuhan, China. *Clin Infect Dis.* (2020) 71:762–8. doi: 10.1093/cid/ciaa248
43. Ruan Q, Yang K, Wang W, Jiang L, Song J. Clinical predictors of mortality due to COVID-19 based on an analysis of data of 150 patients from Wuhan, China. *Intensive Care Med.* (2020) 46:846–8. doi: 10.1007/s00134-020-05991-x
44. Giamarellos-Bourboulis EJ, Netea MG, Rovina N, Akinosoglou K, Antoniadou A, Antonakos N, et al. Complex immune dysregulation in COVID-19 patients with severe respiratory failure. *Cell Host Microbe.* (2020) 27:992–1000.e3. doi: 10.1016/j.chom.2020.04.009
45. Zhang C. The role of inflammatory cytokines in endothelial dysfunction. *Basic Res Cardiol.* (2008) 103:398–406. doi: 10.1007/s00395-008-0733-0
46. Leo N, Alexander L, Sophia B, Rainer K, Tobias W, Michael W, et al. Immunothrombotic dysregulation in COVID-19 pneumonia is associated with respiratory failure and coagulopathy. *Circulation.* (2020) 142:1176–89. doi: 10.1161/CIRCULATIONAHA.120.048488
47. Winterbourn CC, Kettle AJ, Hampton MB. Reactive oxygen species and neutrophil function. *Annu Rev Biochem.* (2016) 85:765–92. doi: 10.1146/annurev-biochem-060815-014442
48. Chaudhry H, Zhou J, Zhong Y, Ali MM, Mcguire F, Nagarkatti PS, et al. Role of cytokines as a double-edged sword in sepsis. *In Vivo.* (2015) 27:669–84.
49. Sarkar M, Niranjan N, Banyal PK. Mechanisms of hypoxemia. *Lung India.* (2017) 34:47–60. doi: 10.4103/0970-2113.197116
50. Millar FR, Summers C, Griffiths MJ, Toshner MR, Proudfoot AG. The pulmonary endothelium in acute respiratory distress syndrome: insights and therapeutic opportunities. *Thorax.* (2016) 71:462–73. doi: 10.1136/thoraxjnl-2015-207461
51. Pober JS, Sessa WC. Evolving functions of endothelial cells in inflammation. *Nat Rev Immunol.* (2007) 7:803–15. doi: 10.1038/nri2171
52. Bikdeli B, Madhavan M V., Jimenez D, Chuich T, Dreyfus I, Driggin E, et al. COVID-19 and thrombotic or thromboembolic disease: implications for prevention, antithrombotic therapy, and follow-up: JACC state-of-the-art review. *J Am Coll Cardiol.* (2020) 75:2950–73. doi: 10.1016/j.jacc.2020.04.031
53. Eltzschig HK, Carmeliet P. Hypoxia and inflammation. *N Engl J Med.* (2011) 364:656–65. doi: 10.1056/NEJMra0910283
54. Görlach A, Dimova EY, Petry A, Martínez-Ruiz A, Hernansanz-Agustín P, Rolo AP, et al. Reactive oxygen species, nutrition, hypoxia and diseases: problems solved? *Redox Biol.* (2015) 6:372–85. doi: 10.1016/j.redox.2015.08.016
55. Mellado-Artigas R, Ferreyro BL, Angriman F, Hernández-Sanz M, Arruti E, Torres A, et al. High-flow nasal oxygen in patients with COVID-19-associated acute respiratory failure. *Crit Care.* (2021) 25:1–10. doi: 10.1186/s13054-021-03469-w
56. The RECOVERY Collaborative Group. Dexamethasone in hospitalized patients with Covid-19 — preliminary report. *N Engl J Med.* (2020) 384:693–704. doi: 10.1056/NEJMoa2021436
57. Hong W, Chen Y, You K, Tan S, Wu F, Tao J, et al. Celebrex adjuvant therapy on coronavirus disease 2019: an experimental study. *Front Pharmacol.* (2020) 11:1–9. doi: 10.3389/fphar.2020.561674
58. Chow JH, Khanna AK, Kethireddy S, Yamane D, Levine A, Jackson AM, et al. Aspirin use is associated with decreased mechanical ventilation, ICU admission, and in-hospital mortality in hospitalized patients with COVID-19. *Anesth Analg.* (2021) 132:930–41. doi: 10.1213/ANE.0000000000005292
59. Bizien N, Noel-Savina E, Tromeur C, Delluc A, Mottier D, Leroyer C, et al. Age is a major risk factor of venous thromboembolism (VTE). *Eur Respir J.* (2011) 38:3936. doi: 10.1097/01.mcp.0000174246.15386.69
60. Pijls BG, Jolani S, Atherley A, Derckx RT, Dijkstra JIR, Franssen GHL, et al. Demographic risk factors for COVID-19 infection, severity, ICU admission and death: a meta-analysis of 59 studies. *BMJ Open.* (2021) 11:e044640. doi: 10.1136/bmjopen-2020-044640
61. Roach REJ, Cannegieter SC, Lijfering WM. Differential risks in men and women for first and recurrent venous thrombosis: the role of genes and environment. *J Thromb Haemost.* (2014) 12:1593–600. doi: 10.1111/jth.12678
62. Zakai NA, Mcclure LA. Racial differences in venous thromboembolism. *J Thromb Haemost.* (2011) 9:1877–82. doi: 10.1111/j.1538-7836.2011.04443.x
63. Golestaneh L, Neugarten J, Fisher M, Billett HH, Gil MR, Johns T, et al. The association of race and COVID-19 mortality. *EClinicalMedicine.* (2020) 25:100455. doi: 10.1016/j.eclinm.2020.100455
64. Groot HE, Sierra LEV, Said MA, Lipsic E, Karper JC, Van Der Harst P. Genetically determined ABO blood group and its associations with health and disease. *Arterioscler Thromb Vasc Biol.* (2020) 40:830–8. doi: 10.1161/ATVBAHA.119.313658
65. Wu B, Gu D, Yu J, Yang J, Shen W. Association between ABO blood groups and COVID-19 infection, severity and demise: a systematic review and meta-analysis. *Infect Genet Evol.* (2020) 84:104485. doi: 10.1016/j.meegid.2020.104485
66. Pomp ER, Lenselink AM, Rosendaal FR, Doggen CJM. Pregnancy, the postpartum period and prothrombotic defects: risk of venous thrombosis in the MEGA study. *J Thromb Haemost.* (2008) 6:632–37. doi: 10.1111/j.1538-7836.2008.02921.x
67. Qeadan F, Mensah NA, Tingey B, Stanford JB. The risk of clinical complications and death among pregnant women with COVID-19 in the Cerner COVID-19 cohort: a retrospective analysis. *BMC Pregn Childbirth.* (2021) 21:1–14. doi: 10.1186/s12884-021-03772-y
68. Silverstein MD, Heit JA, Mohr DN, Petterson TM, O'Fallon WM, Melton J. Trends in the incidence of deep vein thrombosis and pulmonary embolism. *Arch Intern Med.* (1998) 158:585–593. doi: 10.1001/archinte.158.6.585
69. Boudin L, Dutasta F. Relationship between ABO blood groups and coronavirus disease 2019: study design matters. *Clin Infect Dis.* (2021) 72:e927–8. doi: 10.1093/cid/ciaa1473
70. Zaki N, Alashwal H, Ibrahim S. Association of hypertension, diabetes, stroke, cancer, kidney disease, and high-cholesterol with COVID-19 disease severity and fatality: a systematic review. *Diabetes Metab Syndr Clin Res Rev.* (2020) 14:1133–42. doi: 10.1016/j.dsx.2020.07.005
71. Chu Y, Yang J, Shi J, Zhang P, Wang X. Obesity is associated with increased severity of disease in COVID-19 pneumonia: a systematic review and meta-analysis. *Eur J Med Res.* (2020) 25:1–15. doi: 10.1186/s40001-020-00464-9
72. Veghari G, Sedaghat M, Joshghani H, Banihashem S, Moharloei P, Angizeh A, et al. Obesity and risk of hypercholesterolemia in Iranian northern adults. *ARYA Atheroscler.* (2013) 9:2–6.
73. Veghari G, Sedaghat M, Maghsodlo S, Banihashem S, Moharloei P, Angizeh A, et al. The association between abdominal obesity and serum cholesterol level. *Int J Appl Basic Med Res.* (2015) 5:83. doi: 10.4103/2229-516X.157150
74. Wei X, Zeng W, Su J, Wan H, Yu X, Cao X, et al. Hypolipidemia is associated with the severity of COVID-19. *J Clin Lipidol.* (2020) 14:297–304. doi: 10.1016/j.jacl.2020.04.008
75. Wang S, Ma P, Zhang S, Song S, Wang Z, Ma Y, et al. Fasting blood glucose at admission is an independent predictor for 28-day mortality in patients with COVID-19 without previous diagnosis of diabetes: a multi-centre retrospective study. *Diabetologia.* (2020) 63:2102–11. doi: 10.1007/s00125-020-05209-1
76. Wu J, Huang J, Zhu G, Wang Q, Lv Q, Huang Y, et al. Elevation of blood glucose level predicts worse outcomes in hospitalized patients with COVID-19: a retrospective cohort study. *BMJ Open Diabetes Res Care.* (2020) 8:1–7. doi: 10.1136/bmjdrc-2020-001476
77. Avogaro A, Albiero M, Menegazzo L, De Kreutzenberg S, Fadini GP. Endothelial dysfunction in diabetes: the role of reparatory mechanisms. *Diabetes Care.* (2011) 34:S285–S90. doi: 10.2337/dc11-s239
78. Loomans CJM, De Koning EJP, Staal FJT, Rookmaaker MB, Verseyden C, De Boer HC, et al. Endothelial progenitor cell dysfunction: a novel concept in the pathogenesis of vascular complications of type 1 diabetes. *Diabetes.* (2004) 53:195–9. doi: 10.2337/diabetes.53.1.195
79. Rogers SC, Zhang X, Azhar G, Luo S, Wei JY. Exposure to high or low glucose levels accelerates the appearance of markers of endothelial cell senescence and induces dysregulation of nitric oxide synthase. *J Gerontol Ser A Biol Sci Med Sci.* (2013) 68:1469–81. doi: 10.1093/gerona/glt033
80. Brownlee M. The pathobiology of diabetic complications: a unifying mechanism. *Diabetes.* (2005) 54:1615–25. doi: 10.2337/diabetes.54.6.1615

81. Zuin M, Rigatelli G, Zuliani G, Rigatelli A, Mazza A, Roncon L. Arterial hypertension and risk of death in patients with COVID-19 infection: systematic review and meta-analysis Dear. *J Infect.* (2020) 81:e84–6. doi: 10.1016/j.jinf.2020.03.059
82. Bleakley C, Hamilton PK, Pumb R, Harbinson M, Mcveigh GE. Endothelial function in hypertension: victim or culprit? *J Clin Hypertens.* (2015) 17:651–4. doi: 10.1111/jch.12546
83. Taniyama Y, Griendling KK. Reactive oxygen species in the vasculature: molecular and cellular mechanisms. *Hypertension.* (2003) 42:1075–81. doi: 10.1161/01.HYP.0000100443.09293.4F
84. Sattelmair J, Pertman J, Ding EL, Kohl HW, Haskell W, Lee I-M. Dose-response between physical activity and risk of coronary heart disease: a meta-analysis. *Circulation.* (2011) 124:789–95. doi: 10.1161/CIRCULATIONAHA.110.010710
85. Tavakol Z, Ghannadi S, Tabesh MR, Halabchi F, Noormohammadpour P, Akbarpour S, et al. Relationship between physical activity, healthy lifestyle and COVID-19 disease severity; a cross-sectional study. *Z Gesundh Wiss.* (2021) 1–9. doi: 10.1007/s10389-020-01468-9
86. Hackshaw A, Morris JK, Boniface S, Tang JL, Milenkovi D. Low cigarette consumption and risk of coronary heart disease and stroke: meta-analysis of 141 cohort studies in 55 study reports. *BMJ.* (2018) 360:j5855. doi: 10.1136/bmj.j5855
87. Reddy RK, Charles WN, Sklavounos A, Dutt A, Seed PT, Khajuria A. The effect of smoking on COVID-19 symptom severity: systematic review and meta-analysis. *J Med Virol.* (2020) 93:1045–56. doi: 10.1002/jmv.26389
88. Blaizot A, Vergnes J-N, Nuwwareh S, Amar J, Sixou M. Periodontal diseases and cardiovascular events: meta-analysis of observational studies. *Int Dent J.* (2009) 59:197–209.
89. Marouf N, Cai W, Said KN, Daas H, Diab H, Chinta VR, et al. Association between periodontitis and severity of COVID-19 infection: a case–control study. *J Clin Periodontol.* (2021) 48:483–91. doi: 10.1111/jcpe.13435
90. Rosengren A, Hawken S, Ôunpuu S, Sliwa PK, Zubaid M, Almahmeed WA, Ngu Blackett K, et al. Association of psychosocial risk factors with risk of acute myocardial infarction in 11 119 cases and 13 648 controls from 52 countries (the INTERHEART study): case-control study. *Lancet.* (2004) 364:953–62. doi: 10.1016/S0140-6736(04)17019-0
91. Tant T, Khoot B, Mills EG, Phylactou M, Patel B, Eng PC, et al. Association between high serum total cortisol concentrations and mortality from COVID-19. *Lancet Diabetes Endocrinol.* (2020) 8:659–60. doi: 10.1016/S2213-8587(20)30216-3
92. Nicholson A, Kuper H, Hemingway H. Depression as an aetiologic and prognostic factor in coronary heart disease: a meta-analysis of 6362 events among 146 538 participants in 54 observational studies. *Eur Heart J.* (2006) 27:2763–74. doi: 10.1093/eurheartj/ehl338
93. Yang H, Chen W, Hu Y, Chen Y, Zeng Y, Sun Y, et al. Pre-pandemic psychiatric disorders and risk of COVID-19: a UK Biobank cohort analysis. *Lancet Heal Longev.* (2020) 1:e69–79. doi: 10.1016/S2666-7568(20)30013-1
94. Shah NA, Yaggi HK, Concato J, Mohsenin V. Obstructive sleep apnea as a risk factor for coronary events or cardiovascular death. *Sleep Breath.* (2010) 14:131–6. doi: 10.1007/s11325-009-0298-7
95. Strausz S, Kiiskinen T, Broberg M, Ruotsalainen S, Koskela J, Bachour A, et al. Sleep apnoea is a risk factor for severe COVID-19. *BMJ Open Respir Res.* (2021) 8:6–11. doi: 10.1136/bmjresp-2020-000845
96. Sofi F, Cesari F, Casini A, Macchi C, Abbate R, Gensini GF. Insomnia and risk of cardiovascular disease: a meta-analysis. *Eur J Prev Cardiol.* (2014) 21:57–64. doi: 10.1177/2047487312460020
97. Kim H, Hegde S, Lafiura C, Raghavan M, Luong E, Cheng S, et al. COVID-19 illness in relation to sleep and burnout. *BMJ Nutr Prev Heal.* (2021) 4:132–9. doi: 10.1136/bmjnph-2021-000228
98. Ronksley PE, Brien SE, Turner BJ, Mukamal KJ, Ghali WA. Association of alcohol consumption with selected cardiovascular disease outcomes: a systematic review and meta-analysis. *BMJ.* (2011) 342:d671. doi: 10.1136/bmj.d671
99. Dong JY, Zhang YH, Wang P, Qin LQ. Meta-analysis of dietary glycemic load and glycemic index in relation to risk of coronary heart disease. *Am J Cardiol.* (2012) 109:1608–13. doi: 10.1016/j.amjcard.2012.01.385
100. Baigent C, Blackwell L, Emberson J, Holland LE, Reith C, Bhala N, et al. Efficacy and safety of more intensive lowering of LDL cholesterol: a meta-analysis of data from 170 000 participants in 26 randomised trials. *Lancet.* (2010) 376:1670–81. doi: 10.1016/S0140-6736(10)61350-5
101. Zhang XJ, Qin JJ, Cheng X, Shen L, Zhao YC, Yuan Y, et al. In-hospital use of statins is associated with a reduced risk of mortality among individuals with COVID-19. *Cell Metab.* (2020) 32:1–12. doi: 10.1016/j.cmet.2020.06.015
102. Collins R, Peto R, Hennekens C, Doll R, Bubes V, Buring J, et al. Aspirin in the primary and secondary prevention of vascular disease: collaborative meta-analysis of individual participant data from randomised trials. *Lancet.* (2009) 373:1849–60. doi: 10.1016/S0140-6736(09)60503-1
103. Boersma E, Harrington RA, Moliterno DJ, White H, Théroux P, Van De Werf F, et al. Platelet glycoprotein IIb/IIIa inhibitors in acute coronary syndromes: a meta-analysis of all major randomised clinical trials. *Lancet.* (2002) 359:189–98. doi: 10.1016/S0140-6736(02)07442-1
104. Tang N, Bai H, Chen X, Gong J, Li D, Sun Z. Anticoagulant treatment is associated with decreased mortality in severe coronavirus disease 2019 patients with coagulopathy. *J Thromb Haemost.* (2020) 18:1094–9. doi: 10.1111/jth.14817
105. Wallentin L, Wilcox RG, Weaver WD, Emanuelsson H, Goodvin A, Nyström P, et al. Oral ximelagatran for secondary prophylaxis after myocardial infarction: the ESTEEM randomised controlled trial. *Lancet.* (2003) 362:789–97. doi: 10.1016/S0140-6736(03)14287-0
106. Flam B, Wintzell V, Ludvigsson JF, Mårtensson J, Pasternak B. Direct oral anticoagulant use and risk of severe COVID-19. *J Intern Med.* (2021) 289:411–9. doi: 10.1111/joim.13205
107. Verdecchia P, Reboldi G, Angeli F, Gattobigio R, Bentivoglio M, Thijs L, et al. Angiotensin-converting enzyme inhibitors and calcium channel blockers for coronary heart disease and stroke prevention. *Hypertension.* (2005) 46:386–92. doi: 10.1161/01.HYP.0000174591.42889.a2
108. Hippisley-Cox J, Young D, Coupland C, Channon KM, Tan PS, Harrison DA, et al. Risk of severe COVID-19 disease with ACE inhibitors and angiotensin receptor blockers: cohort study including 8.3 million people. *Heart.* (2020) 106:1503–11. doi: 10.1136/heartjnl-2020-317393
109. Savarese G, Costanzo P, Cleland JGF, Vassallo E, Ruggiero D, Rosano G, et al. A meta-analysis reporting effects of angiotensin-converting enzyme inhibitors and angiotensin receptor blockers in patients without heart failure. *J Am Coll Cardiol.* (2013) 61:131–42. doi: 10.1016/j.jacc.2012.10.011
110. Gao C, Cai Y, Zhang K, Zhou L, Zhang Y, Zhang X, et al. Association of hypertension and antihypertensive treatment with COVID-19 mortality: a retrospective observational study. *Eur Heart J.* (2020) 41:2058–66. doi: 10.1093/eurheartj/ehaa433
111. De Peuter OR, Lussana F, Peters RJG, Büller HR, Kamphuisen PW. A systematic review of selective and non-selective beta blockers for prevention of vascular events in patients with acute coronary syndrome or heart failure. *Neth J Med.* (2009) 67:284–94.
112. Ren L, Yu S, Xu W, Overton JL, Chiamvimonvat N, Thai PN. Lack of association of antihypertensive drugs with the risk and severity of COVID-19: a meta-analysis. *J Cardiol.* (2021) 77:482–91. doi: 10.1016/j.jjcc.2020.10.015
113. Psaty BM, Lumley T, Furberg CD, Schellenbaum G, Pahor M, Alderman MH, et al. Health Outcomes associated with various antihypertensive therapies used as first-line agents: a network meta-analysis. *J Am Med Assoc.* (2003) 289:2534–44. doi: 10.1001/jama.289.19.2534
114. Selvin E, Bolen S, Yeh HC, Wiley C, Wilson LM, Marinopoulos SS, et al. Cardiovascular outcomes in trials of oral diabetes medications: a systematic review. *Arch Intern Med.* (2008) 168:2070–80. doi: 10.1001/archinte.168.19.2070
115. Khunti K, Knighton P, Zaccardi F, Bakhai C, Barron E, Holman N, et al. Prescription of glucose-lowering therapies and risk of COVID-19 mortality in people with type 2 diabetes: a nationwide observational study in England. *Lancet Diabetes Endocrinol.* (2021) 8587:1–11. doi: 10.1016/S2213-8587(21)00050-4
116. Scherrer JF, Garfield LD, Lustman PJ, Hauptman PJ, Chrusciel T, Zeringue A, et al. Antidepressant drug compliance: reduced risk of MI and mortality in depressed patients. *Am J Med.* (2011) 124:318–24. doi: 10.1016/j.amjmed.2010.11.015
117. Lenze EJ, Mattar C, Zorumski CF, Stevens A, Schweiger J, Nicol GE, et al. Fluvoxamine vs placebo and clinical deterioration in outpatients

with symptomatic COVID-19: a randomized clinical Trial. *JAMA*. (2020) 324:2292–300. doi: 10.1001/jama.2020.22760

118. Sallis R, Young DR, Tartof SY, Sallis JF, Sall J, Li Q, et al. Physical inactivity is associated with a higher risk for severe COVID-19 outcomes: a study in 48 440 adult patients. *Br J Sports Med*. (2021) 55:1099–105. doi: 10.1136/bjsports-2021-104080
119. Nieman DC, Wentz LM. The compelling link between physical activity and the body's defense system. *J Sport Heal Sci*. (2019) 8:201–17. doi: 10.1016/j.jshs.2018.09.009
120. Facchini FS, Hollenbeck CB, Jeppesen J, Ida Chen YD, Reaven GM. Insulin resistance and cigarette smoking. *Lancet*. (1992) 339:1128–30. doi: 10.1016/0140-6736(92)90730-Q
121. Reaven G, Tsao PS. Insulin resistance and compensatory hyperinsulinemia: the key player between cigarette smoking and cardiovascular disease? *J Am Coll Cardiol*. (2003) 41:1044–7. doi: 10.1016/S0735-1097(02)02982-0
122. Takefuji S, Yatsuya H, Tamakoshi K, Otsuka R, Wada K, Matsushita K, et al. Smoking status and adiponectin in healthy Japanese men and women. *Prev Med*. (2007) 45:471–5. doi: 10.1016/j.ypmed.2007.07.001
123. Badrick E, Kirschbaum C, Kumari M. The relationship between smoking status and cortisol secretion. *J Clin Endocrinol Metab*. (2007) 92:819–24. doi: 10.1210/jc.2006-2155
124. Craig WY, Palomaki GE, Haddow JE. Cigarette smoking and serum lipid and lipoprotein concentrations: an analysis of published data. *BMJ*. (1989) 298:784–8. doi: 10.1136/bmj.298.6676.784
125. Lee J, Taneja V, Vassallo R. Cigarette smoking and inflammation: cellular and molecular mechanisms. *J Dent Res*. (2012) 91:142–9. doi: 10.1177/0022034511421200
126. Barua RS, Sy F, Srikanth S, Huang G, Javed U, Buhari C, et al. Effects of cigarette smoke exposure on clot dynamics and fibrin structure: an *ex vivo* investigation. *Arterioscler Thromb Vasc Biol*. (2010) 30:75–9. doi: 10.1161/ATVBAHA.109.195024
127. Deshpande RG, Khan MB, Genco CA. Invasion of aortic and heart endothelial cells by Porphyromonas gingivalis. *Infect Immun*. (1998) 66:5337–43. doi: 10.1128/IAI.66.11.5337-5343.1998
128. Fan X, Yin C, Wang J, Yang M, Ma H, Jin G, et al. Pre-diagnostic circulating concentrations of insulin-like growth factor-1 and risk of COVID-19 mortality: results from UK Biobank. *Eur J Epidemiol*. (2021) 36:311–8. doi: 10.1101/2020.07.09.20149369
129. Kong Y, Han J, Wu X, Zeng H, Liu J, Zhang H. VEGF-D: a novel biomarker for detection of COVID-19 progression. *Crit Care*. (2020) 24:1–4. doi: 10.1186/s13054-020-03079-y
130. Chen Y, Wang J, Liu C, Su L, Zhang D, Fan J, et al. IP-10 and MCP-1 as biomarkers associated with disease severity of COVID-19. *Mol Med*. (2020) 26:1–12. doi: 10.1186/s10020-020-00230-x
131. Merzon E, Green I, Shpigelman M, Vinker S, Raz I, Golan-Cohen A, et al. Haemoglobin A1c is a predictor of COVID-19 severity in patients with diabetes. *Diabetes Metab Res Rev*. (2020) 2019:1–6. doi: 10.1002/dmrr.3398
132. Saengow U, Assanangkornchai S, Casswell S. Alcohol: a probable risk factor of COVID-19 severity. *Addiction*. (2021) 116:202–8. doi: 10.1111/add.15194
133. Simou E, Leonardi-Bee J, Britton J. The effect of alcohol consumption on the risk of ARDS: a systematic review and meta-analysis. *Chest*. (2018) 154:58–68. doi: 10.1016/j.chest.2017.11.041
134. Keddie S, Ziff O, Chou MKL, Taylor RL, Heslegrave A, Garr E, et al. Laboratory biomarkers associated with COVID-19 severity and management. *Clin Immunol*. (2020) 221:1–5. doi: 10.1016/j.clim.2020.108614
135. Malik P, Patel U, Mehta D, Patel N, Kelkar R, Akrmah M, et al. Biomarkers and outcomes of COVID-19 hospitalisations: systematic review and meta-analysis. *BMJ Evidence-Based Med*. (2020) 26:107–8. doi: 10.1136/bmjebm-2020-111536
136. Jalali Nadoushan M, Ahmadi S, Jalali Nadoushan P, Azzi L, Carcano G, Gianfagna F, et al. Hematologic, biochemical and immune biomarker abnormalities associated with severe illness and mortality in coronavirus disease 2019 (COVID-19): a meta-analysis. *Clin Chem Lab Med*. (2020) 58:1021–8. doi: 10.1515/cclm-2020-0369
137. Ji P, Zhu J, Zhong Z, Li H, Pang J, Li B, et al. Association of elevated inflammatory markers and severe COVID-19: a meta-analysis. *Medicine*. (2020) 99:e23315. doi: 10.1097/MD.0000000000023315
138. Akhmerov A, Marbán E. COVID-19 and the Heart. *Circ Res*. (2020) 126:1443–55. doi: 10.1161/CIRCRESAHA.120.317055
139. Mcelvaney OJ, Mcevoy NL, Carroll P, Murphy MP, Dunlea DM, Orna N, et al. Characterization of the Inflammatory Response to Severe COVID-19 Illness. *Am J Respir Crit Care Med*. (2020) 202:812–21. doi: 10.1164/rccm.202005-1583OC
140. Luis García de Guadiana R, Mulero MDR, Olivo MH, Rojas CR, Arenas VR, Morales MG, et al. Circulating levels of GDF-15 and calprotectin for prediction of in-hospital mortality in COVID-19 patients: a case series. *J Infect*. (2020) 82:e40–42. doi: 10.1016/j.jinf.2020.08.010
141. Milionis HJ, Liberopoulos EN, Achimastos A, Elisaf MS, Mikhailidis DP. Statins: another class of antihypertensive agents? *J Hum Hypertens*. (2006) 20:320–35. doi: 10.1038/sj.jhh.1002001
142. Amann R, Peskar BA. Anti-inflammatory effects of aspirin and sodium salicylate. *Eur J Pharmacol*. (2002) 447:1–9. doi: 10.1016/S0014-2999(02)01828-9
143. Undas A, Brummel-Ziedins KE, Mann KG. Antithrombotic properties of aspirin and resistance to aspirin: beyond strictly antiplatelet actions. *Blood*. (2007) 109:2285–92. doi: 10.1182/blood-2006-01-010645
144. Young E. The anti-inflammatory effects of heparin and related compounds. *Thromb Res*. (2008) 122:743–52. doi: 10.1016/j.thromres.2006.10.026
145. Siddiqi HK, Libby P, Ridker PM. COVID-19 –a vascular disease. *Trends Cardiovasc Med*. (2021) 31:1–5. doi: 10.1016/j.tcm.2020.10.005
146. Marchetti M. COVID-19-driven endothelial damage: complement, HIF-1, and ABL2 are potential pathways of damage and targets for cure. *Ann Hematol*. (2020) 99:1701–7. doi: 10.1007/s00277-020-04138-8
147. Danta CC. SARS-CoV-2, hypoxia, and calcium signaling: the consequences and therapeutic options. *ACS Pharmacol Transl Sci*. (2021) 4:400–2. doi: 10.1021/acsptsci.0c00219
148. Jahani M, Dokaneheifard S, Mansouri K. Hypoxia: a key feature of COVID-19 launching activation of HIF-1 and cytokine storm. *J Inflamm*. (2020) 17:1–10. doi: 10.1186/s12950-020-00263-3
149. Mathews I, Mathews EH, van Laar JH, Hamer W, Kleingeld M. A simulation-based prediction model for coal-fired power plant condenser maintenance. *Appl Therm Eng*. (2020) 174:115294. doi: 10.1016/j.applthermaleng.2020.115294
150. Caly L, Druce JD, Catton MG, Jans DA, Wagstaff KM. The FDA-approved drug ivermectin inhibits the replication of SARS-CoV-2 *in vitro*. *Antiviral Res*. (2020) 178:3–6. doi: 10.1016/j.antiviral.2020.104787
151. Mody V, Ho J, Wills S, Mawri A, Lawson L, Ebert MCCJC, et al. Identification of 3-chymotrypsin like protease (3CLPro) inhibitors as potential anti-SARS-CoV-2 agents. *Commun Biol*. (2021) 4:1–10. doi: 10.1038/s42003-020-01577-x
152. Lehrer S, Rheinstein PH. Ivermectin docks to the SARS-CoV-2 spike receptor-binding domain attached to ACE2. *In Vivo*. (2020) 34:3023–26. doi: 10.21873/invivo.12134
153. Swargiary A. Ivermectin as a promising RNA-dependent RNA polymerase inhibitor and a therapeutic drug against SARS-CoV2: evidence from *in silico* studies. *Res Sq. [Preprint]* (2020). doi: 10.21203/rs.3.rs-73308/v1
154. Kory P, Meduri GU, Varon J, Iglesias J, Marik PE. Review of the emerging evidence demonstrating the efficacy of ivermectin in the prophylaxis and treatment of COVID-19. *Am J Ther*. (2021) 28:e299–318. doi: 10.1097/MJT.0000000000001377
155. Bryant A, Lawrie T, Fordham E, Scott M, Hill S, Tham T. Ivermectin for prevention and treatment of COVID-19 infection: a systematic review and meta-analysis. *Am J Ther*. (2021) 27:e1–27. doi: 10.31219/osf.io/k37ft
156. Whitworth JAG, Hay CRM, Nicholas AM, Morgan D, Maude GH, Taylor DW. Coagulation abnormalities and ivermectin. *Ann Trop Med Parasitol*. (1992) 86:301–5. doi: 10.1080/00034983.1992.11812667

157. Jin L, Feng X, Rong H, Pan Z, Inaba Y, Qiu L, et al. The antiparasitic drug ivermectin is a novel FXR ligand that regulates metabolism. *Nat Commun.* (2013) 4:1–8. doi: 10.1038/ncomms2924
158. Ci X, Li H, Yu Q, Zhang X, Yu L, Chen N, et al. Avermectin exerts anti-inflammatory effect by downregulating the nuclear transcription factor kappa-B and mitogen-activated protein kinase activation pathway. *Fundam Clin Pharmacol.* (2009) 23:449–55. doi: 10.1111/j.1472-8206.2009.00684.x
159. DiNicolantonio JJ, Arranda JB-, McCarty M. Ivermectin may be a clinically useful anti-inflammatory agent for late-stage COVID-19. *Open Hear.* (2020) 7:e001350. doi: 10.1136/openhrt-2020-001350
160. Gracia-Ramos AE, Jaquez-Quintana JO, Contreras-Omaña R, Auron M. Liver dysfunction and SARS-CoV-2 infection. *World J Gastroenterol.* (2021) 27:3951–70. doi: 10.3748/wjg.v27.i26.3951
161. Kory P, Meduri GU, Iglesias J, Varon J, Berkowitz K, Kornfeld H, et al. Review of the emerging evidence demonstrating the efficacy of ivermectin in the prophylaxis and treatment of COVID-19. *Front Pharmacol.* (2021) 1–32. doi: 10.31219/osf.io/wx3zn
162. Roth GA, Johnson C, Abajobir A, Abd-Allah F, Abera SF, Abyu G, et al. Global, regional, and national burden of cardiovascular diseases for 10 causes, 1990 to 2015. *J Am Coll Cardiol.* (2017) 70:1–25. doi: 10.1016/j.jacc.2017.04.052

Conflict of Interest: This study received funding from HumanSim (Pty) Ltd. The funder was not involved in the study design, collection, analysis,interpretation of data, the writing of this article or the decision to submit it for publication.

The authors declare that the research was conducted in the absence of any commercial or financial relationships that could be construed as a potential conflict of interest.

NOMENCLATURE

ACE, Angiotensin-converting-enzyme
β-blocker, Beta-adrenergic antagonists
BDNF, Brain-derived neurotrophic factor
BNP, B-type natriuretic peptide
Covid-19, Coronavirus disease of 2019
COX, Cyclooxygenase
CRP, C-reactive protein
CHD, Coronary heart disease
D-dimer, Fibrin degradation product D
EC, Endothelial cell
FFA, Free fatty acids
GCF, Gingival crevicular fluid
GM-CSF, Granulocyte-Macrophage Colony-Stimulating Factor
HbA1c, Glycated hemoglobin A1c
HDL, High-density lipoprotein
HGD, High Glycemic Diet
HR, Hazard Ratio
Hs, Homocysteine
ICAM, Intracellular adhesion molecule
IGF-1, Insulin-like growth factor-1
IL, Interleukin
LDL, Low-density lipoprotein
MAPK, Mitogen-activated protein kinase
MCP, Monocyte chemoattractant protein
MIF, Macrophage migration inhibitory factor
MMP, Matrix metalloproteinase
MOA, Mechanism Of Action
MPO, Myeloperoxidase
NFκβ, Nuclear factor-kappa-beta
NLRP3, Nod-like receptor family pyrin domain containing 3
NO, Nitric oxide
NO-NSAID, Nitric oxide-non-steroidal anti-inflammatory drug
OPG, Osteoprotegerin
OR, Odds Ratio
oxLDL, Oxidized LDL
PAI, Plasminogen activator inhibitor
PDGF, Platelet-derived growth factor
P. gingivalis, Porphyromonas gingivalis
PI3K, Phosphatidylinositol 3-kinase
RANKL, Receptor activator of nuclear factor kappa-beta ligand
ROS, Reactive oxygen species
RR, Relative Risk
SARS-CoV-2, Severe acute respiratory syndrome coronavirus 2
SCD-40, Recombinant human sCD40 ligand
SMC, Smooth muscle cell
SSRI, Serotonin reuptake inhibitors
TF, Tissue factor
TMAO, Oxidation product of trimethylamine
TNF-α, Tumor necrosis factor-alpha
VCAM, Vascular cell adhesion molecule
vWF, von Willebrand factor.

Appendix E: NECSA pilot study protocol

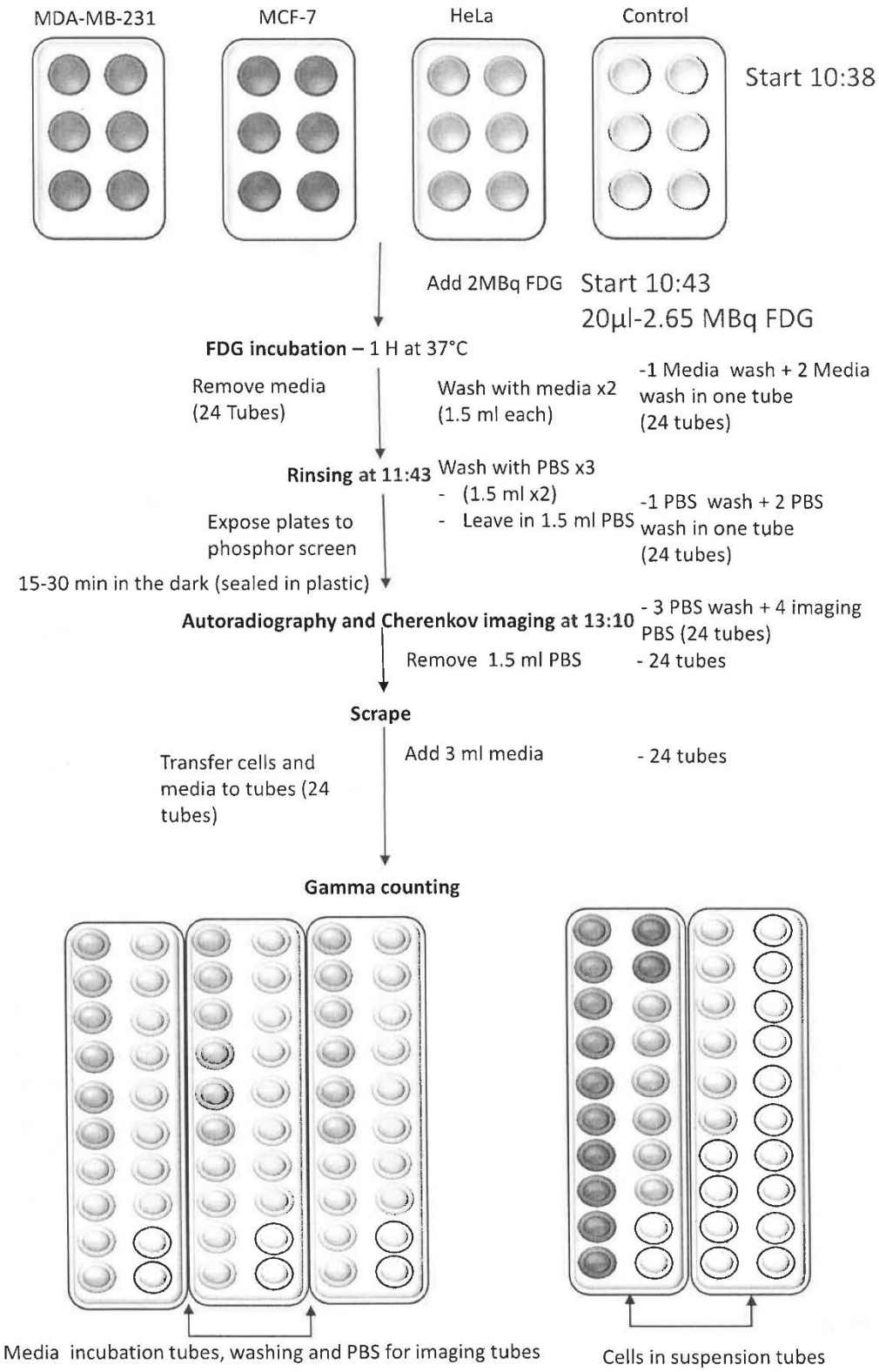

METHOD FOR
FDG IN VITRO IMAGING

On _____ the following method was conducted at NECSA

Steps	Time	Description
1		Added 3 mL of glucose-free DMEM (expose for 2 hours)
2		Measured FDG radioactivity: ___μL = ___MBq (require ≈ 2 MBq) @ ___:___
3		Added ___μL of FDG to cells in 6-well plates (expose for 1 hour)
4		Remove 20μL of solution containing FDG from each well for analysis in gamma counter
5		Removed FDG & Media from 6-well plates into tubes
6		Add 1.5 mL DMEM media (Wash 1) into 6-well plates
7		Removed DMEM media (Wash 1) from 6-well plates into new tubes
8		Add 1.5 mL PBS (Wash 2) into 6-well plates
9		Removed PBS (Wash 2) from 6-well plates into the same corresponding tubes as wash 1
10		Add 1.5 mL PBS (Wash 3) into 6-well plates
11		Removed PBS (Wash 3) from 6-well plates into new tubes
12		Add 1.5 mL PBS (Wash 4) into 6-well plates for imaging
13		Expose cells in 6-well plates to the phosphor screen for 35 minutes
14		Start phosphor imaging
15		Expose cells to optical Cherenkov imaging (Radioactivity was too low)
16		Start nano-PET/CT scans of each cell line separately in the following order: • MDA-MB-231, MCF-7, HeLa and Control
17		Removed PBS (Wash 4) from 6-well plates into the same corresponding tubes as wash 3
18		Add 3 mL of DMEM media into 6-well plates and scrape cells off of the surface
19		Removed cells from 6-well plates and add into new tubes
20		Repeat steps 15 to 17 for all cell lines
21		FDG stock concentration ____Mbq @ ___:___ • FDG 1 x Dilution: • FDG 10 x Dilution: • FDG 100 x Dilution:
22		Insert cells to gamma counter imager in the following order: 1. Solution with FDG (20 μL) 2. FDG tubes 3. Wash 1&2 tubes 4. Wash 3&4 tubes 5. FDG dilution tubes 6. Cells tubes Cell line order: MDA-MB-231, MCF-7, HeLa and Control